



Analytical Methods for Dynamic Open Channel Heat and Mass Transfer

Methodology for the Heat Source Model Version 7.0



Prepared by:

Matthew Boyd & Brian Kasper

The methods presented in this document formulate the programmed modules utilized by Heat Source and TTools (versions 7.0). These computer models are used to create spatial data sets for stream networks, simulate dynamic hydraulics and thermodynamics. Appropriate use and application are the sole responsibility of the user.

This document may be downloaded from the web site at the following URL:
<http://www.deq.state.or.us/wq/TMDLs/tools.htm>

Updated February 12, 2003 & February 20, 2007

Cite this document as:

Boyd, M., and Kasper, B. 2003. Analytical methods for dynamic open channel heat and mass transfer: Methodology for heat source model Version 7.0.

Table of Contents

CHAPTER I. INTRODUCTION

1.1 Overview of Methodology	1
1.1.1 The State of the Science	2
1.1.2 Acknowledgement of Limitations	6
1.2 Stream Heating and Cooling Processes	7
1.2.1 Common Nonpoint Sources of Stream Temperature Change	9
1.2.2 Point Sources of Stream Warming	20
1.2.3 Natural Sources of Stream Warming and Cooling	21
1.3 Model Application: Scope, Scale & Cumulative Effects	23
1.4 Salmonid Life Stage Thermal Ranges	24

CHAPTER II. HEAT TRANSFER

2.1 Overview	27
2.2 Solar Radiation	29
2.2.1 Solar Time Relative to Earth	30
2.2.2 Solar Position Relative to Earth	31
2.2.3 Solar Position Relative to Stream Position	36
2.2.4 Solar Radiation Heat above Topographic Features	38
2.2.5 Solar Radiation Heat below Topographic Features	40
2.2.6 Solar Radiation Heat below Land Cover	41
2.2.6 Solar Radiation Heat above Stream Surface	44
2.2.7 Solar Radiation Heat Penetrating the Stream Surface	46
2.2.8 Solar Radiation Heat Received by Water Column and Substrate	47
2.2 Longwave (Thermal) Radiation	51
2.3 Substrate Conduction Flux	53
2.4 Evaporation Flux	58
2.4.1 Evaporation Rate	59
2.4.2 Wind Functions	62
2.5 Convection Flux	64
2.6 Stream Temperature Simulation Method	65
2.6.1 Non-Uniform Heat Energy Transfer Methodology	65
2.6.2 Finite Difference Approximation	68

CHAPTER III. DYNAMIC MASS TRANSFER

3.1 Overview	71
3.2 Channel Geometry & Manning's Relationships	73
3.3 Dynamic Hydraulic Flow Routing	76
3.3.2 Muskingum-Cunge Approximation	78
3.3.2 Explicit Finite Difference Method	81
3.3.3 Comparison of Methods	84
3.4 Quantifying External Mass Transfers	87

3.4.1 Temperature Change Resulting from Mixing	87
3.4.2 Thermal Infrared Radiometry Derived Mass Balance Approach	88
3.4.3 Surface Inflows (Springs, Tributaries and Return Flows)	92
3.4.4 Subsurface Inflows (Seeps, Springs and Accretion Flows)	93
3.4.5 Hyporheic Flows	94
3.4.6 Evaporation Losses	97
3.5 Flow Volume Continuity	98
3.6 Controlled Flows and Depths	99
3.7 Dewatered Channels	99
3.8 Tendency to Stratify	99

CHAPTER IV. MODEL OPERATION

4.1 Overview	101
4.2 Finite Difference Steps	102
4.3 General Setup Procedure	102
4.3.1 General Inputs	103
4.3.2 Model Setup - Data Sheets	104
4.3.3 Model Setup – Continuous Data	105
4.3.4 Model Setup – Mass Transfer Data	108
4.3.5 Model Setup – TTools Data	111
4.3.6 Model Setup – Land Cover Codes and Attribute Associations	111
4.3.7 Model Setup – Morphology Data	113
4.3.8 Model Setup – Evaporation Rate Methods	118
4.3.9 Model Setup – Stream Bed Conduction	119
4.3.10 Model Setup – Physically Based Flow Routing Methods	120
4.3.11 Model Setup – Clear All Data Sheets	121
4.3.12 Model Setup – Validation Data	122
4.4 Executables	123
4.4.1 Executables – Shade-a-lator	124
4.4.2 Executables – Flow Router	125
4.4.3 Executables – Heat Source	126
4.5 Model Outputs	127
4.5.1 Chart – Diel Temperature	127
4.5.2 Chart – TIR Temperature	128
4.5.3 Chart – Longitudinal Temperature	129
4.5.4 Chart – Solar Flux	129
4.5.5 Chart – Heat Flux	130
4.5.6 Chart – Effective Shade	131
4.5.7 Other Output Data Worksheets	131
4.6 Common Sources of Problems	133
4.7 Dialogue Windows – Purpose and Meaning	134
4.7.1 Progress Window	134
4.7.2 Message Boxes	134
4.8 Other 'Utility' Applications	137
4.8.1 Land Cover Positioner	137

CHAPTER V. SPATIAL DATA DERIVATIONS

5.1 Introduction	139
5.2 Geospatial Data Overview	140
5.3 Aerial Imagery - Digital Orthophoto Quadrangles and Rectified Aerial Photos	141
5.3.1 Digitized Stream Position from Aerial Imagery	141
5.3.2 Stream Aspect	142
5.3.3 Channel Width from Aerial Imagery	143
5.3.4 Near Stream Land Cover Mapping from Aerial Imagery	145
5.4 Digital Elevation Model (DEM)	149
5.4.1 Stream Elevation	149
5.4.2 Stream Gradient	150
5.4.3 Topographic Shade Angle	150
5.5 Thermal Infrared Radiometry (TIR) Temperature Data	152
5.5.1 Overview of TIR Data	152
5.5.2 TIR Data Collection and Validation Methods	152
5.5.2 Interpretation of FLIR Images	154
5.5.3 TTools Sampling of TIR Data	156
5.6 Other TTools applications:	156
5.6.1 Stream Sinuosity	156
5.6.2 Meander Width Ratio	157
5.6.3 Entrenchment Ratio	157
5.7 Digitizing a Stream Layer	158
5.7.1 Cleaning and Unionizing a Stream Layer	159
5.7.2 Cleaning the Overshoots	161
5.7.3 Cleaning the Undershoots	163
5.7.4 Unionizing the Cleaned Stream Polyline	164
5.8 Digitizing Channel Width (Near Stream Disturbance Zone Width)	165
5.9 Digitizing Near Stream Land Cover	167
5.10 TTools Operation	175
Turning on the TTools Extension	175
Step 1: Segmenting the Stream and Calculating the Aspect	176
Step 2: Measuring Channel Widths	177
Step 3: Measuring Stream Elevation and Gradient	177
Step 4: Measuring Topographic Shade	178
Step 5: Sampling the Riparian Land Cover	179
Step 6: Sample FLIR Data	181
 Symbols	 183
 References	 189

Chapter

I

Introduction

Statement of Purpose, Acknowledgement of Limitations and Overview of Heat and Mass Transfer



Varied landscapes, complex morphology and multiple land uses are common challenges in water temperature analysis (Nehalem River, Oregon)

1.1 OVERVIEW OF METHODOLOGY

This document is intended to serve as a reference for the stream heat and mass transfer analytical methodology Heat Source¹. Chapters that follow describe in detail the mathematics and solution techniques suited for heat and mass transfer quantification. Simulation of water temperature and flow dynamics over various scales (i.e. reach, watershed to basin scales) is made possible with high resolution spatially continuous data, coupled with deterministic modeling of hydrologic and landscape processes. These processes are often interrelated and occur simultaneously (and can amplify or mask the effect of other processes). The methods presented in this paper are predicated foremost on data accuracy and resolution, and then analytical methodology robustness.

¹ **Heat Source** model is comprised of modules that can simulate dynamic open channel hydraulics, flow routing, heat transfer, effective shade and stream temperature. This documentation is developed to support Heat Source version 7.0.

Methods for spatial data derivation have been developed and packaged as an ArcView (version 3.0 or higher) extension, and is referred to as TTools². The sampling methods within TTools allow for continuous measurements of channel morphology, land cover and topography. Spatial data derivations sampled and calculated by TTools are then imported into Heat Source as data inputs.

Heat Source consists of a Microsoft Excel (version 2000 or higher) spreadsheet that contains model input and output. No calculations are made in the spreadsheet itself. Instead, Visual Basic programming computes all dynamic mass and heat transfer simulation algorithms. Modules (executables) include simulation of effective shade, comprehensive heat and mass transfer and water temperature (these modules, along with setup routines, are controlled from a central 'Main Menu').

1.1.1 THE STATE OF THE SCIENCE

The models used for stream temperature prediction are becoming standardized and widely available. However, data availability and the increased ease of monitoring, coupled with aerial imagery, GIS data and remote sensing, and finally model operation considerations, offer significant advancements in stream temperature analysis.

RIVERS AND STREAMS ARE THERMALLY UNIQUE

A definition of stream temperature uniqueness recognizes that the longitudinal temperature profile, as well as spatial and temporal dynamics defined at virtually any scale, applies only to one stream, river or network. Recently published literature is offering the scientific community evidence that stream and river systems are not only hydrologically and thermally unique, but also complex (Boyd M. and B. Kasper 2002, Faux et al. 2001, Torgersen et al. 2001, Torgersen et al. 1999, Torgersen et al. 1995). Stream temperature distributions are highly characteristic of individual stream/river reaches and these unique temperature patterns are expressed inter-annually.

An example of unique thermal patterns between similar streams can be found in the North and South Forks of the Sprague River. Thermal infrared radiometry (TIR) measured stream temperature data suggest that the North and South Forks of the Sprague River exhibit temperature dynamics specific to each stream across multiple scales. Both stream have similar summertime low flows of ≈ 0.85 cms (≈ 30 cfs) and originate from similar sized drainages with similar topography, geology and land use patterns. TIR sampling occurred within the same period of the day $\approx 4:00$ PM on August 12 and August 16, 1999 (see **Figure 1.1**). Despite these apparent similarities, each stream exhibits different stream temperature patterns. The reasons for these thermal differences are found in the cumulative effects of highly variable characteristics of the land cover, morphology, mass transfer inflow and withdrawal distributions (Boyd and Kasper 2002).

² **TTools** sampling Tool samples spatial data sets such as stream position, elevation, gradient, channel width, topographic shade and land cover types from GIS data at user defined intervals. This documentation is developed to support TTools version 7.0.

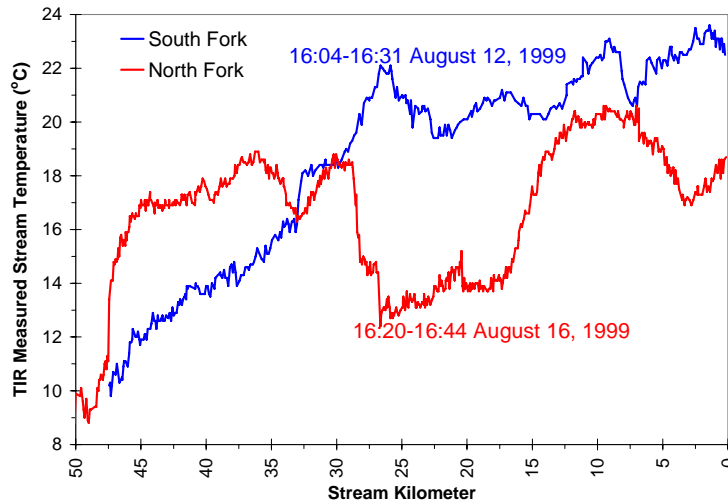


FIGURE 1.1
TIR Sampled Stream Temperature Patterns for the North and South Fork Sprague River

HOW DOES HEAT SOURCE ADDRESS THESE UNIQUE THERMAL PATTERNS?

With recognition of the unique thermal dynamics of streams and rivers comes the need for an analytical framework that accommodates the variability and spatial distributions inherent to land cover, morphology and hydrology. The past ten years have brought about increased use of remote sensing, computational power and ease of programming, ground level data collection methods, and other improvements that are all part of the basis for proposing an improved stream temperature analytical framework.

Analytical Methodology Robustness

Heat Source was born out of the exploration of the causal factors that affect dynamic thermal regimes, with a focus on the data and methods suited for riverine thermodynamics and hydrodynamics that capture complex analytical procedures, robust and comprehensive methods and considerations for the interrelatedness between parameters. Important processes are included in the methodology, such as: mass transfers from tributaries, groundwater inflows, landscape thermal radiation, adiabatic cooling, robust radiation modeling, multiple evaporation methods, and complex hydrodynamic routing with hyporheic exchange within the substrate, to name a few. Very few efforts of simplification are evident in the methodology, and instead, the inclusion of all complex processes is generally the guiding principle in the methodology development and application.

Aside from computational speed, analytical modeling can be performed using deterministic methods over relatively small time and distance finite difference steps. Model operation resolution should match the dynamic nature of stream temperature that tends to occur over small scales across a variable landscape, and sometimes in a brief period of time.

High Resolution Application of the Methodology

By design, spatial input data is derived and sampled at a high resolution, offering a second source of robustness. This method of stream temperature simulation minimizes assumptions and includes all input parameters, even those

considered by some to be less important and/or too difficult to quantify. Simply stated, model robustness is also derived from high input data resolution (in addition to the analytical methodology, scope and input data types).

The authors contend that coarse application of the methodology will cause output errors (the model will perform poorly) because the impacts of human, landscape and hydrologic influences often occur at a high spatial resolution. Observed or simulated stream temperatures result from a multitude of parameters and processes. Even small changes (or omissions) in these parameters or processes (both thermal and hydrologic) may cause significant temperature changes. By definition, such changes are cumulative effects. The methodology is intended to be applied over large scales (i.e. network scale) with the intent of capturing cumulative effects.

These forms of robustness manifest themselves with results that are typically accurate, data driven and inherently unbiased by underlying simplifications or assumptions (because they are minimized to the best practical extent).

A New Way to Model Hydrology and Water Quality

For these reasons, Heat Source represents part of a growing shift in stream temperature analytical approach. This shift is facilitated by the application of model inputs derived from rich spatial data sources and analytically robust methods designed to analyze stream temperature dynamics at any level of complexity. Rejection of model simplification, and instead, embracing the rigors of data and analytical complexity is the basis for the model. Generalizations only apply to basic thermodynamic (heat transfer physics) and physically based processes (mass transfer physics). Generalizations of thermodynamic behavior cannot be made at all, until that is, a comprehensive data rich analysis has been conducted at a network scale. An acknowledgement of thermal uniqueness requires investigators of water temperature dynamics to challenge generalizations in the literature and perform analysis without preconceived notions of parameter and process sensitivity, and ultimately, model outputs.

A COMPREHENSIVE ANALYTICAL APPROACH

As a rule, a comprehensive analysis should be data rich, draw from deterministic methods, operated at high resolution and provided statistically validated results.

So you want to complete a comprehensive stream temperature assessment? Or perhaps you need to calculate the thermal effect of solar radiation exposure to a water body? What is the thermal effect of a point source? Each question raises others. What are the flow dynamics inherent to a stream? What heat transfer processes dominate, and which are of lesser importance? Which parameters are within human control? What are the cumulative impacts of mass and heat transfer? The list of questions directed at a stream temperature analytical effort can often be quite long (and is always much longer than the list of preceding questions).

Regardless of whether the study area is large and complex or simply a stream segment, a primary question posed in this section is, "what is a comprehensive assessment?" The answer to this question seems to have changed recently, as data collection and analytical techniques have evolved over past several years. A comprehensive assessment utilizes integrated remotely

sensed and ground level continuous temperature data, weather data, channel morphology, hydraulics and near stream land cover data. Sampled GIS data should be incorporated into the analysis for many of these parameters. When possible, thermal infrared remote sensing should be used to quantify stream mixing, thermal gradients and mass transfer processes that cannot be measured at the ground level. Other forms of spatial data allow quantification of topography and land form. Model inputs can be dramatically improved simply by drawing from morphologic and land cover assessments methods (i.e. Kovalchik 1987, Hall 1998, Rosgen 1996).

Amidst these advances, some factors have remained constant. You will not have all the data that you want. Unresolved questions will remain when you are finished with your analytical effort. While our ability to measure and quantify landscape and hydrologic processes has dramatically improved over the last decade, there remain several limitations for some parameters, and these are often compounded by the limited resources often available for these analytical efforts. Therefore, we simply cannot address stream temperature in all of its complexity. Although analytical modeling is helpful in understanding the interrelated hydrodynamic and thermodynamic processes associated with stream temperature, it is not a panacea. Let me quickly explain before you toss this document in the recycling bin.

While many heat and mass transfer processes are well understood and even easily measured (and independently modeled) at various levels of complexity (i.e. flow, shade, humidity, wind speed, etc.), the variation and interdependence of some of these parameters across a drainage is poorly documented. For example, near stream microclimates that control humidity, wind speed and air temperature are a function of the near stream land cover type and condition, as well as topography and atmospheric processes. Since the physical attributes of both land cover and topography vary in spatial distributions, often dramatically, we should assume that microclimates also vary across the landscape. Spatial variability is compounded by the temporal variation associated with atmospheric parameters. Now consider that data collection methods are not available to quantify this variability. Consequently, such complexity (variability and interdependence) is not easily accounted for in most analytical methods, at least in a practical sense. Further, even if algorithms are developed to simulate these processes, validation of model performance will be difficult due to the aforementioned data and instrumentation limitations, along with methodology limitations. The result is that microclimates are not included in stream temperature analysis in a complete fashion.

Changes in rates of heat transfer can vary considerably across relatively small spatial and temporal scales. In quantifying and understanding stream heat and mass transfer processes, the challenge is not represented in theoretical conceptions of thermodynamics and relations to flowing water. Thermodynamics is a well-established academic discipline that offers a scientifically tested methodology for understanding stream temperature. In fact, the methodology used to evaluate stream temperature is quite simple when compared to other thermodynamic applications that have become common technological necessities to the American way of life (i.e. a car radiators, cooling towers, solar thermal panels, insulation, etc.). Instead, the true challenge in understanding stream temperature materializes with the recognition that thermally significant heat and mass transfer processes occur in very fine spatial and temporal scales. Tremendous spatial variability occurs across a watershed, and is compounded

by adding the temporal component. At any stream reach, thermal processes constantly change throughout the day, month and year. Stream temperatures are a result of a multitude of heat transfer and mass transfer process. The conceptual and analytical challenge is to develop a framework that captures these forms of variability to the best possible extent while constantly investigating potential analytical improvements.

The recognition of limitations, such as those presented by microclimates, is important for several reasons. While these limitations outline potential areas of weakness in the methodology presented in this document, acknowledgement of data and methodology weaknesses makes it possible to undertake a comprehensive approach, define the limitations, maintain credibility and identify future research needs. Acknowledgement of the limitations is in accordance with the scientific method and recognizes that analytical efforts should provide a rigorous, comprehensive, statistically valid and advanced treatment of stream temperature dynamics.

1.1.2 ACKNOWLEDGEMENT OF LIMITATIONS

Capturing and understanding the thermally important parameter variation across a complex landscape, coupled with quantifying hydrology and morphology parameters and variation, is a common challenge before us. Identifying specific limitations, increases analytical credibility and focuses our efforts on future monitoring and analytical advancements.

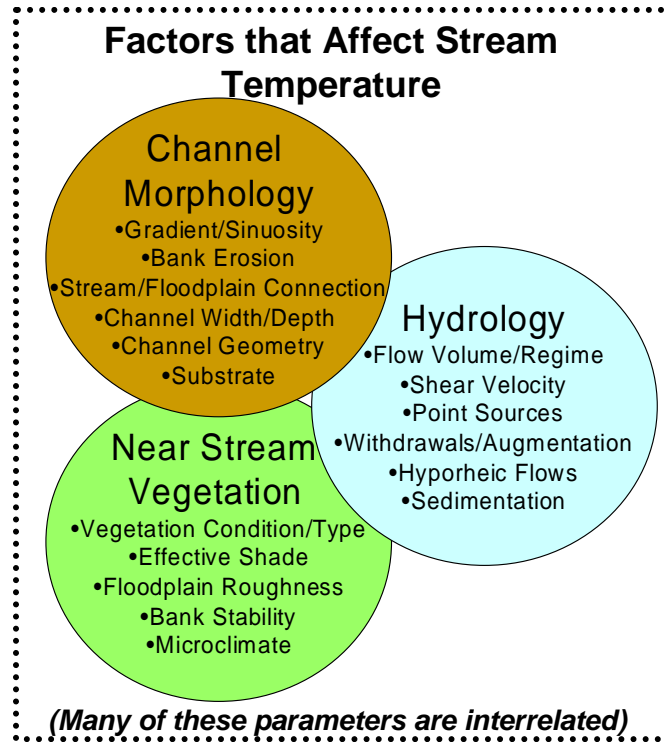
- At any scale, it is challenging to capture spatial variability in stream and landscape data. Ground level measurements are particularly unsuited for detecting spatial variability.
- Simple instream measurements of flow above and below a study reach can be insufficient to detect subsurface interactions with the stream due to instrumentation limitations. Without remote sensing, such data may not describe high-resolution instream flow conditions making validation of derived mass balances difficult. While analytical techniques exist for describing subsurface/stream interactions, they may be beyond the scope of an effort with regard to data availability, technical rigor and resource allocations.
- Water quality issues are complex and interrelated. The state of the science is still evolving in the context of landscape scaled water quality analysis. The degree to which one parameter affects another, may not be fully understood. Analytical methods may capture primary effects, but miss secondary (more subtle) effects. An example is the relationship between channel form/function and flood plain land cover distributions. While both can be quantified independently, the extent that each affects the other may be variable and/or site specific, and therefore not easily quantified in a broad application such as Heat Source.
- Land use patterns often vary through any drainage from heavily impacted areas to areas with little human impacts. However, it is often difficult to find large areas without some level of either current, past or upstream human impacts. Few sites represent historical conditions. Further, some human impacts are 'permanent' in the context of geologic time scales. Attempts at simulating historical conditions cannot be validated and are likely inadequate

on multiple counts. Modeling applications should consider the degree of divergence between the hypothetical simulation conditions and the calibrated model condition.

- Uncertainties will persist, since stream temperature dynamics are complex and analytical methods have limitations. With this acknowledgement of limitations comes the responsibility to use your experience, consult with others when needed, engage in scientific reviews of your work and document limitations inherent to model output and interpretations of results. Always statistically validate model results so that others can easily recognize model performance and advise others to use your results appropriately.
- With recognition of inherent complexity in mass and heat transfer, avoid simple analytical techniques that fail to capture the multitude of important stream parameters and processes that affect stream thermodynamics. Stream temperature does not easily lend itself to simple statistical analysis. For example, simple regression analysis can result in spurious correlations that offer limited or poor insight into the complex thermodynamic and hydrologic processes that vary over space and time.
- As a general rule, do not use a model to create data that can be measured. It is usually cheaper to measure stream temperature via ground level and remote sensing than to derive simulated temperature data. Obviously, measured values (i.e. ground level and remote sensing) are more accurate than modeled results.

1.2 STREAM HEATING AND COOLING PROCESSES

Parameters that affect stream temperature can be grouped as near stream land cover (vegetation), channel morphology and hydrology. Many of these stream parameters are interrelated (i.e., the condition of one may impact one or more of the other parameters). These parameters affect stream *heat transfer processes* and stream *mass transfer processes* to varying degrees. The analytical techniques employed to evaluate stream temperature can be designed to include all of the parameters that affect stream temperature provided that available data and methodologies allow accurate quantification.



Regardless of scale, stream temperature dynamics are complicated when these three parameters (i.e. near stream land cover, channel morphology and hydrology) are evaluated. Many parameters exhibit considerable spatial variability. For example, channel width measurements can vary greatly over small stream lengths. Some parameters can have a diurnal and seasonal temporal component as well as spatial variability. Analytical approaches developed for stream temperature assessment that consider all of these parameters must rely on ground level, GIS data and remotely sensed spatial data. To understand temperature on a landscape scale is a difficult and often resource intensive task. General analytical techniques employed to evaluate stream temperature are statistical and deterministic modeling of hydrologic and thermal processes.

Water temperature change (ΔT_w) is a function of the heat transfer in a discrete volume and may be described in terms of changes in heat per unit volume. With this basic conceptual framework of water temperature change it is possible to discuss stream temperature change as a function of two variables: heat and mass transfer.

Water Temperature Change as a Function of Heat Exchange per Unit Volume,

$$\Delta T_w \propto \frac{\Delta \text{Heat}}{\text{Volume}} \quad (1-1)$$

1. **Heat transfer** relates to processes that change heat in a defined water volume. There are several thermodynamic pathways that can introduce or remove heat from a stream. For any given stream reach heat exchange is closely related to the season, time of day and the surrounding environment and the stream characteristics. Heat transfer processes can be dynamic and

change over relatively small distances and time periods. Several heat transfer processes can be affected by human activities.

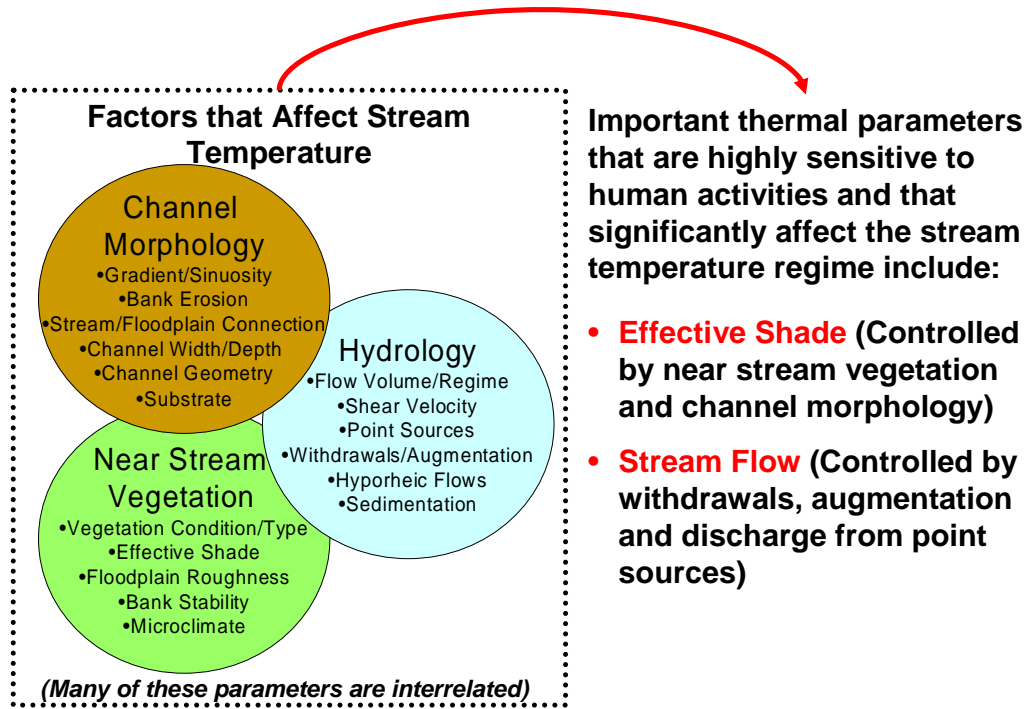
2. **Mass transfer** relates to transport of flow volume downstream, instream mixing and the introduction or removal of water from a stream. For instance, flow from a tributary will cause a temperature change if the temperature is different from the receiving water. Mass transfer commonly occurs in stream systems as a result of advection, dispersion, groundwater exchange, hyporheic flows, surface water exchange and other human related activities that alter stream flow volume.

1.2.1 COMMON NONPOINT SOURCES OF STREAM TEMPERATURE CHANGE

A dominant purpose for analytical modeling is to quantify human-related stream change. Brown (1969) identified temperature change as a function of heat and stream volume (1-1). Using this simple relationship, it becomes apparent that stream temperature change is a function of the heat transfer processes and mass transfer processes. To isolate the human influence on this expression, it is important to associate the human influence on the heat transfer processes and/or mass transfer processes.

Effective shade is consistently identified in the literature as an important thermal control that is often influenced by human activity. The combined effect of land cover physical attributes and channel morphology control the timing and extent of effective shade cast upon the stream surface. It is important to consider that land cover type and condition affects, and is affected by, channel morphology (bank stability, shallow ground water characteristics, riparian nutrient cycles, aerobic or anaerobic rooting conditions, etc.). A meaningful assessment of effective shade should include both land cover and morphologic spatial data and analysis.

Flow volume is also an important thermodynamic and hydrologic parameter that is subject to obvious human manipulations. Many parameters are affected by flow volume. In fact, the flow regime of a riverine system formulates the basic connectivity of instream and riparian processes. The thermodynamic influences of the flow regime cannot be easily summarized simply because of the wide and diverse influences that flow has upon the thermal regime.



The following subsections expand upon the role of effective shade and flow volume in recognition that these two parameters are often implicated in human caused stream temperature modifications.

LAND COVER, MORPHOLOGY AND EFFECTIVE SHADE

The solar radiation heat process considered in the stream thermal budget is often the most significant heat transfer process and can be highly influenced by human-related activity. Decreased levels of stream shade increase solar radiation loading to a stream. The primary factors that determine stream surface shade are near stream land cover type (and associated physical characteristics) and channel morphology. Near stream land cover height controls the shadow length cast across the stream surface and the timing of the shadow. Channel width determines the shadow length necessary to shade the stream surface.

Near stream land cover and channel morphology are often interrelated. Stream bank erosion rates are often a partial function of near stream land cover type and condition. Similarly, the type of land cover that can establish, grow and reproduce at any given near stream site is a partial function of the hydrologic regime, the subsurface water table dynamics and the floodplain condition. An obvious feedback mechanism exists between channel morphology and land cover establishment and success. *Human activities that change the type or condition of near stream land cover and/or alter stream channels (beyond what is considered channel equilibrium dimensions) will likely result in altered stream surface shading patterns. By definition, a decrease in stream surface effective shade will have a warming effect upon water temperature.*

Examples of Two Different Land Cover and Morphology Conditions



Meadow complex with high rates of summertime heating, little effective shade, unstable stream banks, a pattern of downcutting, lowered floodplain water tables and wide/shallow morphology (Sycan River, Oregon)



Another meadow complex with minimal summertime heating, moderate effective shade, stable stream banks, high flood plain water table (Sprague River, Oregon)

Relationships Between Effective Shade, Near Stream Vegetation and Channel Morphology

*Effective Shade is a Function of Two Interrelated Parameters:
Land Cover and Morphology*

Stream surface shade is the primary control over the daytime rate of stream heating from direct beam solar radiation. Simply put, shade is a dominant control over the rate of stream heating.



Near Stream vegetation controls shadow length, and therefore, the timing of stream surface shade.

Near stream vegetation and **channel morphology** conditions are highly interrelated, since each affects the condition of the other.



Channel morphology determines the shadow length necessary to shade stream. In effect, channel morphology controls the size of the stream surface area.

Channel morphology condition and **near stream vegetation** combine to control the amount of stream surface shade that occurs on any given stream segment.



EFFECTIVE SHADE: DEFINED AND DESCRIBED

Stream surface shade is an important parameter that controls the stream heating derived from solar radiation. Recall that solar radiation has the potential to be the largest heat transfer mechanism in a stream system. Human activities can degrade near stream land cover and/or channel morphology, and in turn, decrease effective shade. It follows that human-caused reductions in stream surface shade have the potential to cause significant increases in heat delivery to a stream system. Stream shade levels can also serve as an indicator of near stream land cover and channel morphology condition. For these reasons, stream shade is traditionally a focus of stream temperature analysis.

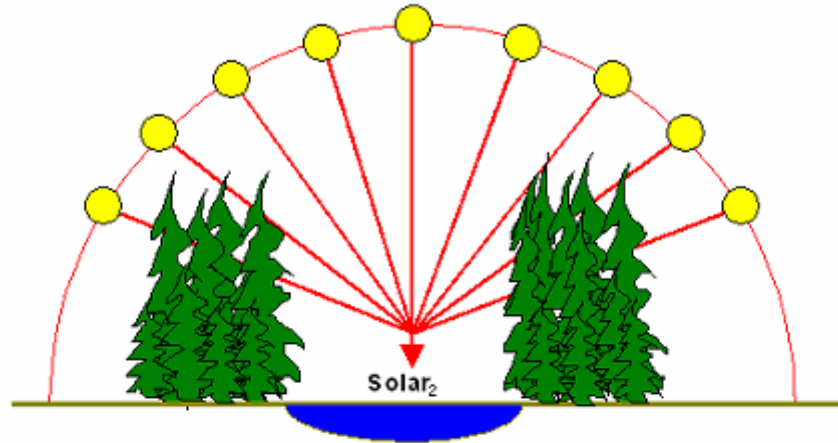
Table 1.1
Factors that Influence Stream Surface Shade

	Blue – Not Influenced by Land Management
	Red - Influenced by Land Management
Season/Time:	Date/Time
Stream Morphology:	Aspect, Channel Width, Incision
Geographic Position:	Latitude, Longitude, Topography
Land Cover:	Near Stream Land cover Height, Width, Density
Solar Position:	Solar Altitude, Solar Azimuth

In the Northern Hemisphere, the earth tilts on its axis toward the sun during summertime months allowing longer day length and higher solar altitude, both of which are functions of solar declination (i.e., a measure of the earth's tilt toward the sun). Geographic position (i.e., latitude and longitude) fixes the stream to a position on the globe, while aspect provides the stream/riparian orientation. Near stream land cover height, width and density describe the physical barriers between the stream and sun that can attenuate and scatter incoming solar radiation (i.e., produce shade). The solar position has a vertical component (i.e., solar altitude) and a horizontal component (i.e., solar azimuth) that are both functions of time/date (i.e., solar declination) and the earth's rotation (i.e., hour angle measured as 15° per hour). While the interaction of these shade variables may seem complex, the mathematics that describes them is relatively straightforward geometry (see **Figure 1.2**). Using solar tables or mathematical simulations, the *potential daily solar load* can be quantified. The *measured solar load* at the stream surface can easily be measured with a Solar Pathfinder[®], hemispherical canopy photography or estimated using mathematical shade simulation computer programs (Boyd, 1996, Chen 1994, Park, 1993).

Effective Shade Defined

Solar₁ – Potential daily direct beam solar radiation load adjusted for julian day, solar altitude, solar azimuth and site elevation.



$$\text{Effective Shade} = \frac{(\text{Solar}_1 - \text{Solar}_2)}{\text{Solar}_1}$$

Where,

Solar₁: Potential Daily Direct Beam Solar Radiation Load

Solar₂: Daily Direct Beam Solar Radiation Load Received at the Stream Surface

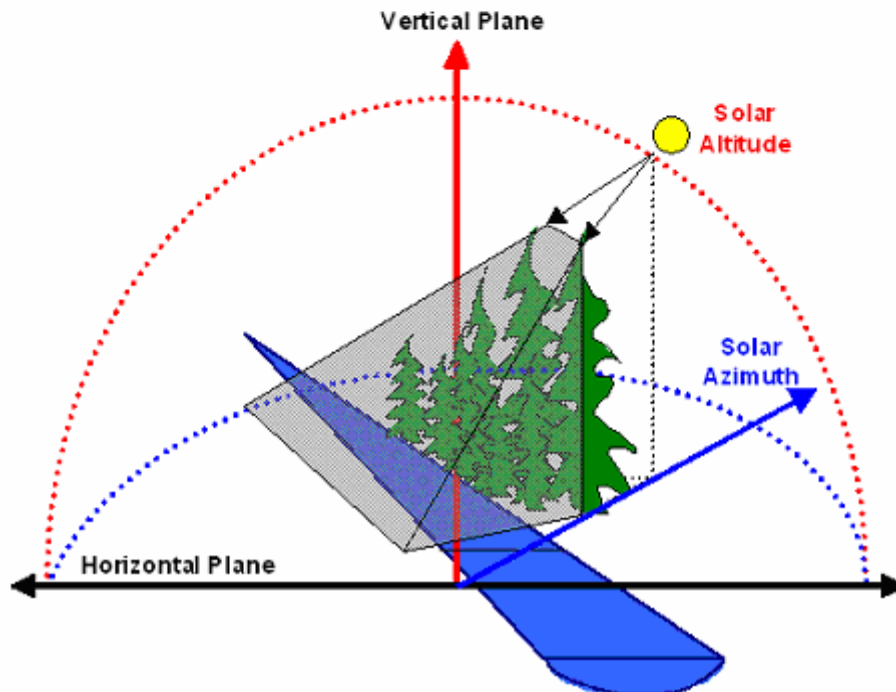


FIGURE 1.2
Shade geometric relationships and effective shade definition

EFFECTIVE SHADE: CASE STUDIES

Recent studies have isolated the thermal effects of solar loading, and consequently, the importance of stream surface shade in moderating localized increases in water temperature. Through controlled water bath studies Moore et al. (1999) found solar radiation to be a warming influence in both daily maximum and daily minimum water temperatures. The study was conducted in varying locations (at various elevations and climatic conditions) in Oregon and found similar results at each study site (see **Figure 1.3**).

The Effect of Shade on Water: A Tub Study

J. Moore, J. Miner and R. Bower
Department of Bioresource Engineering
Oregon State University - 1999

Two tanks with equal volumes of water and similar initial temperatures were insulated on the sides and bottom. One was exposed to August solar radiation, while the other was completely shaded. Results are presented in the graph below.

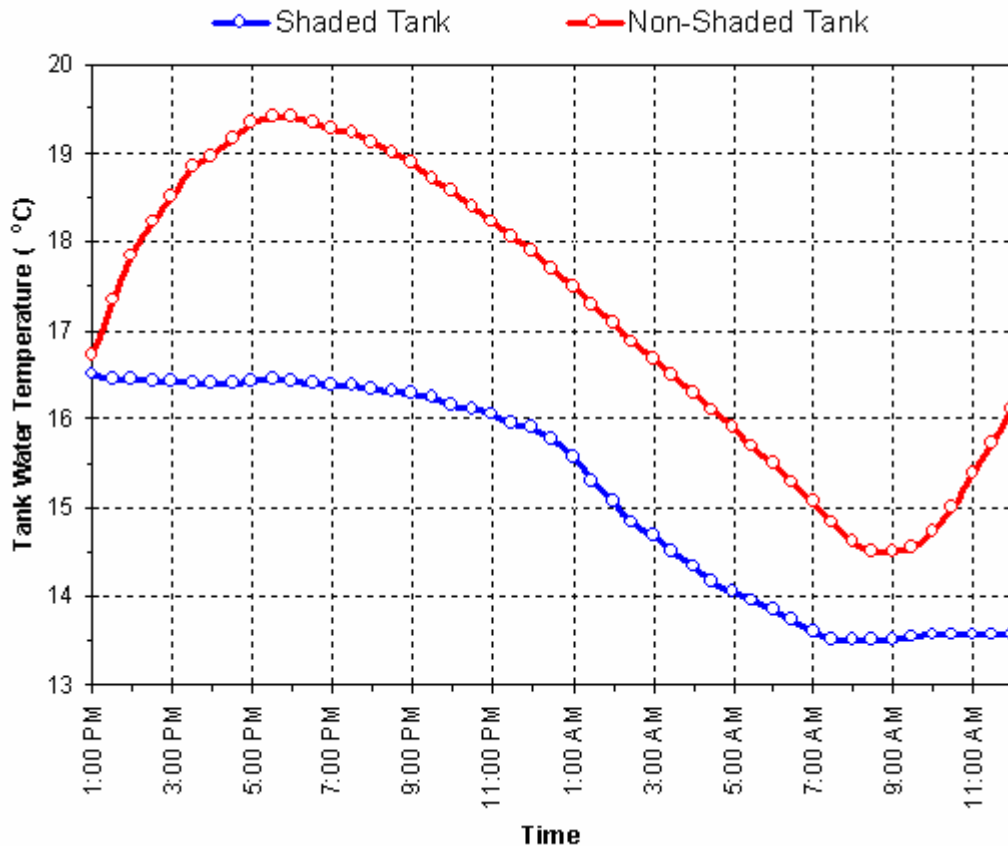


FIGURE 1.3
Solar Radiation 'Tub' Study: Effect of Shade on Water is Apparent (Moore et al. 1999)

Petersen et al. (1999) closely monitored central Oregon irrigation ditches in control and shaded test conditions and found that shade overwhelmingly influenced flowing water heating rates. Of particular importance was the discovery that even small increases in shade produced measurable decreases in water temperature. The study also found that air temperature is a minor thermal parameter.

The Impact of Shade on the Temperature of Running Water

B. Petersen, T. Stringham and W. Krueger
Department of Rangeland Resources
Oregon State University - 1999

Results

"Shade from tarps provided a significant amount of protection from additional heating of the water at all shade levels tested... affirms the importance of even small amounts of shade in moderating stream heating."

Conclusion

"At the scale of this study, air temperature appears to have a minor impact on the temperature of water. The dominant factor seemed to be solar radiation."

In the Upper Grande Ronde River, remotely sensed TIR stream temperature data and effective shade comparisons mimic the results found by Moore et al. (1999) and Petersen et al. (1999). Lack of shade corresponds to increased rates of stream temperature heating, while moderate increases in effective shade correspond to lower rates of stream heating (see **Figure 1.4**). While we should always start discussions of stream temperature with an acknowledgement of complexity, simply matching observed (measured) thermal responses to theoretical science can serve as a powerful method of assessment.



Poor shade results from near stream vegetation removal and is compounded by channel morphology response to near stream vegetation removal (Vey Meadow, Grande Ronde River, Oregon)

With this context, the TIR and instream temperature data was collected for the Grande Ronde River on August 4, 1999. From the TIR data (flown around 4:00 PM) it is apparent that stream temperatures are warmer at the end of the meadow by roughly 3°C where shade levels are very low (near zero) when compared to the upstream temperatures entering the meadow. Stream heating is moderated by increased shade levels (20% to 40%) in the forested downstream reach. Further, a close inspection of the graph reveals corresponding cooler temperatures associated with minor increases in shade levels. This observation fits well with the accepted body of science; the literature supports the theory that shade has a moderating effect upon stream temperatures.

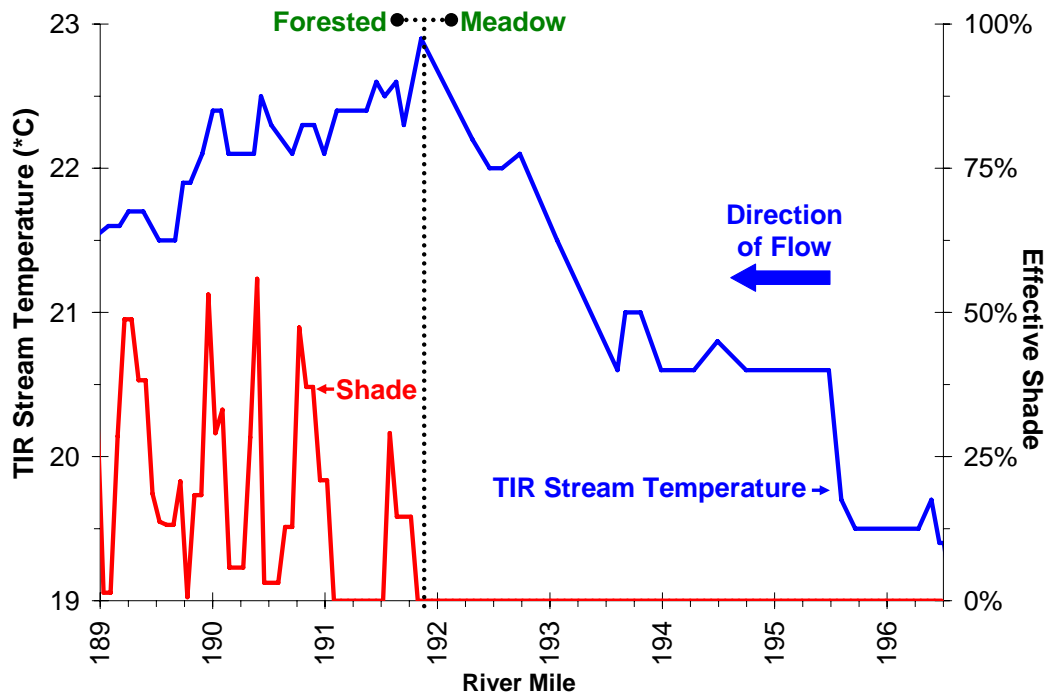


FIGURE 1.4

TIR derive stream temperature data and effective shade modeling indicate that 3°C stream heating corresponds to reduced shade distributions. Reduced rates of stream heating are apparent in the shaded (forested) downstream reach (Vey Meadow, Grande Ronde River, Oregon).

Terminology used to describe the observed thermal response can be complex, and rather academic. Terms such as ‘cooling’ and ‘heating’ imply a change over distance or time. The temporal change in temperature should be referred to as a ‘rate’. The spatial change in temperature should be referred to as a ‘gradient’. For example, in the meadow (unshaded) reach, the above plot shows a 0.6°C change per river mile and 1.3°C change per hour. In the forested (shaded) reach, the above plot shows a -0.4°C change per river mile and 1.2°C change per hour. By definition, the meadow reach has a heating gradient and the forested reach has a cooling gradient. Both reaches have rates of heating

(over the time period 8:00 to 16:00), however, the rate of heating is less in the forested reach than in the meadow reach.

This discussion of semantics is necessary simply because the terms heating and cooling are used so frequently without reference to the dimension (space or time) over which the change is occurring. Statements are often made that shade cannot cool water, but instead, shade only reduces stream warming. Such a generalization is true as long as the dimension of change is time. Spatial representations of shade-induced stream temperature change can, however, represent cooling gradients (see **Figure 1.5**). It becomes easy to see that as streams heat over time at variable rates, that actual temperatures at specific locations will be different. With this background, the temperature change over distance will likely represent cooling gradients in shaded stream reaches. In this context the generalization that shade does not cool water is in fact incorrect, overly simple and poorly defined.

Aside from the terminology of heating and cooling, we do not want to lose focus of the primary finding represented in the temperature and shade comparison. The lack of shade correlates to warmer stream temperatures. This finding is consistent with the literature and theoretical constructs of stream temperature dynamics.

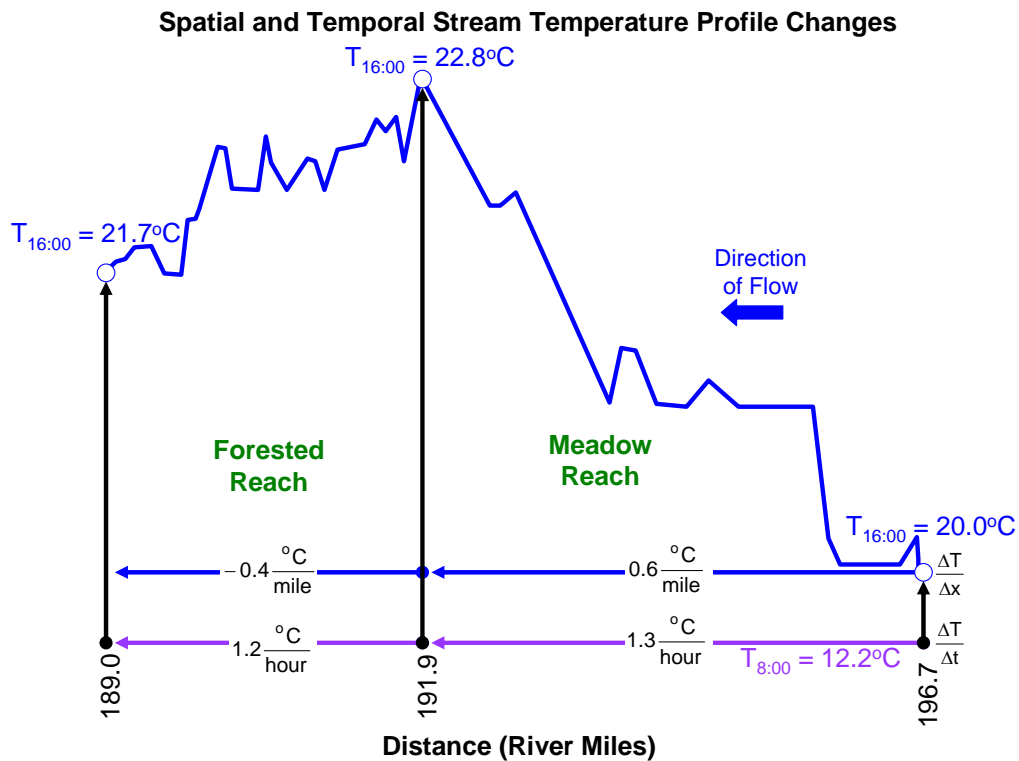
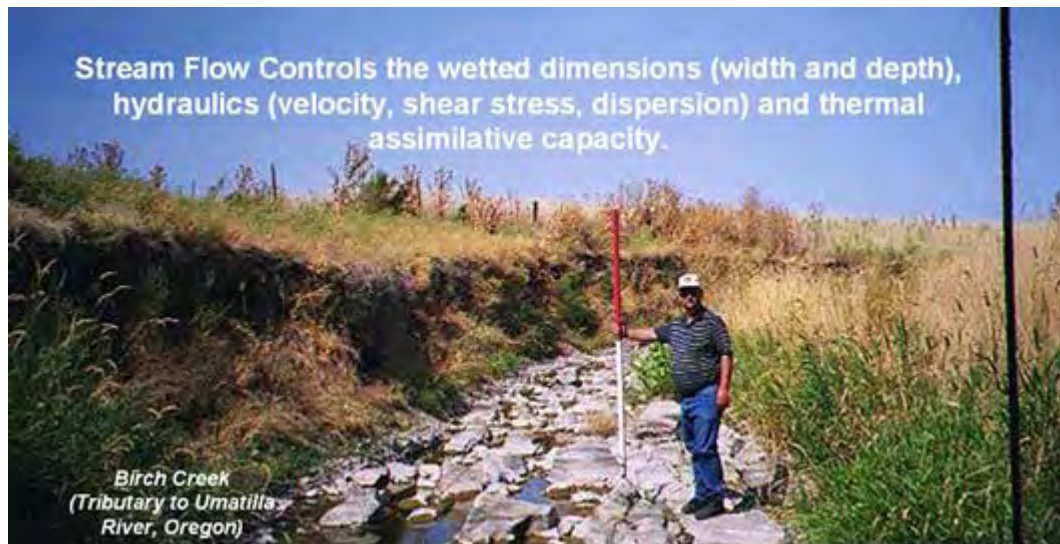


FIGURE 1.5
 Rates of temperature change over time and distance (Vey Meadow, Grande Ronde River, Oregon).

STREAM FLOW MODIFICATIONS

The simple relationship presented by Brown (1969) ($\Delta T_w \propto \frac{\Delta \text{Heat}}{\text{Volume}}$) demonstrates that large volume streams are less responsive to temperature change, and conversely, low flow streams will exhibit greater temperature sensitivity (and greater rates of stream temperature change). Specifically, stream flow volume will affect the wetted channel dimensions (width and depth), flow velocity (and travel time) and the thermal assimilative capacity³. *Human related reductions in flow volume can have a significant influence on stream temperature dynamics, most likely increasing diurnal variability in stream temperature.*

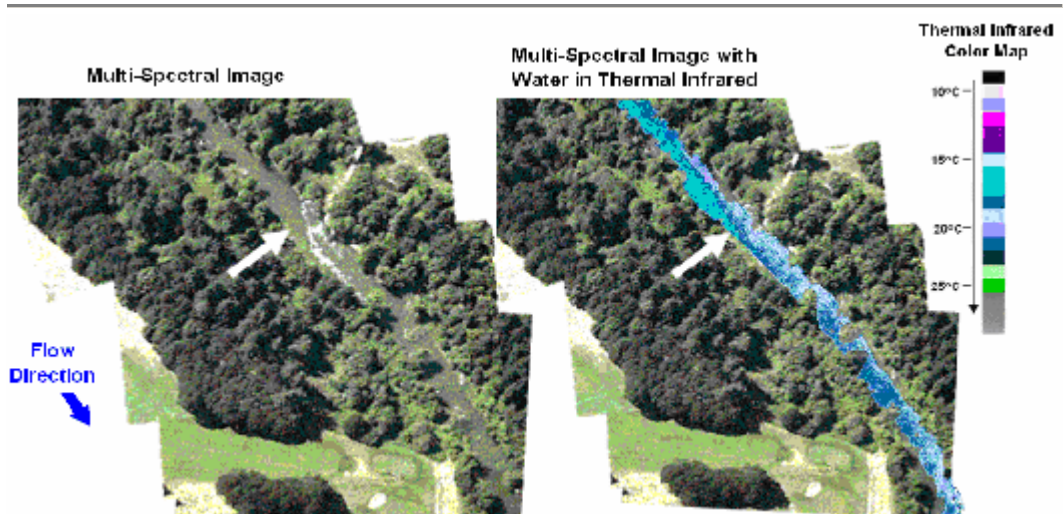


Beyond the simple conception of reduced flow and corresponding reduced thermal assimilative capacity, flow modifications can be highly complex in nature. Diversions can reroute surface waters through irrigation systems of various efficiencies. Often a portion of irrigated water returns to the stream system at some down gradient location. For example, diversions route water (over varying distances) in canals and irrigation systems causing an immediate decrease in instream flow volume. A secondary effect is that the portion of irrigation flows returned to the stream system is often very warm, further increasing instream temperatures. Remotely sensed TIR stream temperature data is particularly suited to detecting these warmed return flows.

Other important considerations include altered instream hydraulics and wetted channel dimensions. Flow velocity and travel times are highly related to flow volume. Reduced flow velocity will translate to reduced shear stress and dispersion, which result in obvious changes water column mixing. A well mixed stream segment may become poorly mixed or stratified when flow volumes and corresponding flow velocities are reduced from instream withdrawals or natural low flow conditions.

³ The thermal assimilative capacity refers to an amount of heat a water column can receive to meet a desired condition (i.e. temperature).

1.2.2 POINT SOURCES OF STREAM WARMING



Multi-Spectral and thermal infrared radiometry (TIR) of a point source discharge and mixing zone measure the direct thermal effect (Tualatin River, Oregon). The warm waste water discharge (22°C) is located at the white arrow and is received into 17.4°C river water.

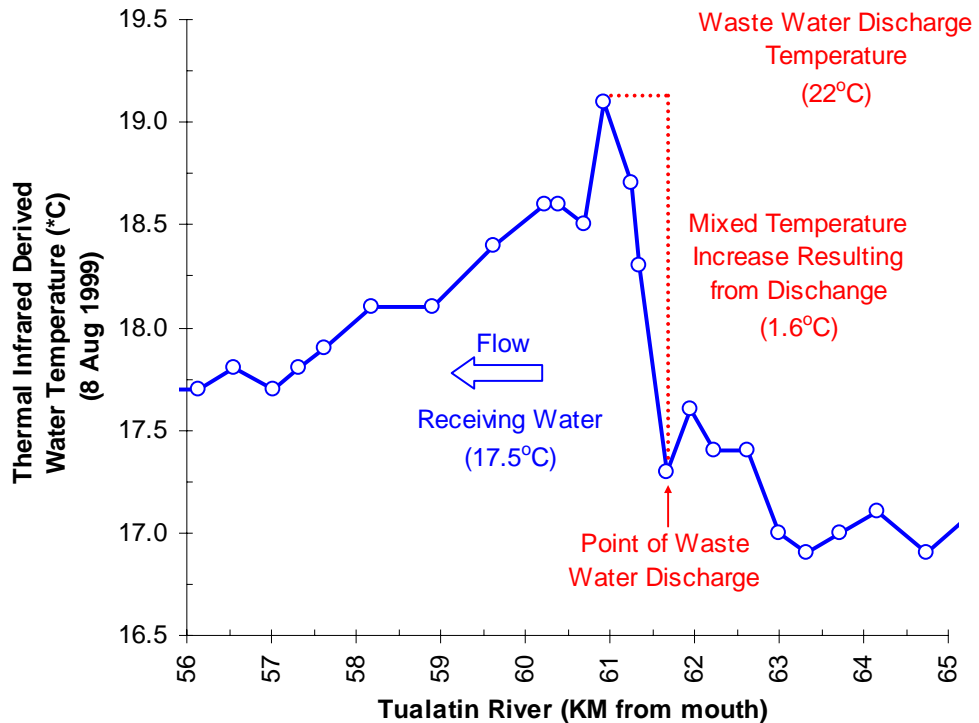


FIGURE 1.6
 Measured TIR data indicates a 1.6°C increase in water temperature after complete mix (Tualatin River, Oregon).

The discharge of waste water into receiving waters can affect a thermal change if the two waterbodies have different temperatures. The receiving waters will change heat as a function of thermal differences and mass transfer from point sources. Associated temperature changes resulting from a discharge (after complete mixing with the receiving water) will have a more profound thermal effect when mass transfer rates are large and the temperature of the point source is different than the receiving water. It is important to keep in mind that most stream and river temperatures have daily and seasonal temperature fluctuations, while point source discharges tend to remain fairly constant. Therefore, the thermal effect of a point source on a receiving waterbody will also follow a diurnal cycle, with maximum thermal effects occurring when the receiving water and stream temperatures are most dissimilar (typically at night in the diurnal cycle or seasonally in winter).

1.2.3 NATURAL SOURCES OF STREAM WARMING AND COOLING

Stream and river temperatures are dynamic over large spatial scales, regardless of anthropogenic activities and human sources of heating/cooling. Dynamic temperature change rates and gradients are reflective of variable background conditions. And, the temporal variability in natural background hydrology, land cover succession and morphology combine to create a complex and somewhat dynamic background thermal condition. The thermal background condition is a range instead of a static condition.

Natural sources that may elevate stream temperature above background conditions include scouring effects on morphology and floodplain vegetation, drought, fires, insect damage to near stream land cover, diseased near stream land cover and windthrow and blowdown in riparian areas. The processes in which natural sources affect stream temperatures include increased stream surface exposure to heat transfer processes, altered microclimates and flow modifications. Legacy morphology conditions and land cover distributions can sometimes be caused by natural disturbances. Overall, the extent of natural disturbances on near stream land cover, channel morphology and hydrology is not well documented and complicated by geologic time scales.

Factors that cool streams and rivers that are of non-human origin can be broken into mass and heat transfer sources. Conditions that reduce radiant heat exposure will prevent or reduce rates of stream heating, and in some cases reduce stream heating rates and gradients. Such conditions include the persistent effects of shade produced from riparian vegetation, stream surface area reduction via healthy equilibrium morphology, and cool near stream microclimates that occur in well vegetated riparian corridors. There are also episodic cooling effects that reduce radiant heat exposure such as cloudiness (or any other form of vapor and particulate matter in the overlaying air mass) and cool air temperatures that reduce thermal radiation emission from the atmosphere, vegetation and topography that is received by a stream.

Natural mass transfers of inflow (tributaries, springs, etc.) can obviously heat and cool the receiving water. Typically subsurface water is cooler than surface water. Cooler subsurface waters tend to come from deeper ground water sources and snowmelt sources. Shallow groundwater and hyporheic flows typically have warmer temperatures relative to deep cold subsurface sources of flow. As with any generalization, there are exceptions. And, no generalizations

can be made when considering the effects of surface inflows and confluences since each stream system and waterbody has a unique thermal behavior. To the extent that tributaries and subsurface flows are unaffected by human activities, an argument can be made that changes from some mass transfers reflect background conditions.

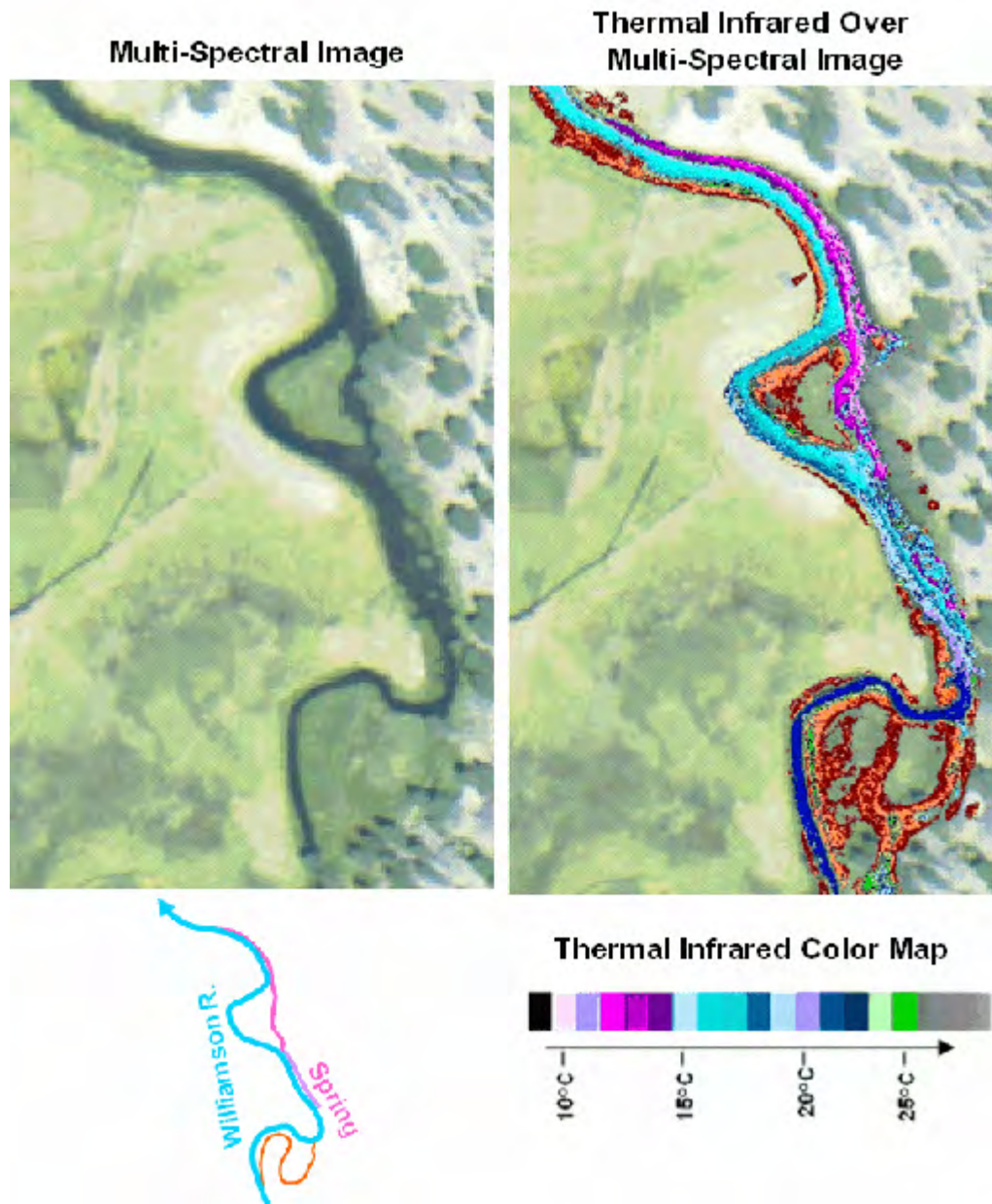


FIGURE 1.7
Subsurface inflows can significantly cool streams and rivers.

1.3 MODEL APPLICATION: SCOPE, SCALE & CUMULATIVE EFFECTS

"Cumulative effects are those effects on the environment that result from the incremental effect of the action when added to past, present and reasonably foreseeable future actions... Cumulative effects can result from individually minor but collectively significant actions taking place over a period of time".

- *Forest Ecosystem Management: An Ecological, Economic and Social Assessment. Report of the Forest Ecosystem Management Assessment Team*

Analytical methods listed in this paper allow dynamic simulation of both heat and mass transfer. Applications include open channel flows, distributed stream networks, wetlands and large rivers systems. An obvious limitation is one-dimensional flow routing. This methodology does not include vertical temperature variations, but instead, simulates an average water column temperature. This methodology is intended to simulate variable longitudinal temperature gradients and temporal rate changes as a function of physically based formulae to meet regulatory, agency and academic modeling needs. As with any analytical model, the application (including spatial and temporal scales) is determined at the discretion of the user, largely as a function of the model application.

Stream temperature changes result from upstream and local conditions. Incremental increases can combine to create relatively warm stream temperatures. Water has a relatively high heat capacity ($c_p = 10^3 \text{ cal kg}^{-1} \text{ K}^{-1}$) (Satterlund and Adams 1992). Conceptually, water is a heat sink. Heat energy that is gained by the stream is retained and only slowly released back to the surrounding environment. Any given measurement of stream temperature is the result of a multitude of processes occurring upstream, as well as those processes acting at the site of measurement. For this reason it is important to consider stream temperature at a stream network scale.

In its current form, Heat Source is developed to simulate temperatures for three weeks for any period of a year. The only limitation to the simulation duration is output storage. Future modifications will include an output storage file that will allow longer simulation periods.

By design, this methodology will simulate complex mass and heat transfers over very large scales, at a very high resolution ($\approx 1:5,000$ scale). Limitations to scale and resolution will largely depend on the complexity of the system and data quality. It is recommended that users derive spatial data sets from high resolution and accurate GIS and remotely sensed data, using the methods outlined in this document.

Operation of the model should include acknowledgements of data quality and quantity, a statement of assumptions and statistical validation (with measured data) of simulation results. Users should be reminded that methodologies for heat and mass transfer are largely physically based. When model output is inaccurate, it is a common practice to 'calibrate' the model with calibration parameters. By design, few calibration parameters are incorporated in this methodology, with the exception being the mass transfer term for evaporation rates. Evaporation varies regionally and warrants user calibration (a and b)

parameters. However, it is the author's opinion that most forms of model inaccuracy result from poor data input quality/quantity, rather than model algorithm error. Users should consider that inaccurate model results may signal a problem with data inputs. It is the experience of the authors that high resolution and accurate data inputs facilitate straight forward model operation and accurate simulation results.

1.4 SALMONID LIFE STAGE THERMAL RANGES

Salmonids and some amphibians are highly sensitive to temperature. In particular, bull trout (*Salvelinus confluentus*) are among the most temperature sensitive of the cold water fish species in the Pacific Northwest. Water temperature protective benchmarks usually employ logic that relies on using *indicator species*, which are the most sensitive. If temperatures are protective of *indicator species*, other species will share in this level of protection.

If water temperatures become too hot, fish die almost instantaneously due to denaturing of critical enzyme systems in their bodies (Hogan, 1970). The ultimate *instantaneous lethal limit* occurs in high temperature ranges (upper-90°F). Such warm temperature extremes are rare natural aquatic systems. More common and widespread are summertime water temperatures in the mid-70°F range (mid- to high-20°C range). These temperatures cause death of cold-water fish species during exposure times lasting a few hours to one day. The exact temperature at which a cold water fish succumbs to such a thermal stress depends on the temperature that the fish is acclimated, as well as, particular development life-stages. This cause of mortality, termed the *incipient lethal limit*, results from breakdown of physiological regulation of vital processes such as respiration and circulation (Heath and Hughes, 1973). The most common and widespread cause of thermally induced fish mortality is attributed to interactive effects of decreased or lack of metabolic energy for feeding, growth or reproductive behavior, increased exposure to pathogens (viruses, bacteria and fungus), decreased food supply (impaired macroinvertebrate populations) and increased competition from warm water tolerant species. This mode of thermally induced mortality, termed indirect or *sub-lethal*, is more delayed, and occurs weeks to months after the onset of elevated temperatures in the mid-60°F to low-70°F (17.8°C - 22°C).

The temperature needs of aquatic organisms are used largely as a primary design criterion for water temperature regulatory programs. Summertime temperatures tend to target sub-lethal ranges (see table below).



Cold water fish population protection and rehabilitation is the primary purpose for stream temperature assessments and modeling. Conclusions based on analytical outputs should relate back to salmonid life stage thermal ranges.

Table 1.2
 Modes of Thermally Induced Cold Water Fish Mortality
 (Brett 1952, Bell 1986, Hokanson et al. 1977)

Modes of Thermally Induced Fish Mortality	Temperature Range	Time to Death
<i>Instantaneous Lethal Limit</i> – Denaturing of bodily enzyme systems	> 90°F > 32°C	Instantaneous
<i>Incipient Lethal Limit</i> – Breakdown of physiological regulation of vital bodily processes, namely: respiration and circulation	72°F - 77°F 22°C - 25°C	Hours to Days
<i>Sub-Lethal Limit</i> – Conditions that cause decreased or lack of metabolic energy for feeding, growth or reproductive behavior, encourage increased exposure to pathogens, decreased food supply and increased competition from warm water tolerant species	64°F – 72°F 17.8°C - 22°C	Weeks to Months

Chapter

II

Heat Transfer

Description of Processes, Analytical Methods and Finite Difference Approximation



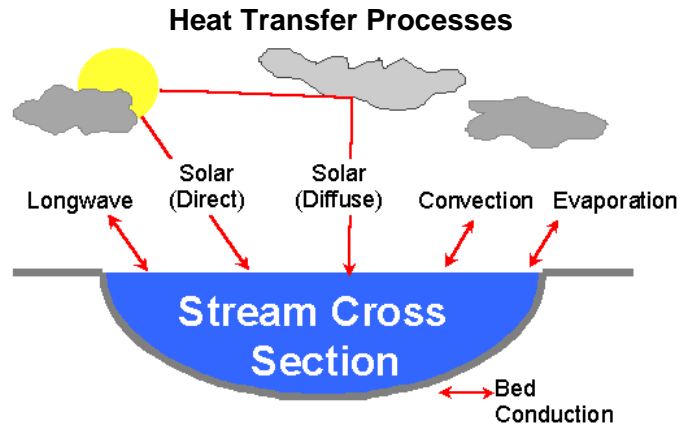
The ultimate source of terrestrial and atmospheric heat energy is solar radiation (images from SOHO telescope and Apollo 17 mission).

2.1 OVERVIEW

Stream temperature change is an expression of heat exchange between a stream and its environment. The heat transfer processes that control stream temperature include solar radiation (Φ_{solar}), longwave (thermal) radiation (Φ_{longwave}), streambed conduction ($\Phi_{\text{streambed}}$), stream/air convection⁴ ($\Phi_{\text{convection}}$) and evaporation ($\Phi_{\text{evaporation}}$) (Wunderlich 1972, Jobson and Keefer 1979, Beschta and Weathered 1984, Sinokrot and Stefan 1993, Boyd 1996). Hence, the net heat energy flux (Φ_{total}) consists of summation of these heat transfer processes. With the exception of solar radiation, which only delivers heat energy, these

⁴ Air/Water convection includes both turbulent and free surface conduction.

processes are capable of both introducing and removing heat from a stream. Stream shade is an important regulator of shortwave radiation heat transfer to a stream that can create significant instream temperature increases (i.e. by 1°C or more) over spatial scales ranging from a stream segment (i.e. ≈1 km) to the watershed scale (Brown 1969, Beschta and Weatherred, 1984, Boyd 1996).



Net Heat Energy Continuity,

$$\Phi_{\text{total}} = \Phi_{\text{solar}} + \Phi_{\text{longwave}} + \Phi_{\text{evaporation}} + \Phi_{\text{convection}} + \Phi_{\text{streambed}} \quad (2-1)$$

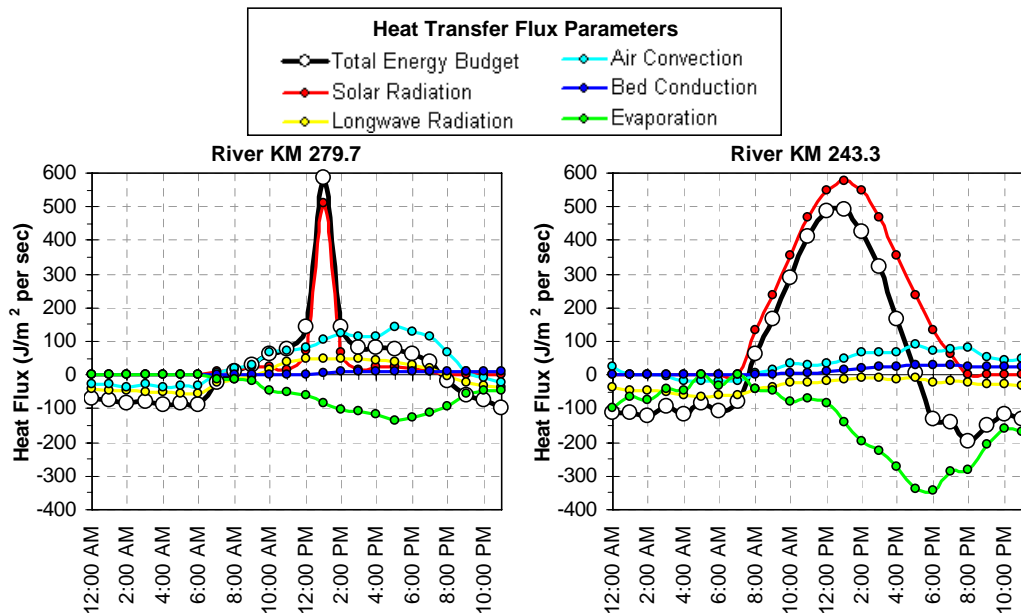


FIGURE 2.1
 Heat Transfer Terms (Grande Ronde River, Oregon - August 20, 1999). Note the variability between sites, the temporal variability and the combined effect (i.e. total energy budget term) of the five heat transfer mechanisms.

The ultimate source of heat energy to a stream is solar radiation (both diffuse and direct). Secondary sources of heat energy include longwave radiation, from the atmosphere and near stream vegetation, streambed conduction and in some cases, groundwater exchange at the water-substrate interface. Several processes dissipate heat energy at the air-water interface, namely: evaporation, convection and back radiation. Heat energy is acquired by the stream system when the flux of heat energy entering the stream is greater than the flux of heat energy leaving. The net heat energy flux provides the rate at which energy is gained or lost per unit area and is represented as the instantaneous summation of all heat energy components (see Equation 2-1). Examples of heat transfer processes developed for the Grande Ronde River in ODEQ (2000) are presented in **Figure 2.1**.

2.2 SOLAR RADIATION: Φ_{SOLAR}

Water column solar radiation exposure rates can be simulated at a various scales (stream segment to landscape scales) with prediction algorithms and methods. Stream surface shade production is a function of geometric relationships between the predictable nature of the sun's position and topography, near stream land cover and morphology. Provided an accurate location description (i.e. latitude and longitude), the exact position of the sun for any given time can be simulated as a function of time (i.e. season and time of day). Topographic, land cover and/or stream channel features that obstruct the sun→stream vector create shade. Opaque features that obstruct solar radiation, such as topography and channel banks, completely attenuate received direct beam and diffuse solar radiation. The atmospheric air mass and land cover exhibits some level of transparency and these bodies only partially attenuate received direct beam and diffuse solar radiation. Routing the direct solar beam through these partially transparent mediums results in attenuation and scattering of only portions of the direct beam and diffuse solar flux. Diffuse solar radiation is received from all directions above a stream surface, and will penetrate to the stream through openings in canopy. While shade is occurring, there is still light penetrating to the stream derived from diffuse sources. Shading algorithms mimic the travel direction of photons from the sun to the stream for both direct beam and diffuse solar radiation.

Radiation penetration through the water surface is largely a function of solar altitude and transmission through the water column is more of a function of water column depth. Water column turbidity will also alter attenuation and scattering, and thus the water transmission of radiation.

The stream bed will reflect a portion of received solar radiation as a function of received radiation, solar altitude and substrate properties. All radiant heat that is absorbed by the stream bed is treated separately in the stream bed conduction heat transfer pathway. Radiation reflected from the stream bed is subjected to the same path length and transmission rates through the water column experienced from the surface to the stream bed.

2.2.1 SOLAR TIME RELATIVE TO EARTH

*All expressions presented in this section are taken from Meeus (1988 and 1991).
 Definition of terminology taken largely from The Astronomical Almanac⁵ (1998)*

The Gregorian calendar time corrected for daylight savings refers to the calendar introduced by Pope Gregory XIII in 1582 to replace the Julian calendar. Every year that is exactly divisible by four is a leap year (except for centurial years, which instead must be divisible by 400 to be leap years). By this definition, the year 2000 is a leap year.

Daylight Savings Corrected Time⁶,

$$t_{\text{DST}} = t + \frac{1}{24} \text{ hours} \quad (2-2)$$

Greenwich mean time is the corresponding time in Greenwich, England, calculated as a function of daylight savings time and the time zone correction factor.

Greenwich Mean Time,

$$t_{\text{GMT}} = t_{\text{DST}} + \frac{t_{\text{zone}}}{24 \text{ hours}} \quad (2-3)$$

Table 2.1
 Time Zone Correction and Meridian as a Function of Time Zone

United States Time Zone Name	Time Zone Correction Factor (t_{zone})	Central Meridian
East	5 hours	-75°
Central	6 hours	-90°
Mountain	7 hours	-105°
Pacific	8 hours	-120°

The Julian day is commonly used to calculate solar parameters as a continuous numeric expression of calendar day. The Julian (ephemeris) date is then converted in Julian centuries (units of 36525 ephemeris days) from the epoch 1900 January 0.5 ET. Julian centuries are calculated since epoch 1900 January 0.5 ET (this time variable will be used heavily in calculating the earth's position).

Julian Day,

$$t_{\text{JD}} = \text{INT}[365.25 \cdot (Y + 4716)] + \text{INT}[30.6001 \cdot (M + 1)] + D + B - 1524.5 \quad (2-4)$$

⁵ United States Government Printing Office. [The Astronomical Almanac for the Year 1998](#). Washington, DC: Navy Dept., Naval Observatory, Nautical Almanac Office.

⁶ If the date is between the first Sunday in April and the last Sunday in October then a correction for daylight savings time is made.

where,

$$A = \text{INT}\left(\frac{Y}{100}\right) \quad B = 2 - A + \text{INT}\left(\frac{A}{4}\right)$$

Julian Century,

$$t_{\text{JDC}} = \frac{[(t_{\text{JD}} + t_{\text{GMT}}) - 2451545]}{36525} \quad (2-5)$$

Variables,

Measured/Known

- D: Day of Month (1 to 31)
- M: Month (1 to 12)
- t: Time (day fraction)
- t_{zone}: Time Zone (see Table 2.1)
- Y: Year (If month is less than 2, then Y = Year-1)

Calculated

- t_{JD}: Julian days since epoch 1900 January 0.5 ET
 - t_{JDC}: Julian centuries since epoch 1900 January 0.5 ET
 - t_{DST}: Daylight Savings Time (day fraction)
 - t_{GMT}: Greenwich Mean Time (day fraction)
-

2.2.2 SOLAR POSITION RELATIVE TO EARTH

*All expressions presented in this section are taken from Meeus (1988 and 1991).
 Definition of terminology taken largely from The Astronomical Almanac (1998)*

The mean plane of the Earth's orbit around the Sun is called the elliptic. Obliquity refers to the angle between the equatorial and orbital planes of the Earth, which is equivalently between the rotational and orbital poles. Specifically, for the Earth, the obliquity of the ecliptic is the angle between the planes of the equator and the ecliptic. The obliquity of the elliptic is a function of the mean obliquity (θ_{OB}) and time measured in Julian centuries (t_{JDC}).

Mean Obliquity of the Elliptic (degrees),

$$\theta_{\text{OB}} = 23 + \frac{\left[26 + \frac{S}{60}\right]}{60} \quad (2-6)$$

where,

$$S = 21.448 - t_{\text{JDC}} \cdot (46.815 + t_{\text{JDC}} (0.00059 - (t_{\text{JDC}} \cdot 0.001813)))$$

Obliquity of the Elliptic (degrees),

$$\theta_{\text{OB}} = \theta_{\text{OB}} + 0.00256 \cdot \text{Cos}\left(125.04 - 1934.136 \cdot t_{\text{JDC}} \cdot \frac{\pi}{180^\circ}\right) \quad (2-7)$$

Eccentricity is a parameter that specifies the shape of a conic section, which is one of the standard elements used to describe an elliptic orbit (position and motion of the Earth's orbit). The eccentricity (E_C) of the Earth's orbit relative to the earth-sun distance is calculated as a function of time measured in Julian centuries (t_{JDC}). The eccentric anomaly accounts for an undisturbed elliptic motion as the angle measured at the center of the ellipse from pericenter to the point on the circumscribing auxiliary circle from which a perpendicular to the major axis would intersect the orbiting body.

Earth's Eccentricity of Orbit,

$$E_C = 0.016708634 - t_{JDC} \cdot (0.000042037 + 0.0000001267 \cdot t_{JDC}) \quad (2-8)$$

The angular distance of the solar sphere (sun) is measured eastward along the ecliptic from the dynamical equinox to the circle passing through the poles of the ecliptic and the sun. The term geometric mean refers to the average geometric position, which can be conceptualized as the geocentric position of an object on the celestial sphere (which is the true equator and equinox, but without the displacement due to planetary aberration). Therefore a geometric mean of the longitude describes the geocentric position as the Earth's mean equator and equinox of a standard epoch (on the celestial sphere) centered at the Sun. A mean position is determined by removing the effects of refraction, geocentric and stellar parallax, and stellar aberration from the directly observed position, and by referring to the coordinates to the mean equator and equinox of a standard epoch. The geometric mean of the longitude of the sun ($\theta_{\overline{LS}}$) is a function of time measured in Julian centuries (t_{JDC}).

Geometric Mean of the Longitude of the Sun ($0 \geq \theta_{\overline{LS}} \leq 360$),

$$\theta_{\overline{LS}} = 280.46646 + t_{JDC} \cdot (36000.76983 + 0.0003032 \cdot t_{JDC}) \quad (2-9)$$

The geocentric position of the anomaly ($\theta_{\overline{AS}}$) is an angular measurement of the Earth in its orbit from its perihelion (the point at which the Earth most closely approaches the sun) and is calculated as a function of time measured in Julian centuries (t_{JDC}).

Geometric Mean of Anomaly of the Sun (degrees),

$$\theta_{\overline{AS}} = 357.52911 + t_{JDC} \cdot (35999.05029 - 0.0001537 \cdot t_{JDC}) \quad (2-10)$$

Variables,

Calculated

- E_C : Eccentricity of Earth's Orbit (unitless)
 - $\theta_{\overline{AS}}$: Geometric Mean of Anomaly of the Sun (degrees)
 - $\theta_{\overline{LS}}$: Geometric Mean of the Longitude of the Sun (degrees)
 - $\theta_{\overline{OB}}$: Mean Obliquity of the Elliptic (degrees)
 - θ_{OB} : Obliquity of the Elliptic (degrees)
 - t_{JDC} : Julian centuries since epoch 1900 January 0.5 ET
-

Consider a celestial sphere as an imaginary sphere of arbitrary radius upon which celestial bodies (in this case Earth) may be located (the celestial sphere is centered at the observer's position). The equation of center of the Sun (θ_{CS}) is calculated as a function of the geometric mean of anomaly of the sun ($\theta_{\overline{AS}}$) and time measured in Julian centuries (t_{JDC}).

Equation of Center of the Sun (degrees),

$$\theta_{CS} = B \cdot [1.914602 - t_{JDC} \cdot (0.004817 + 0.000014 \cdot t_{JDC})] + C \cdot (0.019993 - 0.000101 \cdot t_{JDC}) + D \cdot 0.000289 \quad (2-11)$$

where,

$$A = \left(\theta_{\overline{AS}} \cdot \frac{\pi}{180^\circ} \right) \quad B = \sin(A) \quad C = \sin(B \cdot 2) \quad D = \sin(C \cdot 3)$$

The true longitude of the Sun (θ_{LS}) is the sum of the geometric mean of the longitude of the Sun ($\theta_{\overline{LS}}$) and the equation for the center of the Sun (θ_{CS}).

True Longitude of the Sun (degrees),

$$\theta_{LS} = \theta_{\overline{LS}} + \theta_{CS} \quad (2-12)$$

The true longitude of the Sun (θ_{LS}), centered at the Earth, is determined by removing any topocentric effects of the observer from the directly observed longitude of the Sun. True solar longitude is predicted as a function of time measured in Julian centuries (t_{JDC}).

Apparent Longitude of the Sun (degrees),

$$\theta_{AL} = \theta_{LS} - 0.00569 \cdot \left[0.00478 \cdot \sin \left((125.04 - 1934.136 \cdot t_{JDC}) \cdot \frac{\pi}{180^\circ} \right) \right] \quad (2-13)$$

Variables,

Calculated

- θ_{AL} : Apparent Longitude of the Sun (degrees)
 - $\theta_{\overline{AS}}$: Geometric Mean of Anomaly of the Sun (degrees)
 - θ_{CS} : Equation of the Center of the Sun (degrees)
 - θ_{LS} : True Longitude of the Sun (degrees)
 - $\theta_{\overline{LS}}$: Geometric Mean of the Longitude of the Sun (degrees)
 - t_{JDC} : Julian centuries since epoch 1900 January 0.5 ET
-

The angular distance on the celestial sphere north or south of the celestial equator is measured along the hour circle passing through the celestial object. Declination is usually given in combination with right ascension or hour angle and can be visualized as the latitude at which the sun is directly overhead (Dingman 2002). The earth tilts on its axis, causing the solar declination to vary regularly

between -23.5° and 23.5° . Solar declination (δ) is calculated as a function of the obliquity of the elliptic (θ_{OB}) and the apparent longitude of the sun (θ_{AL}).

Solar Declination (degrees),

$$\delta = \text{Sin}^{-1} \left[\text{Sin} \left(\theta_{OB} \cdot \frac{\pi}{180^\circ} \right) \cdot \text{Sin} \left(\theta_{AL} \cdot \frac{\pi}{180^\circ} \right) \right] \cdot \frac{180^\circ}{\pi} \quad (2-14)$$

The true anomaly of the Sun (θ_{SA}) is the sum of the geometric mean of the longitude of the Sun (θ_{LS}) and the equation for the center of the Sun (θ_{CS}).

Solar True Anomaly (degrees),

$$\theta_{TA} = \theta_{AS} + \theta_{CS} \quad (2-15)$$

The distance to the sun, or radius vector (P), is a function of eccentricity of the Earth's Orbit (E_C) and the true anomaly of the Sun (θ_{SA}) and is measured in AU⁷ units.

Solar Radius Vector,

$$P = \frac{1.000001018 \cdot (1 - E_C^2)}{1 + E_C \cdot \text{Cos} \left(\theta_{TA} \cdot \frac{\pi}{180^\circ} \right)} \quad (2-16)$$

The Equation of time (E_t) is the hour angle of the true position of the sun minus the hour angle of the fictitious mean position of the sun. It can also be explained as the apparent solar time minus mean solar time. The equation of time is calculated as a fairly complex expression below.

Equation of time (minutes),

$$E_t = 4 \cdot \left(A \cdot B - 2 \cdot E_C \cdot C + 4 \cdot + 4 \cdot E_C \cdot A \cdot C \cdot D - \frac{1}{2} \cdot A^2 \cdot E - \frac{4}{3} \cdot E_C^2 \cdot F \right) \cdot \frac{180^\circ}{\pi} \quad (2-17)$$

where,

$$\begin{aligned} A &= \left[\tan \left(\theta_{OB} \cdot \frac{\pi}{360^\circ} \right) \right]^2 & B &= \text{Sin} \left(2 \cdot \theta_{LS} \cdot \frac{\pi}{180^\circ} \right) & C &= \text{Sin} \left(\theta_{AS} \cdot \frac{\pi}{180^\circ} \right) \\ D &= \text{Cos} \left(2 \cdot \theta_{LS} \cdot \frac{\pi}{180^\circ} \right) & E &= \text{Sin} \left(4 \cdot \theta_{LS} \cdot \frac{\pi}{180^\circ} \right) & F &= \text{Sin} \left(2 \cdot \theta_{AS} \cdot \frac{\pi}{180^\circ} \right) \end{aligned}$$

The apparent solar time is a measure of time based on the diurnal motion of the true Sun. The rate of diurnal motion undergoes seasonal variation because of the obliquity of the ecliptic and because of the eccentricity of the Earth's orbit. Additional small variations result from irregularities in the rotation of the Earth on its axis. Solar time (t_s) is calculated as a function of the daylight savings time

⁷ **Astronomical unit (AU)** is the radius of a circular orbit in which a body of negligible mass, and free of perturbations, would revolve around the Sun in $2\pi/k$ days, where k is the Gaussian gravitational constant. This is slightly less than the semi major axis of the Earth's orbit.

(t_{DST}), equation of time (E_t), longitudinal position (on earth), longitude (θ_{long}), time zone (t_{zone}) and of time measured in Julian centuries (t_{JDC}).

Solar Time (minutes),

$$t_s = [60 \cdot h] + m + \left[\frac{s}{60} \right] + E_t - 4 \cdot \theta_{long} + 60 \cdot t_{zone} \quad (2-18)$$

Hour angle is the angular distance on the Earth's sphere measured westward along the equator from the meridian to the hour circle. The hour angle (θ_{HA}) is calculated solely as a function of solar time (t_s).

Hour Angle ($0^\circ \geq \theta_{HA} \leq 360^\circ$),

$$\theta_{HA} = \frac{t_s}{4} - 180 \quad (2-19)$$

Variables,

Measured/Known

- h: Hour based on daylight savings time (hr)
- m: Minute based on daylight savings time (min)
- s: Second based on daylight savings time (sec)
- t_{zone} : Time Zone (see Table 2.1)
- θ_{long} : Longitude (degrees)

Calculated

- δ : Solar Declination (degrees)
 - E_C : Eccentricity of Earth's Orbit (unitless)
 - E_t : Equation of Time (minutes)
 - θ_{AL} : Apparent Longitude of the Sun (degrees)
 - θ_{AS} : Geometric Mean of Anomaly of the Sun (degrees)
 - θ_{CS} : Equation of the Center of the Sun (degrees)
 - θ_{HA} : Hour Angle (degrees)
 - θ_{LS} : Geometric Mean of the Longitude of the Sun (degrees)
 - θ_{OB} : Obliquity of the Elliptic (degrees)
 - θ_{TA} : Solar True Anomaly (degrees)
 - P: Solar Radius Vector (AU)
 - t_s : Solar Time (minutes)
-

2.2.3 SOLAR POSITION RELATIVE TO STREAM POSITION

The uncorrected solar zenith refers to the point at which the sun is directly overhead of the Earth's sphere. The geocentric solar zenith is defined by the line from the center of the Earth through the observer. The uncorrected solar distance ($\theta_{SZ'}$) is the angular distance on the Earth's sphere measured along the great circle from the zenith to the sun calculated as a function of solar declination (δ), latitude (θ_{lat}), and hour angle (θ_{HA}). It may be easier to conceptualize the solar zenith as the angular distance 90° minus solar altitude. The solar altitude is a measure of the angular distance of the sun above or below the horizon, measured along the great circle passing through the Earth and the zenith angle. And, solar altitude is 90° minus the solar zenith angle. Refraction refers to the change in direction of travel (bending) of a light ray as it passes obliquely through the atmosphere. As a result of refraction, the observed altitude of a celestial object is greater than its geometric altitude. The amount of refraction depends on the altitude of the object and on atmospheric conditions. The solar zenith and altitude comprise the vertical position of the sun relative to the stream segment.

Solar Zenith (Corrected for Refraction),

$$\theta_{SZ} = \theta_{SZ'} - C_R \quad (2-20)$$

Solar Altitude (Corrected for Refraction),

$$\theta_{SA} = 90^\circ - \theta_{SZ} \quad (2-21)$$

Solar Zenith - Uncorrected for Refraction (Ibqal 1983),

$$\theta_{SZ'} = \text{Cos}^{-1}(A) \cdot \frac{180^\circ}{\pi} \quad (2-22)$$

where ($-1 \leq A \leq 1$),

$$A = \text{Sin}\left(\theta_{lat} \cdot \frac{\pi}{180^\circ}\right) \cdot \text{Sin}\left(\delta \cdot \frac{\pi}{180^\circ}\right) + \text{Cos}\left(\theta_{lat} \cdot \frac{\pi}{180^\circ}\right) \cdot \text{Cos}\left(\delta \cdot \frac{\pi}{180^\circ}\right) \cdot \text{Cos}\left(\theta_{HA} \cdot \frac{\pi}{180^\circ}\right)$$

Atmospheric Elevation⁸ (Ibqal 1983),

$$\alpha = 90^\circ - \theta_{SZ'} \quad (2-23)$$

⁸ Atmospheric elevation is simply the solar altitude uncorrected for refraction

Refraction Correction Coefficient (C_R)⁹,

If $\alpha > 85^\circ$ then,

$$C_R = 0^\circ$$

If $5^\circ > \alpha \leq 85^\circ$ then,

$$C_R = \frac{\frac{58.1}{\alpha \cdot \frac{\pi}{180^\circ}} - \frac{0.07}{\left(\alpha \cdot \frac{\pi}{180^\circ}\right)^3} + \frac{0.000086}{\left(\alpha \cdot \frac{\pi}{180^\circ}\right)^5}}{3600^\circ}$$

If $-0.575 > \alpha \leq 5^\circ$ then,

$$C_R = \frac{1735 + \alpha \cdot (-518.2 + \alpha \cdot (103.4 + \alpha \cdot (-12.79 + \alpha \cdot 0.711)))}{3600^\circ}$$

If $\alpha \leq -0.575$ then,

$$C_R = \frac{-20.774}{\tan\left(\alpha \cdot \frac{\pi}{180^\circ}\right) \cdot 3600^\circ}$$

(2-24)

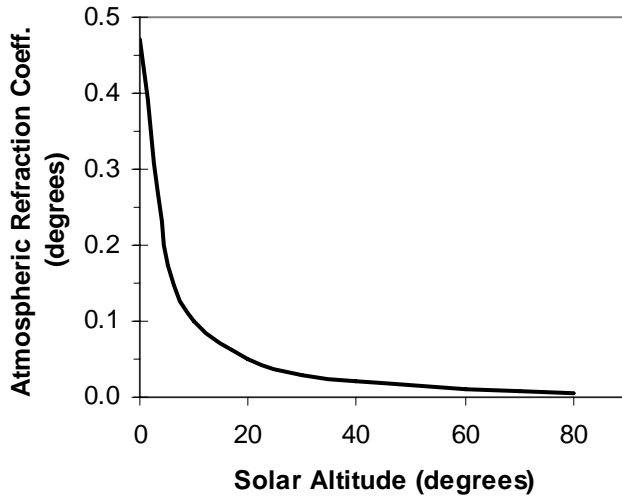


FIGURE 2.2
 Calculated Refraction
 Correction Coefficient (C_R)
 Values Based in Equation 2-
 24.

Solar azimuth is the angular distance measured clockwise along the horizon from a specified location (stream segment) to the intersection with the great circle drawn from the zenith through a body on the celestial sphere. The solar azimuth comprises the horizontal position of the sun relative to the stream segment.

Solar Azimuth (Ibqal 1983) ($0^\circ > \theta_{AZ} \leq 360^\circ$),

$$\theta_{AZ} = \frac{\sin\left(\theta_{lat} \cdot \frac{\pi}{180^\circ}\right) \cdot \cos\left(\theta_{SZ} \cdot \frac{\pi}{180^\circ}\right) - \sin\left(\delta \cdot \frac{\pi}{180^\circ}\right)}{\cos\left(\theta_{lat} \cdot \frac{\pi}{180^\circ}\right) \cdot \sin\left(\theta_{SZ} \cdot \frac{\pi}{180^\circ}\right)} \quad (2-25)$$

⁹ Taken from NOAA Surface Radiation Branch (<http://www.srb.noaa.gov/highlights/sunrise/azel.html>)

Variables,

Measured/Known

θ_{lat} : Latitude (degrees)

Calculated

α : Atmospheric Elevation (degrees)
 C_R : Refraction Coefficient (degrees)
 δ : Solar Declination (degrees)
 θ_{AZ} : Solar Azimuth (degrees)
 θ_{HA} : Hour Angle (degrees)
 θ_{SA} : Solar Altitude (degrees)
 θ_{SZ} : Solar Zenith – Uncorrected (degrees)
 θ_{SZ} : Solar Zenith – Corrected (degrees)

2.2.4 SOLAR RADIATION HEAT ABOVE TOPOGRAPHIC FEATURES

Once emitted from the sun, photons travel through space to the outer edge of the atmosphere, at an average vertical intensity referred to as the *solar constant*. The solar constant is approximately 1367 W/m² (Dingman 2002). The radius vector (r) is the ratio of the actual distance to the mean distance between the Earth and sun and is required for the calculation of extraterrestrial global solar radiation (Φ_{SRG}).

Global Solar Radiation Flux at the Edge of the Atmosphere (Wunderlich 1972),

$$\Phi_{\text{SRG}} = \frac{\Phi_{\text{SRC}}}{r^2} \sin \theta_{\text{SA}} \quad (2-26)$$

Solar Constant (Dingman 2002),

$$\Phi_{\text{SRC}} = 1367 \frac{\text{W}}{\text{m}^2} \quad (2-27)$$

Radius Vector (Wunderlich 1972),

$$r = 1 + 0.017 \cdot \cos\left(2 \cdot \frac{\pi}{365}\right) \cdot \left(186 - \text{JD} + \frac{t_{\text{DST}}}{24}\right) \quad (2-28)$$

While passing through the atmosphere solar radiation is absorbed and scattered by ozone, water vapor, dry air and particulate (McCutcheon 1989). The flux of direct beam solar radiation that traverses the atmospheric air mass must account for attenuation and scattering induced by atmospheric transmissivity (T_A) and cloudiness (C_L) along an instantaneous path length, estimated as the optical air mass thickness (M_A).

Direct Beam Solar Radiation above Topographic Features – Estimate (Wunderlich 1972, Martin and McCutcheon 1999),

$$\Phi_{\text{SRB}} = \Phi_{\text{SRG}} \cdot T_A^{M_A} \cdot (1 - 0.65 \cdot C_L^2) \quad (2-29)$$

Atmospheric Transmissivity (Ibqal 1983),

$$T_A = 0.0685 \cdot \cos \left[\left(2 \cdot \frac{\pi}{365} \right) \cdot (JD + 10) \right] + 0.8 \quad (2-30)$$

Optical Air Mass Thickness (Ibqal 1983),

$$M_A = \frac{35 \cdot e^{(-0.0001184 \cdot Z_s)}}{\sqrt{1224 \cdot \sin \left(\theta_{SA} \cdot \frac{\pi}{180^\circ} \right) + 1}} \quad (2-31)$$

Direct Beam Solar Radiation above Topographic Features (Chen 1994)

$$\Phi_{SRB1} = \Phi_{SRB} \cdot (1 - D_F) \quad (2-32)$$

Diffuse Solar Radiation above Topographic Features (Chen 1994)

$$\Phi_{SRD1} = \Phi_{SRB} \cdot D_F \quad (2-33)$$

Clearness Index (Chen 1994),

$$C_I = \frac{\Phi_{SRB}}{\Phi_{SRG}} \quad (2-34)$$

Diffuse Fraction (Chen 1994),

$$D_F = (0.938 + 1.071 \cdot C_I) - (5.14 \cdot C_I^2) + (2.98 \cdot C_I^3) - \left(\sin \left(2\pi \cdot \frac{(JD - 40)}{365} \right) \right) \cdot (0.009 - 0.078 \cdot C_I) \quad (2-35)$$

Variables,

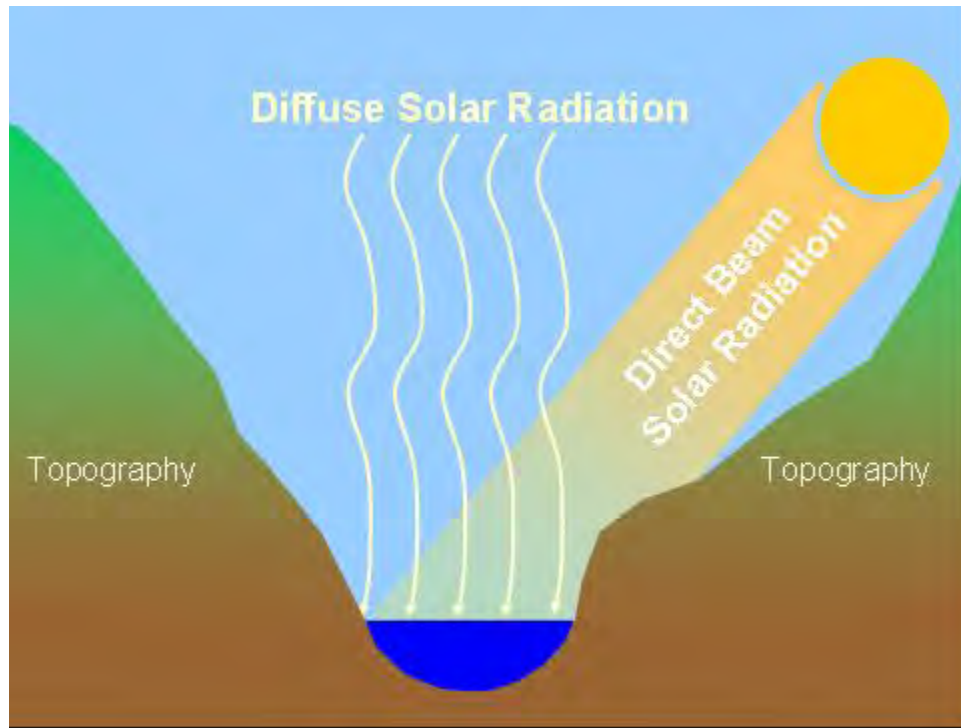
Measured/Known

- C_L: Cloudiness (0 to 1)
- Φ_{SRC}: Solar Constant ($\frac{W}{m^2}$)
- JD: Julian Day (1 to 365)
- t_{DST}: Daylight Savings Time (day fraction)
- Z_s: Stream Elevation (m)

Calculated

- C_I: Clearness Index
 - D_F: Diffuse Fraction of Solar Radiation
 - Φ_{SRB}: Direct Beam Solar Radiation Estimate above Topography ($\frac{W}{m^2}$)
 - Φ_{SRB1}: Direct Beam Solar Radiation above Topography ($\frac{W}{m^2}$)
 - Φ_{SRD1}: Diffuse Solar Radiation above Topography ($\frac{W}{m^2}$)
 - Φ_{SRG}: Global Solar Flux ($\frac{W}{m^2}$)
 - M_A: Air Mass Thickness
 - θ_{SA}: Solar Altitude (degrees)
 - r: Radius Vector (radians)
 - T_A: Air Mass Transmissivity
-

2.2.5 SOLAR RADIATION HEAT BELOW TOPOGRAPHIC FEATURES



In the direction from the sun to the water column, the first encountered potential opaque barrier to direct beam and diffuse solar radiation is often a topographic feature. If the solar altitude (θ_{SA}) is greater than the topographic shade angle¹⁰, then the stream is not shaded from direct beam solar radiation by the surrounding topography. When localized topographic shading is occurring, the direct beam solar radiation is assumed to be zero. Regardless of whether topographic shading is occurring, diffuse solar radiation is reduced in proportion to the horizon that is obscured by topography.

Direct Beam Solar Radiation below Topographic Features (Position 2)

When topographic shade is occurring ($\theta_{SA} \leq \theta_{Tz}$),

$$\Phi_{SRB2} = 0 \quad (2-36)$$

When topographic shade is not occurring ($\theta_{SA} > \theta_{Tz}$),

$$\Phi_{SRB2} = \Phi_{SRB1} \quad (2-37)$$

Diffuse Solar Radiation below Topographic Features (Position 2)

$$\Phi_{SRD2} = \Phi_{SRD1} \cdot \frac{(\theta_{Tw} + \theta_{Ts} + \theta_{Te})}{270^\circ} \quad (2-38)$$

¹⁰ Topographic shade angle: the angle between the center point of the stream and the highest topographic feature. This measurement is performed in 90° intervals for the 360° representing all solar azimuth angles (i.e. west, south and east). The topographic shade angle that is closest to the solar azimuth is used in the model to determine whether topographic shade is occurring.

Variables,

Measured/Known

θ_{T_w} : Topographic Shade Angle – West (degrees)

θ_{T_s} : Topographic Shade Angle – South (degrees)

θ_{T_e} : Topographic Shade Angle – East (degrees)

Calculated

Φ_{SRB1} : Direct Beam Solar Radiation above Topography ($\frac{W}{m^2}$)

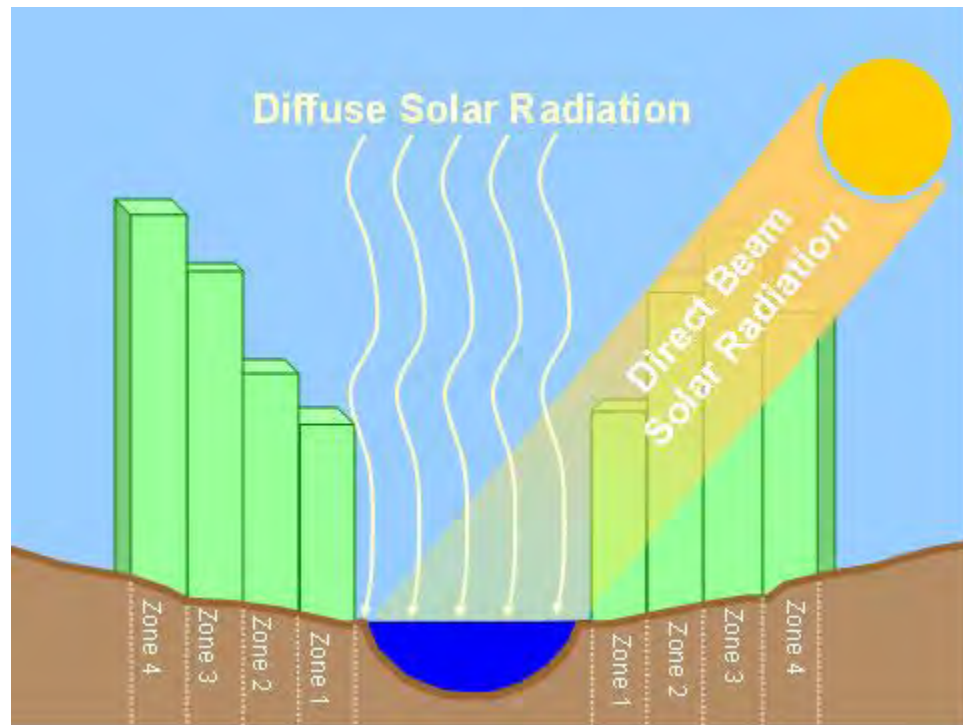
Φ_{SRD1} : Diffuse Solar Radiation above Topography ($\frac{W}{m^2}$)

Φ_{SRB2} : Direct Beam Solar Radiation below Topography ($\frac{W}{m^2}$)

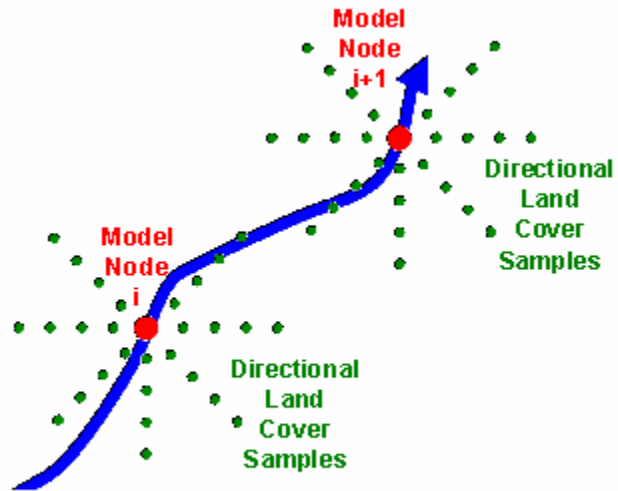
Φ_{SRD2} : Diffuse Solar Radiation below Topography ($\frac{W}{m^2}$)

2.2.6 SOLAR RADIATION HEAT BELOW LAND COVER

Land cover physical attributes (height, overhanging distance and density) are used as model inputs. These data are sampled using TTools in four consecutive zones for seven directions (northeast, east, southeast, south, southwest, west, northwest). Direct beam and diffuse solar radiation is routed through these land cover zones and canopy openings. Direct beam radiation is routed through land cover zones in the direction (i.e. southwest = aspect 225°) closest to the solar azimuth (i.e. solar azimuth = 231°). Routing occurs from the outermost land cover zone (zone 4) to the innermost zone (zone 1).



Shadows that are cast from each land cover zone are calculated as a function of solar altitude and azimuth, in addition to the physical attributes of the land cover and terrain elevation. If the shadow length spans the width of the stream then the stream is shaded. This methodology is based on simulation of the sun → stream vector, and it follows that positional information for both the sun and stream require highly accurate description and analytical methodology. When stream surface shade is determined to be occurring, direct beam attenuation occurs as a function of a light extinction coefficient and the path length through the land cover zone. The path length through the land cover zone is a function of zone width, stream aspect, solar altitude and solar azimuth. Attenuation is calculated using Beer's Law (Oke, 1978). Direct beam radiant energy that passes through a land cover zone is then routed to the next inner land cover zone and the process is repeated. Once through all four land cover zones, the remaining direct beam solar radiation is routed to the stream bank elevation (Position 4). Diffuse solar radiation filters through the openings in land cover and is attenuated as a function of canopy opening, estimated with view to sky and canopy density values for each model node.



Example of land Cover Sampling Performed by TTools and Used as Model Input in Heat Source

Direct Beam Solar Radiation below Land Cover (Position 3):

Step 1. Shadow Length (SL_{LC}) for land cover zones is a function of the sampled land cover height (H_{LC}) and stream bank elevation (Z_{LC}) for each direction and zone, and the solar altitude (θ_{SA}).

For Zone = 4 To 1 Step -1

$$SL_{LC}(\text{Zone}) = \frac{H_{LC}(\text{Zone}) + Z_{LC}(\text{Zone})}{\tan\left(\theta_{SA} \cdot \frac{\pi}{180^\circ}\right)}$$

Next Zone

Visual Basic Code

(2-39)

Step 2. If the shadow length (SL_{LC}) from the zone in question is greater than distance to the center of the stream, then shade is occurring. The path length (PL_{LC}) over which the direct beam must travel through the land cover zone is calculated as a function of the zone width (W_{LC}) and the solar altitude (θ_{SA}). Shade density (Ψ_{LC}) is then calculated as a function of vegetation density (VD) and the path length over which the direct beam must travel through the land cover zone (Zone).

For Zone = 4 To 1 Step -1

If $SL_{LC}(Zone) \geq W(Zone) \cdot Zone$ then

$$PL_{LC}(Zone) = \frac{W_{LC}(Zone)}{\cos\left(\theta_{SA} \cdot \frac{\pi}{180^\circ}\right)}$$

$$\Psi_{LC}(Zone) = 1 - \exp\left(\frac{\log(1 - VD(Zone))}{10} \cdot PL_{LC}(Zone)\right)$$

Else

$$PL_{LC}(Zone) = 0: \Psi_{LC}(Zone) = 0$$

End If

Next Zone

Visual Basic Code (2-40)

Step 3. Direct beam solar radiation is then calculated for each of the land cover zones from the outer most zone to the inner land cover zone as a function of the shade density (Ψ) and the direct beam solar flux leaving the previous zone (A).

$$A = \Phi_{SRB2}$$

For Zone = 4 To 1 Step -1

$$A = A \cdot (1 - \Psi_{LC}(Zone))$$

Next Zone: $\Phi_{SRB3} = A$

Visual Basic Code (2-41)

Diffuse Solar Radiation below Riparian Vegetation (Position 3)

Diffuse solar radiation penetrating below the land cover (Φ_{SRD3}) is calculated as a function of the view to sky (θ_{VTS}) and the diffuse radiation above riparian vegetation (Φ_{SRD2}).

$$\Phi_{SRD3} = \Phi_{SRD2} \cdot \theta_{VTS} \quad (2-42)$$

Variables,

Measured/Known

- H_{LC} : Land Cover Height for each Zone (m)
- VD : Land Cover Density (unitless)
- W_{LC} : Land Cover Zone Width (m)
- Z_{LC} : Ground Elevation Above Stream Surface for each Zone (m)
- Zone: Land Cover Zone

Calculated

- Φ_{SRB2} : Direct Beam Solar Radiation below Topography ($\frac{W}{m^2}$)
 - Φ_{SRD2} : Diffuse Solar Radiation below Topography ($\frac{W}{m^2}$)
 - Φ_{SRB3} : Direct Beam Solar Radiation below Land Cover ($\frac{W}{m^2}$)
 - Φ_{SRD3} : Diffuse Solar Radiation below Land Cover ($\frac{W}{m^2}$)
 - Ψ_{LC} : Land Cover Shade Density (unitless)
 - θ_{SA} : Solar Altitude (degrees)
 - θ_{VTS} : View to Sky (unitless)
 - PL_{LC} : Direct Beam Path Length through each land cover zone (m)
 - SL_{LC} : Shadow Length Cast from each Zone (m)
-

2.2.6 SOLAR RADIATION HEAT ABOVE STREAM SURFACE

To account for shade cast from a stream bank or a near stream topographic feature, the shadow length (SL_{SB}) originating from topography on the appropriate stream bank is calculated for each of the land cover zones. If the bank is shading the stream surface, then the direct beam flux is completely attenuated.

Direct Beam Solar Radiation below Stream Banks,

For Zone = 4 To 1 Step -1

$$SL_{SB}(\text{Zone}) = \frac{Z_{LC}(\text{Zone})}{\tan\left(\theta_{SA} \cdot \frac{\pi}{180^\circ}\right)}$$

If $SL_{SB}(\text{Zone}) \geq W_{LC}(\text{Zone}) \cdot \text{Zone}$ then

$$\Phi_{SRB4} = 0$$

Else

$$\Phi_{SRB4} = \Phi_{SRB3}$$

End If

Next Zone

Visual Basic Code (2-43)

Diffuse Solar Radiation below Stream Banks,

$$\Phi_{SRD4} = \Phi_{SRD3} \tag{2-44}$$

If there are types of emergent vegetation (vegetation growing in the water column and emerging over the stream surface) then shading from this vegetation is also calculated as a function of path length (PL_{LC}) and vegetation density (VD).

Direct Beam Solar Radiation below Emergent Vegetation,

$$PL_{LC}(0) = \frac{H_{LC}(0)}{\sin\left(\theta_{SA} \cdot \frac{\pi}{180^\circ}\right)}$$

If $PL_{LC}(0) > W_W$ then $PL_{LC}(0) = W_W$

$$\Psi_{LC}(0) = 1 - \exp\left(\frac{\log(1 - VD(0))}{10} \cdot PL_{LC}(0)\right)$$

$$\Phi_{SRB4} = \Phi_{SRB4} \cdot (1 - \Psi_{LC}(0))$$

Visual Basic Code (2-45)

Diffuse Solar Radiation below Emergent Vegetation,

$$PL_{LC}(0) = H_{LC}(0)$$

$$\Psi_{LC}(0) = 1 - \exp\left(\frac{\log(1 - VD(0))}{10} \cdot PL_{LC}(0)\right)$$

$$\Phi_{SRD4} = \Phi_{SRD4} \cdot (1 - \Psi_{LC}(0))$$

Visual Basic Code (2-46)

Variables,

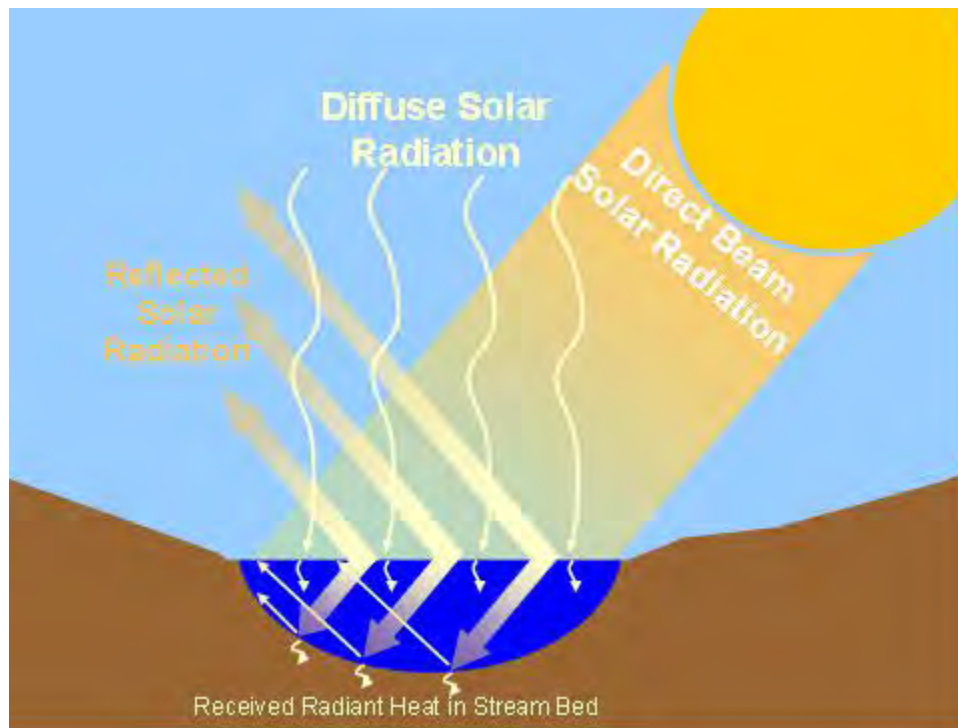
Measured/Known

- H_{LC} : Emergent Vegetation Height (m)
- VD : Emergent Vegetation Density (unitless)
- W_{LC} : Land Cover Zone Width (m)
- Z_{LC} : Ground Elevation Above Stream Surface for each Zone (m)
- Zone: Land Cover Zone

Calculated

- Φ_{SRB3} : Direct Beam Solar Radiation below Land Cover ($\frac{W}{m^2}$)
- Φ_{SRD3} : Diffuse Solar Radiation below Land Cover ($\frac{W}{m^2}$)
- Φ_{SRB4} : Direct Beam Solar Radiation above Stream Surface ($\frac{W}{m^2}$)
- Φ_{SRD4} : Diffuse Solar Radiation above Stream Surface ($\frac{W}{m^2}$)
- θ_{SA} : Solar Altitude (degrees)
- PL_{ZONE} : Direct Beam Path Length through each Zone (m)
- SL_{ZONE} : Shadow Length Cast from each Zone (m)
- W_W : Stream Surface Width (m)
- Ψ_{LC} : Emergent Vegetation Shade Density (unitless)

2.2.7 SOLAR RADIATION HEAT PENETRATING THE STREAM SURFACE



A portion of solar radiation is reflected from the stream surface as a function of reflection, also known as the stream surface albedo, and calculated as a function of the angle of incidence upon the surface. Surface reflection of direct beam solar radiation is calculated from the solar zenith angle (θ_{SZ}) and an assumed 9% reflection rate applies for diffuse solar radiation (Sellers 1965). The portion of solar radiation that is not reflected enters the water column.

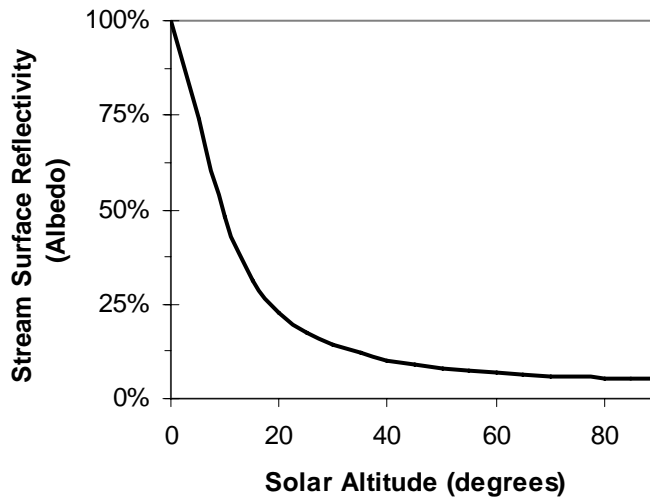


FIGURE 2.3
Calculated Surface Reflection (R_{SS}) Values
Calculated from Equation 2-47.

Stream Surface Reflectivity (Sellers 1965),

If $\theta_{SZ} > 80^\circ$ then

$$R_{SS} = 0.0515 \cdot \left(\theta_{SZ} \cdot \frac{\pi}{180^\circ} \right) - 3.636$$

Elseif $\theta_{SZ} \leq 80^\circ$ then

$$R_{SS} = 0.091 \cdot \left[\cos \left(\theta_{SZ} \cdot \frac{\pi}{180^\circ} \right) \right]^{-1} - 0.0386$$

End If

Visual Basic Code (2-47)

Direct Beam Solar Radiation Penetrating the Stream Surface,

$$\Phi_{SRB5} = \Phi_{SRB4} \cdot (1 - R_{SS}) \quad (2-48)$$

Direct Beam Solar Radiation Penetrating the Stream Surface,

$$\Phi_{SRD5} = \Phi_{SRD4} \cdot 0.91 \quad (2-49)$$

Variables,

Calculated

Φ_{SRB4} : Direct Beam Solar Radiation above Stream Surface ($\frac{W}{m^2}$)

Φ_{SRD4} : Diffuse Solar Radiation above Stream Surface ($\frac{W}{m^2}$)

Φ_{SRB5} : Direct Beam Solar Radiation Penetrating Stream Surface ($\frac{W}{m^2}$)

Φ_{SRD5} : Diffuse Solar Radiation Penetrating Stream Surface ($\frac{W}{m^2}$)

θ_{SZ} : Solar Zenith (degrees)

R_{SS} : Stream Surface Reflectivity (unitless)

2.2.8 SOLAR RADIATION HEAT RECEIVED BY WATER COLUMN AND SUBSTRATE

Upon penetrating the water surface, the portion of the received direct beam solar radiation absorbed by the water column is a function path length (PL_W) and the transmissivity (T_W) of the water column, which in turn, are calculated from the solar angle (θ_{SA}) and average water depth (\bar{d}_W). Solar radiation is received at the stream bed and absorbed as a function of solar angle and literature values for reflectivity properties of quartz (Beschta and Weathered, 1984). Heat absorbed by the streambed will cause differential heating and become part of the substrate↔water column conduction pathway. The remaining portion of solar direct beam radiation is reflected from the stream bed and travels towards the surface of the water column, where again there is absorption of solar radiation as a function of path length and stream transmissivity.

Solar Radiation Flux Attenuated in Water Column,

$$\Phi_{\text{solar}} = \Phi_{\text{SR6}} = \Phi_{\text{SRB6}} + \Phi_{\text{SRD6}} \quad (2-50)$$

Solar Radiation Flux Attenuated in Stream Bed,

$$\Phi_{\text{SR7}} = \Phi_{\text{SRB7}} + \Phi_{\text{SRD7}} \quad (2-51)$$

DIRECT BEAM SOLAR RADIATION ROUTING THROUGH WATER COLUMN

Direct Beam Solar Radiation Water Column Path Length (Jerlov 1976),

$$PL_W = \frac{\bar{d}_W}{\text{Cos} \left[\text{Sin}^{-1} \left[\frac{\text{Sin} \left(\theta_{\text{SZ}} \cdot \frac{\pi}{180^\circ} \right)}{1.333} \right] \right]} \quad (2-52)$$

Transmissivity of Water for Direct Beam Solar Radiation (Austin and Halikas 1976),

$$T_W^B = 0.415 - (0.194 \cdot \text{Log}_{10}(PL_W)) \quad (2-53)$$

Stream Bed Reflectivity (Beschta and Weathered 1984 adopted from Sellers 1965),

$$R_{\text{SB}}^B = \text{Exp} \left(0.0214 \cdot \left(\theta_{\text{SZ}} \cdot \frac{\pi}{180^\circ} \right) - 1.941 \right) \quad (2-54)$$

Direct Beam Solar Radiation Attenuated from Surface to Stream Bed,

$$A1 = \Phi_{\text{SRB5}} \cdot (1 - T_W^B) \quad (2-55)$$

Direct Beam Solar Radiation Reaching Stream Bed,

$$A2 = \Phi_{\text{SRB5}} - A1 \quad (2-56)$$

Direct Beam Solar Radiation Absorbed in Stream Bed,

$$A3 = A2 \cdot (1 - R_{\text{SB}}^B) \quad (2-57)$$

Direct Beam Solar Radiation Absorbed in Stream Bed and Immediately Returned to Water Column as Heat,

$$A4 = A3 \cdot 0.53 \cdot (1 - \eta) \quad (2-58)$$

Direct Beam Solar Radiation Reflected from Stream Bed,

$$A5 = A2 \cdot R_{\text{SB}}^B \quad (2-59)$$

Direct Beam Solar Radiation Attenuated from Stream Bed to Surface,

$$A6 = A5 \cdot (1 - T_W^B) \quad (2-60)$$

Direct Beam Solar Radiation Attenuated in Water Column,

$$\Phi_{\text{SRB6}} = A1 + A4 + A6 \quad (2-61)$$

Direct Beam Solar Radiation Attenuated in Stream Bed,

$$\Phi_{\text{SRB7}} = A3 - A4 \quad (2-62)$$

DIFFUSE SOLAR RADIATION ROUTING THROUGH WATER COLUMN

Transmissivity of Water for Diffuse Solar Radiation (adopted from Austin and Halikas 1976),

$$T_W^D = 0.415 - \left(0.194 \cdot \text{Log}_{10}(\bar{d}_W)\right) \quad (2-63)$$

Stream Bed Reflectivity (adopted from Beschta and Weathered 1984),

$$R_{\text{SB}}^D = \text{Exp}\left(0.0214 \cdot \left(0^\circ \cdot \frac{\pi}{180^\circ}\right) - 1.941\right) \quad (2-64)$$

Diffuse Solar Radiation Attenuated from Surface to Stream Bed,

$$B1 = \Phi_{\text{SRD5}} \cdot \left(1 - T_W^D\right) \quad (2-65)$$

Diffuse Solar Radiation Reaching Stream Bed,

$$B2 = \Phi_{\text{SRD5}} - B1 \quad (2-66)$$

Diffuse Solar Radiation Absorbed in Stream Bed,

$$B3 = B2 \cdot \left(1 - R_{\text{SB}}^D\right) \quad (2-67)$$

Diffuse Solar Radiation Flux Absorbed in Stream Bed and Immediately Returned to Water Column as Heat,

$$B4 = B3 \cdot 0.53 \cdot (1 - \eta) \quad (2-68)$$

Diffuse Solar Radiation Flux Reflected from Stream Bed,

$$B5 = B2 \cdot R_{\text{SB}}^D \quad (2-69)$$

Diffuse Solar Radiation Flux Attenuated from Stream Bed to Surface,

$$B6 = B5 \cdot \left(1 - T_W^D\right) \quad (2-70)$$

Diffuse Solar Radiation Flux Attenuated in Water Column,

$$\Phi_{\text{SRD6}} = B1 + B4 + B6 \quad (2-71)$$

Diffuse Solar Radiation Flux Attenuated in Stream Bed,

$$\Phi_{\text{SRD7}} = B3 - B4 \quad (2-72)$$

Variables,

Measured/Known

η : Porosity of the Stream Bed (unitless)

Calculated

\bar{d}_W : Average Water Column Depth (m)

Φ_{SRB5} : Direct Beam Solar Radiation Penetrating Stream Surface ($\frac{W}{m^2}$)

Φ_{SRD5} : Diffuse Beam Solar Radiation Penetrating Stream Surface ($\frac{W}{m^2}$)

Φ_{SRB6} : Direct Beam Solar Radiation Attenuated in Water Column ($\frac{W}{m^2}$)

Φ_{SRD6} : Diffuse Solar Radiation Attenuated in Water Column ($\frac{W}{m^2}$)

Φ_{SR6} : Solar Radiation Attenuated in Water Column ($\frac{W}{m^2}$)

Φ_{solar} : Solar Radiation Attenuated in Water Column ($\frac{W}{m^2}$)

Φ_{SRB7} : Direct Beam Solar Radiation Attenuated in Stream Bed ($\frac{W}{m^2}$)

Φ_{SRD7} : Diffuse Solar Radiation Attenuated in Stream Bed ($\frac{W}{m^2}$)

Φ_{SR7} : Solar Radiation Attenuated in Stream Bed ($\frac{W}{m^2}$)

θ_{SA} : Solar Altitude (degrees)

θ_{SZ} : Solar Zenith (degrees)

R_{SB}^B : Reflectivity of Stream Bed if Direct Beam Radiation (unitless)

R_{SB}^D : Reflectivity of Stream Bed if Diffuse Radiation (unitless)

T_W^B : Direct Beam Transmissivity of Water Column (unitless)

T_W^D : Diffuse Transmissivity of Water Column (unitless)

PL_W : Direct Beam Path Length through Water Column (m)

2.2 LONGWAVE (THERMAL) RADIATION: Φ_{LONGWAVE}

The longwave radiation flux is comprised of a positive component (atmospheric and land cover) and a negative component (back radiation). The intensity of incoming atmospheric long wave radiation experienced by the stream surface is a function of atmospheric moisture (Anderson et al. 1984). Humidity and air temperature influence longwave radiation greatly, while carbon dioxide and other molecules in the atmosphere have less of an influence. Further, Anderson et al. (1984) found that the height of cloud cover affects the intensity of longwave radiation. Thermal radiation emitted from surrounding land cover is largely controlled by the physical characteristics (i.e. height and density), which combine form the radiating surface area.

Longwave radiation emission from the surface of the stream, termed back radiation, is the second most important component in dissipating heat energy from the stream system (Parker & Krenkal 1969). Back radiation is best described by the Stefan-Boltzmann Fourth Power Radiation Law for a blackbody as a function of the emissivity water (0.96) and water temperature (McCutcheon 1989). The total longwave radiation flux is simply the instantaneous summation of the positive longwave radiation flux (atmospheric and land cover) and the negative longwave radiation flux (back radiation).

Longwave Radiation Flux Attenuated in Water Column (Longwave Continuity),

$$\Phi_{\text{longwave}} = \Phi_{\text{LW}}^{\text{A}} + \Phi_{\text{LW}}^{\text{LC}} + \Phi_{\text{LW}}^{\text{S}} \quad (2-73)$$

Atmospheric Longwave Radiation Flux Attenuated in Water Column (McCutcheon 1989),

$$\Phi_{\text{LW}}^{\text{A}} = 0.96 \cdot \varepsilon_{\text{atm}} \cdot \sigma \cdot (T_{\text{a}} + 273.2)^4 \quad (2-74)$$

Land Cover Longwave Radiation Flux Attenuated in Water Column (adopted from McCutcheon 1989),

$$\Phi_{\text{LW}}^{\text{LC}} = 0.96 \cdot (1 - \theta_{\text{VTS}}) \cdot 0.96 \cdot \sigma \cdot (T_{\text{a}} + 273.2)^4 \quad (2-75)$$

Longwave Radiation Flux Emitted from Water Column - Back Radiation (adopted from McCutcheon 1989),

$$\Phi_{\text{LW}}^{\text{S}} = -0.96 \cdot \sigma \cdot (T_{\text{w}} + 273.2)^4 \quad (2-76)$$

Atmospheric Emissivity (Dingman 2002, Kustas et al. 1994),

$$\varepsilon_{\text{atm}} = 1.72 \cdot \left(\frac{0.1 \cdot e_{\text{a}}}{T_{\text{a}} + 273.2} \right)^{\frac{1}{7}} \cdot (1 + 0.22 + C_{\text{L}}^2) \quad (2-77)$$

Vapor Pressure (Bedient and Huber 1992),

$$e_{\text{a}} = \frac{H}{100\%} \cdot e_{\text{s}} \quad (2-78)$$

Saturation Vapor Pressure (modified from Chapra 1997 and Raudkivi 1979),

$$e_s = 6.1275 \cdot e^{\left(\frac{17.27 \cdot T_a}{237.3 + T_a}\right)} \quad (2-79)$$

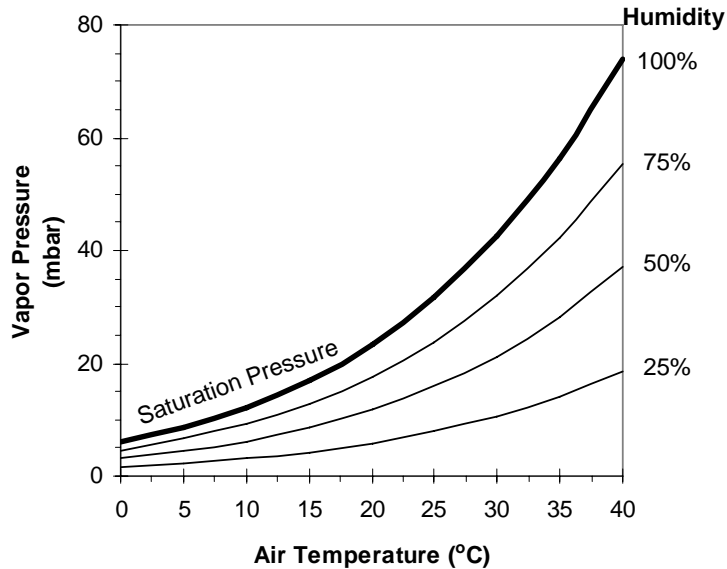


FIGURE 2.4
 Calculated Vapor Pressure (e_a) Values
 Calculated from Equations 2-78 and 2-79.

Variables,

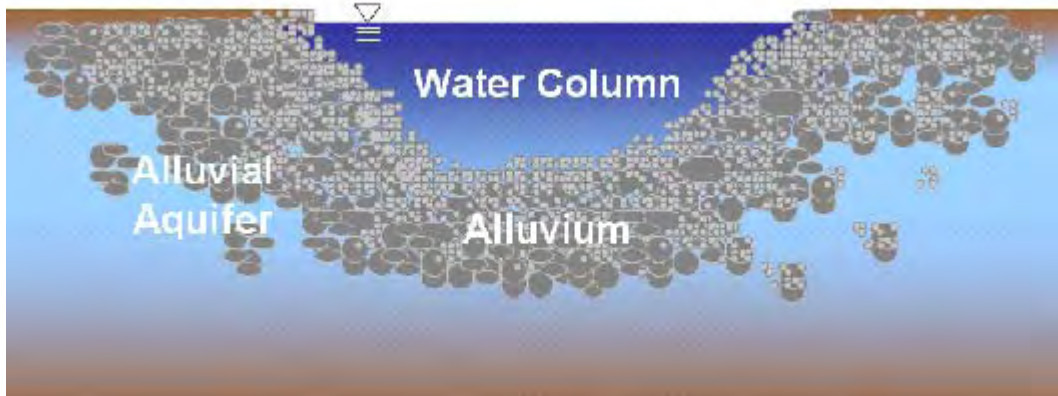
Measured/Known

- C_L : Cloudiness (unitless)
- H : Humidity (unitless)
- σ : Stefan-Boltzmann Constant ($0.0000000567 \frac{W}{m^2 \cdot K^4}$)
- T_a : Air Temperature ($^{\circ}C$)
- T_w : Water Temperature ($^{\circ}C$)

Calculated

- ϵ_{atm} : Emissivity of the Atmosphere (unitless)
- e_a : Vapor Pressure (mbar)
- e_s : Saturation Vapor Pressure (mbar)
- $\Phi_{longwave}$: Water Column Received Longwave Radiation Flux ($\frac{W}{m^2}$)
- Φ_{LW}^A : Atmospheric Emitted Longwave Radiation Flux ($\frac{W}{m^2}$)
- Φ_{LW}^{LC} : Land Cover Emitted Longwave Radiation Flux ($\frac{W}{m^2}$)
- Φ_{LW}^S : Water Column Emitted Longwave Radiation Flux ($\frac{W}{m^2}$)
- θ_{VTS} : View to Sky (unitless)

2.3 SUBSTRATE CONDUCTION FLUX: $\Phi_{\text{CONDUCTION}}$



Heat exchange between alluvium and the water column acts as a heat buffer with the stream and does so as a function of particle size, embeddedness and channel geometry.

Heat energy conduction between the stream bed and the water column is driven by a heat gradient and is rate limited by the size and conductance properties of the substrate. Conduction transfers heat to the stream during periods of the day when thermal differences between the substrate and water column are most pronounced. The effects of conduction can vary greatly. Heat transfer to the water column from conduction typically broadens the diel temperature profile, rather than increasing the maximum daily water temperature (Beschta and Weathered 1984). This is largely because a portion of incoming solar heat is routed through the sediments to the water column, instead of directly attenuating in the water column.

For the purposes of developing the conduction heat flux analytical methodology, the morphologic terminology requires definition. *Substrate* is comprised of various types and sizes of *alluvium* that occupies the stream bed. *Alluvium* consists of depositional materials and substrate that underlies the stream channel. Alluvium material is sorted to some degree by tractive forces and shear stress associated with surface high flow conditions. The distribution of alluvium can vary significantly within the channel and across the floodplain. The depth of alluvium will vary by site and is not predictably quantified without accurate ground level geologic and hydrologic information. The supply of sediments and the flow patterns during peak events affect the distribution and type of sediment found in the alluvium.

Porosity refers to the interstitial spaces (void space) in the alluvium and is assumed to be filled with fine sediments and water. Estimates of porosity are made as a function of substrate size (with an acknowledgement that such an assumption is a simplification and

TABLE 2.2
 Bed Particle Size
 (Bedient & Huber 1992,
 Rosgen 1996)

Size Class	d_{50}
Silt	< 0.062 mm
Sand	0.062 - 2.0 mm
Gravel	2.0 - 63.5 mm
Cobble	63.5 - 254 mm
Boulder	> 254 mm

may misrepresent local variations). Substrate size is typically sieved (measured in terms of diameter) and quantified as a percentage of the total sampled volume. A d_{50} measurement indicates an average alluvium particle size within a sample. *Embeddedness* is a measure of the degree to which substrate is surrounded by fine sediments (silt and sand). It is assumed that embedded fine sediments occupy interstitial spaces in the alluvium. For example, 25% embeddedness indicates that approximately one quarter of the void space in the alluvium is occupied by fine sediments.

Porosity (adopted from Bedient and Huber 1992),

$$\eta = 0.3683 \cdot \left[(d_{50} \cdot (1 - E)) + (d_{50}^{\text{sand}} \cdot E) \right]^{-0.0641} \quad (2-78)$$

where,

- d_{50}^{sand} : Particle Size of Fines (0.0622 mm)
- :
- d_{50} : Sediment Particle Zone (mm)
- E : Embeddedness (unitless)

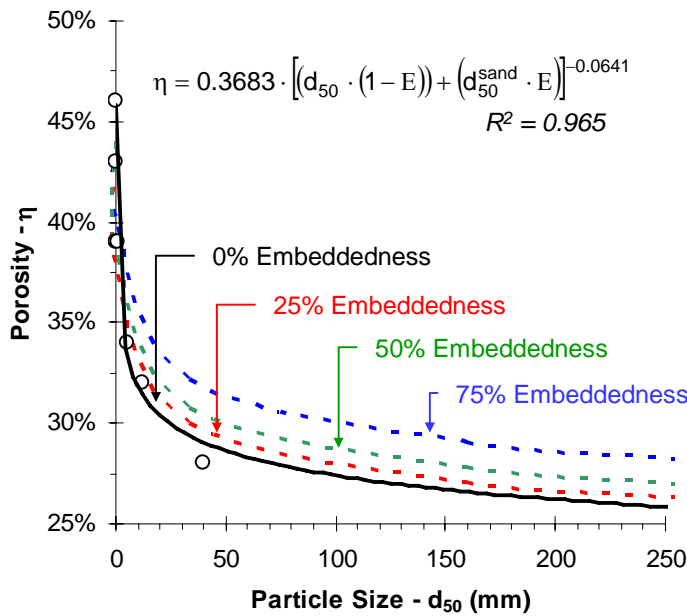


FIGURE 2.5
 Estimated Porosity (η)
 Values as a Function of
 Alluvium Particle Size and
 Embeddedness (Values
 from Bedient and Huber
 1992).

Since both water and alluvium occupy the conduction interface, the thermal conductivity (K_{CL}) is calculated as the volume weighted average of each medium. The thermal conductivity is a calculated as the product of density, thermal diffusivity and specific heat capacity.

The conduction flux can be calculated as a function of the conductivity of the conduction layer and difference between the conduction layer temperature and water column temperature. Recall that during periods of solar exposure (i.e. daytime) that the substrate will attenuate a portion of the radiant heat reaching the stream bed. This heat changes the temperature of the conduction layer and is accounted in the heat budget. A secondary heat transfer occurs between the substrate conduction layer and deeper alluvium. The conduction layer temperature will change at different rates than the water column, allowing for

varying thermal gradients over time and space. The conduction layer initial temperature condition is assumed to be equal with the stream node initial condition. Conduction represents a change in heat and is accounted for in the conduction layer heat budget and temperature. It should be noted that all solar heat is conserved. In effect, a portion of solar heat energy is routed through the substrate, and either remains in the substrate or is returned to the stream system via conduction. Further, conduction can transfer heat from the water column when substrate temperatures are less than the water column temperatures. In essence, the conduction layer represents a heat buffer with the stream and does so as a function of temperature differences between the water and substrate, particle size, embeddedness and channel geometry.

Sediment Thermal Conductivity (Potter and Wiggert 1991),

$$\begin{aligned} K_{\text{sed}} &= \rho_{\text{sed}} \cdot C_{\text{sed}} \cdot \alpha_{\text{sed}} \\ &= 1600 \frac{\text{kg}}{\text{m}^3} \cdot 2219 \frac{\text{J}}{\text{kg} \cdot ^\circ\text{C}} \cdot 0.0000045 \frac{\text{m}^2}{\text{s}} = 15.977 \frac{\text{J}}{\text{m} \cdot \text{s} \cdot ^\circ\text{C}} \end{aligned} \quad (2-79)$$

Water Thermal Conductivity (Potter and Wiggert 1991),

$$\begin{aligned} K_{\text{H}_2\text{O}} &= \rho_{\text{H}_2\text{O}} \cdot C_{\text{H}_2\text{O}} \cdot \alpha_{\text{H}_2\text{O}} \\ &= 1000 \frac{\text{kg}}{\text{m}^3} \cdot 4187 \frac{\text{J}}{\text{kg} \cdot ^\circ\text{C}} \cdot 0.00000014331 \frac{\text{m}^2}{\text{s}} = 0.600 \frac{\text{J}}{\text{m} \cdot \text{s} \cdot ^\circ\text{C}} \end{aligned} \quad (2-80)$$

Variables Used in Thermal Conductivity Calculations,

Density,

$$\rho_{\text{sed}} = 1600 \frac{\text{kg}}{\text{m}^3} \quad \rho_{\text{H}_2\text{O}} = 1000 \frac{\text{kg}}{\text{m}^3}$$

Thermal Diffusivity,

$$\alpha_{\text{sed}} = 0.0000045 \frac{\text{m}^2}{\text{s}} \quad \alpha_{\text{H}_2\text{O}} = 0.00000014331 \frac{\text{m}^2}{\text{s}}$$

Specific Heat Capacity,

$$C_{\text{sed}} = 2219 \frac{\text{J}}{\text{kg} \cdot ^\circ\text{C}} \quad C_{\text{H}_2\text{O}} = 4187 \frac{\text{J}}{\text{kg} \cdot ^\circ\text{C}}$$

Conduction Layer (Assumes 100 Particles Thickness),

$$d_{\text{CL}} = \frac{100 \cdot d_{50}}{1000} : (0.1 \text{ m} < d_{50} < 0.3 \text{ m}) \quad (2-81)$$

Sediment Volume in Conduction Layer,

$$V_{\text{sed}} = (1 - \eta) \cdot P_W \cdot d_{\text{CL}} \cdot dx \quad (2-82)$$

Water Volume in Conduction Layer,

$$V_{\text{H}_2\text{O}} = (\eta) \cdot P_W \cdot d_{\text{CL}} \cdot dx \quad (2-83)$$

Total Volume in Conduction Layer,

$$V_{\text{CL}} = P_W \cdot d_{\text{CL}} \cdot dx \quad (2-84)$$

Volumetric Composite Thermal Conductivity in Conduction Layer,

$$K_{\text{CL}} = \left(K_{\text{sed}} \cdot \frac{V_{\text{sed}}}{V_{\text{CL}}} \right) + \left(K_{\text{H}_2\text{O}} \cdot \frac{V_{\text{H}_2\text{O}}}{V_{\text{CL}}} \right) = (K_{\text{sed}} \cdot (1 - \eta)) + (K_{\text{H}_2\text{O}} \cdot \eta) \quad (2-85)$$

Volumetric Composite Heat Capacity in Conduction Layer,

$$c_{CL} = \left(c_{sed} \cdot \frac{V_{sed}}{V_{CL}} \right) + \left(c_{H_2O} \cdot \frac{V_{H_2O}}{V_{CL}} \right) = (c_{sed} \cdot (1 - \eta)) + (c_{H_2O} \cdot \eta) \quad (2-86)$$

Volumetric Composite Density in Conduction Layer,

$$\rho_{CL} = \left(\rho_{sed} \cdot \frac{V_{sed}}{V_{CL}} \right) + \left(\rho_{H_2O} \cdot \frac{V_{H_2O}}{V_{CL}} \right) = (\rho_{sed} \cdot (1 - \eta)) + (\rho_{H_2O} \cdot \eta) \quad (2-87)$$

Volumetric Composite Thermal Diffusivity in Conduction Layer,

$$\alpha_{CL} = \left(\alpha_{sed} \cdot \frac{V_{sed}}{V_{CL}} \right) + \left(\alpha_{H_2O} \cdot \frac{V_{H_2O}}{V_{CL}} \right) = (\alpha_{sed} \cdot (1 - \eta)) + (\alpha_{H_2O} \cdot \eta) \quad (2-88)$$

Conduction Layer Depth,

$$d_{CL} = 0.2 \text{ m} \quad (2-89)$$

Substrate Conduction Flux with Water Column,

$$\Phi_{conduction} = \rho_{CL} \cdot c_{CL} \cdot \alpha_{CL} \cdot \frac{(T_{CL}^t - T_W^t)}{\frac{d_{CL}}{2}} = K_{CL} \cdot \frac{(T_{CL}^t - T_W^t)}{\frac{d_{CL}}{2}} \quad (2-90)$$

Substrate Conduction Flux with Alluvium,

$$\Phi_{conduction}^{alluvium} = \rho_{CL} \cdot c_{CL} \cdot \alpha_{CL} \cdot \frac{(T_{CL}^t - T_{Alluvium})}{\frac{d_{CL}}{2}} = K_{CL} \cdot \frac{(T_{Alluvium} - T_{CL}^t)}{\frac{d_{CL}}{2}} \quad (2-91)$$

Change in Conduction Layer Temperature from Heat Transfer,

$$\begin{aligned} \Delta T_{CL} &= (\Phi_{SR7} - \Phi_{conduction} + \Phi_{conduction}^{alluvium}) \cdot \frac{A_{CL} \cdot dt}{V_{CL} \cdot \rho_{CL} \cdot c_{CL}} \\ &= (\Phi_{SR7} - \Phi_{conduction} + \Phi_{conduction}^{alluvium}) \cdot \frac{(P_W \cdot dx) \cdot dt}{(d_{CL} \cdot P_W \cdot dx) \cdot \rho_{CL} \cdot c_{CL}} \\ &= (\Phi_{SR7} - \Phi_{conduction} + \Phi_{conduction}^{alluvium}) \cdot \frac{dt}{d_{CL} \cdot \rho_{CL} \cdot c_{CL}} \end{aligned} \quad (2-92)$$

Conduction Layer Temperature,

$$T_{CL}^{t+1} = T_{CL}^t + \Delta T_{CL} \quad (2-93)$$

Variables,

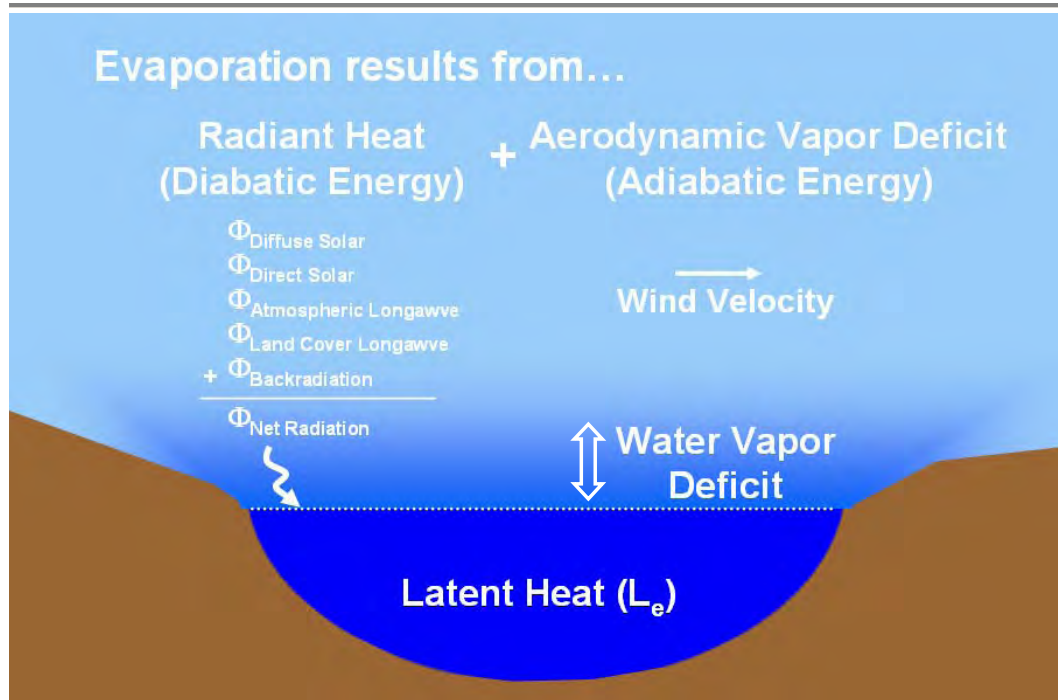
Measured/Known

- d_{50} : Substrate particle size (mm)
- d_{50}^{sand} : Fine sediment particle size (0.062 mm)
- dx : Stream segment length (m)
- E : Embeddedness (unitless)
- c_{sed} : Substrate Specific Heat Capacity ($2219 \frac{\text{J}}{\text{kg} \cdot ^\circ\text{C}}$)
- $c_{\text{H}_2\text{O}}$: Water Specific Heat Capacity ($4187 \frac{\text{J}}{\text{kg} \cdot ^\circ\text{C}}$)
- α_{sed} : Substrate Thermal Diffusivity ($0.0000045 \frac{\text{m}^2}{\text{s}}$)
- $\alpha_{\text{H}_2\text{O}}$: Water Thermal Diffusivity ($0.00000014331 \frac{\text{m}^2}{\text{s}}$)
- ρ_{sed} : Substrate Density ($1600 \frac{\text{kg}}{\text{m}^3}$)
- $\rho_{\text{H}_2\text{O}}$: Water Density ($1000 \frac{\text{kg}}{\text{m}^3}$)
- K_{sed} : Sediment Thermal Conductivity ($15.977 \frac{\text{J}}{\text{m} \cdot \text{s} \cdot ^\circ\text{C}}$)
- $K_{\text{H}_2\text{O}}$: Water Thermal Conductivity ($0.600 \frac{\text{J}}{\text{m} \cdot \text{s} \cdot ^\circ\text{C}}$)
- t : Time (s)

Calculated

- α_{CL} : Volumetric Weighted Thermal Diffusivity ($\frac{\text{m}^2}{\text{s}}$)
- A_{CL} : Surface Area of Conduction Layer (m^2)
- c_{CL} : Volumetric Weighted Specific Heat Capacity ($\frac{\text{J}}{\text{kg} \cdot ^\circ\text{C}}$)
- d_{CL} : Depth of Conduction Layer (m)
- $\Phi_{\text{conduction}}$: Conduction Flux ($\frac{\text{W}}{\text{m}^2}$)
- Φ_{SR7} : Solar Flux Attenuated in Conduction Layer
- η : Porosity of the conduction layer (unitless)
- K_{CL} : Volumetric Weighted Thermal Conductivity ($\frac{\text{J}}{\text{m} \cdot \text{s} \cdot ^\circ\text{C}}$)
- P_{W} : Wetted Perimeter (m)
- ρ_{CL} : Volumetric Weighted Density ($\frac{\text{kg}}{\text{m}^3}$)
- $\Delta T_{\text{CL}}^{\text{solar}}$: Change in Conduction Layer Temperature from Solar Radiation ($^\circ\text{C}$)
- $\Delta T_{\text{CL}}^{\text{cond}}$: Change in Conduction Layer Temperature from Conduction ($^\circ\text{C}$)
- T_{CL} : Conduction Layer Temperature ($^\circ\text{C}$)
- $T_{\text{CL}}^{\text{solar}}$: Conduction Layer Temperature Accounting for Solar Irradiance ($^\circ\text{C}$)
- $T_{\text{CL}}^{\text{cond}}$: Conduction Layer Temperature Accounting for Conduction ($^\circ\text{C}$)
- T_{W} : Water Column Temperature ($^\circ\text{C}$)
- T_{Alluvium} : Deeper Alluvium Temperature ($^\circ\text{C}$)
- V_{sed} : Substrate Volume in Conduction Layer (m^3)
- $V_{\text{H}_2\text{O}}$: Water Volume in Conduction Layer (m^3)
- V_{CL} : Conduction Layer Volume (m^3)

2.4 EVAPORATION FLUX: $\Phi_{\text{EVAPORATION}}$



Evaporation represents the difference in enthalpy of the air near the water surface and the ambient air. Evaporation raises the total energy content of the air near the evaporating surface representing a heat loss to the water column.

As the molecular motion of a water molecule in the liquid phase increases, in response to increased heat energy and aerodynamic energy, it begins to overcome the molecular attraction to liquid water, causing water molecules to escape as water vapor. When the vapor pressure of the air above the stream is low, the released water vapor from the stream has a lower chance of colliding with other molecules in the air, a greater chance of volatilizing away from the water column surface, and thus, a greater chance of remaining in the gaseous phase as water vapor. If the vapor pressure is high, the chance of molecular collisions is greater, with a decreased tendency for the water vapor to remain volatilized into the liquid phase. Saturation vapor pressure occurs when the air mass contains the maximum water vapor content, determined as a function of air temperature. Attainment of a saturated air vapor pressure implies that the rate of water molecules leaving the stream surface is equal to the rate of water vapor molecules being introduced back to the liquid phase of the stream. Under this condition, evaporation stops. Condensation is the reversal of evaporation, and instead the delivery of water vapor molecules to the water column, and represents heat gain to the water column. Condensation occurs when the water vapor deficit is directed from the overlaying air mass to the water column, and predicted when the air temperature is below the dew point (i.e. the air mass is saturated with water vapor).

Water molecules in the liquid phase require energy to overcome the molecular bonds that bind the liquid molecules. The energy needed to change water from a liquid to gaseous phase is known as *the latent heat of vaporization*.

Heat energy necessary for the evaporative process is furnished by the stream system and transferred to the surrounding air mass, representing a net heat energy loss. *Sensible heat exchange* is an upward rate of turbulent heat transfer and is limited by the density and heat capacity of air.

The evaporative heat flux across the air-water interface is generally the most significant factor in dissipation of stream heat (Parker and Krenkel 1969). Special consideration must be taken in addressing the simulation of evaporation rates, since the evaporation flux is the energy process in which streams dissipate most heat energy, and therefore, contributes most to decreases in water column temperature. Further, the evaporation flux is utilized by the Bowen ratio to approximate the convective heat energy flux, and thus, the accuracy of the convection flux is dependent on accurate estimation of the evaporation energy flux.

The vapor pressure gradient between the water surface (e_s) and the air (e_a) directly above the stream drives evaporation (i.e. the vaporization of water molecules) when the gradient is positive ($e_a < e_s$). Only when the air is saturated does evaporation cease to occur ($e_a \approx e_s$). This condition is known as the dew point temperature. The overlying air mass may become supersaturated with resulting condensation when the vapor pressure gradient is negative ($e_a \geq e_s$).

The evaporative flux can be calculated as a summation of the sensible heat carried with evaporated water vapor and the product of the latent heat of evaporation (LHV), density of water (ρ_w) and the rate of evaporation (\bar{E}). The energy needed for water to change from a liquid to a gas, the latent heat of vaporization (LHV), is a function of water temperature (McCutcheon 1989). Brown and Barnwell (1987) found that for practical modeling applications the sensible heat term ($\Phi_{\text{convection}}$) is negligible, however, convection heat transfer is included in this methodology and is described in the following section.

Evaporation Flux,

$$\Phi_{\text{evaporation}} = \rho_{\text{H}_2\text{O}} \cdot L_e \cdot \bar{E} \quad (2-94)$$

Latent Heat of Vaporization,

$$L_e = 1000 \cdot (2501.4 + (1.83 + T_w)) \quad (2-95)$$

Evaporation Rate (\bar{E}) is defined in the following section

2.4.1 EVAPORATION RATE

The rate of evaporation is derived by assuming that heat transfer and turbulent mixing are responsible for the transport of momentum, heat and water vapor in the atmospheric boundary layer directly above the stream surface (McCutcheon 1989). Evaporation is an extremely important area of hydrologic study. For example, in the United States, 70% of the received precipitation is returned to the atmosphere via evaporation and transpiration (Dingman 2002). Accurate water balance and heat balance methods must devote considerable attention to robust analytical treatment of evaporative water loss. It follows that the evaporative process has been the topic of vigorous research. Several

methods, namely the mass transfer method, energy budget method and the combination method, are available in the literature and are described below.

MASS TRANSFER METHOD

A primary focus on the turbulent transfer of water vapor from a waterbody to the atmospheric air mass allows a simple expression of evaporation as an approximation of the vapor gradient ($e_s - e_a$) and the movement of the air (\vec{W}) directly above the water surface width of exposure. Numerous expressions closely follow Dalton type equations similar to Equation 2-96. Special attention should be paid to the measurement height above the free water surface for the input variables (wind speed, air temperature and humidity). Each expression typically has unique data constraint and are developed for specific applications and regions. The mass transfer evaporation rate method is available for use in the model methodology.

Mass Transfer Evaporation Rate (Dingman 2002),

$$\bar{E} = f(\vec{W}) \cdot (e_s - e_a) \quad (2-96)$$

Saturation Vapor Pressure Using Stream Temperature (modified for units from Chapra 1997),

$$e_s = 6.1275 \cdot e^{\left(\frac{17.27 \cdot T_{wi}}{237.3 + T_{wi}} \right)} \quad (2-97)$$

Vapor Pressure Based on Saturation Vapor Pressure Using Stream Temperature (Bedient and Huber 1992),

$$e_a = \frac{H}{100\%} \cdot e_s \quad (2-98)$$

Wind Function ($f(\vec{W})$) is described in detail in following section (Wind Functions)

ENERGY BUDGET METHOD

The energy budget method calculates the evaporation rate as a function of heat transfer processes. It is the most accurate and complex method for estimating evaporation dynamics (Bedient and Huber 1992). As would be expected, application of this method requires accurate measurements of free water surface temperature, radiation attenuation and emission. Atmospheric data also must be detailed and highly accurate, and is considered a serious limitation of application of this method (Bedient and Huber 1992). Despite these limitations, the energy budget evaporation rate method is a widely used methodology. However, the calculated evaporation rate is a function of surface water temperature, which is often an estimated or simulated condition. A feedback mechanism resulting from errors in temperature simulation may create errors in evaporation simulation with a compounding effect. Lastly, unlike the other two evaporation simulation methods presented in this section, there are not calibration parameters (a and b), and results cannot be calibrated by the user.

Energy Budget Evaporation Rate (Dingman 2002),

$$\bar{E} = \frac{\Phi_{\text{solar}} + \Phi_{\text{longwave}} + \Phi_{\text{conduction}} + \Phi_{\Delta M} - \Phi_{\Delta Q}}{\rho_{\text{H}_2\text{O}} \cdot L_e \cdot (1 + B_R)} \quad (2-99)$$

Water Advected Heat (Dingman 2002),

$$\Phi_{\Delta M} = \frac{\rho_{\text{H}_2\text{O}} \cdot c_{\text{H}_2\text{O}}}{A_W} \cdot [(Q_{\text{IN}} \cdot T_{\text{IN}}) + (Q_{\text{GW}} \cdot T_{\text{GW}}) - (Q_{\text{OUT}} \cdot T_{\text{OUT}})] \quad (2-100)$$

Change in Stored Heat (Dingman 2002),

$$\Phi_{\Delta Q} = \frac{\rho_{\text{H}_2\text{O}} \cdot c_{\text{H}_2\text{O}}}{A_W} \cdot [(Q \cdot T_W)_i^{t-1} - (Q \cdot T_W)_i^t] \quad (2-101)$$

Bowen's Ratio of Sensible Heat to Evaporative Heat (modified for units from Bedient and Huber 1992),

$$B_R = 0.00061 \cdot P_A \cdot \frac{T_{W_i}^t - T_A}{(e_s^* - e_a^*)} \quad (2-102)$$

Adiabatic Air Pressure (Dingman 2002),

$$P_A = 1013 - 0.1055 \cdot z \quad (2-103)$$

COMBINATION METHOD (PENMAN)

Penman (1948) developed a combination method to capture both the mass transfer and the energy budget components involved in estimating evaporation rates. This method does not require surface water temperatures, which represents a considerable improvement over the energy budget method. Further, heat energy terms are included, extending the simulation to diabatic vaporization processes, as well as the mass transfer adiabatic/aerodynamic processes. The Penman method is widely used since it eliminates the problems associated with the mass transfer and energy budget methods.

Combination Method (Penman) Evaporation Rate (basic form),

$$\bar{E} = \text{Energy Input} + \text{Mass Transfer} \quad (2-104)$$

Combination Method (Penman) Evaporation Rate (Dingman 2002),

$$\begin{aligned} \bar{E} &= \frac{(\Phi_{\text{solar}} + \Phi_{\text{longwave}})}{\rho_{\text{H}_2\text{O}} \cdot L_e} \cdot \frac{\Delta}{\Delta + \gamma} + E_a \cdot \frac{\gamma}{\Delta + \gamma} \\ &= \frac{(\Phi_{\text{solar}} + \Phi_{\text{longwave}})}{\rho_{\text{H}_2\text{O}} \cdot L_e} \cdot \Delta + E_a \cdot \gamma \end{aligned} \quad (2-105)$$

Slope of the Saturation Vapor v. Air Temperature Curve (Dunne and Leopold 1978),

$$\Delta = \frac{e_s^* - e_a^*}{T_s^* - T_a^*} = 6.1275 \cdot e^{\left(\frac{17.27 \cdot T_A}{237.3 + T_A}\right)} - 6.1275 \cdot e^{\left(\frac{17.27 \cdot (T_A - 1)}{237.3 + (T_A - 1)}\right)} \quad (2-106)$$

Psychrometric Constant (Cuenca 1989),

$$\gamma = 1003.5 \cdot \frac{P_A}{0.62198 \cdot L_e} \quad (2-107)$$

Aerodynamic Evaporation (Dingman 2002),

$$E_a = f(\bar{W}) \cdot (e_s - e_a) \quad (2-108)$$

2.4.2 WIND FUNCTIONS

Both the mass transfer and the combination (Penman) method utilize a wind function ($f(\bar{W})$) to estimate adiabatic portion of evaporation. In essence the wind function has the following form.

Wind Function (Shanahan et al. 1984),

$$f(\bar{W}) = a + b \cdot \bar{W} \quad (2-109)$$

where,

a and b are coefficients (see Table 2.3)

\bar{W} : Wind velocity measured at ≈ 2 meters above water surface ($\frac{m}{s}$)

Table 2.3
 Wind Function Coefficients

Source	Location	a ($mb^{-1}m \cdot s^{-1}$)	b (mb^{-1})
Meyer (1928)		$4.18 \cdot 10^{-9}$	$0.95 \cdot 10^{-9}$
Marciano and Harbeck (1952)	Lake Hefner	0	$1.02 \cdot 10^{-9}$
Harbeck et al. (1959)	Colorado City	0	$1.51 \cdot 10^{-9}$
Morton (1965)	Canada	$3.45 \cdot 10^{-9}$	$1.26 \cdot 10^{-9}$
Brady et al. (1969)	South U.S.	$2.81 \cdot 10^{-9}$	$0.14 \cdot 10^{-9}$
Brady et al. (1971)	South U.S.	$2.21 \cdot 10^{-9}$	0
Ryan and Harleman (1973)	Australia	$2.83 \cdot 10^{-9}$	$1.26 \cdot 10^{-9}$
Dunne and Leopold (1978) ¹¹		$1.505 \cdot 10^{-9}$	$1.600 \cdot 10^{-9}$
Bowie et al. (1985)	California	$3.083 \cdot 10^{-9}$	$5.845 \cdot 10^{-9}$

Wind velocity measured at a given elevation above the water surface may not be representative of the wind velocity experienced by the water body surface boundary. The expressions for the wind function are specifically developed to account for this phenomenon and are highly dependent on wind speed sampling elevation above the water surface (Dingman 2002). When emergent vegetation is present, the attenuation of wind will be significant and since the vertical distribution of wind velocity decreases at the water surface due to frictional forces from the emergent vegetation. This wind attenuation is represented as a logarithmic function. Specifically, the Prandtl-von-Karman Universal Velocity-Distribution formulae for turbulent flows can effectively simulate the boundary layer wind flows experienced by the stream surface (Dingman 2002).

¹¹ Developed by Dunne and Leopold (1978) for the Penman Method

Boundary Layer Wind Velocity Prandtl-von-Karman Universal Velocity-Distribution (Dingman 2002),

$$\vec{W}_s = \frac{1}{k} \cdot \vec{W} \cdot \ln\left(\frac{z - z_d}{z_0}\right) \quad (2-110)$$

Variables,

Measured/Known

- c_{H_2O} : Specific Heat of Water
- H: Humidity (unitless)
- H_{LC} : Height of Emergent Vegetation (m)
- k: Wind Velocity Coefficient (k = 0.4)
- ρ_{H_2O} : Density of Water (998.2 $\frac{kg}{m^3}$)
- T_A : Air Temperature ($^{\circ}C$)

Calculated

- a: Wind Function Coefficient ($\frac{m}{mb \cdot s}$)
- b: Wind Function Coefficient ($\frac{1}{mb}$)
- A_W : Stream Segment Surface Area (m^2)
- B_R : Bowens Ratio (unitless)
- Δ : Slope of the Saturation Vapor v. Air Temperature Curve ($\frac{mb}{^{\circ}C}$)
- \bar{E} : Evaporation Rate ($\frac{m}{s}$)
- E_a : Aerodynamic Evaporation ($\frac{m}{s}$)
- e_a : Vapor Pressure Based on e_s (mb)
- e_s : Saturation Vapor Pressure Based on T_W (mb)
- $\Phi_{conduction}$: Substrate Conduction Flux ($\frac{W}{m^2}$)
- $\Phi_{evaporation}$: Evaporation Flux ($\frac{W}{m^2}$)
- $\Phi_{longwave}$: Longwave Radiation Flux ($\frac{W}{m^2}$)
- Φ_{solar} : Solar Radiation Flux ($\frac{W}{m^2}$)
- $\Phi_{\Delta Q}$: Change in Stored Heat ($\frac{W}{m^2}$)
- $\Phi_{\Delta M}$: Water Advected Heat ($\frac{W}{m^2}$)
- γ : Psychrometric Constant ($\frac{mb}{^{\circ}C}$)
- L_e : Latent Heat of Vaporization ($\frac{J}{kg}$)
- P_A : Adiabatic Atmospheric Pressure (mb)
- Q: Flow Rate (m^3)
- Q_{GW} : Subsurface Inflow Rate (m^3)
- Q_{IN} : Surface Inflow Rate (m^3)
- Q_{OUT} : Withdrawal Flow Rate (m^3)
- T_{GW} : Subsurface Inflow Temperature ($^{\circ}C$)

Calculated (continued)

- T_{IN} : Surface Inflow Temperature ($^{\circ}C$)
 - T_{OUT} : Withdrawal Flow Temperature $\approx T_W$ ($^{\circ}C$)
 - T_W : Water Temperature ($^{\circ}C$)
 - $f(\vec{W})$: Wind Function ($\frac{m}{mb \cdot s}$)
 - \vec{W} : Wind Velocity Measured at ≈ 2 meters Above Surface ($\frac{m}{s}$)
 - \vec{W}_s : Wind Velocity Measured at Water Surface ($\frac{m}{s}$)
 - Zero-Plane Displacement (m)
 - z_d : $z_d = 0.7 \cdot H_{LC}$
 - Roughness Height (m)
 - z_0 : $z_d = 0.1 \cdot H_{LC}$
 - Measurement Height (2 m)
 - z : $z > z_d + z_0$
-

2.5 CONVECTION FLUX: $\Phi_{CONVECTION}$

The convection heat flux (also known as sensible heat) at the air-water interface is the result of turbulent and molecular heat exchange that occurs in response to a heat energy gradient. Sensible heat will be transferred between water and air when the respective temperatures are different. From Furrier's heat transfer studies, the rate of heat energy transfer is proportional to the heat gradient (McCutcheon 1989). The Bowen ratio is a constant of proportionality between the convection flux and the evaporation flux at the air-water interface, and is therefore, a function of stream and air temperature and vapor pressure (Bowen 1926). It follows that the convection heat flux at the air-water interface is the product of the Bowen ratio and the evaporative heat flux.

Convection Heat Flux (Bowen 1926),

$$\Phi_{convection} = B_R \cdot \Phi_{evaporation} \quad (2-111)$$

Variables,

Calculated

- B_R : Bowens Ratio Defined in Equation 2-102 (unitless)
 - $\Phi_{convection}$: Convection Flux ($\frac{W}{m^2}$)
 - $\Phi_{evaporation}$: Evaporation Flux Defined in Equation 2-94 ($\frac{W}{m^2}$)
-

2.6 STREAM TEMPERATURE SIMULATION METHOD

2.6.1 NON-UNIFORM HEAT ENERGY TRANSFER METHODOLOGY

The rate change in stream temperature is driven by the total heat flux (Φ_{total}), excluding mass transfer temperature effects. It is easily shown that when mass transfer is excluded, a defined volume of water will attain a predictable rate change in temperature, provided an accurate prediction of the heat energy flux.

Rate Change in Water Temperature from Heat Transfer,

$$\begin{aligned} \frac{\partial T_W}{\partial t} &= \left(\frac{A \cdot \Phi_{total}}{\rho_{H_2O} \cdot c_{H_2O} \cdot V_W} \right) \\ &= \left(\frac{(W_W \cdot dx) \cdot \Phi_{total}}{\rho_{H_2O} \cdot c_{H_2O} \cdot (d_W \cdot W_W \cdot dx)} \right) \\ &= \left(\frac{\Phi_{total}}{\rho_{H_2O} \cdot c_{H_2O} \cdot d_W} \right) \end{aligned} \quad (2-112)$$

The advective movement of water is a function of the flow velocity (U_x)¹². Advection redistributes heat energy in the positive longitudinal direction. No heat energy is lost or gained by the system during advection, and instead, heat energy is transferred downstream as a function of flow velocity. Over a any scale, the rate change in temperature due to advection is expressed in the following first order partial differential equation.

Rate Change in Temperature from Advection,

$$\frac{\partial T_W}{\partial t} = -U \cdot \frac{\partial T_W}{\partial x} \quad (2-113)$$

Dispersion processes occur in both the upstream and downstream direction along the longitudinal axis¹³. Heat energy contained in the system is conserved throughout dispersion, and similar to advection, heat energy is simply moved throughout the system. The rate change in temperature due to dispersion is expressed in the following second order partial differential equation.

Rate Change in Temperature from Dispersion,

$$\frac{\partial T_W}{\partial t} = D_L \cdot \frac{\partial^2 T_W}{\partial x^2} \quad (2-114)$$

The dispersion coefficient (D_L) may be calculated by stream dimensions, roughness and flow (Fischer et. al. 1979). For streams that exhibit high flow velocities and low longitudinal temperature gradients, it may be assumed that the

¹² See Chapter 3 for a detailed description of advection.

¹³ See Chapter 3 for a detailed description of dispersion.

system is advection dominated and the dispersion coefficient may approach zero (Sinokrot and Stefan 1993). Regardless, dispersion is included in the simulation methodology. The longitudinal dispersion coefficient is determined from stream dimensions and flow velocity with a relationship developed by Fischer et al. (1979).

Physical Dispersion Coefficient (Fischer et. al. 1979)

$$D_L = 0.011 \cdot \frac{U^2 \cdot W_W^2}{U_s \cdot \bar{d}_W} \quad (2-115)$$

Shear velocities result from the frictional forces exerted upon flowing water at the substrate boundary. Most formulations of shear velocity are based upon representations of shear stress (Martin and McCutcheon 1999).

Shear Stress as a Function of Slope and Water Column Depth (Martin and McCutcheon 1999),

$$\tau = \rho_{H_2O} \cdot g \cdot \bar{d}_W \cdot S_o \quad (2-116)$$

Shear Velocity as a Function of Shear Stress (Martin and McCutcheon 1999),

$$U_s = \sqrt{\frac{\tau}{\rho_{H_2O}}} = \sqrt{g \cdot \bar{d}_W \cdot S_o} \quad (2-117)$$

The simultaneous non-uniform one-dimensional transfer of heat energy is the summation of the rate change in temperature due to heat energy thermodynamics, advection and dispersion. Given that the stream is subject to steady flow conditions and is well mixed, transverse temperature gradients are negligible (Sinokrot and Stefan 1993). An assumption of non-uniform flow implies that cross-sectional area and flow velocity vary with respect to longitudinal position. Unsteady flow assumptions allow for flows, velocities and wetted dimensions to change over time. The following second ordered parabolic partial differential equation describes the rate change in temperature for non-uniform flow.

Non-Uniform One-dimensional Heat Energy Transfer,

$$\frac{\partial T_W}{\partial t} = \underbrace{-U \cdot \frac{\partial T_W}{\partial x}}_{\text{Advection}} + \underbrace{D_L \cdot \frac{\partial^2 T_W}{\partial x^2}}_{\text{Dispersion}} + \underbrace{\frac{\Phi_{total}}{c_{H_2O} \cdot \rho_{H_2O} \cdot \bar{d}_W}}_{\text{Heat Transfer}} \quad (2-118)$$

Mass Transfer

When combined with the dynamic flow routing (see Chapter 3),

$$\text{Unsteady Flow: } \frac{\partial U}{\partial t} \neq 0 \quad \text{Non-Uniform Flow: } \frac{\partial U}{\partial x} \neq 0$$

Variables,

Measured/Known

- c_{H_2O} : Specific Heat of Water
- dx : Model Distance Step (m)
- g : Acceleration of gravity ($9.8 \frac{m}{s^2}$)
- ρ_{H_2O} : Density of Water ($998.2 \frac{kg}{m^3}$)
- S_o : Channel Slope (unitless)
- x : Longitudinal Distance (m)
- t : Time (s)

Calculated

- A_w : Surface Area (m^2)
 - \bar{d}_w : Average Water Column Depth (m)
 - D_L : Dispersion Coefficient ($\frac{m^2}{s}$)
 - Φ_{total} : Total Heat Flux ($\frac{W}{m^2}$)
 - T_w : Water Temperature ($^{\circ}C$)
 - τ : Shear Stress ($\frac{kg}{m \cdot s^2}$)
 - U : Average Flow Velocity ($\frac{m}{s}$)
 - U_s : Shear Velocity ($\frac{m}{s}$)
 - V_w : Water Reach Volume (m^3)
 - W_w : Wetted Width (m)
-

2.6.2 FINITE DIFFERENCE APPROXIMATION

The methods employed to approximate the *one-dimensional heat energy transfer equation* (2-118) is essentially the summation of thermodynamic heat energy exchange between the stream system and the surrounding environment and physical processes that redistribute heat energy within the stream system (Boyd 1996). It is important to note that all heat energy introduced into the stream is conserved, hydraulically redistributed and partially lost to the surrounding environment via heat transfer processes, with the net result reflected in stream temperature magnitude. Heat energy is transient within the stream system, due to longitudinal advective and dispersive transfer of heat energy. The net heat energy flux (Φ_{total}) is calculated at every distance step and time step based on physical and empirical formulations developed for each heat component. Any effort to accurately simulate stream temperatures must develop a finite difference approximation to the three modes of heat energy transport and change: advection, dispersion and heat transfer.

MacCormick (1969) demonstrates a predictor-corrector approach to approximation of the non-uniform one-dimensional advection dispersion partial differential form. **Figure 2.6** displays the MacCormick solution scheme. In summary the approximation uses two forward slope predictions along with Euler's method, and then averages the slope predictions to calculate a backward difference (Chapra 1997). The MacCormick method is computationally efficient, more stable than traditional explicit approximation solution methods and does not introduce numerical dispersion (since the method uses a time-centered approach). Chapra (1997) note that the MacCormick method is particularly accurate since it employs a time-centered and space-centered approach. A potential limitation is conditionally stability. However, stability greatly exceeds that offered in explicit methods, and approaches constraints more commonly found with Euler's method. Numerical stability criterion cannot be calculated, suffice to say it will be apparent when stability limits are exceeded (the model will fluctuate temperature prediction wildly and then crash).

Forward - First Approximation (t) of the Slope (MacCormick 1969),

$$s_{1,t} = -U \cdot \frac{T_{W_{i+1}}^t - T_{W_i}^t}{dx} + D_L \cdot \frac{T_{W_{i+1}}^t - 2 \cdot T_{W_i}^t + T_{W_{i-1}}^t}{dx^2} + \frac{(\Phi_{total})_i^t}{\rho_{H_2O} \cdot C_{H_2O} \cdot \bar{d}_w} \quad (2-119)$$

Forward - First Approximation (t) Using Euler's Method for Predictor Calculation (MacCormick 1969),

$$T_{W_i}^{t+1} = T_{W_i}^t + s_{1,t} \cdot dt \quad (2-120)$$

Second Approximation ($t+1$) of the Slope (MacCormick 1969),

$$s_{2,t} = -U \cdot \frac{T_{W_i}^{t+1} - T_{W_{i-1}}^{t+1}}{dx} + D_L \cdot \frac{T_{W_{i+1}}^{t+1} - 2 \cdot T_{W_i}^{t+1} + T_{W_{i-1}}^{t+1}}{dx^2} + \frac{(\Phi_{total})_i^{t+1}}{\rho_{H_2O} \cdot c_{H_2O} \cdot \bar{d}_W} \quad (2-121)$$

Backward - Second Approximation (t) for Final Predictor Calculation (MacCormick 1969),

$$T_{W_i}^{t+1} = T_{W_i}^t + \left(\frac{s_{1,t} + s_{2,t}}{2} \right) \cdot dt \quad (2-122)$$

Variables,

Measured/Known

- c_{H_2O} : Specific Heat of Water
- dx : Model Distance Step (m)
- ρ_{H_2O} : Density of Water ($998.2 \frac{kg}{m^3}$)
- x : Longitudinal Distance (m)
- t : Time (s)

Calculated

- D_L : Dispersion Coefficient ($\frac{m^2}{s}$)
- \bar{d}_W : Average Water Column Depth (m)
- Φ_{total} : Total Heat Flux ($\frac{W}{m^2}$)
- $s_{1,t}, s_{2,t}$: Approximation of the Slope ($\frac{^{\circ}C}{s}$)
- T_W : Water Temperature ($^{\circ}C$)
- U : Average Flow Velocity ($\frac{m}{s}$)

Boundary conditions are defined for the finite difference solution and displayed in **Figure 2.7**. The temperatures at the upstream boundary (i_o) for all time steps ($t_o, t-1, t, t+1, \dots$) are supplied by hourly temperature data inputs. It is assumed at the downstream boundary (position x in **Figure 2.7**) that temperature remains constant with respect to time. Initial values of the temperatures at each distance node ($i_o, i-1, i, i+1, \dots$) occurring at the starting time (t_o) are equal to the boundary condition at time t_o . The initial condition of the model is quite irrelevant, since model convergence should be independent of the initial condition. However, convergence will occur faster when the initial condition is a closer to the convergence (final approximation) condition. Further, the substrate temperature is also assumed to equal the initial condition temperatures and will require more simulation time to reach a dynamic equilibrium heat transfer condition (note: this does not imply thermal equilibrium) with the water column.

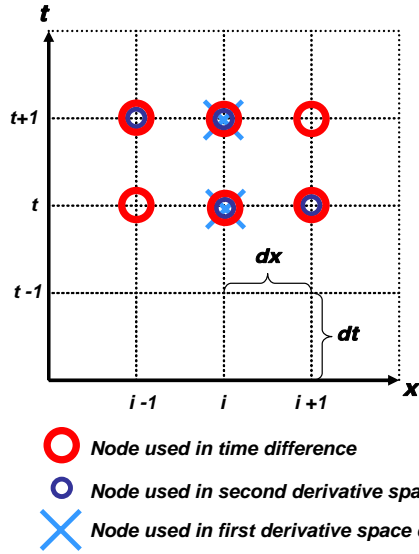


FIGURE 2.6
 MacCormick Finite Difference Scheme

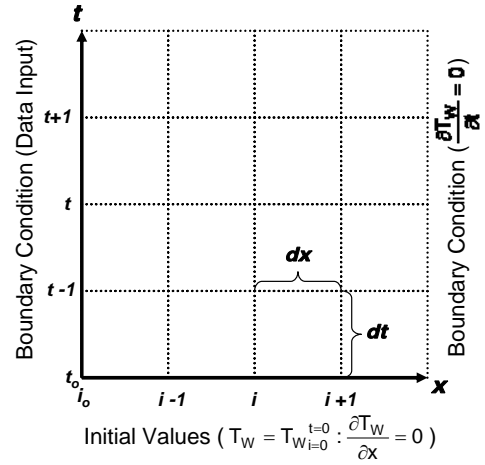


FIGURE 2.7
 Boundary Conditions and Initial Values

Chapter



Dynamic Mass Transfer

Description of Processes, Analytical Methods and Finite Difference Approximation



Mass transfer is simulated as a function of the St. Venant equations which combine continuity and momentum (picture Trask River, Oregon).

3.1 OVERVIEW

Mass transfer processes refer to the movement and mixing of water throughout a stream system. The downstream transport of dissolved/suspended substances and heat associated with flowing water is called *advection*. *Dispersion* results from turbulent diffusion that mixes the water column. In fact, flowing water is usually well mixed vertically, largely a result of dispersion. Stream water mixing with inflows from surface tributaries and subsurface groundwater sources moves water and heat within the stream system. These processes (advection, dispersion and mixing of surface and subsurface waters) redistribute the heat of a stream system via mass transfer.

Water that is transported by river flow is referred to as advection. It follows that advection is a gravity driven process that can only occur in the downstream direction. In the case of water temperature, no heat energy is lost or gained by the system during advection, assuming the heat from mechanical processes, such as friction and compression, is negligible. Advection is simply the rate at which water and the dissolved/suspended substances and heat are transferred downstream.

Dispersion refers to the mixing caused by turbulent diffusion. In natural stream systems flows are often vertically mixed due to turbulent diffusion of water molecules. Turbulent flows result from a multi-dimensional variable flow velocity

profile, with lower velocities occurring near the boundaries of the channel (i.e. channel bottom and stream banks). Higher velocities occur farthest away from channel boundaries, commonly at the top and center of the water column. The velocity profile results from the friction between the flowing water and the rough surfaces of the channel. Since water is flowing at different rates through the channel cross-section, turbulence is created, and vertical mixing results. Dispersion mixes water molecules at a much higher rate than molecular diffusion. Turbulent diffusion can be calculated as a function of stream dimensions, channel roughness and average flow velocity. Dispersion occurs in both the upstream and downstream directions.

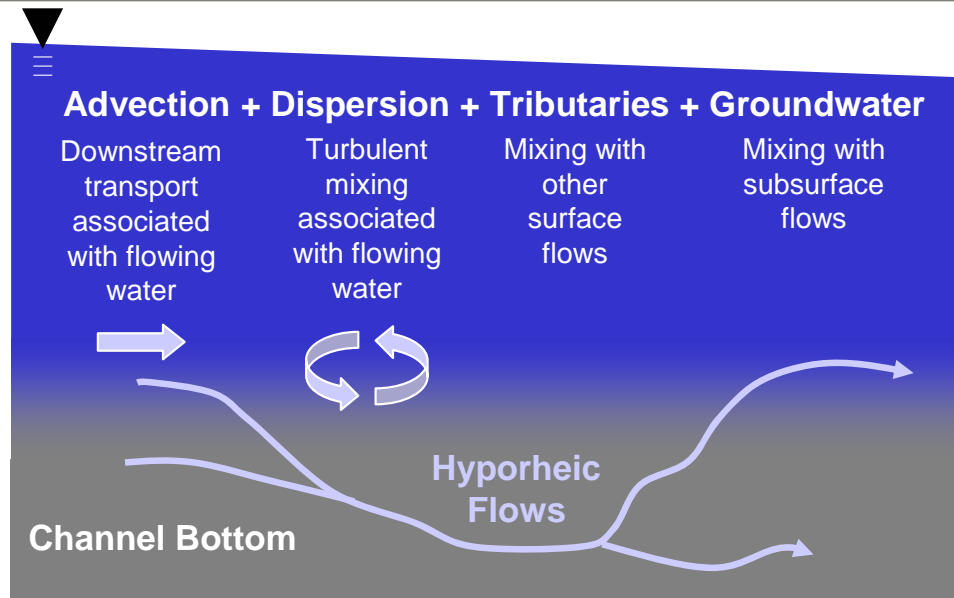


FIGURE 3.1
 Mass Transfer Processes: Advection, Dispersion, and Mixing

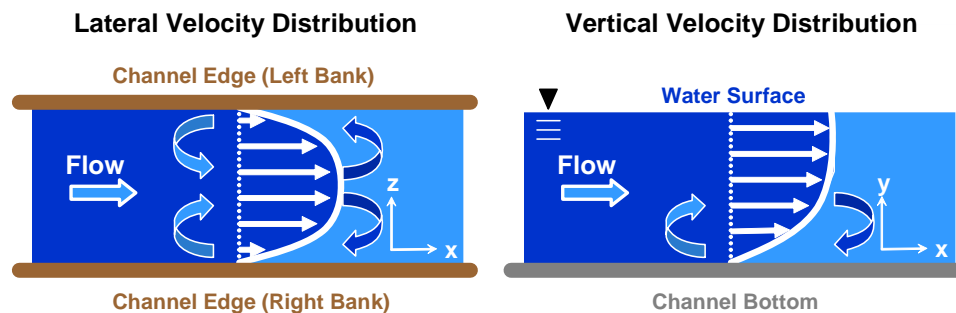


FIGURE 3.2
 Dispersion Defined. Dispersion is the mixing that occurs from turbulence caused by vertical and lateral flow variations. Velocity is a function of depth, width and channel roughness (frictional forces at the boundaries). The vertical and horizontal gradient in flow velocity causes tumbling and eddy effect mixing.

Mixing external flows (tributaries, groundwater inflows, point sources, etc.) with a receiving water will change the heat when the respective temperatures are different. Mixing simply changes the heat as a function of stream and inflow volumes and temperatures. Remote sensing using thermal infrared radiometry (TIR) can easily identify areas where heat change occurs due to mixing with surface and subsurface waters.

3.2 CHANNEL GEOMETRY & MANNING'S RELATIONSHIPS

A trapezoidal channel shape can be used to estimate bankfull channel dimensions represented by measured bankfull width (W_{BF}) and channel side slope ratio (Z), channel longitudinal slope (S_0) and an assumed/measured width to depth ratio ($W:D$). From these known values it is possible to calculate the remaining unknown bankfull dimensions, namely: average bankfull depth (d_{BF}), bankfull depth (d_{BF}) and bottom width (W_B). Using the equations listed below it is possible to calculate the bankfull channel dimensions for any segment over a stream network.

Manning's equation is commonly used to calculate flow rate and flow velocity for flows as a function of wetted channel dimensions (d , W , Z), roughness (n) and slope (S_0). Provided that flow rates are known, the wetted channel dimensions are calculated using basic channel geometry and Manning's equation. A system of equations is developed for cross-sectional area (A_w), wetted perimeter (P_w), hydraulic radius (R_h) and flow volume ($Q = A \cdot U$) that become a function of known variables and one unknown variable: wetted depth (d_w). Convergence on the value of wetted depth, the root for the system of equations, is performed by the Newton-Raphson root finding iterative method.

The use of Manning's equation relies on the assumption that flows are steady ($\frac{dQ}{dt} = 0$) and uniform ($\frac{dQ}{dx} = 0$) over the length of a stream segment (i) at any particular time (t).¹⁴ This methodology, when combined with a finite difference approximation of the St. Venant Equations, allows for calculation of unsteady flows ($\frac{dQ}{dt} \neq 0$) between time steps (t_1, t_2, \dots) and non-uniform flows ($\frac{dQ}{dx} \neq 0$) for each stream segment (i_1, i_2, \dots) (Bedient and Huber 1992).

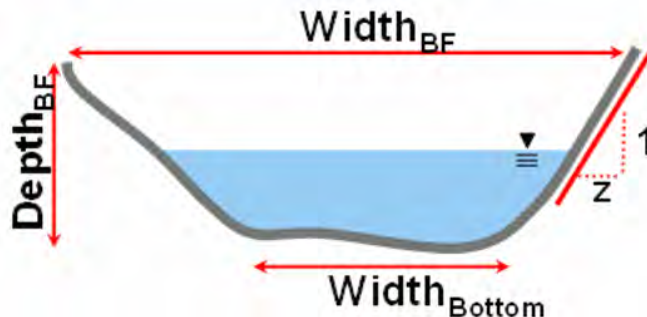


FIGURE 3.3
 Channel Cross-Section
 Represented as a Trapezoid
 and Calculated Dimensions

¹⁴ A **stream segment** is defined as the length of stream that spans one model distance step (dx) and is denoted in listed equations with the subscript 'i'.

Manning's Equation,

$$U = \frac{1}{n} \cdot R_h^{\frac{2}{3}} \cdot S_o^{\frac{1}{2}} \quad (3-1)$$

Flow Volume,

$$Q = A_x \cdot U = \frac{1}{n} \cdot A_x \cdot R_h^{\frac{2}{3}} \cdot S_o^{\frac{1}{2}} \quad (3-2)$$

Hydraulic Radius,

$$R_h = \frac{A_x}{P_w} \quad (3-3)$$

Cross-Sectional Area,

$$A_x = d_w \cdot (W_B + Z \cdot d_w) \quad (3-4)$$

Wetted Perimeter,

$$P_w = W_B + 2 \cdot d_w \cdot \sqrt{1 + Z^2} \quad (3-5)$$

Bottom Width,

$$W_B = W_{BF} - 2 \cdot Z \cdot d_{BF} \quad (3-6)$$

Average Bankfull Depth,

$$\bar{d}_{BF} = \frac{W_{BF}}{W : D} \quad (3-7)$$

Bankfull Depth,

$$d_{BF} = \frac{\bar{d}_{BF}}{\left(\frac{W_{BF} - W_B}{W_{BF}}\right) + \frac{1 - \left(\frac{W_{BF} - W_B}{W_{BF}}\right)}{2}} \quad (3-8)$$

Wetted Width,

$$W_w = W_B + 2 \cdot Z \cdot d_w \quad (3-9)$$

Average Wetted Depth,

$$\bar{d}_w = \left(\frac{W_w - W_B}{W_w}\right) \cdot d_w + \frac{1 - \left(\frac{W_w - W_B}{W_w}\right)}{2} \cdot d_w \quad (3-10)$$

Flow as a Function of Wetted Depth and Other Known Values for Trapezoidal Channel (form of Manning's Equation),

$$Q = \frac{1}{n} \cdot d_w \cdot (W_B + Z \cdot d_w) \cdot \left(\frac{d_w \cdot (W_B + Z \cdot d_w)}{W_B + 2 \cdot d_w \cdot \sqrt{1 + Z^2}}\right)^{\frac{2}{3}} \cdot S_o^{\frac{1}{2}} \quad (3-11)$$

Wetted Depth Calculation Performed with a Newton-Raphson Method,

The Newton-Raphson method offers a computationally efficient procedure for determining the root of a complex mathematical expression. Solution for wetted depth represented in Manning's equation (3-11) offers an application for the Newton-Raphson method that excels over other iterative methods. Below is the technique employed throughout the model to calculate the wetted depth from other wetted dimensions and instream hydraulics. This slope predictor method projects the value of the root by estimating from the first derivative of the function and can quickly converge on a solution stepwise.

Step 1. Write the function so that all variables are on one side and compute first guess of $F(d_w)$,

Recall (3-2),

$$Q = A_x \cdot U = \frac{1}{n} \cdot A_x \cdot R_h^{\frac{2}{3}} \cdot S_o^{\frac{1}{2}}$$

Rearrange to Develop the Function of Depth,

$$F(d_w) = A_x \cdot R_h^{\frac{2}{3}} - \frac{Q \cdot n}{S_o^{\frac{1}{2}}}$$

Step 2. Compute the first derivative of function of depth $F(d_w)$ as follows,

First Derivative of the Function of Depth,

$$F'(d_w) = \frac{F(d_w + \Delta d_w) - F(d_w)}{\Delta d_w}$$

where,

$$\Delta d_w = 0.005 \text{ m}$$

Step 3. Calculate the new approximation for wetted depth (d_w^{k+1}),

Approximation for Wetted Depth,

$$d_w^{k+1} = d_w^k - \frac{F(d_w)}{F'(d_w)}$$

Step 4. Use the new approximation for wetted depth (d_w^{k+1}) to calculate 'Step 1' function of depth $F(d_w)$ and 'Step 2' first derivative of the function of depth $F'(d_w)$. Calculate the 'Step 3' new approximations for wetted depth ($d_w^{k+1, k+2, \dots}$). Repeat until convergence tolerance is achieved.

Convergence Tolerance,

$$|d_w^{k+1} - d_w^k| < 0.0001 \text{ m}$$

Variables,

Measured/Known

- n: Manning's Roughness Coefficient
- S_o : Stream gradient (dimensionless)
- W_{BF} : Bankfull Width (m)
- W : D: Bankfull width to depth ratio (dimensionless)
- Z: Channel Side Slope Ratio (dimensionless)

Calculated

- A_x : Cross-Sectional Wetted Area (m^2)
 - d_{BF} : Bankfull Depth (m)
 - d_w : Water Column Depth (m)
 - \bar{d}_{BF} : Average Bankfull Depth (m)
 - \bar{d}_w : Average Water Column Depth (m)
 - P_w : Wetted Perimeter (m)
 - Q: Flow Rate ($\frac{m^3}{s}$)
 - R_h : Hydraulic Radius (m)
 - U: Average Flow Velocity ($\frac{m}{s}$)
 - W_B : Bottom Width (m)
 - W_w : Wetted Width (m)
-

3.3 DYNAMIC HYDRAULIC FLOW ROUTING

Dynamic water routing methods are based on simultaneous solution of the St. Venant equations for continuity and one-dimensional momentum. Numeric methods are available that approximate solutions to these governing equations. Two such methods are developed and utilized in the Heat Source model and the approximation methodology is discussed in detail in this section. The user has the choice of using either the Muskingum-Cunge method or explicit finite difference method for dynamic hydraulic flow routing approximation.

The Muskingum method uses storage assumptions to calculate the storage terms in the continuity equation. Cunge (1969) modified this method to take the finite difference form of the kinematic wave equation, and thus incorporate the conservation of momentum. The Muskingum-Cunge method is a computationally efficient, numerically stable, physically based numeric approximation. It is less sensitive to bathymetric data gaps or inaccuracies when compared to the explicit finite difference approximation forms of the St. Venant and momentum equations.

The three point centered difference form of the explicit finite difference numeric approximation of the continuity and momentum conservation equations offers a straightforward finite element derivation. Due to stability limits, the numerical approximation scheme is less computationally efficient than the Muskingum-Cunge method. The time step used for the model is dynamic to minimize the finite difference time steps, while ensuring numeric stability (however, there are other forms of instability with this approximation method). This explicit approximation is completely physically based and therefore highly

sensitive to bathometric data. It is fundamentally important that the quality and spatial resolution of bathometric data is excellent. Other forms of instability may result from rapidly varied flows (event driven, highly managed, major mass transfers), which bolsters the concern of the suitability of this numerical solution technique.

The overall performance of each method will vary based on the application. Both methods are included in the model because strong cases can be made for the selection of one method over the other based on the spatial scale of model application, the complexity of system hydrodynamics and data availability.

ST. VENANT GOVERNING EQUATIONS

Continuity Equation (form 1) (Bedient and Huber 1992),

$$\frac{dS}{dt} = Q_i - Q_{i+1} \quad (3-12)$$

Continuity Equation (form 2) (Bedient and Huber 1992),

$$\frac{\partial d_w}{\partial t} + d_w \cdot \frac{\partial U}{\partial x} + U \cdot \frac{\partial d_w}{\partial x} = 0 \quad (3-13)$$

Momentum Equation (Bedient and Huber 1992),

$$\frac{\partial U}{\partial t} + U \cdot \frac{\partial U}{\partial x} + g \cdot \frac{\partial d_w}{\partial x} = g \cdot (S_o - S_f) \quad (3-14)$$

Flows Assumed to be Unsteady and Varied (Non-Uniform)

$$\frac{\partial d_w}{\partial t} \neq 0, \quad \frac{\partial U}{\partial t} \neq 0 \quad \text{and} \quad \frac{\partial d_w}{\partial x} \neq 0, \quad \frac{\partial U}{\partial x} \neq 0 \quad (3-15)$$

Variables,

Measured/Known

g: Acceleration of Gravity ($9.8 \frac{m}{s^2}$)

S_o: Stream gradient (unitless)

t: Time (s)

x: Longitudinal Distance (m)

Calculated

d_w: Average Water Column Depth (m)

Q: Flow Rate ($\frac{m^3}{s}$)

S: Storage (m³)

S_f: Friction slope (unitless)

U: Average Flow Velocity ($\frac{m}{s}$)

3.3.2 MUSKINGUM-CUNGE APPROXIMATION

Conceptually the storage volume of water for any time 't' is the prism and the wedge storage of the stream segment 'i' (see **Figure 3.4**). The theoretical wedge that forms the basis for the Muskingum Method can occur in the upstream or downstream direction depending on whether flows are increasing ($Q_i > Q_{i+1}$) or decreasing ($Q_i < Q_{i+1}$) over the longitudinal distance. A basic assumption of this method is that the cross-sectional area (A) as defined by Manning's equation is proportional to flow rate for any give stream segment. Such an assumption allows the volume storage (S) to become a function of discharge, the ratio of storage to discharge (K) and a weighting factor (X) that controls the wedge height and thus, the wedge storage that occurs in response to flow rate changes over a stream segment. Cunge (1969) shows that the Muskingum expression represents the kinematic wave equation when the effects of diffusion are included.

The following derivation develops the Muskingum-Cunge finite difference solution used to simulate dynamic flow routing. It is important to consider that the calculation of wetted channel dimensions (d_w, W_w, A_x, P_w, R_h) and Manning's velocity (U) at each distance and time steps is necessary for this method. Where these terms are listed, such calculations are performed as a function of constant and known parameters ($W_{BF}, W_B, d_{BF}, Z, S_o$) and flow rate (Q).

The procedure for approximating the Muskingum-Cunge finite approximation follows a three point scheme. The derivation of the partial derivatives relies on a three point finite difference form, largely taken from Bedient and Huber (1992).

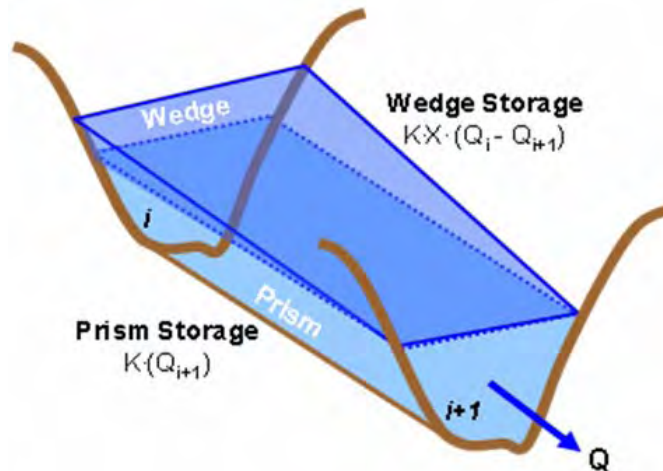


FIGURE 3.4
 Muskingum-Cunge Wedge
 and Prism Storage

Recall the Continuity Equation Form 1 (3-12),

$$\frac{dS}{dt} = Q_i - Q_{i+1}$$

Volume Storage (S) (Bedient and Huber 1992),

$$S = K \cdot Q_{i+1} + K \cdot X \cdot (Q_i - Q_{i+1}) \quad (3-16)$$

Change in Flow (ΔQ) with Respect to Stream Segment (Cunge 1969),

$$\Delta Q = (Q_i - Q_{i+1}) = K \cdot \frac{d}{dt} [X \cdot Q_i + (1 - X) \cdot Q_{i+1}] \quad (3-17)$$

Finite Difference Form of (3.17) (Bedient and Huber 1992),

$$\begin{aligned} \frac{K}{dt} \cdot [X \cdot Q_i^{t+1} + (1 - X) \cdot Q_{i+1}^{t+1} - X \cdot Q_i^t - (1 - X) \cdot Q_{i+1}^t] \\ = \frac{1}{2} \cdot [Q_i^{t+1} - Q_{i+1}^{t+1} + Q_i^t - Q_{i+1}^t] \end{aligned} \quad (3-18)$$

It can be shown that when $K = dx/c_K$ that equation (3-18) is the finite difference form of the kinematic wave equation (3-19) provided that $c_K = dQ/dA_x$ and diffusion is included (Bedient and Huber 1992).

Kinematic Wave Equation,

$$\frac{\partial Q}{\partial t} + c_K \cdot \frac{\partial Q}{\partial x} = D_x \cdot \frac{\partial^2 Q}{\partial x^2} \quad (3-19)$$

Wave Celerity (c_K) (Bedient and Huber 1992),

$$c_K = \frac{dQ}{dA_x} = \frac{5}{3} \cdot U = \frac{5}{3} \cdot \left(\frac{R_h^{2/3} \cdot S_o^{1/2}}{n} \right) \quad (3-20)$$

Diffusion Coefficient (D_x) (Bedient and Huber 1992),

$$D_x = \left(\frac{1}{2} - X \right) \cdot c_K \cdot dx \quad (3-21)$$

The weighting factor¹⁵ ($0 \leq X \leq 0.5$) can be calculated (or input by the user) (Bedient and Huber 1992),

$$X = \frac{1}{2} - \frac{D_x}{c_K \cdot dx} = \frac{1}{2} - \frac{\frac{1}{2} \cdot \frac{Q}{W_W \cdot S_o}}{c_K \cdot dx} = \frac{1}{2} \cdot \left(1 - \frac{Q}{c_K \cdot dx} \right) \quad (3-22)$$

¹⁵ The weighting factor (X) will be zero when there is no wedge storage (in most cases this term is zero in reservoirs and greater than zero in flowing stream and river reaches. For natural river flows, X will usually be between 0.1 and 0.3, with an average value of 0.2.

The Muskingum coefficients are calculated as follows (Bedient and Huber 1992),

$$C_1 = \frac{dt - (2 \cdot K \cdot X)}{D} \qquad C_2 = \frac{dt + (2 \cdot K \cdot X)}{D}$$

$$C_3 = \frac{[2 \cdot K \cdot (1 - X)] - dt}{D} \qquad D = 2 \cdot K \cdot (1 - X) + dt$$

$$\sum C = C_1 + C_2 + C_3 + C_4 = 0 \qquad (3-23)$$

The Muskingum method finite difference form of (3-19) then becomes,

$$Q_{i+1}^{t+1} = C_1 \cdot Q_i^{t+1} + C_2 \cdot Q_i^t + C_3 \cdot Q_{i+1}^t \qquad (3-24)$$

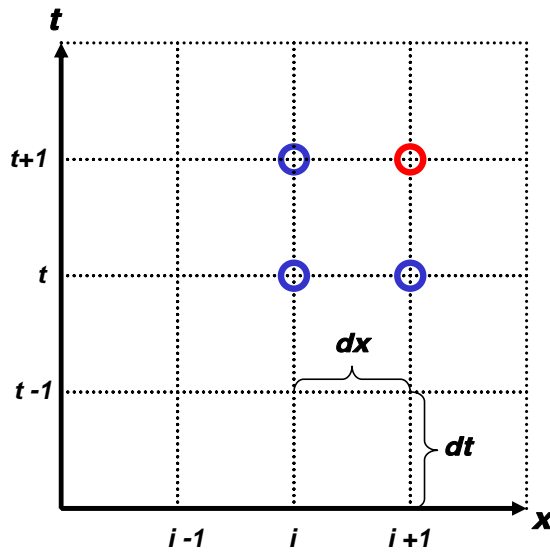


FIGURE 3.5
 Muskingum-Cunge Finite Difference Scheme

Variables,

Measured/Known

- dx: Model Distance Step (m)
- dt: Model Time Step (s)
- n: Manning's Roughness Coefficient
- S_o: Stream gradient (unitless)
- t: Time (s)
- x: Longitudinal Distance (m)

Calculated

- A_x: Cross-Sectional Wetted Area (m²)
 - c_K: Wave Celerity ($\frac{m}{s}$)
 - C₁...C₃: Muskingum Coefficients
 - D_x: Diffusion Coefficient ($\frac{m^2}{s}$)
 - d_w: Average Water Column Depth (m)
 - K: Travel time Parameter (s)
 - R_h: Hydraulic Radius (m)
 - Q: Flow Rate ($\frac{m^3}{s}$)
 - S: Storage (m³)
 - U: Average Flow Velocity ($\frac{m}{s}$)
 - X: Wedge Weighting Coefficient
 - W_w: Wetted Width (m)
-

3.3.2 EXPLICIT FINITE DIFFERENCE METHOD

The derivation of the explicit method for flow routing based on the equations of continuity and conservation of momentum originated with Stoker (1957) and Issacson et al. (1956). While derivations of the finite forms are limitless and computational power has increased dramatically, the basic approach for approximating solutions using the explicit method has remained unchanged. The following example is for a three point central difference approximation. The governing equations are the St. Venant equations:

Recall the Continuity Equation (form 2) (3-13),

$$\frac{\partial d_w}{\partial t} + d \cdot \frac{\partial U}{\partial x} + U \cdot \frac{\partial d_w}{\partial x} = 0$$

Recall the Conservation of Momentum Equation (3-14),

$$\frac{\partial U}{\partial t} + U \cdot \frac{\partial U}{\partial x} + g \cdot \frac{\partial d_w}{\partial x} - g \cdot (S_o - S_f) = 0$$

The procedure for approximating the continuity equation and the conservation of momentum equation follows basic finite approximation schemes. The partial derivatives are written in three point finite difference forms with respect to distance 'i' and time 't'. These forms are then substituted into the two governing

equations and rearranged to solve for the central difference parameter in time t . The time step (dt) must be small relative to the distance step (dx) to calculate an accurate approximate. The stability conditions listed in (3-30) and (3-31) will ensure that this assumption is correct and prevent numeric instability and minimize numerical diffusion. The smaller of the two time step values should be used.

THE COMPUTATIONAL PROCEDURE CONSISTS OF THE FOLLOWING STEPS:

- (1) Determine stability condition for each distance step 'i' for the time step 't' using the Courant (3-30) and friction stability equations (3-31). For each time 't' calculate the smallest dt value for all segments 'i'.
- (2) Solve for $d_{w_i}^t$ using the finite difference form of the continuity equation (3-26)
- (3) Calculate the friction slope(s_f) from equation (3-28)
- (4) Solve for U_i^t using the finite difference form of the conservation of momentum equation (3-29)
- (5) Calculate Q_i^t as a function of $d_{w_i}^t$ and U_i^t

Finite Difference Form of the Derivatives,

$$\begin{aligned}\frac{\partial U}{\partial x} &= \frac{U_{i+1}^{t-1} - U_{i-1}^{t-1}}{2 \cdot dx} & \frac{\partial U}{\partial t} &= \frac{U_i^{t-1} - U_i^t}{dt} \\ \frac{\partial d_w}{\partial x} &= \frac{d_{w_{i+1}}^{t-1} - d_{w_{i-1}}^{t-1}}{2 \cdot dx} & \frac{\partial d_w}{\partial t} &= \frac{d_{w_i}^{t-1} - d_{w_i}^t}{dt}\end{aligned}\quad (3-25)$$

Substitution into the Continuity Equation (3-13) yields,

$$\frac{d_{w_i}^{t-1} - d_{w_i}^t}{dt} + d_{w_i}^{t-1} \cdot \left(\frac{U_{i+1}^{t-1} - U_{i-1}^{t-1}}{2 \cdot dx} \right) + U_i^{t-1} \cdot \left(\frac{d_{w_{i+1}}^{t-1} - d_{w_{i-1}}^{t-1}}{2 \cdot dx} \right) = 0$$

Which is rearranged to represent the Finite Difference Form of the Continuity Equation,

$$d_{w_i}^t = d_{w_i}^{t-1} + \frac{dt}{2 \cdot dx} \cdot \left[d_{w_i}^{t-1} \cdot (U_{i+1}^{t-1} - U_{i-1}^{t-1}) + U_i^{t-1} \cdot (d_{w_{i+1}}^{t-1} - d_{w_{i-1}}^{t-1}) \right] \quad (3-26)$$

Substitution into (3-14) Conservation of Momentum Equation yields,

$$\frac{U_i^{t-1} - U_i^t}{dt} + U_i^{t-1} \cdot \frac{U_{i+1}^{t-1} - U_{i-1}^{t-1}}{2 \cdot dx} + g \cdot \frac{d_{w_{i+1}}^{t-1} - d_{w_{i-1}}^{t-1}}{2 \cdot dx} = g \cdot (S_o - S_f)$$

Which is rearranged to represent the Finite Difference Form of the Conservation of Momentum Equation (3-14),

$$\begin{aligned}U_i^t &= U_i^{t-1} + \frac{dt}{2 \cdot dx} \cdot U_i^{t-1} \cdot (U_{i+1}^{t-1} - U_{i-1}^{t-1}) \\ &\quad + \frac{dt \cdot g}{2 \cdot dx} \cdot (d_{w_{i+1}}^{t-1} - d_{w_{i-1}}^{t-1}) - dt \cdot g \cdot (S_o - S_f)\end{aligned}\quad (3-27)$$

For a trapezoidal channel where $U = \frac{U_{i+1}^{t-1} + U_{i-1}^{t-1}}{2}$ the friction slope becomes,

$$S_f = \frac{U^2 \cdot n^2}{R_h^{\frac{4}{3}}} = \frac{U^2 \cdot n^2}{\left(\frac{A_x}{P_w}\right)^{\frac{4}{3}}} = \frac{U^2 \cdot n^2}{R_h^{\frac{4}{3}}} = \frac{\left(\frac{U_{i+1}^{t-1} + U_{i-1}^{t-1}}{2}\right)^2 \cdot n^2}{\left(\frac{d_{w_i}^t \cdot (W_B + Z \cdot d_{w_i}^t)}{W_B + 2 \cdot d_{w_i}^t \cdot \sqrt{1 + Z^2}}\right)^{\frac{4}{3}}} \quad (3-28)$$

Substitution of (3-28) into (3-27) provides the final finite difference form of the Conservation of Momentum Equation,

$$U_i^t = U_i^{t-1} + \frac{dt}{2 \cdot dx} \cdot U_i^{t-1} \cdot (U_{i+1}^{t-1} - U_{i-1}^{t-1}) + \frac{dt \cdot g}{2 \cdot dx} \cdot (d_{w_{i+1}}^{t-1} - d_{w_{i-1}}^{t-1}) - dt \cdot g \cdot \left[S_o - \frac{\left(\frac{U_{i+1}^{t-1} + U_{i-1}^{t-1}}{2}\right)^2 \cdot n^2}{\left(\frac{d_{w_i}^t \cdot (W_B + Z \cdot d_{w_i}^t)}{W_B + 2 \cdot d_{w_i}^t \cdot \sqrt{1 + Z^2}}\right)^{\frac{4}{3}}} \right] \quad (3-29)$$

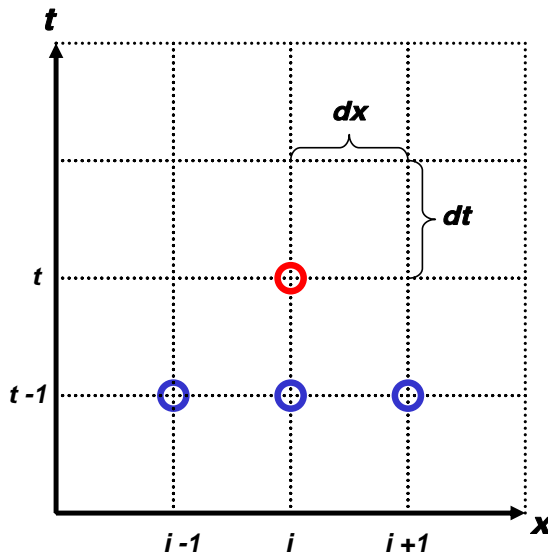


FIGURE 3.6
Explicit Finite Difference Scheme

COURANT STABILITY,

$$dt \leq \frac{dx}{U + c} \leq \frac{dx}{U + \sqrt{g \cdot d_w}} \quad (3-30)$$

FRICION STABILITY,

$$dt \leq \frac{R_h^{\frac{4}{3}}}{g \cdot n^2 \cdot U} \quad (3-31)$$

Variables,

Measured/Known

- dx: Model Distance Step (m)
- dt: Model Time Step (s)
- g: Acceleration of Gravity ($9.8 \frac{m}{s^2}$)
- n: Manning's Roughness Coefficient
- S_o : Stream gradient (unitless)
- t: Time (s)
- x: Longitudinal Distance (m)
- Z: Channel Side Slope Ratio (dimensionless)

Calculated

- A_x : Cross-Sectional Wetted Area (m^2)
 - \bar{d}_w : Average Water Column Depth (m)
 - P_w : Wetted Perimeter (m)
 - R_h : Hydraulic Radius (m)
 - Q: Flow Rate ($\frac{m^3}{s}$)
 - S_f : Friction Slope (unitless)
 - U: Average Flow Velocity ($\frac{m}{s}$)
 - W_B : Bottom Width (m)
 - W_w : Wetted Width (m)
-

3.3.3 COMPARISON OF METHODS

The Muskingum-Cunge method simulates volume storage and dynamic flow routing using a finite difference solution that is based on the continuity and kinematic wave equations. There are several methods available for dynamic flow routing, each requiring different kinds of data input and each offering varying degrees computational stability and accuracy. Of these, the Muskingum-Cunge method is particularly suited for simulation of hydrodynamics over large and complex stream systems. Channel bathymetric data is often unavailable over a large hydrologic scale. While such data is required for *accurate* explicit solutions to complete unsteady hydraulic models, the Muskingum-Cunge method allows for less bathymetric detail since segment storage is approximated (Bedient and Huber 1992). Segment storage and flow routing is simulated as a function of derived spatial channel data (geometry and slope) and input values for channel roughness (n) and wedge storage (X). The numeric approximation is relatively efficient and stable, even in highly varied flow regimes. The methodology is fundamentally dependent on the assumption of wedge storage and travel time approximations. Inherent to these approximations are Manning's based calculations that span time and distance steps, for which it is assumed that flows are steady and uniform. The duration of the time step may become a limiting factor, if in fact, flows vary over the course of any one time step. The same concern also applies to the distance step. However, it is likely that finite difference mesh size will not pose these limiting factors when time and distance steps are small (for example: dt = one minute, dx = 100 meters).

The explicit finite difference method simulates storage of volume in stream segments and dynamic flow routing using an approximation that is based on the continuity and conservation of momentum equations. In general, the explicit method is used to simulate dynamic flows over well defined river reaches where channel data is robust. Storage within a segment is completely dependent on channel bathymetry and frictional forces. Therefore, the sensitivity to bathymetric data is very high, facilitating the need for accurate and spatially varied channel geometry and elevation data. The need for such data can create a potential problem when applying this method since it is likely that such data (in the detail required) is not available for most stream systems over a large spatial extent. It is generally not acceptable to rely on assumed input values for data parameters in which model sensitivity is high. For this reason alone, it may prove difficult to apply the explicit finite difference method to large stream/river systems or in stream/river segments where bathymetric data is limited.

An additional limitation to the explicit finite difference approximation is model stability. Both the Courant and frictional stability conditions must be met at all times, adding several important consequences. Depending on wave celerity and flow velocity, computational efficiency may be reduced since the time step must change to accommodate variations in these parameters. Beyond these traditional explicit method stability concerns, the method is not stable when flows, velocities or depths are highly variable. Therefore highly managed flows (withdrawals, point sources, etc.) or naturally variable flows (springs, large tributaries, flashy flows, etc.) become difficult to simulate using the explicit method.

Table 3.1
 Summary of Muskingum-Cunge and Explicit Finite Difference Methods

	Muskingum-Cunge	Explicit Finite Difference
Governing Equations	-Continuity Equation -Kinematic Wave Equation	-Continuity Equation -Conservation of Momentum Equation
Bathometric Data Requirements	-Moderate	-Very High
Computational Efficiency	-Efficient	-Low to Moderately Efficient -Variable time step is required for model stability
Stability Requirements	-Highly Stable	-Moderately Stable -Courant Stability Condition -Friction Stability Condition -Unstable with Variable Flows
Varied Flow Limitations	-None (Provided that $Q > 0$)	-Severely Limited -Flows, velocity and depths must vary gradually
Assumptions	-Wedge storage is accurately represented -Travel time is accurately represented -Manning's calculations are appropriate over any given time and distance step	-Vertical acceleration is negligible when compared to total acceleration -Boundary friction is accurately represented -Manning's calculations are appropriate over any given time and distance step -Tributary flows or withdrawals do not significantly change instream flows -Flows are not highly managed -Manning's calculations are appropriate over any given time and distance step
Common Applications	-Watershed Scaled Modeling -Stream Network Modeling	-River Reach Modeling -Flood waves -Tidal flows -Waves generated by slow control structures (sluice gates, gates, locks, etc.)

3.4 QUANTIFYING EXTERNAL MASS TRANSFERS

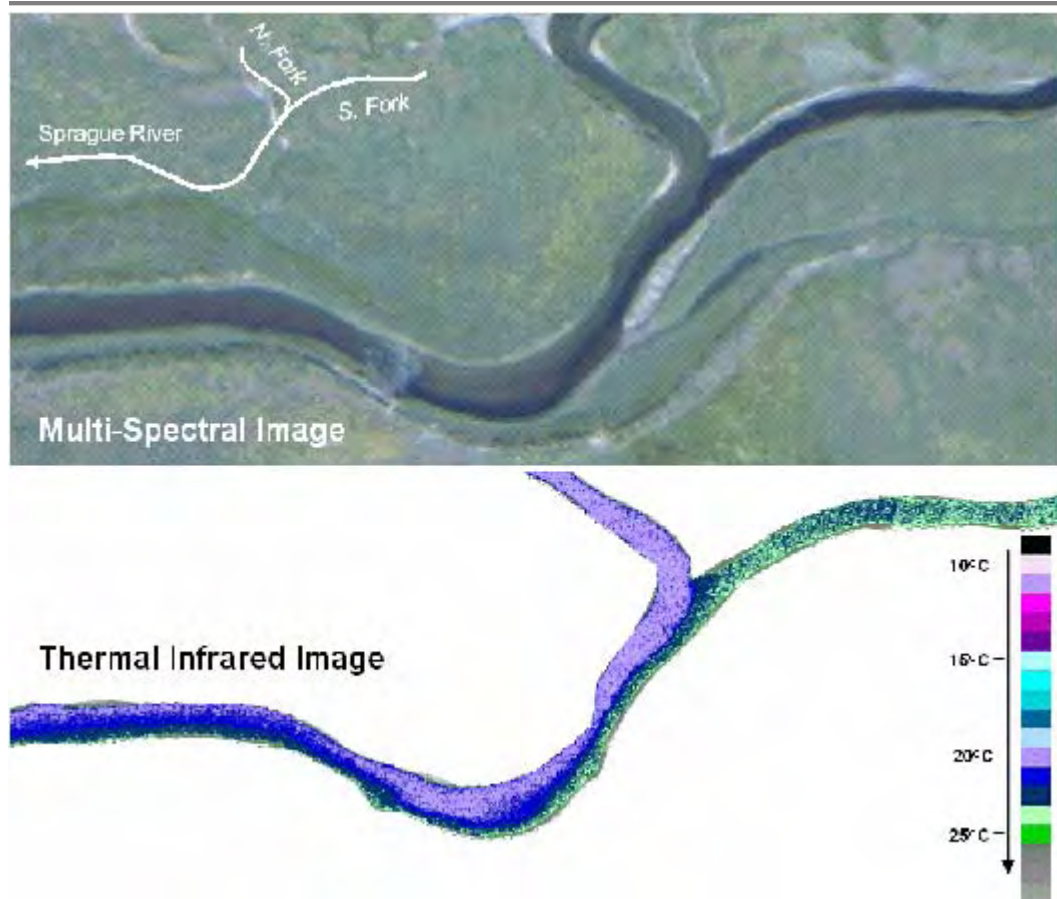


FIGURE 3.7
Example of mixing at a confluence (North and South Forks of the Sprague River, Oregon)

3.4.1 TEMPERATURE CHANGE RESULTING FROM MIXING

Receiving water mixing of inflows from surface and subsurface sources will result in the change in temperature and heat as a function of flow volumes and associated water temperatures. Such mass transfers occur at specific locations and can have pronounced heating or cooling effects. The thermal effect of mixing is more localized and pronounced than temperature changes resulting from heat transfer process. The temperature resulting from mixing two volumes (or flow rates) is easily calculated.

Resulting Temperature after Complete Mix with Inflow,

$$T_{Wi} = \frac{(T_{Wi} \cdot Q_i) + (T_{IN} \cdot Q_{IN})}{(Q_i + Q_{IN})} \quad (3-32)$$

Variables,

Calculated

- Q: Flow Rate ($\frac{m^3}{s}$)
- Q_{IN} : Inflow Rate ($\frac{m^3}{s}$)
- T_{IN} : Inflow Temperature ($^{\circ}C$)
- T_W : Water Temperature ($^{\circ}C$)

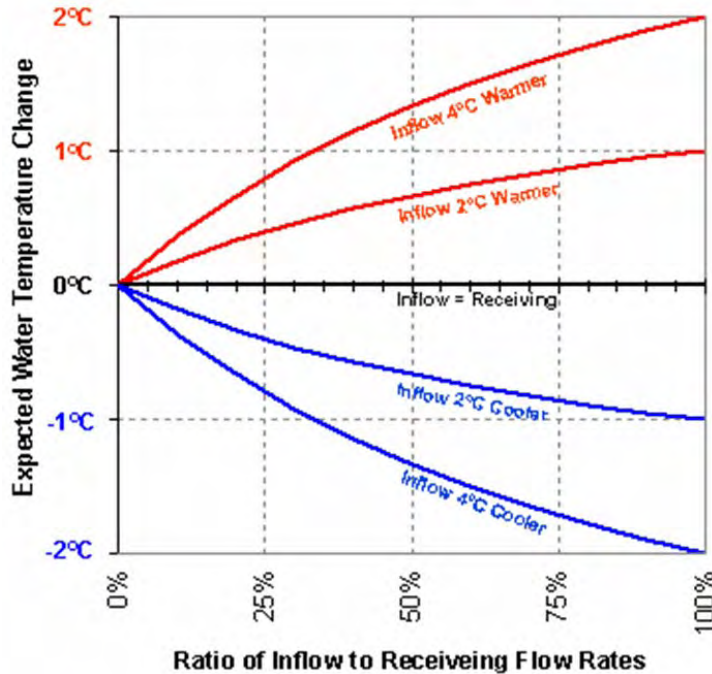


FIGURE 3.8.
 Temperature Changes that Accompany Mixing

3.4.2 THERMAL INFRARED RADIOMETRY DERIVED MASS BALANCE APPROACH

Remote sensing using thermal infrared radiometry (TIR) can easily identify areas where heat change occurs due to mixing with surface and subsurface waters. All water temperatures are apparent in TIR sampled stream temperature data, and provided that at least one instream flow rate is known, the other flow rates can be calculated. In this fashion, TIR sampled stream temperature data can be used to develop a mass balance for stream flow using minimal ground level data collection points. Simply identifying mass transfer areas is an important step in quantifying heat transfer within a stream network. For example, using TIR data, thirty-one discrete mass transfer processes were located and quantified in the North Fork Sprague River, Oregon (Boyd and Kasper 2002). Several of the subsurface mass transfer areas were unmapped and the relative thermal and hydrologic impact to the stream system was not previously quantified. Further, surface returns from agriculture irrigation were previously unmapped, and consequently were not quantified in terms of flow rates or temperatures.

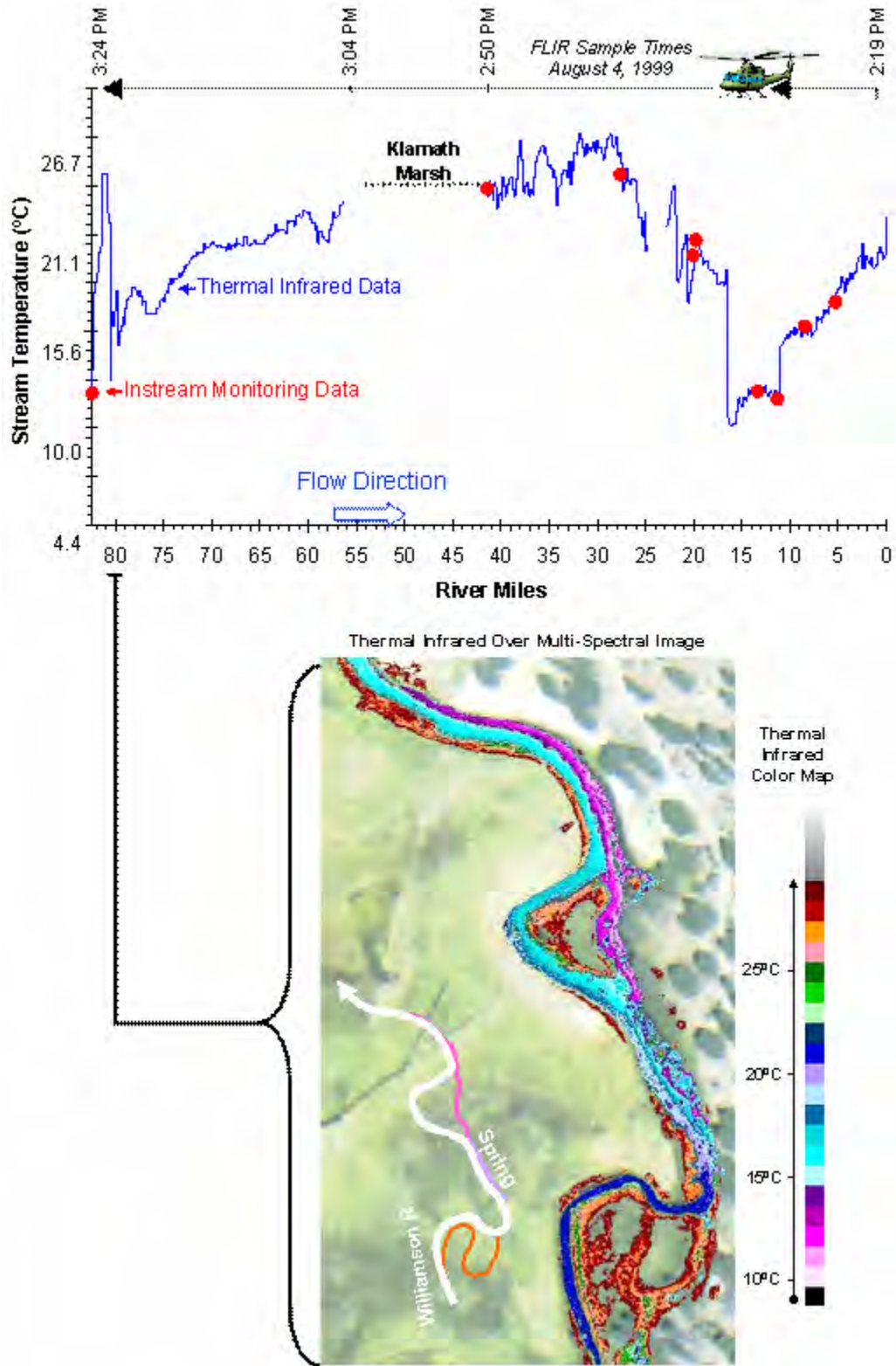


FIGURE 3.9
(Above) Instream and TIR Monitoring Data. (Below) An Example of TIR Imagery – Cooling from a Spring (River Miles 80.41 to 80.65 Williamson River, Oregon)

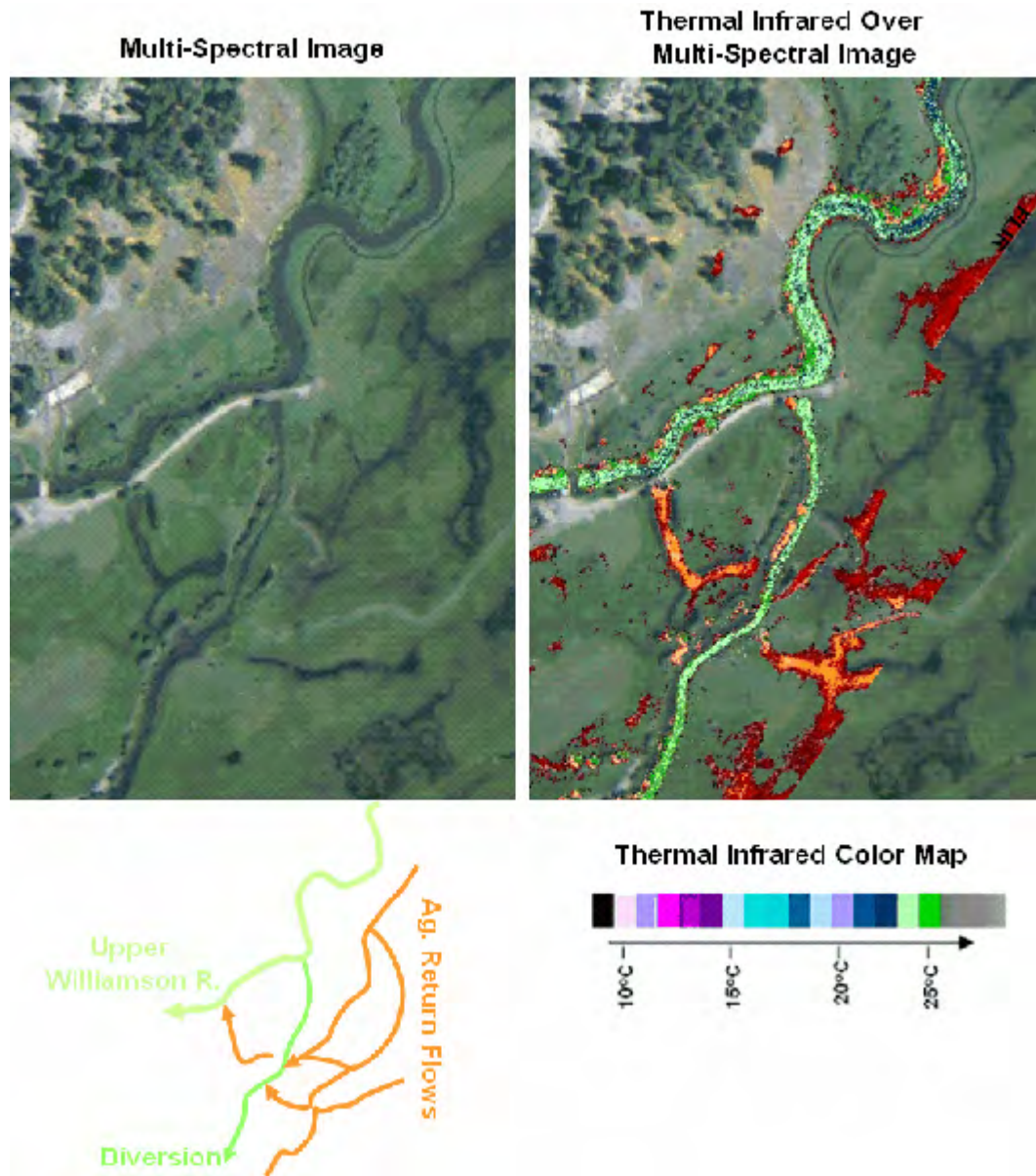


FIGURE 3.10
Water Withdrawal and Return Flows Located and Measured with TIR remote sensing (Williamson River, Oregon)

Water volume losses are often visible in TIR imagery since diversions and water withdrawals usually contrast with the surrounding thermal signature of landscape features (see **Figure 3.10**). Highly managed stream flow regimes can become complicated where multiple diversions and return flows mix or where flow diversions and returns are unmapped and undocumented. In such cases it becomes important to establish the direction of flow (i.e. influent or effluent). With the precision afforded by TIR sampled stream temperatures, effluent flows can be determined when temperatures are the same. Temperature differences indicate that the flow is influent. This holds true even when observed

temperature differences are very small. The rate of water loss from diversions or withdrawals cannot be easily calculated. Oregon DEQ estimates water withdrawal flow rates from the water right information maintained by Oregon Water Resources Department (OWRD).

A mass balance can be developed from relatively few instream measurements, FLIR stream temperature data and water rights data. Potential flow rates¹⁶ are easily calculated by removing all water withdrawals and agriculture return flows. An example of a derived mass balance is presented in **Figure 3.11**.

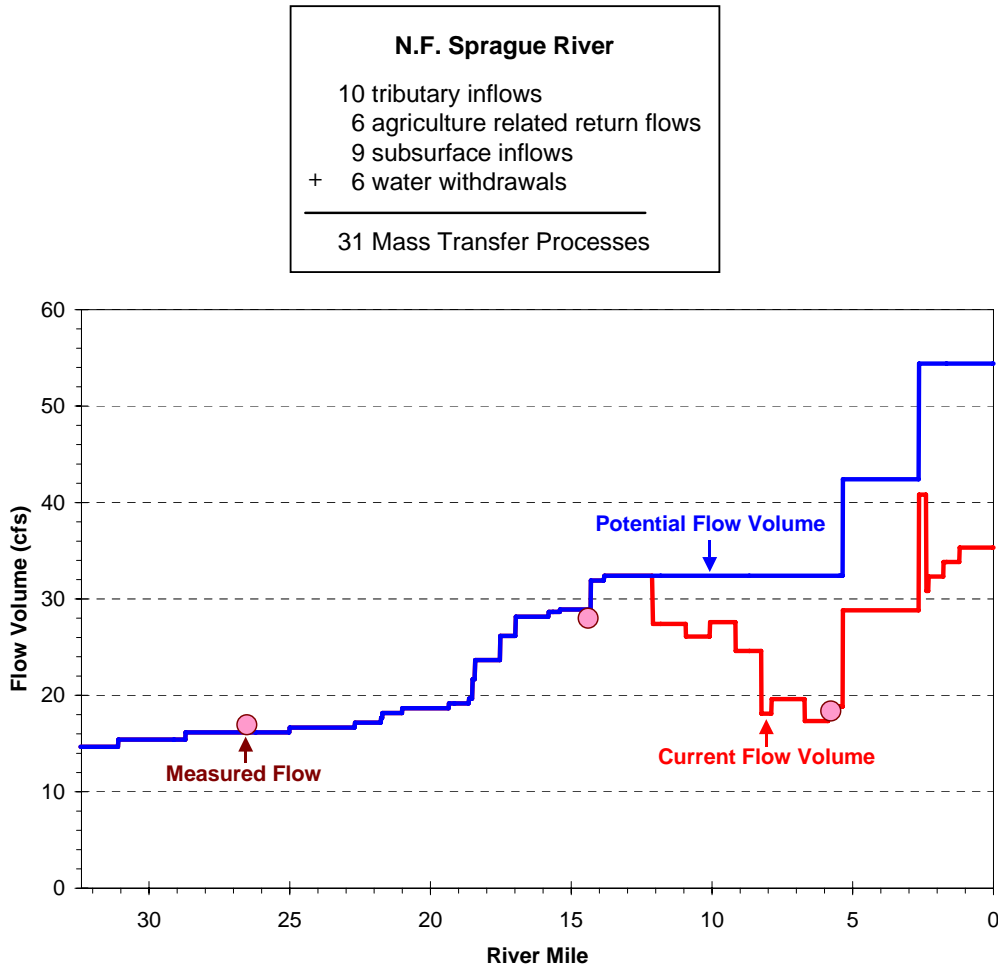


FIGURE 3.11
Mass balance developed using instream gage data, TIR temperature data and water rights data (North Fork Sprague River, Oregon)

¹⁶ In this case, potential flow rate refers to the flow condition that would exist without anthropogenic modifications (withdrawals, returns, discharges, augmentation).

DISCUSSION OF ASSUMPTIONS AND LIMITATIONS FOR TIR DATA BASED MASS BALANCE METHODOLOGY

Small mass transfer processes cannot be accounted since TIR data often has an accuracy of $\pm 0.5^{\circ}\text{C}$. A limitation of the methodology is that only mass transfer processes with measured ground level flow rates or those that cause a TIR quantifiable change in stream temperature with the receiving waters (i.e. identified by TIR data) can be analyzed and included in the mass balance. For example, a tributary with an unknown flow rate that cause small temperature changes (i.e. less than $\pm 0.5^{\circ}\text{F}$) to the receiving stream cannot be accurately included. *This assumption can lead to an under estimate of influent mass transfer processes.*

Limited ground level flow data limit the accuracy of derived mass balances. Errors in the calculations of mass transfer can become cumulative and propagate in the methodology since validation can only be performed at sites with known flow rates. *These mass balance profiles should be considered estimates of a steady state flow condition.*

Water withdrawals are not directly quantified. Instead, water right data is simply the upper limit of volume allowed to be withdrawn. An assumption is made that these water rights are being used if water availability permits. *This assumption can lead to an over estimate of water withdrawals.*

Water withdrawals are assumed to occur only at mapped points of diversion sites or those visible in TIR data. There may be additional diversions occurring throughout the stream network (small pumps, piped flows, etc.). *This assumption can lead to an underestimate of water withdrawals and an under estimate of potential flow rates.*

Return flows may deliver water that is diverted from another watershed. In some cases, irrigation canals transport diverted water to application areas in another drainage. This is especially common in low gradient meadows, cultivated fields and drained wetlands used for agriculture production. *When return flows are removed in the potential flow condition this assumption can lead to an under estimate of potential tributary flow rates.*

3.4.3 SURFACE INFLOWS (SPRINGS, TRIBUTARIES AND RETURN FLOWS)

Surface inflows (tributaries, springs, and return flows) are associated in the model with longitudinal stream distances, and thus, with model reaches. The total number of model reaches is a function of the distance step (dx), which is user defined, and the simulation longitudinal distance. Several surface inflows in close proximity creates a possibility that more than one surface inflow is associated with any given model reach over the distance step. The methodology accounts for all surface inflows and their associated temperatures, and mixes these inflows with the water column.

Instantaneous Flow Summation of Surface Inflows,

$$Q_{\text{TRIB}i}^t = \sum_{i=1}^i Q_{\text{TRIB}}^t \quad (3-33)$$

Instantaneous Flow Weighted Temperature of Surface Inflows,

$$T_{\text{TRIB}_i}^t = \frac{\sum_{i-1}^i (T_{\text{TRIB}^t} \cdot Q_{\text{TRIB}^t})}{\sum_{i-1}^i Q_{\text{TRIB}^t}} \quad (3-34)$$

Resulting Temperature after Complete Mix with Surface Inflow,

$$T_{W_i}^t = \frac{(T_{W_i}^t \cdot Q_i^t) + (T_{\text{TRIB}_i}^t \cdot Q_{\text{TRIB}_i}^t)}{(Q_i^t + Q_{\text{TRIB}_i}^t)} \quad (3-35)$$

Variables,

Measured/Known

dx: Model Distance Step (m)

Q_{TRIB^t} : Surface Inflow Flow Rate ($\frac{\text{m}^3}{\text{s}}$)

T_{TRIB^t} : Surface Inflow Temperature ($^{\circ}\text{C}$)

Calculated

Q: Flow Rate ($\frac{\text{m}^3}{\text{s}}$)

Q_{TRIB} : Instantaneous Flow Summation of Surface Inflows ($\frac{\text{m}^3}{\text{s}}$)

T_{TRIB} : Instantaneous Flow Weighted Temperature of Surface Inflows ($^{\circ}\text{C}$)

T_W : Water Column Temperature ($^{\circ}\text{C}$)

3.4.4 SUBSURFACE INFLOWS (SEEPS, SPRINGS AND ACCRETION FLOWS)

In a similar fashion as used for surface inflows, subsurface inflows (seeps, spring and accretion flows) are associated with model reaches. The total subsurface inflow rate and the flow volume weighted average temperature are mixed with the model reach water column.

Instantaneous Summation of Subsurface Inflows,

$$Q_{\text{GW}_i}^t = \sum_{i-1}^i Q_{\text{GW}^t} \quad (3-36)$$

Instantaneous Flow Weighted Temperature of Subsurface Inflows,,

$$T_{\text{GW}_i}^t = \frac{\sum_{i-1}^i (T_{\text{GW}^t} \cdot Q_{\text{GW}^t})}{\sum_{i-1}^i Q_{\text{GW}^t}} \quad (3-37)$$

Resulting Temperature after Complete Mix with Subsurface Inflows,

$$T_{W_i}^t = \frac{(T_{W_i}^t \cdot Q_i^t) + (T_{\text{GW}_i}^t \cdot Q_{\text{GW}_i}^t)}{(Q_i^t + Q_{\text{GW}_i}^t)} \quad (3-38)$$

Variables,

Measured/Known

dx: Model Distance Step (m)

Q_{GW} : Subsurface Inflow Flow Rate ($\frac{m^3}{s}$)

T_{GW} : Subsurface Inflow Temperature ($^{\circ}C$)

Calculated

Q: Flow Rate ($\frac{m^3}{s}$)

Q_{GW} : Instantaneous Flow Summation of Subsurface Inflows ($\frac{m^3}{s}$)

T_{GW} : Instantaneous Flow Weighted Temperature of Subsurface Inflows ($^{\circ}C$)

T_w : Water Column Temperature ($^{\circ}C$)

3.4.5 HYPORHEIC FLOWS

Hyporheic flows occur when surface water from a stream or river infiltrates into the *alluvial aquifer* and eventually travel back to the surface water column down gradient (Poole and Berman 2001, Poole et al. 2000). *Alluvium* comprised of depositional materials and substrate underlies the stream channel. This material is sorted to some degree by tractive forces and shear stress associated with surface high flow conditions. The distribution of alluvium can vary significantly within the channel and across the floodplain. The supply of sediments and the flows patterns during peak flow events affect the distribution and type of sediment found in the alluvium.

The *alluvial aquifer* refers to the water that occupies the interstitial spaces in the alluvium. This water moves directionally based on the elevation of the stream water column relative to the shallow groundwater elevation. If the shallow ground water elevation is lower than the surface water column elevation, the potential energy gradient will be directed away from the stream. In this case, water will likely be lost from the stream to the alluvial aquifer. If this water stays in the alluvial aquifer, and is not lost to deeper subsurface storage less prone to be connected to down gradient surface waters, it will reemerge back to the surface water column when the potential energy gradient is directed from the alluvial aquifer to the stream. The rate of hyporheic water movement depends on the hydraulic head (potential energy) and physical properties of the alluvium. Consider that water is incompressible. If we assume that water lost to deeper ground water sources is negligible, then a discrete volume transferred to the alluvial aquifer from surface waters must result in an equal volume transferred back to surface waters from the alluvial aquifer.

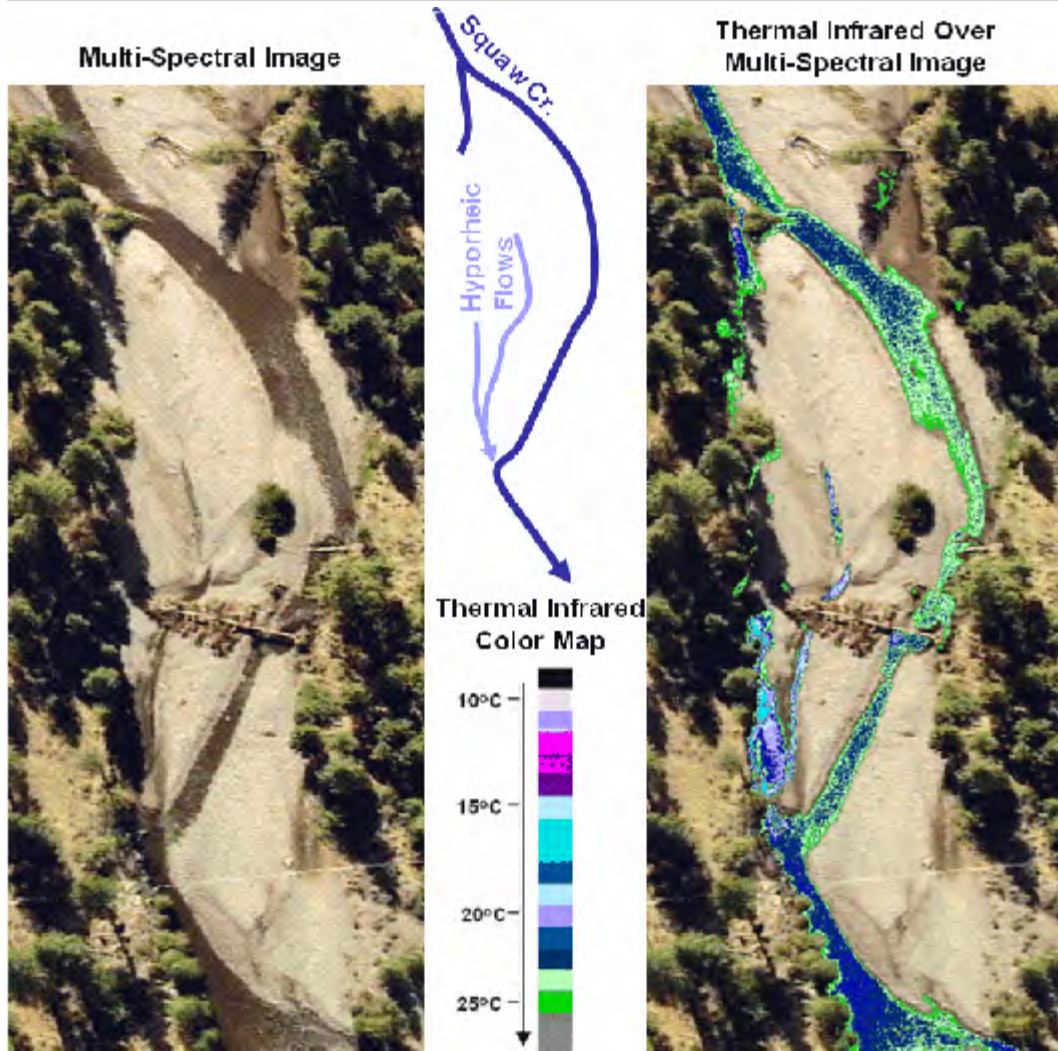


FIGURE 3.12
 Hyporheic flows through stream bar substrate (Squaw Creek, Oregon)

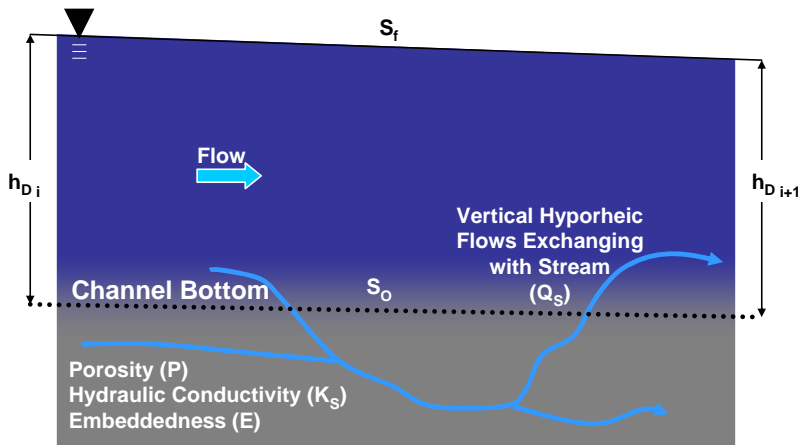


FIGURE 3.13
 Surface and subsurface parameters used to calculate hyporheic exchange

Darcy's Law is used to calculate the seepage flow exchange with water column flows as a function of hydraulic head, seepage cross-sectional area and hydraulic conductivity. It is assumed that hyporheic flows are conserved (volume is not lost from the water column or saturated streambed via this process). This assumption allows that hyporheic flow additions at the downstream boundary of a stream segment are accompanied by equal water column additions at the upstream boundary. The cross-sectional area of the seepage face (A_S) is the product of the seepage face thickness (h_S) and the wetted perimeter (P_W) of the channel. The hydraulic head is calculated as a function of streambed slope, friction slope and stream depth.

Darcy's Law for Calculating for Hyporheic Flow (Domenico and Schwartz 1990),

$$Q_{hyp} = A_S \cdot K_S \cdot \frac{dh_D}{dx} \quad (3-33)$$

Change in hydraulic head per unit distance,

$$\frac{dh_D}{dx} = \frac{(h_{D_i} - h_{D_{i+1}})}{dx} \quad (3-34)$$

Cross-Sectional Area of the Seepage Face,

$$A_S = h_S \cdot P_W \quad (3-35)$$

Seepage Face Thickness,

$$h_S = dx \cdot S_o \quad (3-36)$$

Hydraulic Head Calculations,

$$h_{D_i} = d_{W_i} \quad (3-37)$$

$$h_{D_{i+1}} = d_{W_{i+1}} - dx \cdot S_o = d_{W_i} - dx \cdot (S_o - S_f) \quad (3-38)$$

Composite Substrate Hydraulic Conductivity,

$$K_S = K_S \cdot (1 - C_E) + K_E \cdot C_E \quad (3-39)$$

Variables,

Measured/Known

C_E : Embeddedness

dx : Model Distance Step (m)

K_S : Dominant Substrate Hydraulic Conductivity ($\frac{m}{s}$)

K_E : Embedded Substrate Hydraulic Conductivity for Silt/Sand ($\frac{m}{s}$)

S_o : Stream gradient (unitless)

Calculated

A_s : Cross-Sectional Area Across Seepage Face (m^2)

K_S : Composite Substrate Hydraulic Conductivity ($\frac{m}{s}$)

h_D : Hydraulic Head for Darcy Calculation (m)

h_s : Hydraulic Head Across Seepage Face (m)

d_W : Water Column Depth (m)

P_W : Wetted Perimeter (m)

Q_{hyp} : Hyporheic Exchange Rate Across Seepage Face ($\frac{m^3}{s}$)

S_f : Friction Slope (unitless)

3.4.6 EVAPORATION LOSSES

Loss from the mass transfer (liquid phase change to gas) associated with evaporation (calculated in order to account for heat transfer) from the water column is included as a negative term. The rate of water loss that accompanies the phase change and mass transfer from water column to the overlying air mass is a function of the evaporation rate and water surface area. The evaporative process is described in detail in **Section 2.4.1**.

$$Q_{evap} = \bar{E} \cdot W_W \cdot dx \quad (3-40)$$

Variables,

Measured/Known

dx : Model Distance Step (m)

Calculated

\bar{E} : Evaporation Rate ($\frac{m}{s}$)

Q_{evap} : Evaporation Loss Rate ($\frac{m^3}{s}$)

W_W : Wetted Width (m)

3.5 FLOW VOLUME CONTINUITY

Mass transfer to and from the water column, coupled with dynamic flow routing, makes it possible to account for volumes of water at any time (t) and location (model node 'i'). Inflows ($\sum Q_{IN}$) are the summation of surface tributary flows, subsurface springs, seeps and accretion flows, and hyporheic flow. Flow losses ($\sum Q_{OUT}$) are simply the summation of withdrawal rates and evaporation losses. The flow rate (Q_i^t) presented in (3-44) is calculated from the dynamic flow routing methods discussed in **Section 3.2**.

Instantaneous Summation of Inflows,

$$Q_{INi}^t = \sum Q_{TRIBi}^t + \sum Q_{GWi}^t + (Q_{hypi-1}^t - Q_{hypi}^t) \quad (3-41)$$

Instantaneous Summation of Outflows,

$$Q_{OUTi}^t = \sum Q_{WITHi}^t + Q_{evapi}^t \quad (3-42)$$

Instantaneous Model Reach Volume When Flow Rate (Q_{i-1}^t) is Known,

$$V_{Wi-1}^t = [Q_{i-1}^t + \sum Q_{INi-1}^t - \sum Q_{OUTi-1}^t] \cdot dt \quad (3-43)$$

Instantaneous Model Reach Volume When Flow Rate (Q_i^t) is Unknown,

$$V_{Wi}^t = [Q_i^t + \sum Q_{INi}^t - \sum Q_{OUTi}^t] \cdot dt \quad (3-44)$$

Variables,

Measured/Known

dt: Model Time Step (s)

Calculated

Q: Flow Rate ($\frac{m^3}{s}$)

Q_{evap} : Evaporation Loss Rate ($\frac{m^3}{s}$)

Q_{GW} : Instantaneous Flow Summation of Subsurface Inflows ($\frac{m^3}{s}$)

Q_{hyp} : Hyporheic Exchange Rate Across Seepage Face ($\frac{m^3}{s}$)

Q_{IN} : Surface Inflow Rate (m^3)

Q_{OUT} : Withdrawal Flow Rate (m^3)

Q_{IN} : Inflow Rate ($\frac{m^3}{s}$)

Q_{OUT} : Outflow Rate ($\frac{m^3}{s}$)

Q_{TRIB} : Instantaneous Flow Summation of Surface Inflows ($\frac{m^3}{s}$)

Q_{WITH} : Withdrawal Flow Rate ($\frac{m^3}{s}$)

V_W : Instantaneous Model Reach Volume (m^3)

3.6 CONTROLLED FLOWS AND DEPTHS

Controlled flows are common where instream structures meter flow releases. Obvious examples include dams, weirs, irrigation pushups, etc. It is recommended that these control flows be associated with the appropriate modeled stream reach. As with controlled flows, depth is often also controlled by instream structures. For example, a reservoir, wetland, or backwater depth can be entered to override the simulated condition if needed. Model accuracy will be enhanced by accounting for controlled flows and/or depths.

3.7 DEWATERED CHANNELS

Inherent to all of the flow routing methods presented in this Chapter is requirement that flow volumes are greater than zero. Unfortunately, in the western United States, in some stream and river reaches are completely dewatered through diversions and withdrawals. In these cases, flow routing cannot be performed in the traditional manners outlined in this Chapter. In terms of modeling, low flows are extremely difficult to simulate (recall that stream temperature change is inversely proportional to flow volume).

A method is developed in Heat Source that allows flow volumes to reach zero without model failure (i.e. division by zero errors). Heat Source will notify the user once stream flows have reached $\frac{1}{4}$ cfs (0.0071 cms), or less, and will ask whether the operator would like to continue. This message is basically asking the user whether the low flows being simulated reflect the true condition. At this time the model operator can either stop the model run or continue the simulation. The model will not ask the user again about encountered flow volumes for the duration of the simulation.

Once a user selects to continue the simulation, the model simply skips the stream nodes without sufficient flows to route (i.e. less than $\frac{1}{4}$ cfs). In these stream nodes, hydrologic and heat processes are not calculated and output variables are assumed to be zero. Proceeding downstream, the model will detect when flows become sufficient to commence flow routing again (i.e. greater than $\frac{1}{4}$ cfs).

Of particular concern is the estimation of the water temperature in this first stream node below the dewatered section, where flows are sufficient for flow routing and heat transfer modeling. In essence, this stream node represents a boundary condition. The model estimates this stream node temperature as the last known stream temperature value in the closest proximity to the stream node. It is likely that this assumption will be minimized since instream flows will be very small relative to the inflows and the inflow temperatures should dominate.

3.8 TENDENCY TO STRATIFY

Martin and McCutcheon (1999) present the densimetric Froude number as a measure of the tendency of a water body to stratify. Norton et al. (1968) first developed the densimetric Froude number and used it for prediction of stratification potential of reservoirs.

Densimetric Froude Number,

$$F_d = \sqrt{\frac{1}{g \cdot e}} \cdot \frac{dx \cdot Q}{d_w \cdot V} = \sqrt{\frac{1}{g \cdot e}} \cdot \frac{Q}{d_w \cdot A_x} \quad (3-45)$$

Variables,

Measured/Known

- dx: Model Distance Step (m)
- g: Acceleration of Gravity ($9.8 \frac{m}{s^2}$)
- e: Density Gradient ($10^{-6} \frac{1}{m}$)

Calculated

- A_x : Cross-Sectional Wetted Area (m^2)
- \bar{d}_w : Average Water Column Depth (m)
- F_d : Densimetric Froude Number (unitless)

$F_d > 1.25$ *Low Tendency to Stratify*

$0.75 \geq F_d \leq 1.25$ *Moderate Tendency to Stratify*

$F_d < 0.75$ *High Tendency to Stratify*

Q: Flow Rate ($\frac{m^3}{s}$)

V: Water Column Volume (m^3)

Chapter

IV

Model Operation

Input Data, Procedures and Modules

4.1 OVERVIEW

Important: Analytical methods are presented in preceding Chapters I-III and can be found in the Visual Basic programming in the model. Since this model is shareware, we invite user suggestions for improvements in methodology and coding. The collective intuition of the modeling community can contribute to the refinement of these and related analytical methods. Please let us know what improvements or changes you have made or are considering (our contact information is listed on the cover page).

The Heat Source methodology is unique and will prove to be a different modeling experience, especially to the uninitiated. Microsoft Excel is used to store and configure the model inputs and chart/store the model outputs. Visual Basic programming is utilized from all of the model functions (model setup, executables and data formatting). The 'Main Menu' can be accessed from all of the worksheets, except those containing charts and contains all of the model functions, as well as the fundamental general inputs. This model format has been selected for the ease of model design, programming and the widespread availability of Excel. The large quantity of input and output data required for Heat Source modeling is easily handled by using multiple worksheets in Excel for storage. No calculations are performed within the spreadsheets to minimize model size and maximize computational efficiency. Further, cell formatting is minimized due to Excel's tendency to count formatted cells as occupied and greatly increase the Excel file size (a phenomenon widely known as spreadsheet bloat). The only way to remove unwanted formatted or occupied cells is to delete them completely. For this reason, when Heat Source asks the user to delete/or clear data from the worksheets, the cells are in fact deleted.

TTools is designed to develop the spatial data inputs for Heat Source. It is necessary to use TTools to operate Heat Source in the fashion in which it is designed (i.e. the use of multiple spatial data sets). In particular, the land cover information can only developed with the sampling routines contained in TTools. The variability inherent to spatial data parameters warrants the measurement capability afforded by TTools. Assuming such data is not an appropriate use of this methodology.

A utility program called the 'Land Cover Positioner' is packaged with Heat Source to help users to reposition typical transverse land cover data (i.e. left bank and right bank) to the radial sampling pattern used by Heat Source. Further, the 'Land Cover Positioner' also can be used to position land cover inputs following changes to the bankfull morphology (i.e. bankfull width narrowing or widening).

4.2 FINITE DIFFERENCE STEPS

Important: *The distance step should always be equal to or greater than the longitudinal spatial data sampling rate used in TTools. A typical distance step is 100 meters and with a corresponding time step of one minute.*

Model time and distance steps are left to the user's discretion. These finite difference steps are used for all finite element methods (Heat and Mass Transfer, Dynamic Flow Routing) and thus, have multiple stability criteria¹⁷. Familiarity with the methods, and the analytical needs of the user, are fundamental to the selection of appropriate time and distance steps. As a basic rule the distance step should always be equal to or greater than the longitudinal spatial data sampling rate used in TTools. Keep in mind that the longitudinal spatial data sampling rate used in TTools should always be equal to or greater than the data resolution (including horizontal accuracy). Time and distance steps are interrelated and changes in one will affect the limits applied to the other. While changes in time and distance steps should not significantly affect (mathematically) simulation results, other effects may manifest altered simulation results. Heat Source averages spatial data inputs between finite difference nodes (as determined by the selected distance step). Therefore, a large distance step (relative to the sampling step) will reduce data resolution and spatial accuracy simply by averaging the uniqueness and variability. Further, a larger distance step often requires a large corresponding time step, which decreases model temporal resolution. Ultimately, the selection of time and distance steps is left to the user's discretion, creating a tradeoff between model resolution and computational efficiency.

4.3 GENERAL SETUP PROCEDURE

A general setup stepwise procedure can be summarized as follows:

- Step 1.** Complete data fields (text boxes) found in the 'General Inputs' tab from the 'Main Menu'
- Step 2.** Setup the spatial data worksheets from the 'Data Sheets' tab
- Step 3.** Setup the temporal data worksheet from the 'Continuous Data' tab
- Step 4.** Setup the flow data worksheet from the 'Mass Transfer Data' tab
- Step 5.** Assign physical attributes to land cover classifications
 - ⇒ Enter codes and associated physical attribute information into the 'Land Cover Codes' worksheet
 - ⇒ Run 'Vegematic' to assign height, density and overhang information to sampled land cover classifications

¹⁷ Stability criteria are a function of the selected finite approximation methods. Heat transfer methods are highly stable. Mass transfer stability criteria are listed in Table 3.1.

Step 6. Enter morphology input data

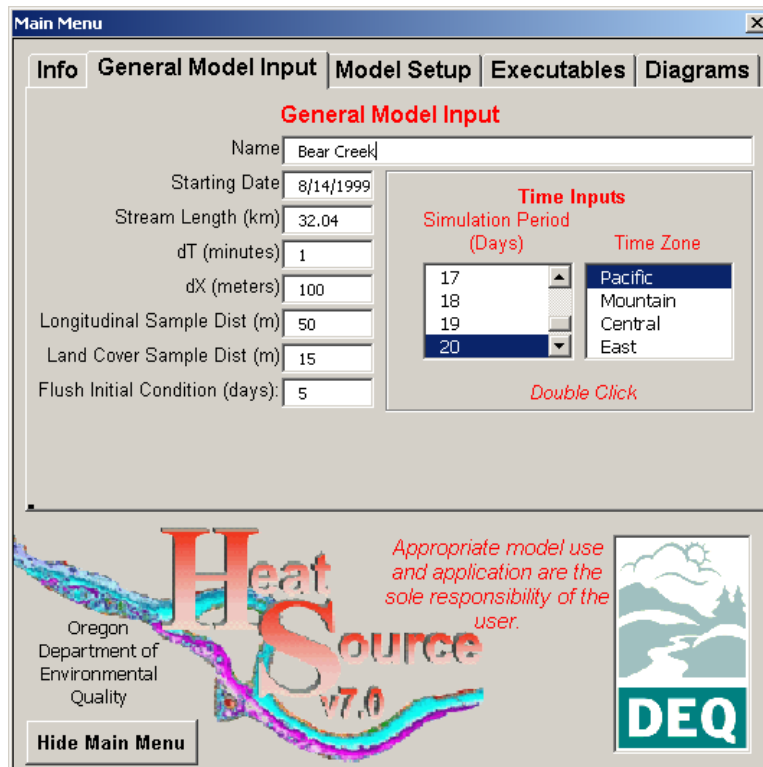
- ⇒ Either enter or assign W:D based on Rosgen Level I information under the 'Associate W:D' tab
- ⇒ Calculate the bankfull morphology under the 'Bankfull Morph.' tab.

Step 7. Select evaporation rate model and 'a' and 'b' constants under the 'Evaporation' tab

Step 8. Select dynamic flow routing method under the 'Flow Routing' tab

4.3.1 GENERAL INPUTS

The first step in the model setup is to enter the general information that will be used to setup input data sheets, control the model simulation length and finite difference time and distance steps. To access the 'Main Menu', click on the 'Main Menu' buttons located on most worksheets (except those containing charts) and then select the 'General Model Input' tab. Enter the data with attention to units of measurement. The 'Time Inputs' list drop boxes contain the input information for the simulation per and the time zone. Selections are made by double clicking (and should be done after the other inputs are entered). The information entered as 'General Model Inputs' will be visible on most of the worksheets (except those containing charts), listed as 'Simulation Information'.

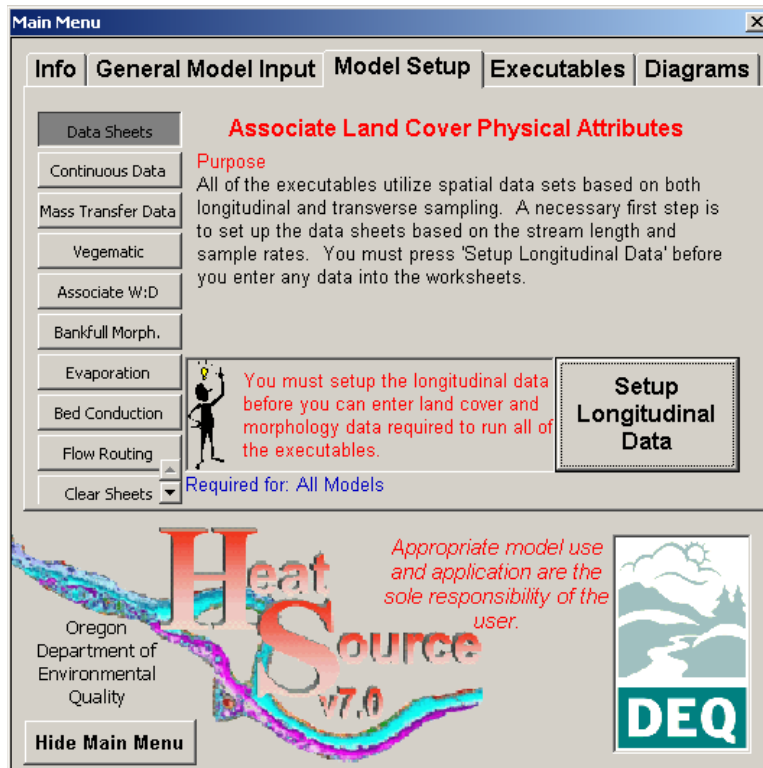


Important:

- Do not change the 'General Model Inputs' on the worksheets. Instead use the text boxes and list boxes found under the 'General Model Inputs' tab in the 'Main Menu'.
- Be exact when entering stream length and longitudinal sampling distance.
- Make sure that you double click on the 'Time Inputs'. You may want to check the worksheet input summaries to see if these have been properly selected.

4.3.2 MODEL SETUP - DATA SHEETS

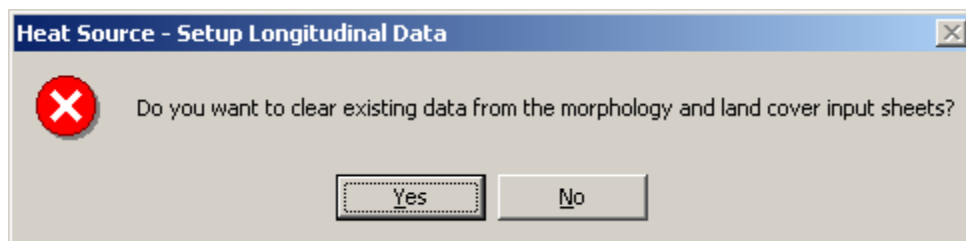
The next step for model setup includes developing the longitudinal input distance and model node information for the 'TTools Data', 'Morphology Data' and 'Validation Data'. Model nodes should match those created by TTools. The distance information is the longitudinal distance from the upstream boundary condition and the stream kilometer, which is the distance from the downstream boundary condition. These longitudinal distances and model nodes must match those found in the TTools derived database. Check the entered values for 'Stream Length' and 'Longitudinal Sampling Dist' if there are discrepancies.



Important:

- Do not proceed until you have confirmed that distance information matches the TTools derived database.

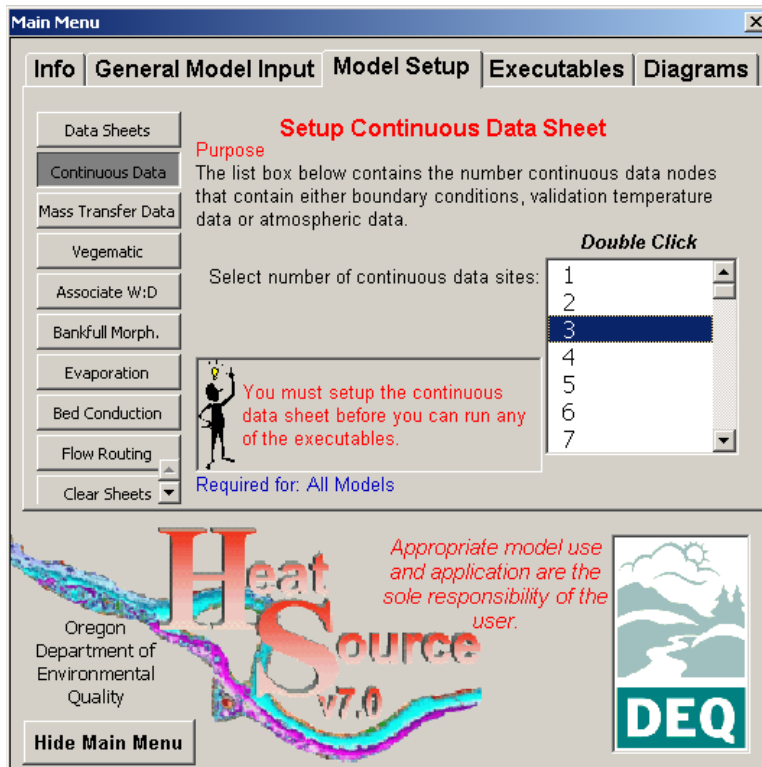
A message box will ask the user to confirm that they want to delete input data. Configuring the longitudinal data involves changing location data in the model. The user is asked whether they want to delete the current inputs associated with existing longitudinal data, since these data are about to be changed. If the user can keep track of existing data associations, it may be easier to choose not to delete existing data and simply move it appropriately after the longitudinal setup configuration.



4.3.3 MODEL SETUP – CONTINUOUS DATA

Important: Since continuous data are time dependent, make sure that you have entered the appropriate date in the 'Starting Date' text box located under the 'General Model Input' tab. The first time will be 12:00 AM for the starting date and incrementally increase one hour to the ending date (determined by the 'Simulation Period').

Continuous data refers to ground level information (measured over time) such as flow rate, stream temperature, air temperature, wind speed and relative humidity. These data are used for boundary conditions, heat transfer calculations and validation data. Select the 'Continuous Data' tab under the 'Model Setup' tab in the 'Main Menu' and then double click on the number of continuous data sites that contain any data that you intend to include as validation data or atmospheric inputs. This step will format the worksheet 'Continuous Data', which is then ready for input of these data.



Important:

- The maximum number of 'Continuous Nodes' is 100. This is a large number of continuous data nodes.
- A more typical number of nodes would be roughly one per ten kilometers.
- Data availability largely determines the number of 'Continuous Data Nodes'.

CONTINUOUS DATA NODE LOCATIONS

Continuous data node locations must be associated with longitudinal positional data (i.e. stream KM), in the upper (headwaters) to lower (mouth) downstream direction. 'Continuous Node' number 1 is the data site that will be used for atmospheric data, until the model (simulating in the downstream direction) encounters the next continuous data node, where the data associated with that node will then be used as atmospheric data. Climatic variations such as

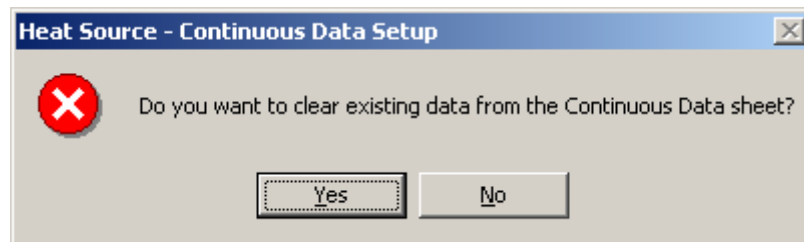
microclimate, adiabatic air temperature effects, etc. should be represented in the continuous data.

BOUNDARY CONDITIONS

The stream temperature boundary conditions for flow and stream temperature should be entered in columns H⇒I. Column J represents the cloudiness index (the percentage of average daily cloudiness). Boundary conditions should consist of measured values. Due to the cumulative effects, the boundary conditions may seriously alter simulations outputs.

DELETE CONTINUOUS DATA?

A message box will ask the user to confirm that they want to delete existing continuous data. Configuring the number of continuous data sites data involves changing the entire continuous worksheet. If the user can keep track of existing data associations, it may be easier to choose not to delete existing data and simple move it appropriately after the continuous data setup configuration. If the setup involves significant changes in the number of continuous sites, then you may want to delete all of the data and reenter this information.



'Continuous Data' Worksheet

Simulation Information
 Simulation Name: Lostine River
 Date: 3/14/2009
 Time Step: 6T (min): 1
 Distance Step: dx (m): 700
 Stream Length (km): 51.04
 Longitudinal Sample Rate (m): 60
 Transverse Sample Rate (m): 15
 Inflow Sites: 24
 Continuous Data Sites: 2
 Flush Initial Condition (days): 2
 Time Zone: Pacific
 Simulation Period (days): 20

Continuous Data Node Locations

Local Information (optional)	Continuous Node	Local Source Node (optional)	Stream km
d/s E. Lostine R.	1	193	41.89
SWCD monitoring site	2	694	16.84

Boundary Conditions

Time	Flow (cms)	Stream Temperature (°C)	Cloudiness (0-1)	Wind Speed (m/s)	Relative Humidity (%)	Air Temp (°C)	Stream Temp (°C)
8/14/99 12:00 AM	0.673903061	8	0	1.48	0.53	5.50	8.10
8/14/99 1:00 AM	0.673903061	8	0	1.48	0.51	6.33	8.00
8/14/99 2:00 AM	0.673903061	8	0	1.48	0.53	7.16	7.70
8/14/99 3:00 AM	0.673903061	8	0	1.48	0.57	7.99	7.50
8/14/99 4:00 AM	0.673903061	8	0	1.48	0.61	8.82	7.40
8/14/99 5:00 AM	0.673903061	8	0	1.48	0.65	9.65	7.30
8/14/99 6:00 AM	0.673903061	8	0	1.48	0.56	10.48	7.10
8/14/99 7:00 AM	0.673903061	8	0	1.48	0.54	11.31	7.00
8/14/99 8:00 AM	0.673903061	8	0	1.48	0.54	12.13	7.00
8/14/99 9:00 AM	0.673903061	8	0	1.48	0.50	12.96	7.00
8/14/99 10:00 AM	0.673903061	8	0	1.48	0.72	13.79	7.10
8/14/99 11:00 AM	0.673903061	8	0	1.48	0.74	14.62	7.40
8/14/99 12:00 PM	0.673903061	8	0	1.48	0.74	15.45	8.00
8/14/99 1:00 PM	0.673903061	8	0	1.48	0.80	16.28	9.30
8/14/99 2:00 PM	0.673903061	8	0	1.48	0.80	17.11	8.40
8/14/99 3:00 PM	0.673903061	8	0	1.48	0.72	17.94	8.70
8/14/99 4:00 PM	0.673903061	8	0	1.48	0.62	16.87	8.70
8/14/99 5:00 PM	0.673903061	8	0	1.48	0.56	15.00	9.00
8/14/99 6:00 PM	0.673903061	8	0	1.48	0.49	14.73	9.00
8/14/99 7:00 PM	0.673903061	8	0	1.48	0.46	13.02	9.00

Continuous Data Node Locations

Local Information (optional)	Continuous Node	Local Source Node (optional)	Stream km
d/s E. Lostine R.	1	193	41.89
SWCD monitoring site	2	694	16.84

Boundary Conditions

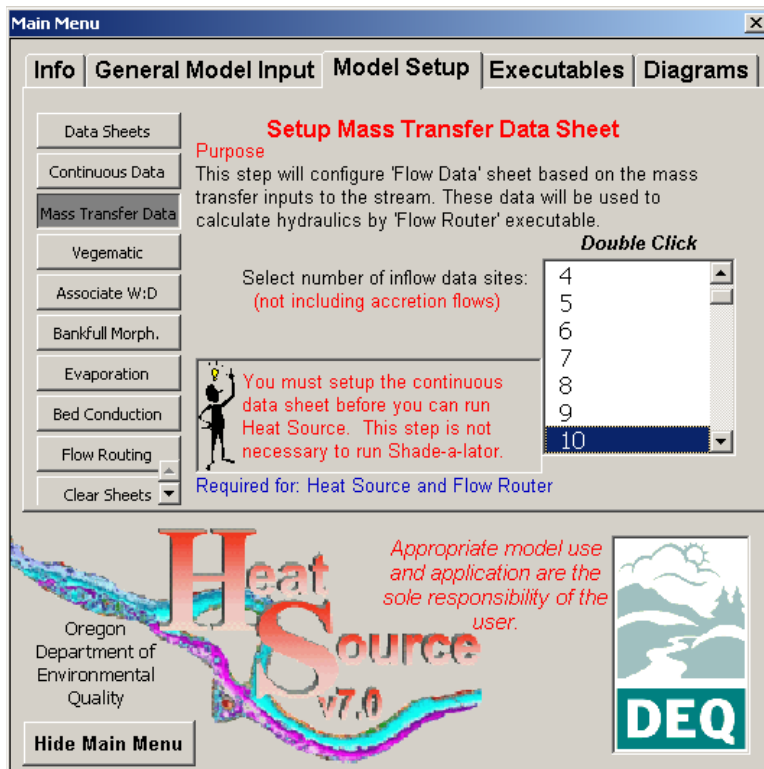
Time	Flow (cms)	Stream Temperature (°C)	Cloudiness (0-1)	Wind Speed (m/s)	Relative Humidity (%)	Air Temp (°C)	Stream Temp (°C)
8/14/99 12:00 AM	0.673903061	8	0	1.48	0.53	5.50	8.10
8/14/99 1:00 AM	0.673903061	8	0	1.48	0.51	6.33	8.00
8/14/99 2:00 AM	0.673903061	8	0	1.48	0.53	7.16	7.70
8/14/99 3:00 AM	0.673903061	8	0	1.48	0.57	7.99	7.50

Continuous Data Node Locations

Continuous Data Node Locations will control where these data are used in the model.

4.3.4 MODEL SETUP – MASS TRANSFER DATA

Mass transfer data include site specific (at discrete locations) surface and subsurface inflows. These flows do not including hyporheic exchange inflows, accretion (distributed) inflows and withdrawals. Double clicking on the 'number of inflow data sites' allows the model to format the 'Flow Data' worksheet. On this worksheet there are longitudinal inputs for accretion flows and withdrawals, which are handles separately from site specific (at discrete locations) surface and subsurface inflows.



Important:

- You can always come back to add or delete inflow data sites without deleting the data on the worksheet.
- These data need to be in longitudinal order from upper (headwaters) to lower (mouth) longitudinal position.
- The maximum number of localized inflow processes is 100.

INFLOW DATA SITES

Inflows rates and temperatures can be associated with location information and entered at a one-hour interval. It is important to differentiate between localized inflows and accretion flows (see following subsections). 'Inflow Data Sites' refers to localized (non-accretion) type flows such as tributaries, springs, returns, point sources, etc. Double click on the 'number of inflow data sites from' the list located in the 'Mass Transfer Data' tab of the 'Main Menu'. This will trigger the automated setup of the 'Flow Data' worksheet for localized inflow data with a time/date interval of one-hour.

The next step is to input the localized inflow positional information in columns I⇒L. This data associates a localized inflow to a point in the longitudinal stream length. For each inflow data site, you need to enter (in columns O⇒...) the time series inflow rates and inflow temperatures (at a one-hour interval) for the entire

simulation period. When inflows are close enough, so that more than one occurs in a model distance step, the inflow rates will be summed and a flow based average inflow temperature will be derived and used in the mixing calculations.

ACCRETION (DISTRIBUTED) FLOWS

Accretion flows are inflows that enter the stream over more than one stream data node, and typically are subsurface seeps that occur over longer distances than discrete subsurface inflows (i.e. a spring). The temperature of the accretion flows, along with the flow rates, should be input in columns E⇒F in the 'Flow Data' worksheet. When accretion flows are close enough so that more than one occurs in a model distance step, the accretion flow rates will be summed and a flow based average accretion temperature will be derived and used in the mixing calculations.

Important: Zero values indicate that no accretion flow is occurring.

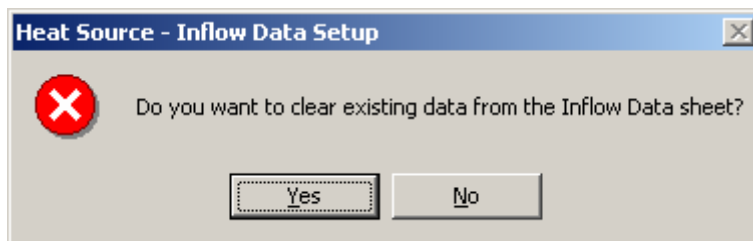
FLOW WITHDRAWALS

Withdrawals can be entered to represent known flow losses such as diversions from the stream or other human caused flow reductions. Withdrawal flow rates are assumed to remain constant throughout the simulation period. Withdrawal flows should be input in column G in the 'Flow Data' worksheet. When withdrawal flows are close enough so that more than one occurs in a model distance step, the withdrawal flow rates will be summed.

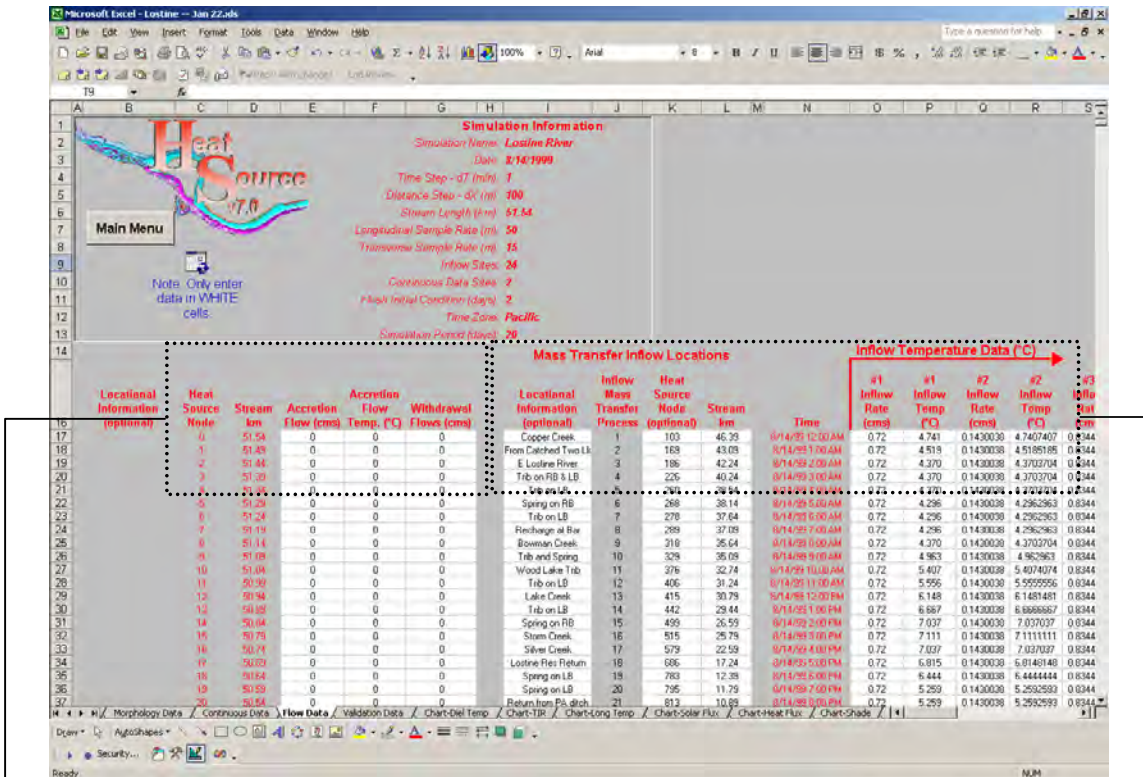
Important: Zero values indicate that no withdrawal is occurring.

DELETE INFLOW DATA?

A message box will ask the user to confirm that they want to delete existing inflow data. Configuring the number of inflow data sites data involves changing the entire Inflow worksheet. If the user can keep track of existing data associations, it may be easier to choose not to delete existing data and simply move it appropriately after the continuous data setup configuration. If the setup involves significant changes in the number of inflow sites, then you may want to delete all of the data and reenter this information.



'Flow Data' Worksheet



Heat Source Node	Stream km	Accretion Flow (cms)	Accretion Flow Temp. (°C)	Withdrawal Flows (cms)
0	51.54	0	0	0
1	51.49	0	0	0
2	51.44	0	0	0
3	51.39	0	0	0
4	51.34	0	0	0

- Important:**
- Zero values indicate that no accretion flows or withdrawals are occurring.
 - Mass Transfer Inflow Locations should be input in the downstream direction.

Locational Information (optional)	Inflow Mass Transfer Process	Heat Source Node (optional)	Stream km	Time	Inflow Temperature Data (°C)			
					#1 Inflow Rate (cms)	#1 Inflow Temp (°C)	#2 Inflow Rate (cms)	#2 Inflow Temp (°C)
Copper Creek	1	103	46.39	8/14/99 12:00 AM	0.72	4.741	0.1430038	4.7407407
From Caughted Two Lk	2	169	43.09	8/14/99 1:00 AM	0.72	4.519	0.1430038	4.5185185
E Lostine River	3	186	42.24	8/14/99 2:00 AM	0.72	4.370	0.1430038	4.3703704
Trib on RB & LB	4	226	40.24	8/14/99 3:00 AM	0.72	4.370	0.1430038	4.3703704
Trib on LB	5	260	38.54	8/14/99 4:00 AM	0.72	4.370	0.1430038	4.3703704
Spring on RB	6	268	38.14	8/14/99 5:00 AM	0.72	4.296	0.1430038	4.2962963

4.3.5 MODEL SETUP – TTOOLS DATA

The data in the TTools database file is formatted to be simply copied and pasted into the appropriate 'TTools Data' worksheet columns. Starting with longitude (column F), the columns are arranged in the same order so that multiple columns of data can be inserted (copied and pasted) directly from the TTools derived *dbf* file. After you have inserted the data, scroll down to the bottom of data set and check to see that the data row count matches the longitudinal row count (red font color, columns B⇒E).

Important: To minimize spreadsheet bloat, you should copy only the cells that have data and then paste special⇒values into Heat Source. If you choose to numerically format the cells on this page, keep in mind that you will increase the spreadsheet file size.

'TTools Data' Worksheet

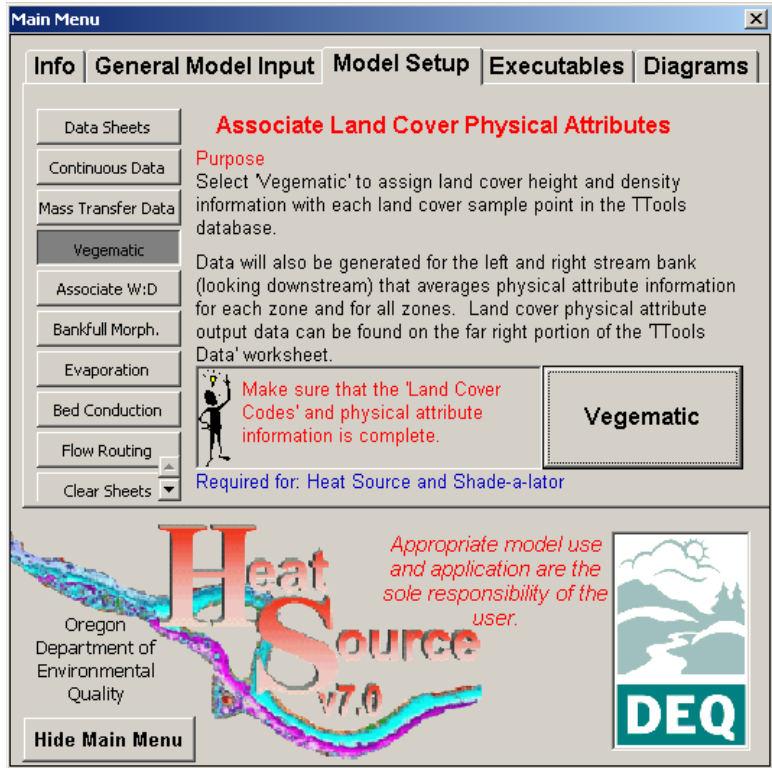
Heat Source Node	Long. Distance (km)	Stream km	Enter Sampled TTools Data						Topo Shade (deg)		
			Longitude (deg)	Latitude (deg)	Stream Elevation (m)	Bankfull Width (m)	Aspect (deg)	West	South	East	
0	0	51.54	-117.35	45.19	2246.1	3	333.4	12	3.6	19.3	
1	0.05	51.49	-117.35	45.19	2245.2	3	325.9	12	3.8	19	
2	0.1	51.44	-117.35	45.19	2242.1	3	318.8	12.4	3.2	18.6	
3	0.15	51.39	-117.35	45.19	2241.2	3	323.1	12.9	3.2	17.3	
4	0.2	51.34	-117.35	45.19	2241.2	3	2.9	13.3	3.5	17.1	

4.3.6 MODEL SETUP – LAND COVER CODES AND ATTRIBUTE ASSOCIATIONS

The 'TTools Data' worksheet should now contain all of the TTools data. A portion of these data are the sampled land cover classifications. The 'Land Cover Codes' worksheet will contain the physical attribute information associated with each classification. Data entry is fairly straightforward. Land cover codes must be integers (non zero values) and physical attribute data must be numeric. There cannot be skipped rows (i.e. rows without information in between rows with information) because the model routines see a blank row as the end of the data sequence. These land cover physical attribute data will be associated with the classification data in the next step.

Due to the radial sampling pattern utilized (where directional sampling occurs around each data node), the data are well suited for directional shade simulation, but are not easily summarized for graphical presentation. Part of 'Vegematic' accounts for the stream aspect and land cover orientation/location and creates a left /right bank summary of the land cover height and density. While these data are not used in the simulations, they should be used to quantify the spatial distributions of land cover physical attributes. See columns DX ⇒ EN on the 'TTools Data' worksheet for these data.

'Vegetatic' is a simple routine that associates, organizes and summarizes the land cover physical attribute information. Output data from 'Vegetatic' will be located in the 'TTools Data' worksheet in columns BS ⇒ FE. Land cover physical attribute data used in solar routing and shade simulations can be found in columns BS ⇒ DV in the 'TTools Data' worksheet.



- Important:**
- Run 'Vegetatic' only after all TTools data and the physical attribute codes/data are entered.
 - If you are missing a code, 'Vegetatic' will stop and identify the cell with the undefined land cover code.

'Land Cover Codes' Worksheet

Enter Land Cover Physical Attributes →

Land Cover Name (optional)	Code	Height (m)	Density (%)	Overhang (m)
Water	301	0.0	0%	0.0
Pasture/Cultivated Ag	302	0.9	90%	0.0
Tree Farm	303	4.6	80%	0.7
Barren - Rock	304	0.0	0%	0.0
Barren - Bank	305	0.0	0%	0.0

4.3.7 MODEL SETUP – MORPHOLOGY DATA

DEVELOPMENT OF WIDTH TO DEPTH RATIO INFORMATION

The data contained in the 'Morphology' worksheet contain both measured TTools data and assumed or derived values. The general procedure for setting up this sheet should start with inserting gradient and bankfull width data from the TTools database. The next step is to assign a width to depth ratio (W:D) to each model data node. There are two ways to provide the needed W:D information.

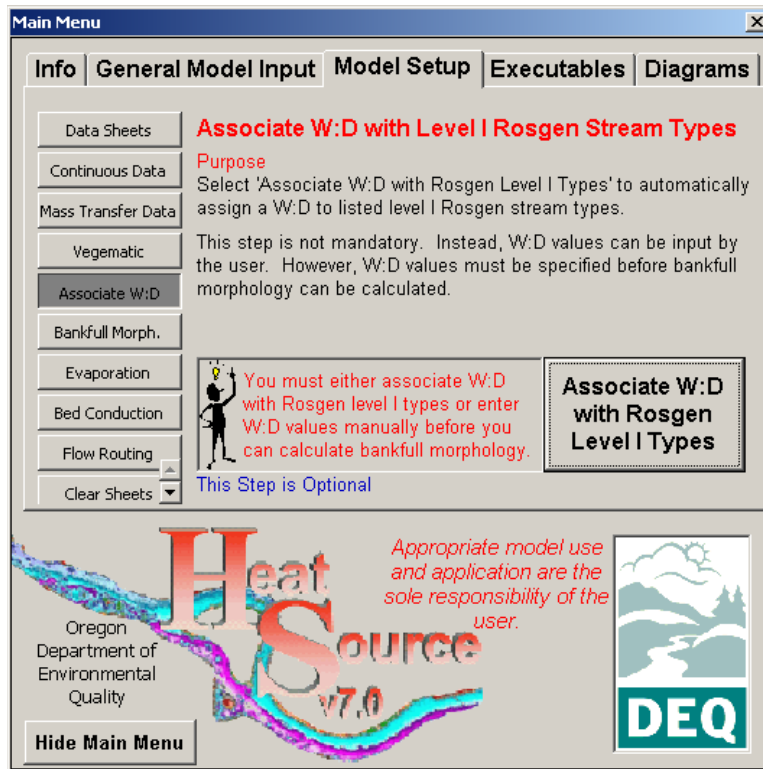
The first method (and easiest method) is to simply insert the W:D values directly into the worksheet. There is an optional procedure that can be used to associate W:D values based on Rosgen level I information. To associate W:D data to a Rosgen stream type, press the 'Enter W:D Data' button and change the W:D data manually. Notice that the 'Rosgen Level I Stream Type' column is optional. This column must be completely filled in with the stream types (A ⇒ G) before you can proceed, after which you can access 'Associate W:D' tab in the 'Main Menu' to assign Rosgen based W:D values.

**Enter Average W:D
as a Function of
Rosgen Stream
Type**

Enter W:D Data

Stream Type	W:D
A	8
B	12
C	20
E	7
F	28
G	8

Users can enter W:D values to associate with Level I Rosgen stream types.



Important:

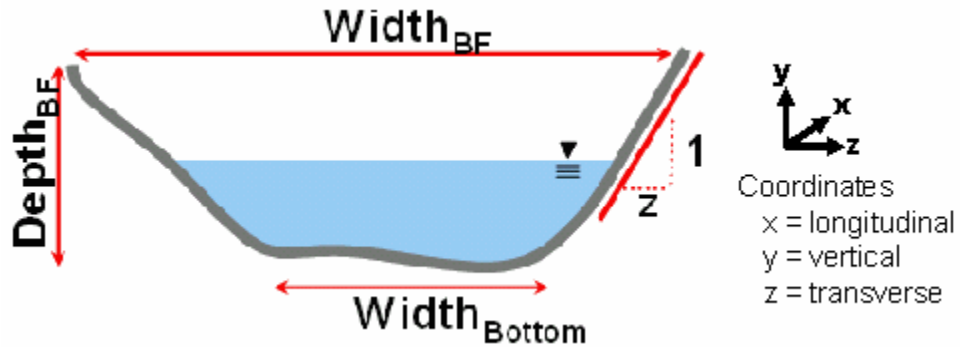
- Do not spend too much time with W:D or channel angle-z values right now. You will have the opportunity to fine tune this information once the model is completely setup.
- You will need to estimate the Rosgen Level I stream type.

If the letters used for stream typing are not found in the listed Rosgen stream types (see graphic above), then a message will appear and stop the association routine. The cell that contains the unrecognizable stream type letter will be identified.



BANKFULL CHANNEL GEOMETRY – CHANNEL SIDE SLOPE ‘Z’

The next step is to input the ‘Channel Angle – z’ data to represent the channel side slope ratio. The ultimate goal is to configure a basic trapezoidal channel dimension to match the basic channel geometry. Channel profile information (commonly measured when collecting instream flow data) can be useful for estimating the channel side slope angle.

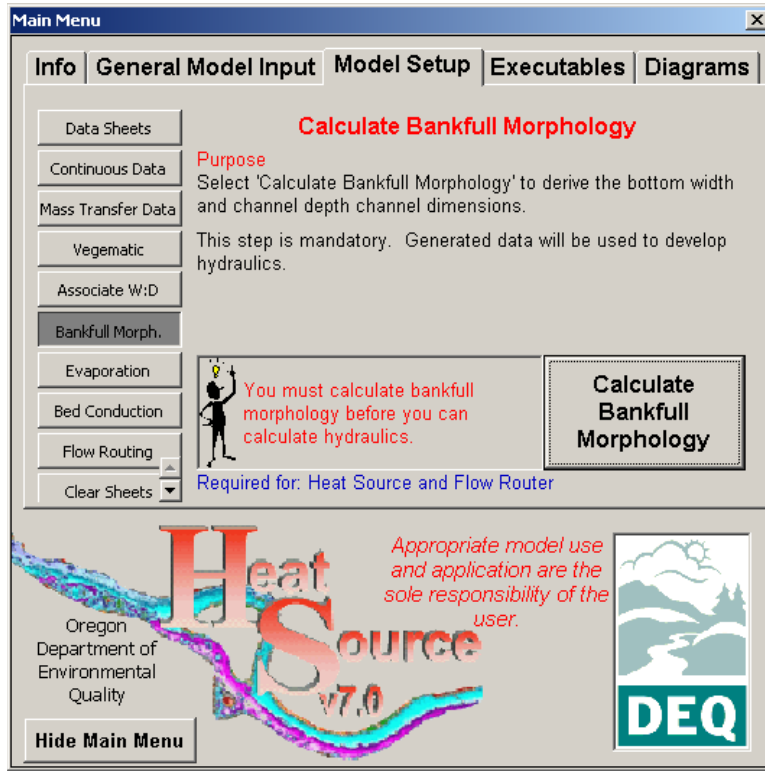


‘Morphology Data’ Worksheet – Channel Side Slope ‘Z’

Cross-Sectional Area (m ²)	Channel Angle -z	X Factor (0.0-0.5)
4.500	1.98	0.2
3.120	1.98	0.2
3.250	1.98	0.2
3.120	1.98	0.2
0.780	1.98	0.2

CALCULATE BANKFULL CHANNEL DIMENSIONS

With these data inputs entered, the next step is to calculate the bankfull channel bottom width, bankfull depth and average bankfull depth. Select the 'Bankfull Morph.' tab from the 'Main Menu.' If the channel 'Channel Angle – z' is too large (i.e. the channel sides converge) then the morphology determined to resemble a 'V' shape and the bankfull bottom width is zero.



Important:

- Make sure that you have entered stream gradient, bankfull width and channel slope z-angle before you press the 'Calculate Bankfull Morphology' button.
- You will be able to modify these inputs later, so do not spend too much time on this step right now.

'Morphology Data' Worksheet –Bankfull Morphology

Gradient	Mannings n	Rosgen Level I Stream Type (optional)	W:D Ratio	Bankfull Width (m)	Estimated Bottom Width (m)	Maximum Bankfull Depth (m)	Average Bankfull Depth (m)	Cross-Sectional Area (m ²)	Channel Angle -z
1.8%	0.015		8.00	6.000	0.570	1.370	0.750	4.500	1.98
4.4%	0.015		8.00	5.000	0.510	1.130	0.620	3.120	1.98
3.6%	0.015		8.00	5.100	0.520	1.160	0.640	3.250	1.98
2.4%	0.015		8.00	5.000	0.510	1.130	0.620	3.120	1.98

Known/Estimated Values of Bankfull Morphology

Calculated Values of Bankfull Morphology

MUSKINGUM 'X-FACTOR'

Users should reference **Section 3.3.2 Muskingum-Cunge Approximation** (used for dynamic flow routing) for an overview of the Muskingum-Cunge Method and the importance of the X-factor parameter. In summary the X-factor ranges between 0 and 0.5, where a 0 value represents no wedge storage (in reservoirs for example) and 0.5 represents full wedge storage in the finite element method. The average X-factor in a flowing river reach is often approximately 0.3. If you plan to use the Muskingum-Cunge dynamic flow routing method (and we recommend that for distributed stream network modeling that you use this method) then you will either need to enter X-factor values (that can be used as a calibration parameter) or leave these values blank and select 'Calculate Muskingum Storage Factor 'X' from the 'Flow Router' tab in the 'Main Menu'.

Cross-Sectional Area (m ²)	Channel Angle -z	X Factor (0.0-0.5)
4.500	1.98	0.2
3.120	1.98	0.2
3.250	1.98	0.2
3.120	1.98	0.2
0.780	1.98	0.2

Important: If you do not understand the Muskingum Storage X-Factor select the option so to calculate the appropriate values (for more information see **Section 3.3.2 Muskingum-Cunge Approximation**)

SUBSTRATE INFORMATION: HYDRAULIC CONDUCTIVITY, BED PARTICLE SIZE AND PERCENT EMBEDDEDNESS

Heat energy conduction between the alluvium and the water column and hyporheic flow methodologies utilize substrate data. Hydraulic conductivity can be estimated from the dominant bed particle size (silt, sand, gravel, cobble and boulder). Embeddedness refers to the ratio of fine sediment occupying the interstitial spaces in the alluvium. Input of these data is very straightforward, however, derivations of data values can become complex and should draw from advanced morphology classifications and/or measured instream data. In the state of Oregon, many stream networks have been surveyed for aquatic habitats, and substrate measurements have been summarized in GIS databases.

Important: In the state of Oregon, many stream networks have been surveyed for aquatic habitat and substrate measurements have been summarized in GIS databases (use this link to check GIS habitat survey availability: <http://oregonstate.edu/Dept/ODFW/freshwater/inventory/habitgis.html>).

'Morphology Data' Worksheet – Substrate Information

Horizontal Bed Conductivity (from Bedient & Huber 1992)		
Silt: < 0.02 mm/s (0.00079 in/s)		
Sand: 0.02 - 6.0 mm/s (0.00079 - 0.236 in/s)		
Gravel: 6.0 - 30 mm/s (0.236 - 1.18 in/s)		
Cobble: > 30 mm/s (1.18 in/s)		
Bed Particle Size (from Bedient & Huber 1992, Rosgen 1996)		
Silt: < 0.062 mm (< 0.0024 in)		
Sand: 0.062 - 2.0 mm (0.0024 - 0.0787 in)		
Gravel: 2.0 - 63.5 mm (0.0787 - 2.5 in)		
Cobble: 63.5 - 254 mm (2.5 - 10 in)		
Percent Embeddedness: (Simonson et al., 1994)		
100% = Rocks are completely surrounded by sediment and completely covered by fines.		
75% = Rocks are completely surrounded by sediment and half covered by fines.		
50% = Rocks are completely surrounded by sediment but are not covered by fines.		
25% = Rocks are half surrounded by sediment and are not covered by fines.		
Horizontal Bed Conductivity (mm/s)	Bed Particle Size (mm)	Embeddedness
		Important:
		<ul style="list-style-type: none"> You must input substrate information. Either use stream survey information or assume values based on your knowledge of the substrate types.

THERMAL INFRARED (TIR) DATA

Thermal infrared stream temperature data serves as a valuable tool for model validation. Input of these data is optional; however, it is strongly recommended by the authors that efforts to obtain remotely sensed TIR data. In fact, TIR data alone usually proves to be more informative than any modeling effort in assessing the current spatial distribution of stream temperatures, and should be a primary focus stream temperature assessments. TTools should be used to associate TIR sampled temperature data with individual stream data nodes. These data can then be directly entered into column U from the TTools database.

Important: Pay particular attention to entering exact times for sampling over the stream length. Heat Source will match the closest simulated values (both temporal and spatial) the time and location represented by the TIR data points. A statistical comparison between simulated values and TIR data is provided as model output.

CONTROLLED FLOW, TEMPERATURE AND DEPTH DATA

Most stream and river systems have control structures where hydraulics are subjected to natural, or more commonly, human controls, such as: reservoirs, weirs, check dams, diversion structures, etc. The user has the ability to add these features to the instream hydraulics and flow routing routines, where they cannot be calculated from traditional gravity and friction based methods. Where data are entered, these values become fixed flows, temperatures and depths. For example, behind a bottom release dam there will be a controlled flow that has a fairly constant temperature, and likely, a constant wetted depth. In this case it would be appropriate to add these data to override the other hydraulic

data calculated in the tradition flow routing methods. Any one of these control parameters (flow, temperature, depth) can be added, without the others. Further, any combination can be used, as long as values are realistic and appropriate. Using these control parameters allows the model to simulate through a reservoir (or other control structure) without introducing model error in the heat or mass transfer methods.

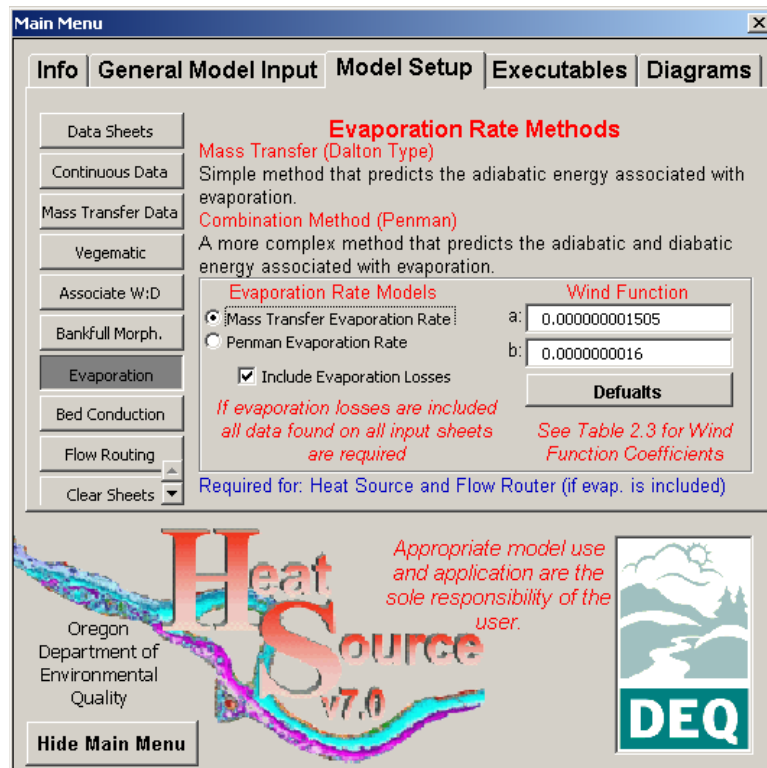
'Morphology Data' Worksheet – Controlled Flows, Depths and Temperatures

Optional - "0" Signifies no data				
TIR Date/Time	TIR Temps. (°C)	Controlled Flows (cms)	Controlled Depth (m)	Controlled Temperature (°C)

Important:
 • Zero (or null) values indicates that no control flows, temperatures or depths are occurring at the corresponding data node.

4.3.8 MODEL SETUP – EVAPORATION RATE METHODS

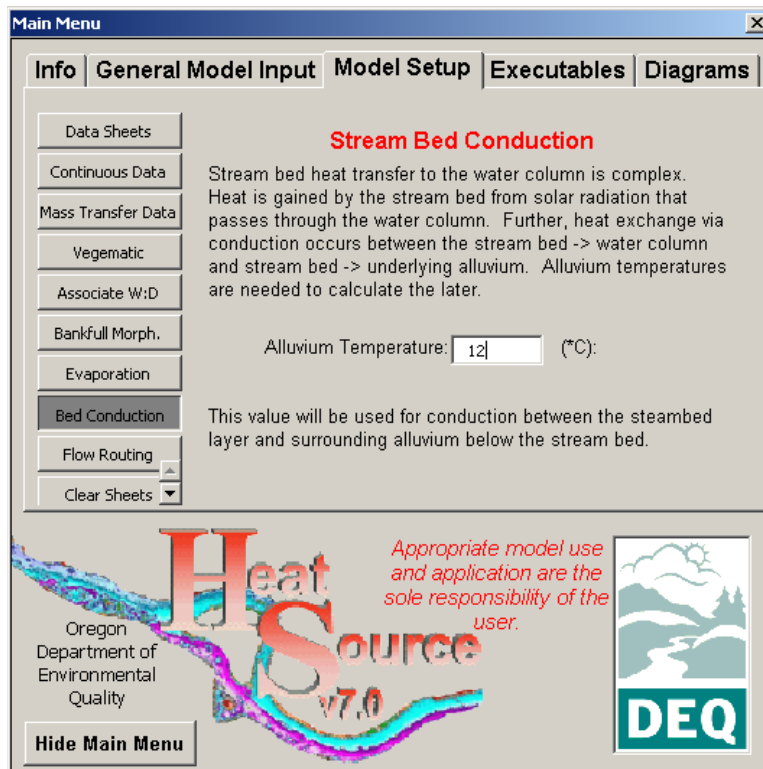
Heat Source allows the user to select the evaporation rate method as either the mass transfer method or the combination method (Penman). For a comprehensive review of these methods see **Section 2.4.1 Evaporation Rate**. Both methods rely on a wind function that utilizes coefficients 'a' and 'b' (See **Table 2.3 Wind Function Coefficients** for appropriate 'a' and 'b' values). Values for these coefficients can be either input by the user or restored by hitting the default button.



Important:
 • Many wind function coefficients are available in the literature.
 • Make sure that you have correctly accounted for the units ($a = mb-1m.s^{-1}$ and $b = mb^{-1}$)

4.3.9 MODEL SETUP – STREAM BED CONDUCTION

Heat Source allows the user to select the alluvium temperature for stream bed conduction. Recall that stream bed conduction is dependent on the stream bed temperature (substrate conduction layer temperature), as well as the water column and underlying alluvium temperatures. For a comprehensive review of these methods see **Section 2.3 Substrate Conduction Flux**.

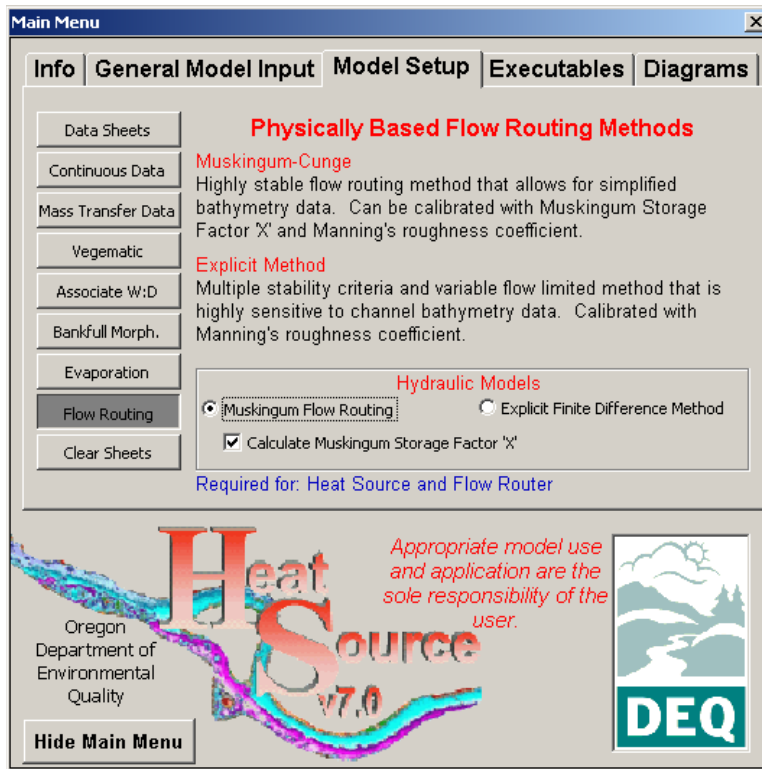


Important:

- The alluvium temperature will serve as the conduction temperature below the substrate conduction layer.

4.3.10 MODEL SETUP – PHYSICALLY BASED FLOW ROUTING METHODS

Two flow routing models are available: Muskingum-Cunge Flow Routing and Explicit Hydraulic Model Routing. Each method has strengths and weaknesses as outlined in **Table 3.1 Summary of Muskingum-Cunge and Explicit Finite Difference Methods**. If using the Muskingum-Cunge Flow Routing method, the user will have the chance to have the model calculate the Muskingum Storage Factor 'X', which simplifies the model inputs and is physically based. One drawback may be a reduction in calibration parameters. Aside from the Muskingum Storage Factor 'X', user's should use morphology and roughness parameters to calibrate flow routing.

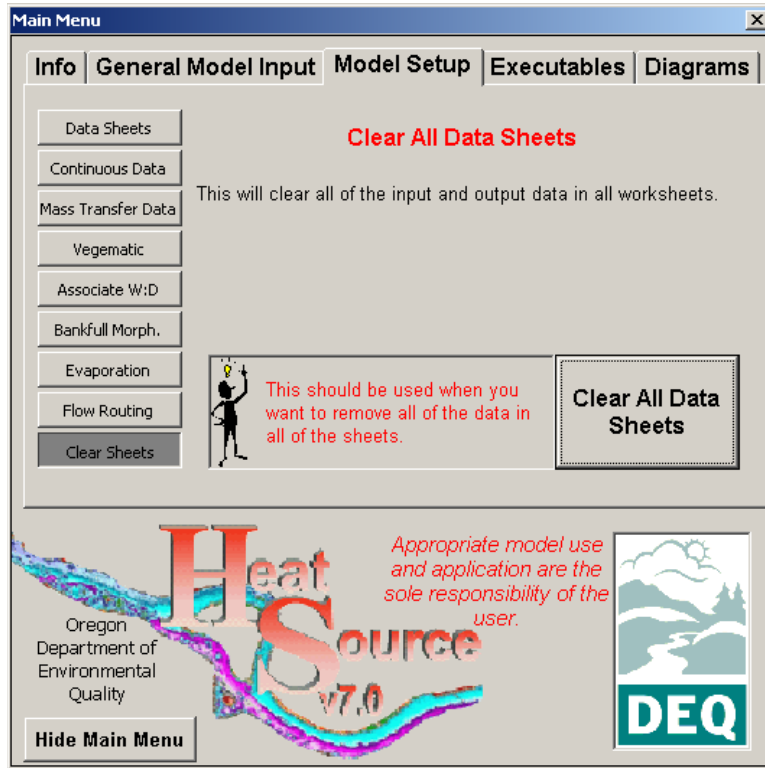


Important:

- Carefully select the mass transfer methodology based on the model application
- Select to Calculate Muskingum Storage Factor 'X' if you are unfamiliar with the methodology.

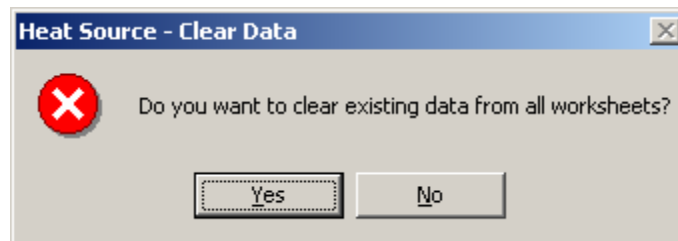
4.3.11 MODEL SETUP – CLEAR ALL DATA SHEETS

This model function will clear all of data in all of the worksheets in the model. Use this function when you want to start over or create a new model. Be careful!



Important:
• Be Careful!

The user is prompted before the model deletes all of the data from all worksheets. This process cannot be undone.



4.3.12 MODEL SETUP – VALIDATION DATA

Hydraulic and shade information can be entered in to the ‘Validation Data’ worksheet and the model will pair simulated values to the location and date of the measured values. Flow rate, velocity and wetted channel dimensions will be paired with measured data at the completion of a simulation.

‘Validation Data’ Worksheet

Measured Data							
Locational Information (optional)	Date	Stream km	Flow (cms)	Velocity (m/s)	Wetted Width (m)	Average Wetted Depth (m)	Max. Wetted Depth (m)
u/s French Camp	8/19/1999	39.10	1.57	0.27	19.81	0.25	0.64
Lake Cr CG	8/19/1999	29.00	2.35	0.39	14.33	0.33	0.67
1st bridge	8/19/1999	21.10	3.10	0.61	9.14	0.42	0.76
Gage at Baker Rd	8/23/1999	9.00	1.42				
Gage at Baker Rd	8/23/1999	1.80	2.12				
DEQ mouth	8/19/1999	0.25	2.79	0.58	11.89	0.28	0.49

Simulated Data				
Flow (cms)	Velocity (m/s)	Wetted Width (m)	Average Wetted Depth (m)	Max. Wetted Depth (m)
0.96	0.20	11.10	0.36	0.60
1.50	0.36	12.60	0.24	0.43
2.04	0.36	13.10	0.34	0.58
1.87	0.29	15.30	0.32	0.56
1.82	0.17	29.90	0.24	0.46
1.84	0.17	27.20	0.28	0.52

Measured and simulated data are paired for validation

4.4 EXECUTABLES

Three executables can be accessed and run independently from the 'Main Menu': Shade-a-lator, Flow Router and Heat Source. Shade-a-lator is the solar routing routine from the sun to the stream surface. It can be used to simulate effective shade and stream surface solar exposure. Flow Router is the dynamic flow routing methodology that can be used to simulate hydraulics and wetted channel dimensions. Heat Source simulates water column temperature, dynamic flow routing and heat transfer processes. Model inputs and outputs are unique for all three executables.

Model performance will vary by computer type and software installations. Microsoft Excel has some issues that may create problems with the model. Namely, model bloat can quickly grow the file to large sizes in the course of one model run. There is not an easy way to prevent this phenomenon, except to manually delete worksheet cells that are not in use by the model. The minimum model size is roughly 5 megabytes, but a model setup and simulation may commonly approach 20 megabytes. We recommend that you run Office2000 or later. Sharing Excel files from a network can cause documented problems from the auto save functions and read/write privileges. These problems can degrade the Excel files. Virus protection programs can prevent VBA code from executing or can cause documented problems with saving Excel files.

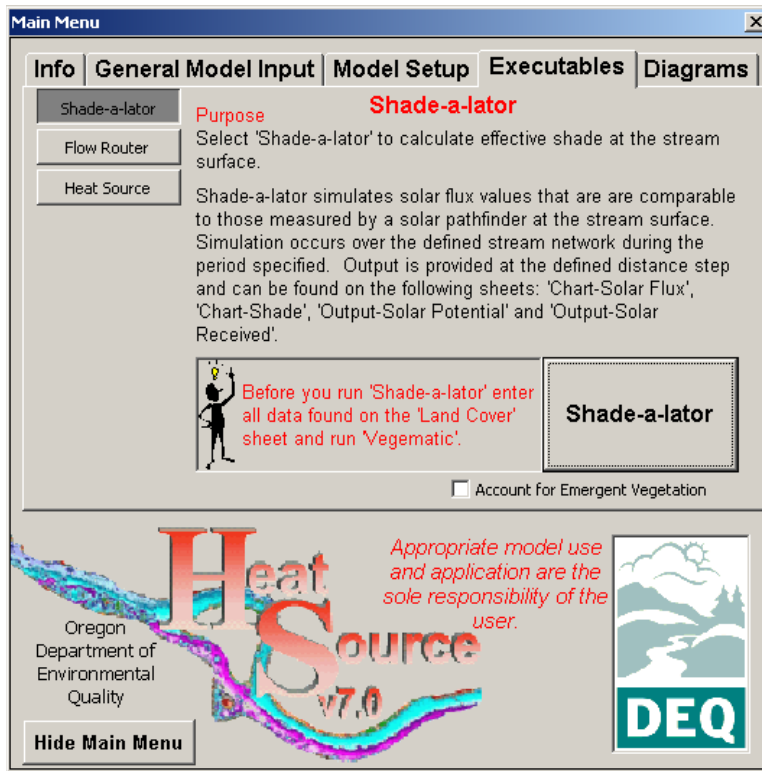
Since the models utilize Visual Basic programming, it will be helpful for users to familiarize themselves with the computer code. In general, the code structure relies on descriptively labeled subroutines (i.e. SubSolarFlux). With this document as a guide, the code should be accessible and moderately easy to follow.

Important:

- (1) *To stop an executable press Ctrl-Break,*
 - (2) *To speed simulation run times increase distance step size,*
 - (3) *To increase model resolution decrease distance step size,*
 - (4) *Be aware of the stability constraints of the models,*
 - (5) *Familiarize yourself with the Visual Basic code,*
 - (6) *Identify causes of code interruptions by inserting a code break above a the problem area and then step through the code,*
 - (7) *A common source of problems is missing data or division by zero errors,*
 - (8) *Submit concerns, suggestions, improvements and/or bugs to the authors.*
-

4.4.1 EXECUTABLES – SHADE-A-LATOR

Shade-a-lator is a solar routing model that calculates the potential and received solar radiation flux at the stream surface and also provides effective shade output data. Note that there is an option to account for emergent vegetation in the solar routing calculations.



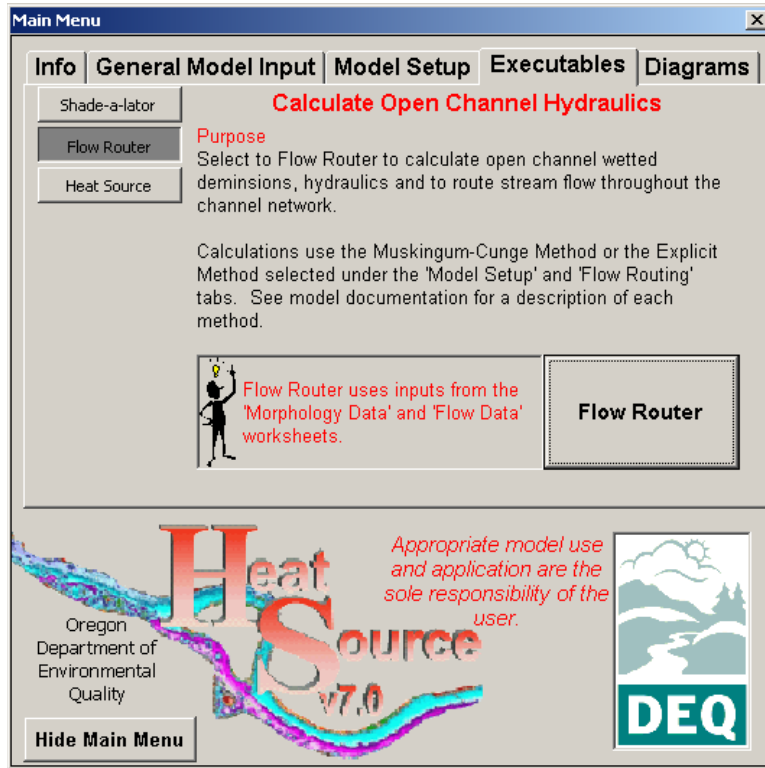
•Application:
Simulate water surface solar exposure and effective shade

•Inputs: *All parameters found in the 'TTools Data' worksheet and Cloudiness (Column J) in the 'Continuous Data' worksheet.*

•Outputs: *'Chart – Solar Flux', 'Chart - Shade', 'Output – Solar Potential' and 'Output – Solar Surface'*

4.4.2 EXECUTABLES – FLOW ROUTER

Flow Router is the hydraulic flow routing model (either Muskingum-Cunge or Explicit Finite Difference Method).



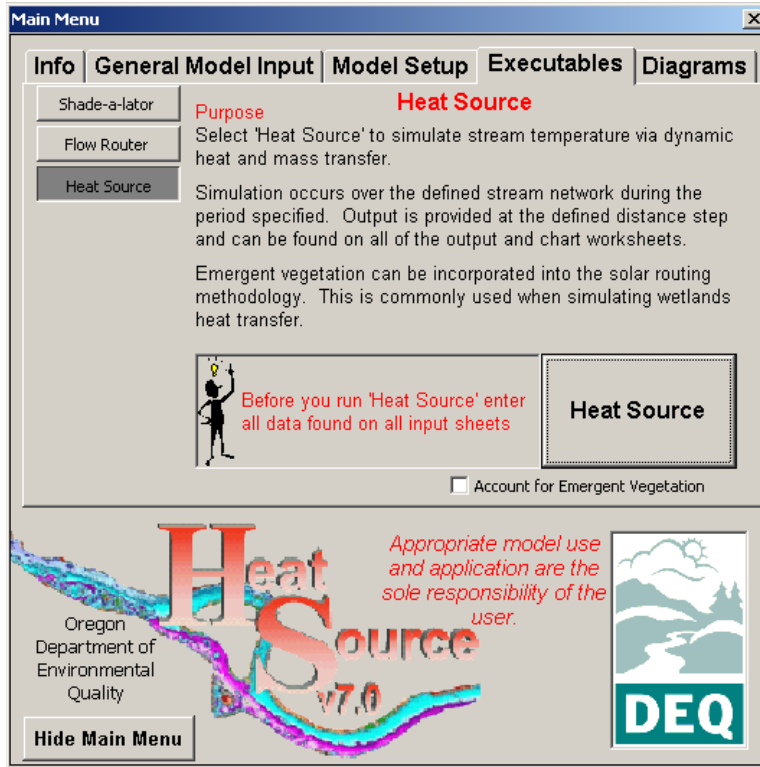
•**Application:**
Simulate dynamic flow routing, wetted channel dimensions and hydraulics (including hyporheic flows).

•**Inputs:** *All parameters found in the 'Morphology Data' worksheet, 'Flow Data' worksheet and 'Flow Boundary Conditions' in the 'Continuous Data' worksheet. If evaporation losses are included, all of the input sheets should be completed.*

•**Outputs:** *'Output – Hydraulics'*

4.4.3 EXECUTABLES – HEAT SOURCE

Heat Source is the combination heat and mass transfer models.



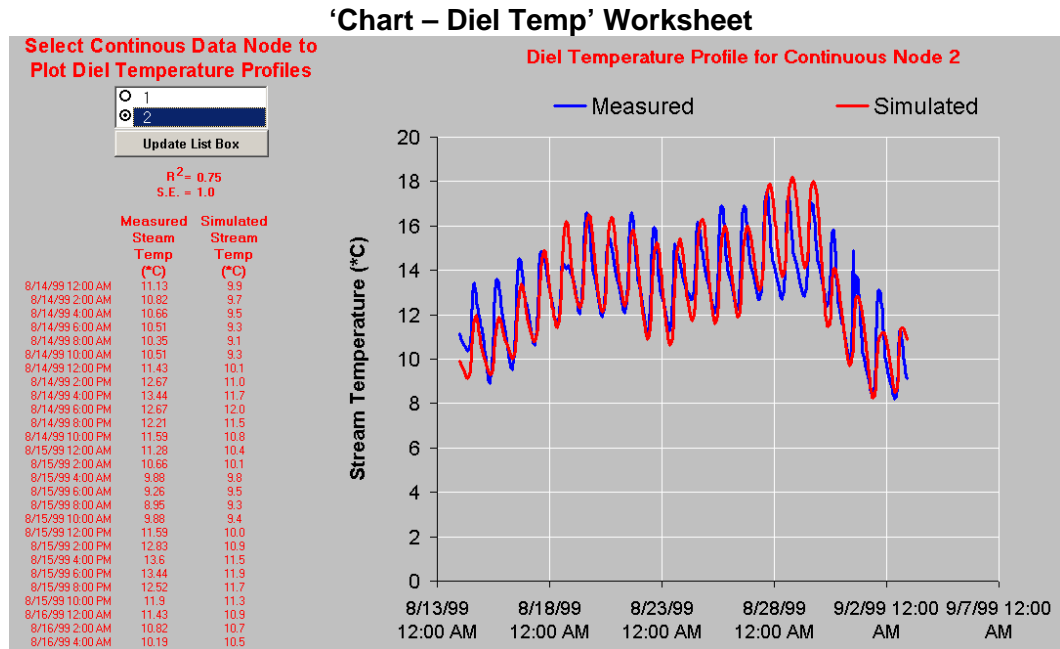
- Application:** Simulate heat transfer, dynamic flow routing, wetted channel dimensions and hydraulics (including hyporheic flows) and water column temperature.
- Inputs:** All of the input sheets should be completed.
- Outputs:** All of the output sheets will be completed.

4.5 MODEL OUTPUTS

4.5.1 CHART – DIEL TEMPERATURE

Measured hourly stream temperatures can be plotted against the simulated values for each 'Continuous Monitoring Node'. When a model run is completed, the 'Continuous Monitoring Node' list box is updated; however, when the model is opened, and not run, it will be necessary to press the 'Update List Box' button. Validation statistics are provided.

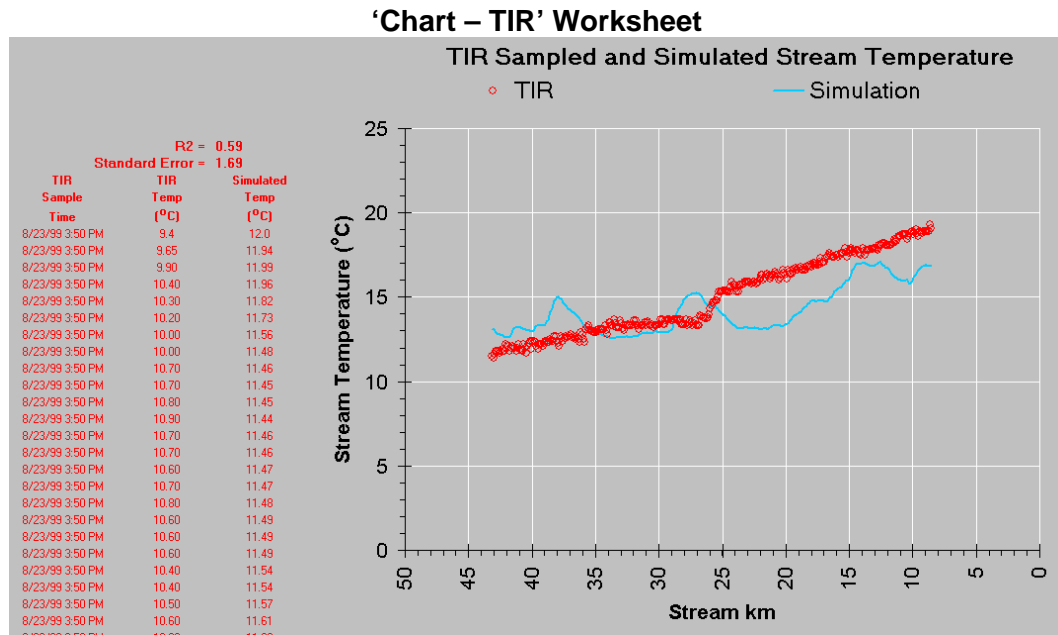
Important: Use this worksheet to validate the model output against measured temporal data.



4.5.2 CHART – TIR TEMPERATURE

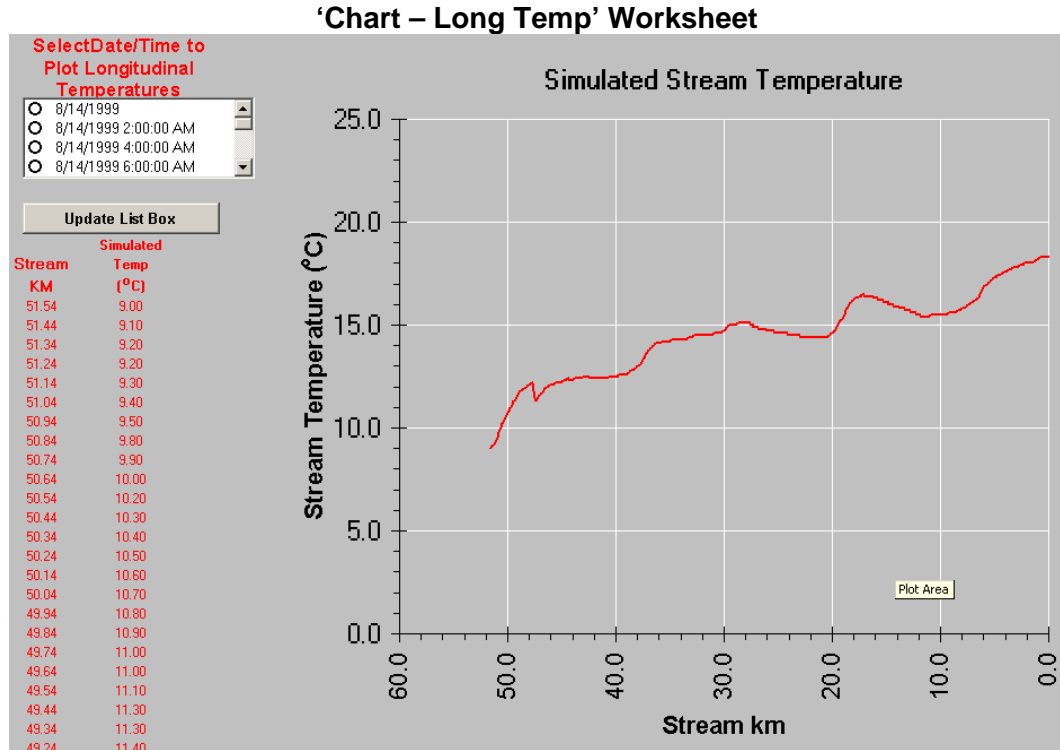
Measured TIR stream temperature data can be plotted against the simulated values that are paired with the closest location and time to the TIR measurement. Pairings are made during the simulation when and where they occur. Validation statistics are provided.

Important: Use this worksheet to validate the model output against measured spatial data. The example provided below would be considered a 'poor' result.



4.5.3 CHART – LONGITUDINAL TEMPERATURE

The spatial distribution of stream temperature can be plotted for any hour within the simulation period. You will need to press ‘Update List Box’ after each simulation run to populate the list box with the hourly data.

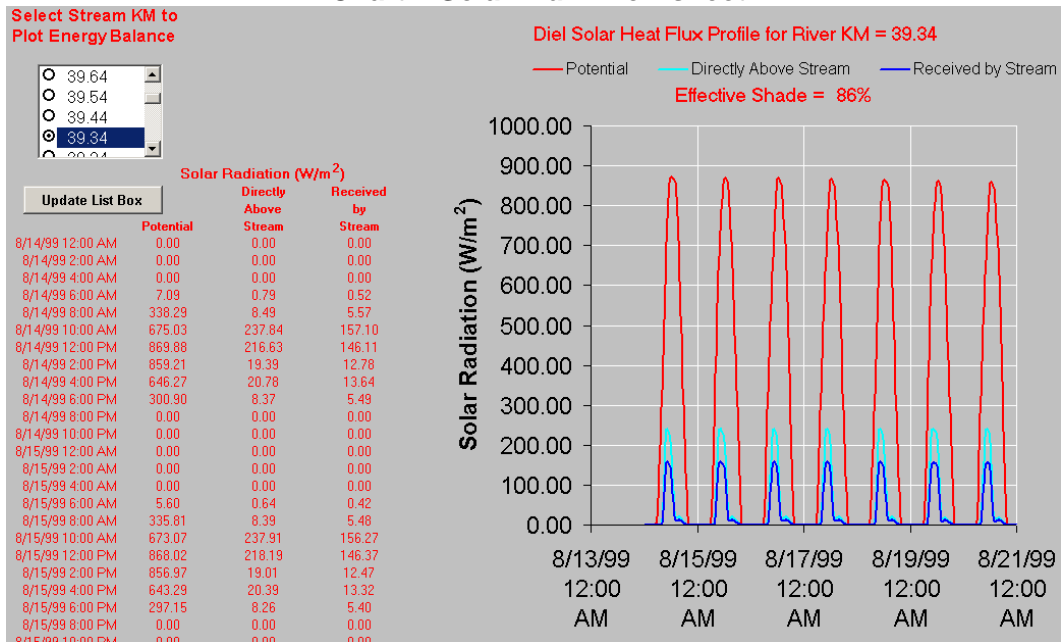


4.5.4 CHART – SOLAR FLUX

The hourly simulated solar heat flux can be plotted for any river kilometer (as determined by the model distance step) by double clicking on the list box.

- **Potential** - represents the solar heat flux (both diffuse and direct beam) that would reach the stream surface without shading or obstructions of any kind attenuate or scatter shortwave radiation (i.e. without land cover, topography, stream banks, etc.). Cloudiness is accounted for in the ‘Potential’ solar heat flux.
- **Directly Above Stream** - represents the solar heat flux that reaches the stream surface with shading and obstructions that attenuate and scatter shortwave radiation (i.e. with land cover, topography, stream banks, etc.). Cloudiness is accounted for in the ‘Directly Above Stream’ solar heat flux.
- **Received by Stream** - represents the solar heat flux that enters the water column after accounting for the surface reflection, transmission through the water column and substrate absorption.

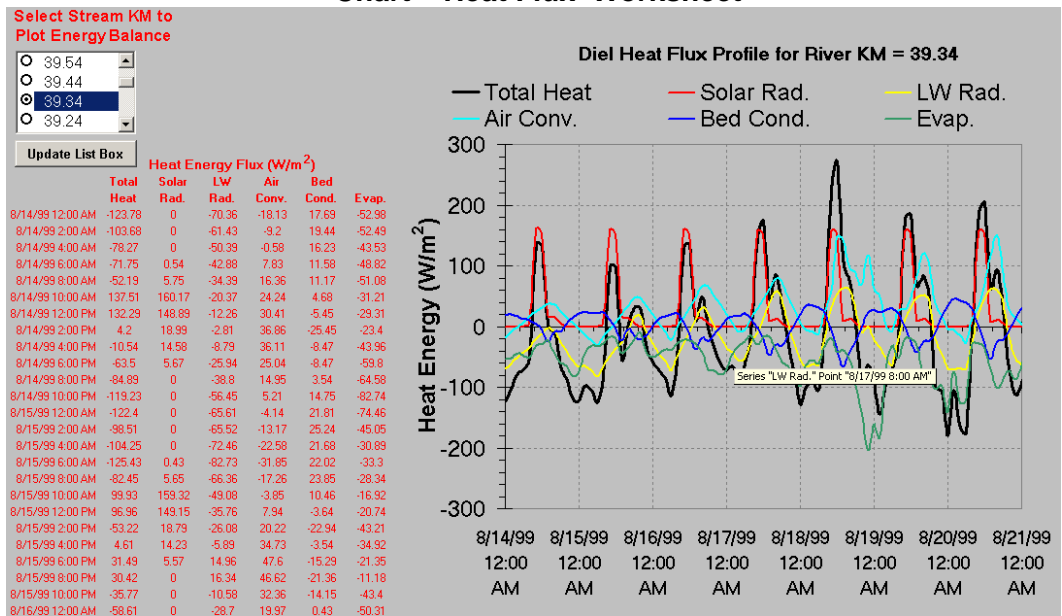
'Chart – Solar Flux' Worksheet



4.5.5 CHART – HEAT FLUX

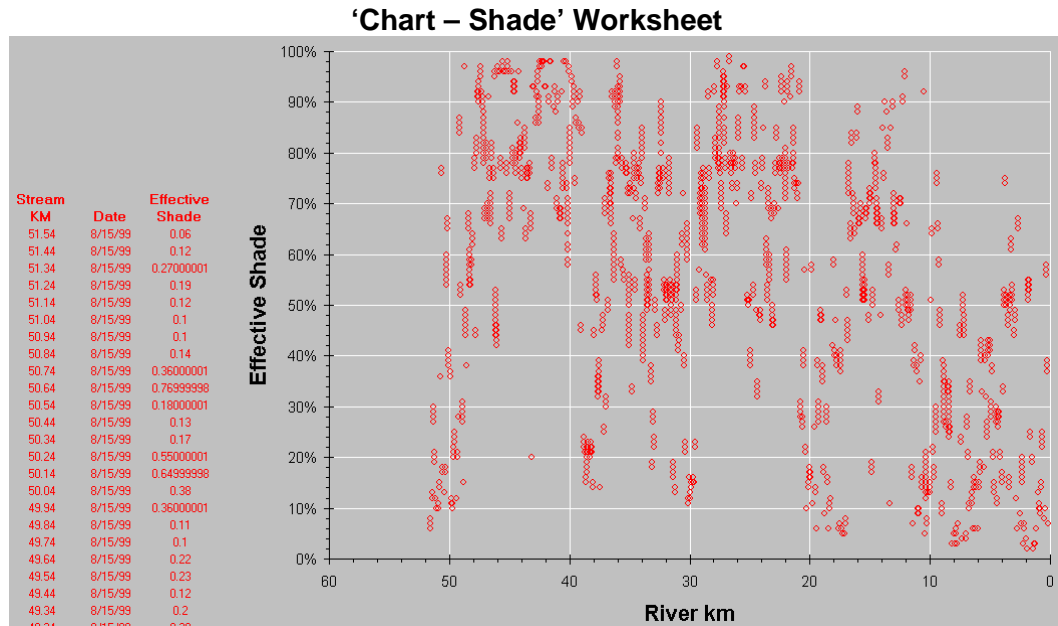
The hourly simulated heat flux parameters can be plotted for any river kilometer (as determined by the model distance step) by double clicking on the list box. These heat flux values represent water column heat transfer.

'Chart – Heat Flux' Worksheet



4.5.6 CHART – EFFECTIVE SHADE

Recall that effective shade is a ratio of potential and received solar radiation heat. Effective shade data is calculated at each model distance step and plotted longitudinally.



4.5.7 OTHER OUTPUT DATA WORKSHEETS

OUTPUT – HYDRAULICS

Daily hydraulics data are listed in the “Output – Hydraulics’ worksheet. The daily data that can be found on this worksheet are:

- Flow Volume (cms)
- Flow Velocity (m/s)
- Wetted Width (m)
- Average Wetted Depth (m)
- Maximum Wetted Depth (m)
- Hyporheic Exchange Volume (cms)
- Tendency to Stratify (via Densimetric Froude Number)

OUTPUT – TEMPERATURE

Hourly water temperature output data are listed in the “Output – Temperature’ worksheet.

OUTPUT – SOLAR POTENTIAL

Hourly solar heat flux (both diffuse and direct beam) data that would reach the stream surface without shading or obstructions of any kind attenuate or scatter shortwave radiation (i.e. without land cover, topography, stream banks, etc.). Cloudiness is accounted for in the 'Potential' solar heat flux.

OUTPUT – SOLAR SURFACE

Hourly solar heat flux output data that reaches the stream surface with shading and obstructions that attenuate and scatter shortwave radiation (i.e. with land cover, topography, stream banks, etc.). Cloudiness is accounted for in the 'Directly Above Stream' solar heat flux.

OUTPUT – SOLAR RECEIVED

Hourly solar heat flux output data that enters the water column after accounting for the surface reflection, transmission through the water column and substrate absorption.

OUTPUT – SOLAR LONGWAVE

Hourly longwave (thermal) radiation heat flux output data that accounts for atmospheric and land cover sources and the backradiation emission from the water surface.

OUTPUT – EVAPORATION

Hourly evaporation heat flux output data at the water surface - air column interface.

OUTPUT – CONVECTION

Hourly convection heat flux output data at the water surface - air column interface.

OUTPUT – CONDUCTION

Hourly conduction heat flux output data at the water column - substrate interface.

OUTPUT – TOTAL HEAT

Hourly total heat flux output data between the water column and the surrounding environment (air column and substrate).

OUTPUT – EVAPORATION RATE

Hourly evaporation rate output data resulting from diabatic and adiabatic processes.

OUTPUT – DAILY HEAT FLUX

Daily output data are listed in the “Output – Daily Heat Flux” worksheet. The daily data that can be found on this worksheet are:

- View to Sky (%)¹⁸
- Effective Shade (%)
- Potential Solar Radiation Heat Flux ($\frac{W}{m^2}$)
- Solar Radiation Heat Flux Above Stream Surface ($\frac{W}{m^2}$)
- Solar Radiation Heat Flux Received by Stream ($\frac{W}{m^2}$)
- Longwave Heat Flux ($\frac{W}{m^2}$)
- Convection Heat Flux ($\frac{W}{m^2}$)
- Conduction Heat Flux ($\frac{W}{m^2}$)
- Evaporation Heat Flux ($\frac{W}{m^2}$)
- Total Heat Flux ($\frac{W}{m^2}$)

4.6 COMMON SOURCES OF PROBLEMS

- **Poor Output Resolution:** Finite difference distance and time steps too coarse.
- **Model Instability (Crashes):** Combinations of finite difference distance and time steps may be creating model instability. If the problem persists when distance steps and time steps are reduced (i.e. $dx = 100$ m and $dt = 1$ minute), then the source of the instability is likely an input entry error. Nonnumeric input values will cause model problems. Null values in the input data set also may crash the model. Unless noted in the worksheets, all white cells should contain the appropriate model input (except in the ‘Land Cover Codes’ and ‘Validation Data’ worksheets).
- **Inaccurate or Sparse Meteorological Data:** When simulating over long distances in the Pacific Northwest, you will likely traverse variable land cover and topographic conditions that will affect the local microclimates. Further, the adiabatic lapse rate will generally reduce atmospheric pressure (affecting vapor pressures and the vapor pressure deficit), cool the air temperature as a function of increasing elevation and affect wind speed variability. This problem is only truly addressed with multiple atmospheric data measurement locations along the simulated stream network. However, such data will often be a limiting factor in model accuracy.
- **Diurnal Water Temperature:** Sometimes simulated stream temperatures will under or over predict when compared to measured diurnal changes. Recall that stream temperature change is inversely proportional to flow

¹⁸ View to sky is not a function of time/day.

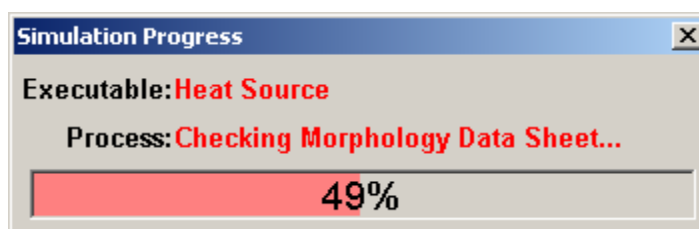
volume and water column depth. An over prediction of the diurnal temperature change indicates that either too much heat transfer to the water column or that the flow rate and/or water column depths are too low. Similarly, an under prediction of the diurnal temperature change indicates that either too little heat is transferred to the water column or that the flow rate and/or water column depth are too large.

4.7 DIALOGUE WINDOWS – PURPOSE AND MEANING

Many dialogue windows and message boxes will appear to help the user make decisions or explain problems. While the meaning is likely fairly clear, the purpose for these windows is explained briefly below.

4.7.1 PROGRESS WINDOW

There is a standard progress bar window that will appear during all model processes that take time to complete. Features of the progress bar window include the title of the procedure, the specific executable that is running, the specific process of the executable, and finally, the progress of the ‘process’ measured in terms of percentage completed.



4.7.2 MESSAGE BOXES

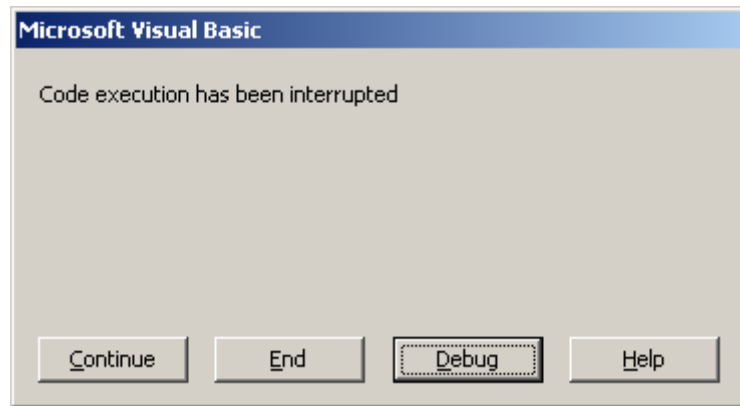
CLEARING INPUT DATA

The user will be asked before operations that delete or change model inputs. Now is a good time to suggest that the users save the model frequently and on local drives. Be careful before deleting data and be sure that you always have a previous version of your work saved. Excel has known bugs that will crash the model unexpectedly, and you should anticipate such problems. The authors also recommend that you refrain from working directly from networks or servers, due to a known Excel problem with completing large saves over networks.

Several message boxes will ask the user to confirm that they want to delete input data. Configuring the longitudinal data, inflow data sites and continuous data sites involves changing location and temporal data in the model. The user is asked whether they want to delete the current inputs associated with existing longitudinal or temporal data, since these data are about to be changed. If the user can keep track of existing data associations, it may be easier to choose not to delete existing data and simply move it appropriately after the location or temporal setup configuration.

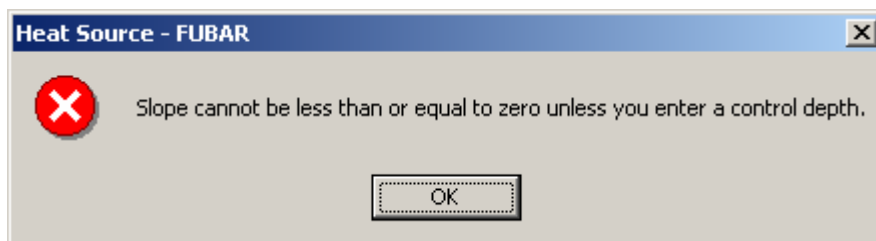
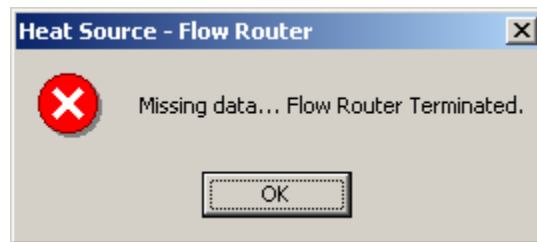
Code Execution Has Been Interrupted

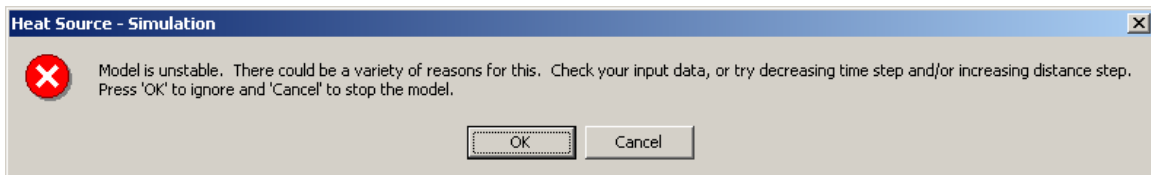
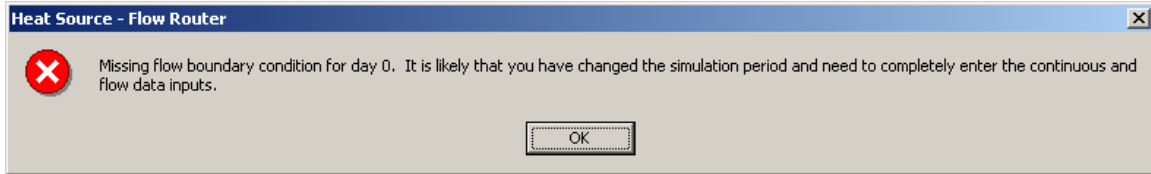
This is a very common Microsoft message box that notifies the user when VBA code has been stopped. You can trigger a code interruption by pressing the control and break keys at the same time (ctrl-break). This message will also appear when an irresolvable error occurs, such as division by zero, illegal math function (i.e. the arctangent of zero, square root of a negative number, etc.), or with illegal code syntax (i.e. open loops and logic statements). Unless triggered by the user, this message signifies serious problems with either the code or the input data that cannot be resolved without changes that address the underlying problem(s).



ERROR MESSAGES

There are embedded in the code several error messages that will notify the user that a problem has occurred. All of these error messages terminate with an end to the model run. Examples of such error message boxes are presented below.





FLOWS ARE APPROACHING ZERO – MODEL OPTIONS

A method is developed in Heat Source that allows flow volumes to reach zero without model failure (i.e. division by zero errors). Heat Source will notify the user once stream flows have reached $\frac{1}{4}$ cfs (0.0071 cms), or less, and will ask whether the operator would like to continue. This message is basically asking the user whether the low flows being simulated reflect the true condition. At this time the model operator can either stop the model run or continue the simulation. The model will not ask the user again about encountered flow volumes for the duration of the simulation.

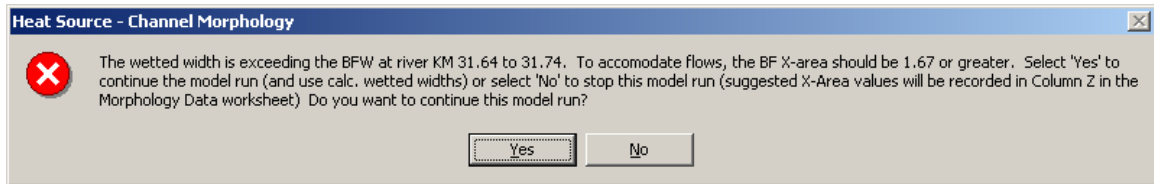
Once a user selects to continue the simulation, the model simply skips the stream nodes without sufficient flows to route (i.e. less than $\frac{1}{4}$ cfs). In these stream nodes, hydrologic and heat processes are not calculated and output variables are assumed to be zero. Proceeding downstream, the model will detect when flows become sufficient to commence flow routing again (i.e. greater than $\frac{1}{4}$ cfs).

Of particular concern is the estimation of the water temperature in this first stream node below the dewatered section, where flows are sufficient for flow routing and heat transfer modeling. In essence, this stream node represents a boundary condition. The model estimates this stream node temperature as the last known stream temperature value in the closest proximity to the stream node. It is likely that this assumption will be minimized since instream flows will be very small relative to the inflows and the inflow temperatures should dominate.



CALCULATED WETTED WIDTHS ARE EXCEEDING BANKFULL WIDTHS

Both Heat Source and Flow Router calculate wetted channel dimensions. If the flows exceed bankfull, per the bankfull channel design and flow inputs, the model will provide a message that warns the user of potential problems. Specifically, the user is notified where the location of the first bankfull flow. The user can choose to ignore this problem, and the model will simply calculate the appropriate wetted width for the flows (which will exceed the bankfull width), or the user can stop the model run and modify inputs. The model will list recommended bankfull cross-sectional areas in column Z in the morphology data worksheet. By changing W:D or channel side slope Z, the user can create a channel that will accommodate flows.



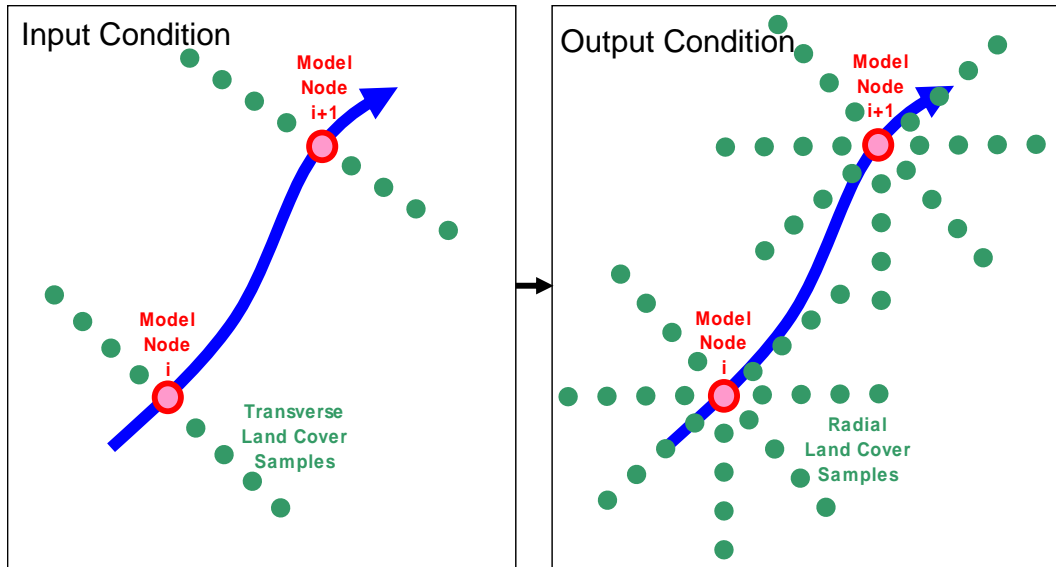
4.8 OTHER 'UTILITY' APPLICATIONS

A utility application (with VBA macros) is available (on the distribution CD) as a stand alone program to help manipulate input data. To date the 'Land Cover Positioner' is the only utility application packaged with Heat Source v. 7.0.

4.8.1 LAND COVER POSITIONER

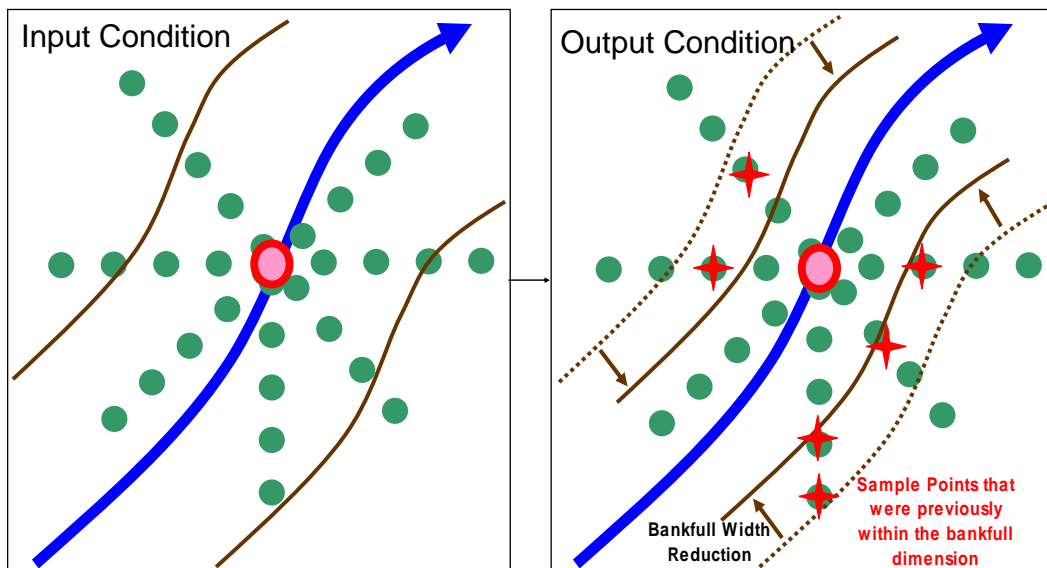
TRANSVERSE TO RADIAL LC VALUES

This worksheet macro will radially distribute transverse land cover inputs for Heat Source v. 7.0. Ttools v. 7.0 samples in a radial pattern and creates land cover data that is formatted for Heat Source. In the event that TTools 7.0 is not used to sample land cover, or a previous version of TTools is used to sample land cover values, this worksheet macro can transform transverse land cover data into radial sampled data.



UPDATE RADIAL LC VALUES

This worksheet macro will calculate whether radial sampled land cover and water sampled values will fall within or outside the channel boundary following a change in bankfull width. Points that are not within the bankfull channel are denoted with 'LC' (for Land Cover) and points that fall within the bankfull channel are denoted with 'W' (for Wet). A comparison of the current and the new channel width output (made by the macro for you) identifies the 'Dried' (no longer within the bankfull channel) and the 'Wetted' (now in the bankfull channel) locations. You can then search for these values ('Dried' and 'Wetted') and make appropriate changes (for example associate the nearest neighboring value).

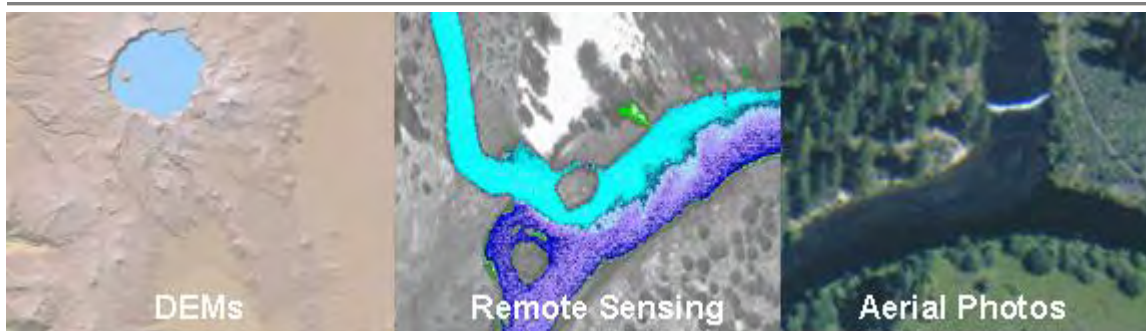


Chapter

V

Spatial Data Derivations

TTools Input Data, Procedures and Methods



Spatial Data Derivations Involved Automated Sampling of Spatial Databases and Performing Simple Calculations

5.1 INTRODUCTION

TTools 7.0 is an ArcView extension developed by the Oregon Department of Environmental Quality. This ArcView extension contains a suite of tools designed to automatically sample spatial data sets used in water quality modeling (mainly stream temperature modeling). TTools 7.0 is designed to assemble high-resolution (1:5,000 geographic scale) spatial databases.

This user manual is divided into three parts, which discuss 1) the types of geospatial data required 2) development of the core geospatial data sets, and 3) the TTools operating instructions. This user manual was written under the assumption that the reader has ArcView experience. Basic skills such as creating and editing themes, mosaicing DEMs, and obtaining and preparing aerial imagery are necessary.

Creating and sampling geospatial data sets requires creativity and the ability to “think outside the box”. This user manual is not going to answer every question that will arise when preparing data for TTools sampling. For example, you may need to figure out how to convert a DEM from one format to another in order for ArcView to recognize it, or you may obtain raw color aerial photographs that need to be scanned into the computer, georeferenced, and rectified before use. Often times, you may encounter a sub-basin that has an existing vegetation layer for the upper watershed area, and you will need to figure out how to incorporate that into the vegetation digitization process.

Once the user has the digitized stream, digitized banks, vegetation grid, and mosaiced DEM, TTools 7.0 may be used. The TTools 7.0 extension contains graphical dialogs and error-checks that prompt the user for inputs. The actual sampling procedure is consistent time after time, and the results are as good as the geospatial data sets that are sampled.

5.2 GEOSPATIAL DATA OVERVIEW

TTools is designed to sample high-resolution spatial data sets. Several GIS data sources that can be used are listed in **Table 5.1**. Developing spatial data sets from existing GIS or remotely sensed data must consider data resolution (map scale and positional accuracy). GIS data sources that describe landscape parameters can be developed at a high resolution (i.e., less than 1:5,000), however, many of the existing spatial data sets are coarse and may fail to capture variable landscape parameters. Modules contained in TTools can employ high-resolution sampling, provided that high-resolution (1:5,000) spatial data sets are available. It should be noted that the sampling density is user-defined and should be scaled to match GIS data resolution/accuracy.

Table 5.1
 Spatial Data Types and Applications

Spatial Data	Application
Digital Elevation Model (DEM)	<ul style="list-style-type: none"> • Measure Valley Morphology • Measure Topographic Shade Angles • Measure Stream Elevations and Gradients
Aerial Imagery (Digital Orthophoto Quadrangles and Rectified Aerial Photos)	<ul style="list-style-type: none"> • Map Streams (1:5,000 scale) • Map Near Stream Vegetation (1:5,000 scale) • Map Channel Morphology • Map Roads, Development, Structures
Thermal Infrared Radiometry Temperature Data (TIR)	<ul style="list-style-type: none"> • Measure Surface Water Temperatures • Develop Longitudinal Temperature Profiles • Identify Subsurface Hydrology, Groundwater Inflow, Springs

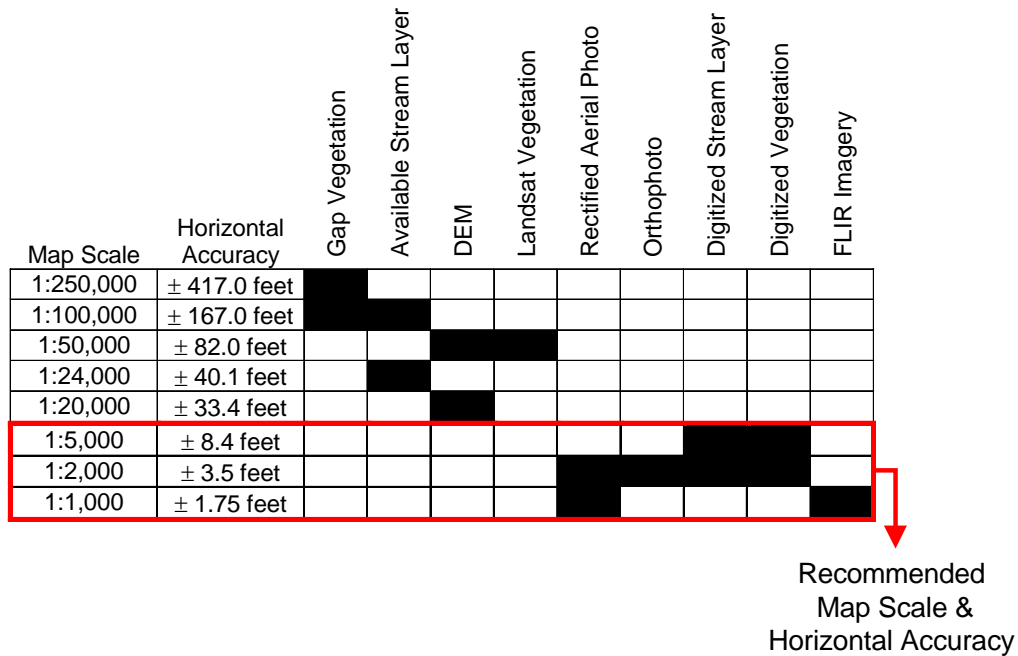


FIGURE 5.1
 Widely Available Spatial Data Types and the Associated Resolution

5.3 AERIAL IMAGERY - DIGITAL ORTHOPHOTO QUADRANGLES AND RECTIFIED AERIAL PHOTOS

Spatial data sets derived from Aerial Imagery include:

- Stream Position
- Stream Aspect
- Channel Width
- Near Stream Riparian Land Cover

A digital orthophoto quadrangle (DOQ) is a digital aerial photograph in which displacements caused by the camera angle and the terrain have been removed. It combines the image characteristics of a photograph with the geometric qualities of a map. The standard DOQ is black-and-white, with a one-meter pixel resolution (color DOQs are also available for some locations).

Standard color aerial photographs can be digitally scanned, georeferenced, and rectified. The product is similar to a DOQ, but is multispectral and usually has less than one-meter resolution. In the very near future high-resolution (one-meter or two-meter pixel) satellite imagery should become available. Certain satellites can record full spectrum imagery for large geographic areas. This imagery is most often georeferenced and can be collected at almost any moment. Hence, the satellite imagery is seamless and can be collected and available in very short time spans.

DOQs and rectified aerial photographs are used to map streams, delineate riparian land cover, and to identify previously unmapped features such as diversions, small dams, etc.

5.3.1 DIGITIZED STREAM POSITION FROM AERIAL IMAGERY

Stream polyline accuracy is a function of the mapping scale. For example, the figure below demonstrates that a stream polyline at 1:100,000 mapping scale (red line) simplifies sinuosity and has local horizontal inaccuracies of over 200 feet. Sampling with a 1:100,000 stream polyline will result in inaccurate sampling reference points and simplified stream sinuosity. As can be seen in the figure below, a stream polyline digitized at 1:5,000 mapping scale will properly identify stream position and will yield accurate reference points for sampling.

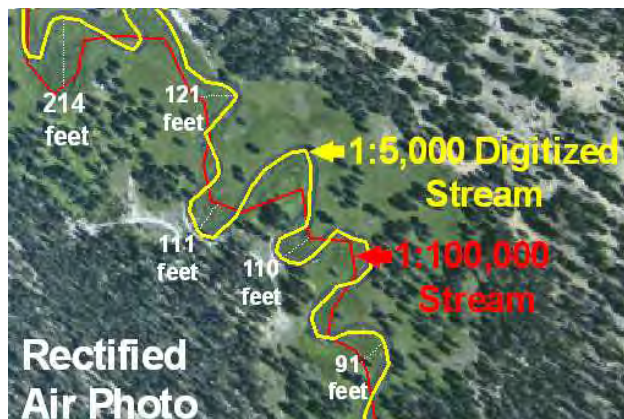


FIGURE 5.2
Comparison of Stream Position Mapped at 1:100,000 and 1:5,000 Scales – Measurements (in white) Indicate Horizontal Positional Errors in the 1:100,000 Scaled Stream Layer

Digitized stream position is used to develop data nodes (reference points) for sampled/derived data generated with the TTools extension. Once a stream polyline has been digitized, it is segmented at a user defined interval to produce a point data layer (shapefile). This point data theme is then used to sample other parameters (and data generated is associated with these discrete points). A common longitudinal sampling distance is 50 meters.



FIGURE 5.3
Digitized Stream Position Polyline and Segmented Stream Data Nodes Point Layer Segmented at 50 meter Interval (Mapped at 1: 5,000 Scale)

5.3.2 STREAM ASPECT

The stream aspect is defined as the angle that exists between the velocity vector (\vec{U}) and true north (0°). TTools calculates this angle as the angle between each of the stream data nodes (see **Figure 5.4**).

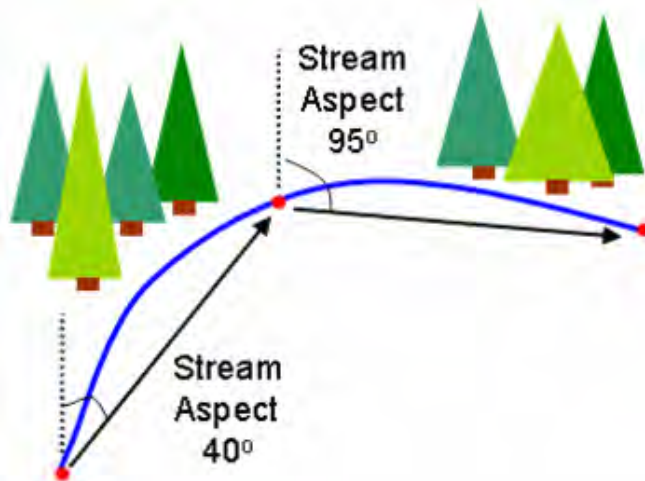


FIGURE 5.4
Stream aspect is calculated by calculating the angle between two stream nodes.

5.3.3 CHANNEL WIDTH FROM AERIAL IMAGERY

Channel width can be measured from digitized channel edge polylines. At each stream segment node TTools measures the distance between the left and right channel edge polylines in the transverse direction (i.e. perpendicular to the aspect).

Channel morphology is largely a function of high flow volume magnitude/frequency, stream gradient, sediment supply and transportation, stream bed and bank materials and stream bank stability (Rosgen 1996 and Leopold et al. 1964). The predominant thermodynamic influence of channel morphology is quite simple. Wider channels result in the combined effect of increased solar radiation loading via decreased stream surface shade and increased stream surface area exposed to solar radiation loading. A wider stream has a larger surface and a corresponding decrease in depth (more water is exposed to surface heat transfer processes). Stream hydraulics are a function of wetted perimeter (bathymetry), gradient and channel roughness. Surface and groundwater interactions may change with channel morphology modifications (relations to alluvial aquifer, groundwater inflow, hyporheic flows, etc.). **Figure 5.6** displays longitudinally sampled channel width for the Williamson River, Oregon.

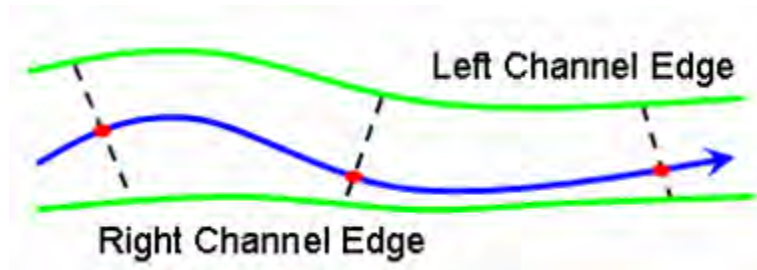
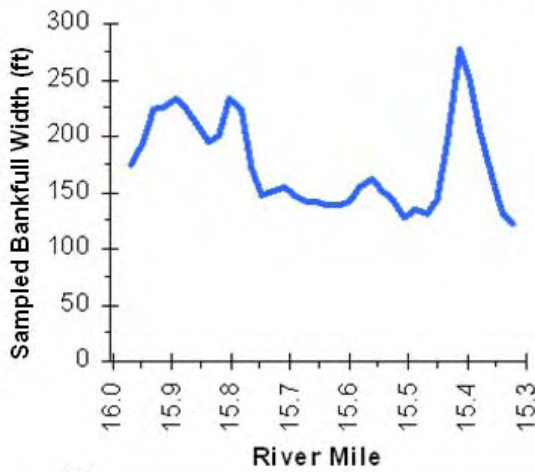


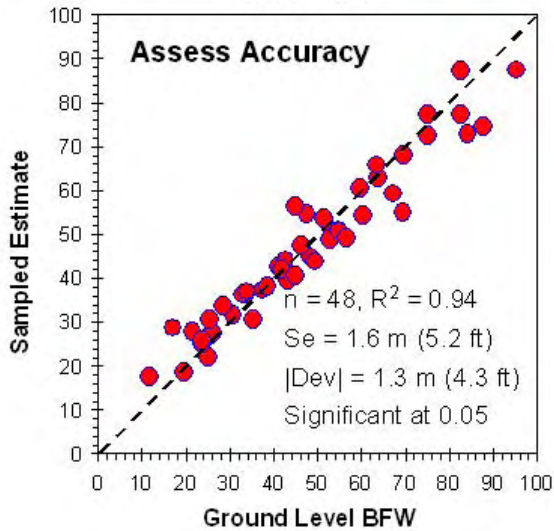
FIGURE 5.5
Channel Width Sampling from Digitized Channel Edges at Each Stream Data Node



Digitized Channel Edges and Stream Data Nodes (Williamson River, Oregon)



Sampled Channel Width (Williamson River, Oregon)



Statistically Assess Sampled Channel Width Accuracy (Williamson and Sprague Rivers, Oregon)

FIGURE 5.6
Digitized Channel Width Sampling, Results and Validation Statistics

5.3.4 NEAR STREAM LAND COVER MAPPING FROM AERIAL IMAGERY

The role of near stream land cover in maintaining a healthy stream condition and water quality is well documented and accepted in scientific literature (Beschta et al. 1987). Near stream land cover has several influences upon the stream and the surrounding environment that warrant listing:

- Near stream land cover plays an important role in regulating radiant heat in stream thermodynamic regimes.
- Channel morphology is often highly influenced by land cover type and condition by affecting flood plain and instream roughness, contributing coarse woody debris and influencing sedimentation, stream substrate compositions and stream bank stability.
- Near stream land cover creates a thermal microclimate that generally maintains cooler air temperatures, higher relative humidity and lower wind speeds along stream corridors.
- Riparian and instream nutrient cycles are affected by near stream land cover.

With the recognition that near stream land cover is an important parameter in influencing water quality, the development of land cover data sets should be a high priority. Variable land cover conditions require a higher resolution than most currently available GIS land cover data sources. To meet this need, one may need to map near stream land cover using rectified color aerial imagery. Using physical attributes associated with land cover classifications, sampling can be completed across a large landscape scale. Summarized land cover attributes (e.g. height, density and overhang data) can then be used to populate the digitized land cover polygons.

The high resolution of orthorectified aerial photographs allows for detailed analysis and mapping of riparian land cover within ArcView. A trained technician can digitize a 600-foot wide riparian corridor for a 50-mile stream in about one day. Ground level data must be applied to determine species composition and height values. Canopy densities can be visually determined from the aerial photographs.

An additional benefit of using orthorectified aerial photographs is that the true color or panchromatic images allow visual decipherment of tree types and canopy densities. Features such as roads and buildings are also easy to map from aerial photographs as opposed to alternative spectrum (i.e., infrared) images. Aerial photograph analysis facilitates the development of dozens of riparian vegetation classes, whereas most alternative spectrum satellite data can be translated into fewer and more general land cover classes. The image below exemplifies some riparian classifications that were developed from black and white DOQ interpretation at a 1:5,000 scale.

Near stream land cover vegetation mapping can be completed on a sub-basin (fourth field watershed) scale. Large rivers/streams (third order and higher) and selected major tributaries are typically the focus. Total river miles mapped may be up to approximately 200 to 500 miles in larger sub-basins.

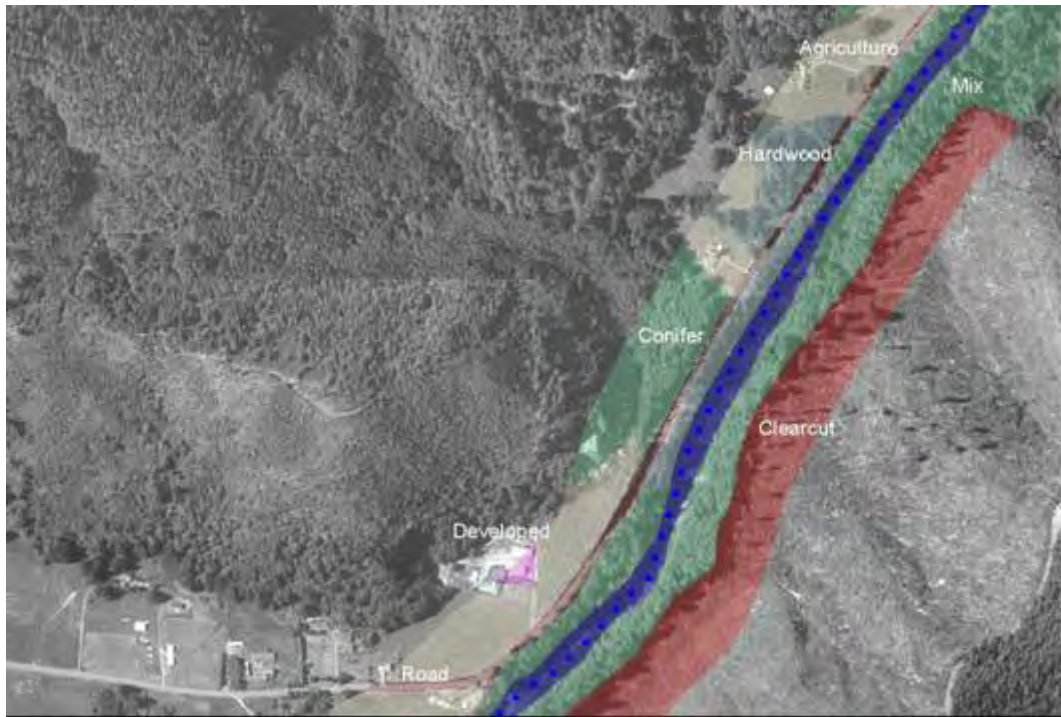
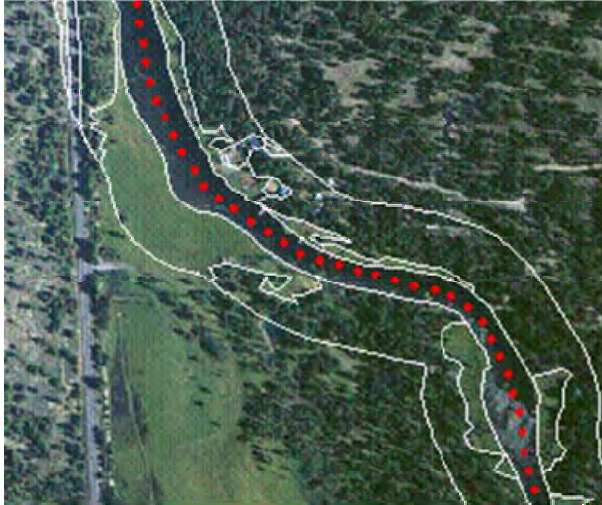


FIGURE 5.7
Digitized Near Stream Land Cover from a DOQ at 1:5,000 (Trask River, Oregon)

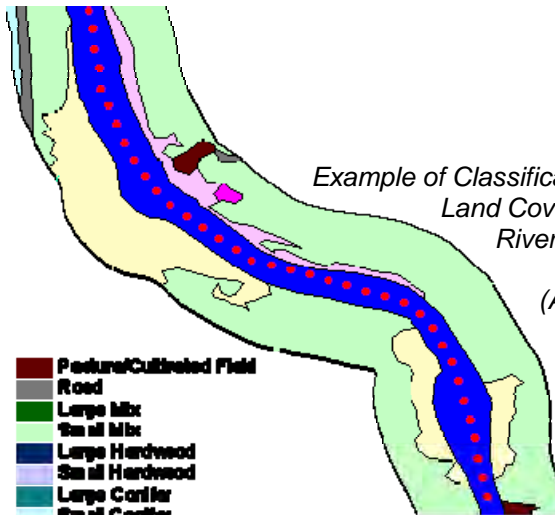
There are a number of potential imagery sources for riparian vegetation mapping (aerial near infrared classified data, satellite classified data, etc.). Accuracy of the mapped riparian vegetation coverage depends upon the spatial resolution, aerial extent of analysis, and spectral resolution of the imagery used. When mapping vegetation in narrow riparian corridors (typically less than 100 meters from the stream), a pixel size of one meter or smaller is desirable to maintain a high spatial resolution.

Regardless of the data or imagery source, there are generally three steps associated with near stream land cover quantification. First, the land cover must be mapped (remotely sensed or digitized) and classified. This basically involved developing polygons and populating each with a numeric code representing a near stream land cover type. Second, TTools sampling of the polygon representations of land cover type at user defined intervals allows the derivation of a landscape scaled land cover type data set. To this point, the discussion has focused on land cover types, and not the physical attributes of each type. The third basic step is then to assign physical attributes (height, canopy density and overhang) to each of the land cover types. Physical attribute information can be a summary of ground level information and data (measurements, growth curves, best professional judgment, etc.) With this association, an estimate of both land cover type and physical dimension is available for assessment and input into the Heat Source methodology.



Example of Polygon Mapping of Near Stream Land Cover from Aerial Color Imagery (Williamson River, Oregon)

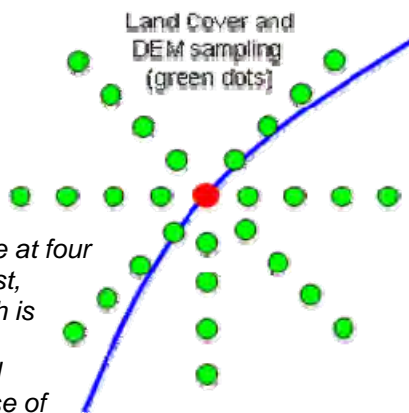
(At this point only the line work is complete and no data is associated with the polygons.)



Example of Classification of the Land Cover Polygons Associating a Land Cover Type to Each of the Polygons (Williamson River, Oregon)

(At this point a land cover type numeric code is associated with each polygon.)

- Pasture/Cultivated Field
- Road
- Large Mix
- Small Mix
- Large Hardwood
- Small Hardwood
- Large Conifer
- Small Conifer
- Shrub - Upland
- Shrub - Wetland
- Grasses - Upland
- Grasses - Wetland
- Water
- Developed - Residential
- 25% Distribution of Shrub
- 75% Distribution of Shrub



TTools radial sampling pattern for near stream land cover (sampling interval is user defined). Radial land cover sampling occurs for every stream data node at four user-defined intervals in the northwest, west, southwest, south, southeast, east, and north east directions (North is not sampled since the sun does not shine from that direction in the northern hemisphere, and shadows will hence not be cast in a southerly direction). A database of land cover type in created for each stream data node.

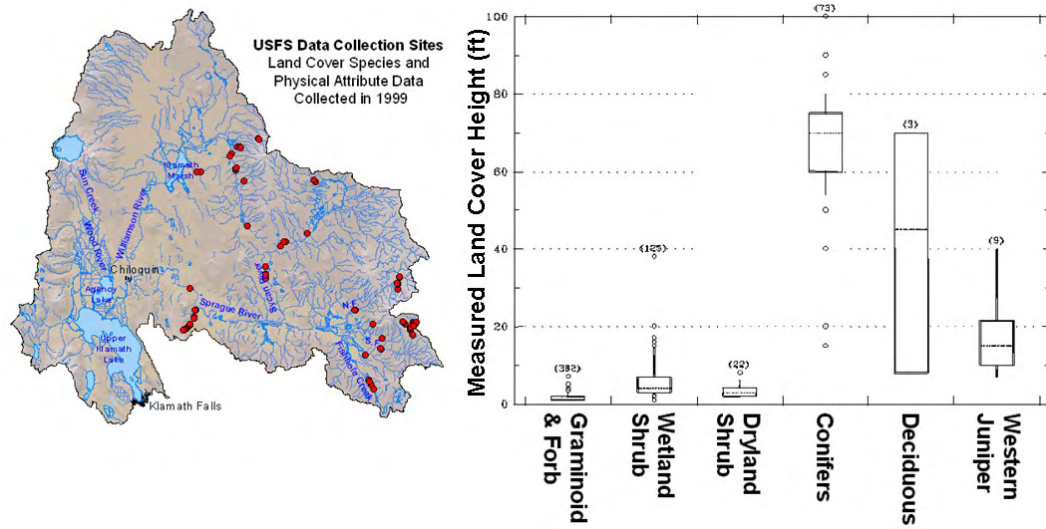


FIGURE 5.8
 Example of Near Stream Land Cover Ground Level Monitoring Sites and Summarized Physical Attribute Data (Williamson and Sprague Rivers, Oregon). These data allow the near stream land cover classifications to be associated with local physical attribute information specific to the basin of interest.

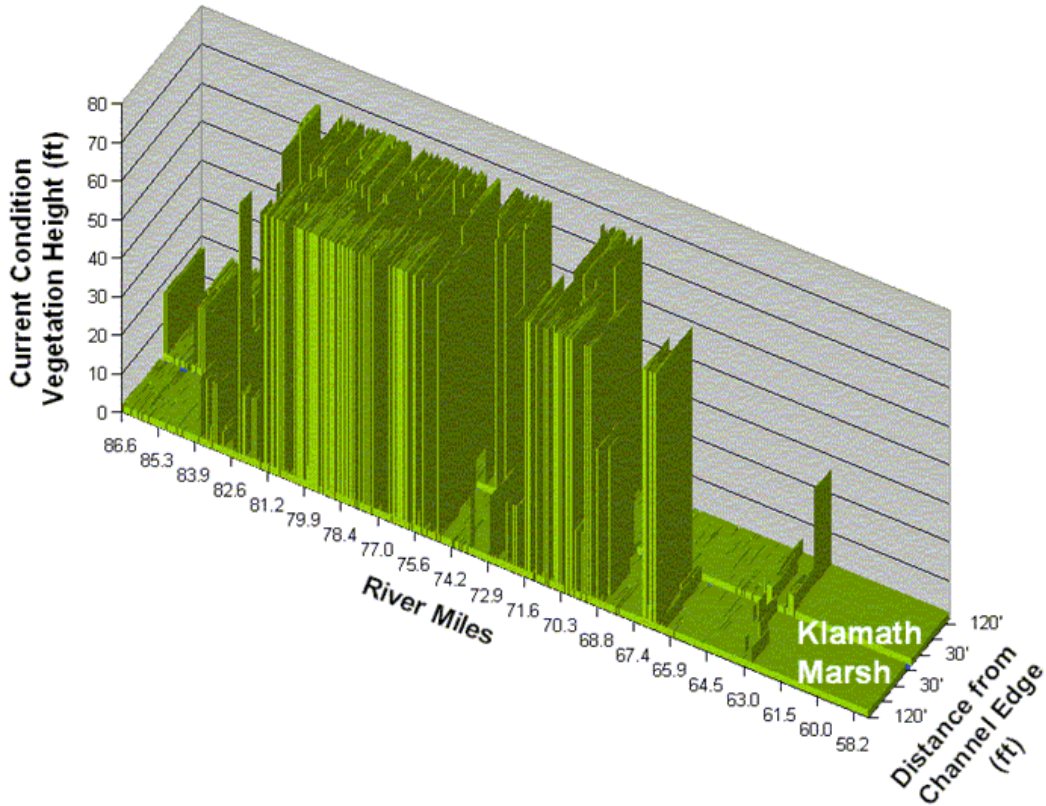


FIGURE 5.9
 Near Stream Land Cover Height (Upper Williamson River, Oregon)

5.4 DIGITAL ELEVATION MODEL (DEM)

Spatial data sets derived from DEMs include:

- Stream Elevation
- Stream Gradient
- Maximum Topographic Shade Angles (East, South, West),

The Digital Elevation Model (DEM) data files are grids, in which each cell contains a land surface elevation value. The U.S. Geological Survey, as part of the National Mapping Program produces these digital cartographic/geographic data files. DEMs typically have either a 30-meter cell size or a 10-meter cell size. DEMs are used to determine stream elevation, stream gradient, valley gradient, valley shape/landform and topographic shade angles.

5.4.1 STREAM ELEVATION

Stream elevation is measured from a DEM. TTools will auto-detect the pixel size (either 10 meter or 30 meter) of the DEM. In order to find the lowest pixel nearest to the stream segment node, TTools samples 25 pixels: the pixel that falls directly on the stream segment node and two pixels in each direction surrounding it. The lowest elevation sampled is assigned to the stream segment node.

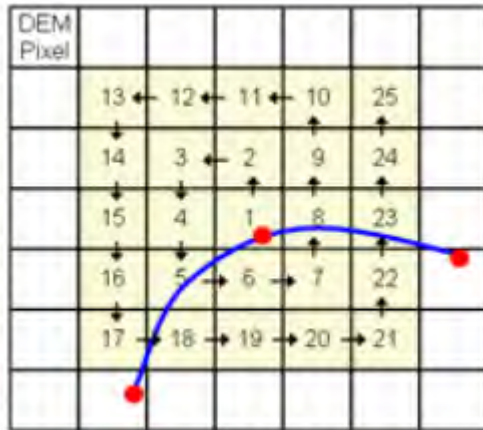


FIGURE 5.10
The procedure for sampling stream elevation involves twenty five discrete samples in a radial pattern to locate the lowest datum.

5.4.2 STREAM GRADIENT

Stream gradient is calculated from the elevation of the stream node and the distance between nodes. The DEMs have a 3.3 feet (one meter) elevation resolution. It commonly occurs that a measurable (i.e. greater than 3.3 feet) elevation drop spans several of the stream segment nodes. Gradients are calculated as:

Stream Gradient Calculation,

$$S_o = \frac{z_i - z_{i^*}}{(i - i^*) \cdot dx} \quad (5-1)$$

Variables,

Measured/Known

- dx : Distance Step (m)
- i : Stream Data Node
- i* : Last Stream Node Where ($z_{i^*} > z_i$)
- z : Elevation (s)

Calculated

- S_o : Stream Gradient (unitless)
-

5.4.3 TOPOGRAPHIC SHADE ANGLE

The maximum topographic shade angle is calculated to the east, south and west, relative to the stream segment node. In each direction (east, south and west) TTools steps away from the stream sampling the DEM pixels for elevation and calculating topographic shade angle. TTools records the value and the X and Y coordinates of the point that represents maximum topographic shade angle. While this description is fairly simple, the methodology is actually quite complex.

The overriding intent of topographic shade calculation focuses on locating the local maximum associated with each data node in the three direction (East, West and South). Generally, there are near field (stream bank, valley morphology, etc.) and far field (hills, mountains, etc.) topographic features that combine to form topographic shade. In terms of the local effect of topographic shade, only the highest directional topographic angle (and not necessarily the highest topographic feature) is a controlling factor. With this background, it becomes apparent that the search regime for the maximum topographic feature must include both the near and far field.

A near field search must be high resolution, because the distance from the stream is small, increasing the importance of even small elevation differences from stream banks and morphology. The near field search directionally samples each DEM pixel for a total of twenty five pixels¹⁹. The highest near field

¹⁹ For a 10-meter DEM, the near field search distance is 250 meters (820 feet). For a 30-meter DEM, the near field search distance is 750 meters (2460 feet).

topographic shade angle, for all three directions, is stored in memory for each stream node.

The far field search for the maximum topographic shade angle typically targets large features (hills, mountains, etc.) and spans greater distances from the stream. These factors allow fewer restrictions for sampling resolution (and allow greater sampling interval distances). Computationally, this is very important because grid data sampling can be long and expose ArcView bugs that may interfere with application functions. The user is allowed to enter the far field sampling interval and the distance to sample. The higher of the two maximum topographic shade angles (near field and far field) is entered in the stream node database.

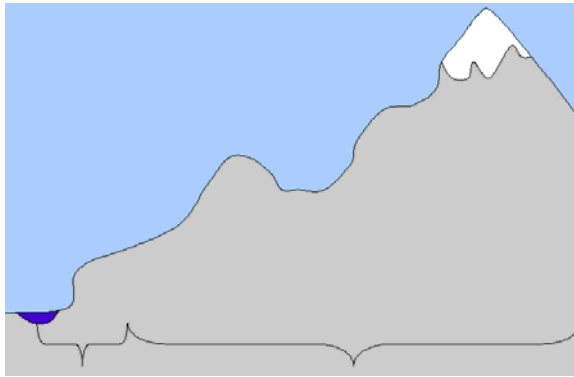


FIGURE 5.11
*Near and Far Field
Topographic Shade Angle
Calculations from DEM Data*

Near-field:

Each of first 25 DEM cells is sampled.

Far-Field:

User determines sample distance and interval

TTools records the max topographic shade angle.

Topographic Shade Calculation,

$$\theta_T = \tan^{-1}\left(\frac{z_T - z_i}{L_T}\right) \quad (5-2)$$

Variables,

Measured/Known

dx : Distance Step (m)

i : Stream Data Node

L_T : Distance from Stream Data Node "i" to topographic feature

z : Elevation (s)

z_T : Elevation of Topographic Feature (s)

Calculated

θ_T : Topographic Shade (degrees)

5.5 THERMAL INFRARED RADIOMETRY (TIR) TEMPERATURE DATA

5.5.1 OVERVIEW OF TIR DATA

TIR thermal imagery measures the temperature of the outermost portions of the bodies/objects in the image (i.e., ground, riparian vegetation, stream, etc.). The bodies of interest are opaque to longer wavelengths (Atwell et al. 1971). On free flowing streams, water columns are usually well mixed and surface temperatures represent the temperature of the water column. The exception is in thermally stratified areas, which may occur in slow, deep channels or upstream of impoundments.

For Oregon DEQ TIR remote sensing, a sensor mounted on a helicopter records digital data to an on-board computer at a rate that insures the imagery maintains a continuous image overlap of at least 40%. The radiometer detects emitted radiation at wavelengths from 8-12 microns (long-wave) and records the level of emitted radiation as a digital image across the full 12-bit dynamic range of the sensor. Each image pixel contains a measured value that is directly converted to a temperature. Each thermal image has a spatial resolution of less than one-half meter per pixel. A visible wavelength video sensor captures the same field-of-view as the TIR sensor. Geographic position system (GPS) time is encoded on the recorded video as a means to correlate visible video images with the TIR images during post-processing.

Data collection is timed to capture maximum daily stream temperature, which typically occur between 14:00 and 18:00 hours. The helicopter is flown longitudinally over the center of the stream channel with the sensors in a vertical (or near vertical) position. In general, the flight altitude is selected so that the stream channel occupies approximately 20-40% of the image frame. A minimum altitude of approximately 300 meters is used both for maneuverability and for safety reasons. If the stream splits into two channels that cannot be covered in the sensor's field of view, the survey is conducted over the larger of the two channels.

5.5.2 TIR DATA COLLECTION AND VALIDATION METHODS

A calibrated FLIR radiometer is used to collect a series of digital thermal infrared images along a stream reach with the sensor maintained at a normal angle of incidence (approx. 90°) to minimize the variability in emissivity (and hence reflectivity) at the water surface. Sensing in the 8-12 μ wavelengths minimizes shortwave reflections (i.e. the solar spectrum occurs between 0.3 to 2.2 μ , with a peak at 0.5 μ) from the water surface (Wunderlich 1972).

Prior to the airborne survey, in-stream data loggers are distributed in the basin in order to ground truth (i.e. verify the accuracy) of the TIR images. Data loggers are placed evenly over the planned flight area with three to six in situ measurements per survey. Weather conditions including sky conditions, air temperature, and relative humidity are collected for the times of the survey at fixed weather stations (e.g. USFS remote automated weather stations, RAWS, Agrimet, local airports) or using portable weather stations. The recorded TIR images contain measured radiance values that are then converted to surface temperatures based on the calibration factor of the sensor, emissivity of natural

water, atmospheric transmission, and ambient reflections (multi-scattering). For the calculations, the emissivity of the stream is assumed to be 0.96, which is within the 0.92 to 0.96 range published for natural water (Avery and Berlin 1992). This assumption is made while also recognizing that slight changes in emissivity result from differences in surface roughness (Torgersen et al. 2001) and suspended sediments (Wen-Yao et al. 1987). The error contribution from these factors in TIR derived stream temperature measurement is quite small (i.e. less than 0.5°C). The atmospheric transmission of the emitted energy between the water surface and the sensor is simulated with the MODTRAN atmospheric transmission model and using the measured weather conditions at the time of the survey (Berk et al. 1989). The ambient reflection component is modeled using an estimation of average longwave energy emitted from bank side vegetation and the reflectivity of natural water at normal viewing angles (i.e. 4%). Variable near stream land cover and topography over the survey extent can alter the reflective component. However, the reflected energy from the stream surface is 4% or less of the energy received at the sensor. If reflections from land cover were not accounted for, the calculated apparent temperature of the water could potentially increase by 0.4°C (Kay et al. 2001). Including a calculated estimate for the reflected component received at the sensor improves the absolute accuracy of the radiant temperature.

For validation purposes, the calibrated radiant water temperatures are then compared to in situ measurements from the instream data loggers at the time of the over-flight. If a consistent difference is observed between the radiant temperature and the in-stream temperatures, the atmospheric transmittance, as the most sensitive variable, is adjusted to provide a more accurate measurement of temperature. The resultant accuracy is then reported for each airborne TIR survey as a validation statistic that quantifies error. In most cases, the radiant temperatures are further validated against independent instream data collected by various federal and state agencies as part of ongoing monitoring efforts. Stream temperatures are sampled from the imagery through the center of the stream channel to derive spatial temperature patterns over the surveyed reach. Derived stream temperature profiles illustrate how stream temperatures vary longitudinally along the stream course.

Kay et al. (2001) suggests that an accuracy of 1.0°C is required to quantify stream temperature gradients, identify ground and surface water inputs, and create a boundary condition for basin scale hydrologic models. In the Upper Grande Ronde River subbasin, Oregon, ODEQ found radiant measurements of stream temperatures, to be accurate within 0.5°C (**Figure 5.12**). Torgersen et al. (2001) report similar levels of TIR data accuracy.

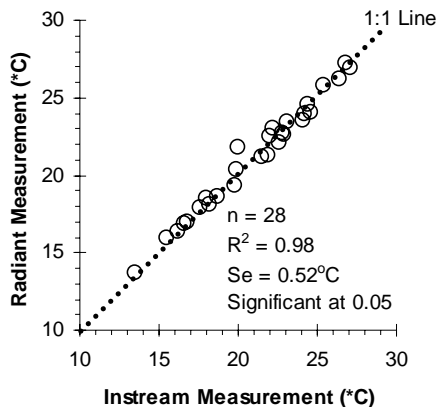


FIGURE 5.12
TIR Data Validation - Instream measured and radiant measured stream water temperatures in the Grande Ronde Basin, Oregon, excluding stratified areas (August 19-20, 1999).

5.5.2 INTERPRETATION OF FLIR IMAGES

What temperature does TIR data actually measure? In short, the answer to this question is that TIR images represent water surface (or skin) temperatures because water is essentially opaque to the electromagnetic spectrum greater than 2.65μ (Wunderlich 1972). By measuring surface temperature the accuracy of the radiant temperature is not influenced by a transmissive component from the stream bed and is therefore not a function of stream depth.

TIR images measure the global water temperatures in stream systems where turbulent mixing occurs (Torgersen et. al. 2001, ODEQ 2000, Boyd and Kasper 2002). The instream data loggers that are used to calibrate and validate the TIR images also can be used to confirm that the water column is mixed and that the measured radiant temperatures are representative of the global water temperatures. Furthermore, visible band color video is collected simultaneously with the TIR images and directly shows areas of obvious mixing such as riffles and rapids.

Flowing water is inherently mixed from dispersion (i.e. turbulent diffusion) and the vertical mixing that occurs from a variable flow profile (i.e. slower velocities occur near the stream boundaries and faster velocities occur away from channel boundaries) (Martin and McCutcheon 1999). Thermal stratification often develops in areas where little or no mixing occurs such as behind impoundments or in deeper low velocity channels. When a stream is stratified, TIR measurements represent only the surface temperatures. It follows that recognition of a thermally stratified, as opposed to a mixed water column, will control how TIR images are interpreted. Under mixed flow conditions visible shadows have no influence on thermal infrared signatures at the stream surface (**Figure 5.13**).

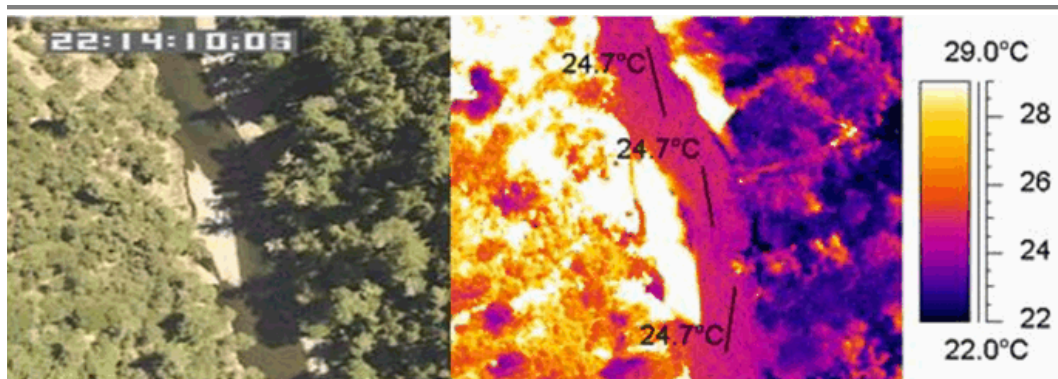


FIGURE 5.13
An Example of Mixed Stream with Shaded Surface from TIR Image without Differential Surface Heating (Faux, personal communication)

Even heavily stratified stream reaches have some level of mixing that is visible where cooler deeper water mixes to the surface around bends, instream objects or from wind kinetic energy. As a result, TIR imagery can be used to

identify thermal stratification (**Figure 5.14**). The presence or absence of a thermal stratification provides information about both flow conditions and stream temperature. Over a stream network, a portion of the stream segments will tend to display thermal stratification. For example, of the 442 km stream length surveyed in the upper Grande Ronde River sub-basin, Oregon, a total of 67 km (15%) were determined to be thermally stratified (ODEQ 2000).

Modern TIR sensors have sensitivities from 0.2 to 0.02°C. Under thermally stratified conditions, the TIR sensor detects surface temperature patterns that result from slight mixing (from wind and flow) and differential heating relationships in multiple directions (i.e. longitudinal and transverse). Under these conditions, differential heating at the stream surface results from large variations in rates of heat transfer, such as solar heat and the absence of solar heat in shade. A TIR image of a stratified stream reach can be interpreted to show differential heating (shade versus no shade) at the stream surface. However, these images should not be interpreted to suggest that these differences represent short scale cooling in bulk water temperatures.

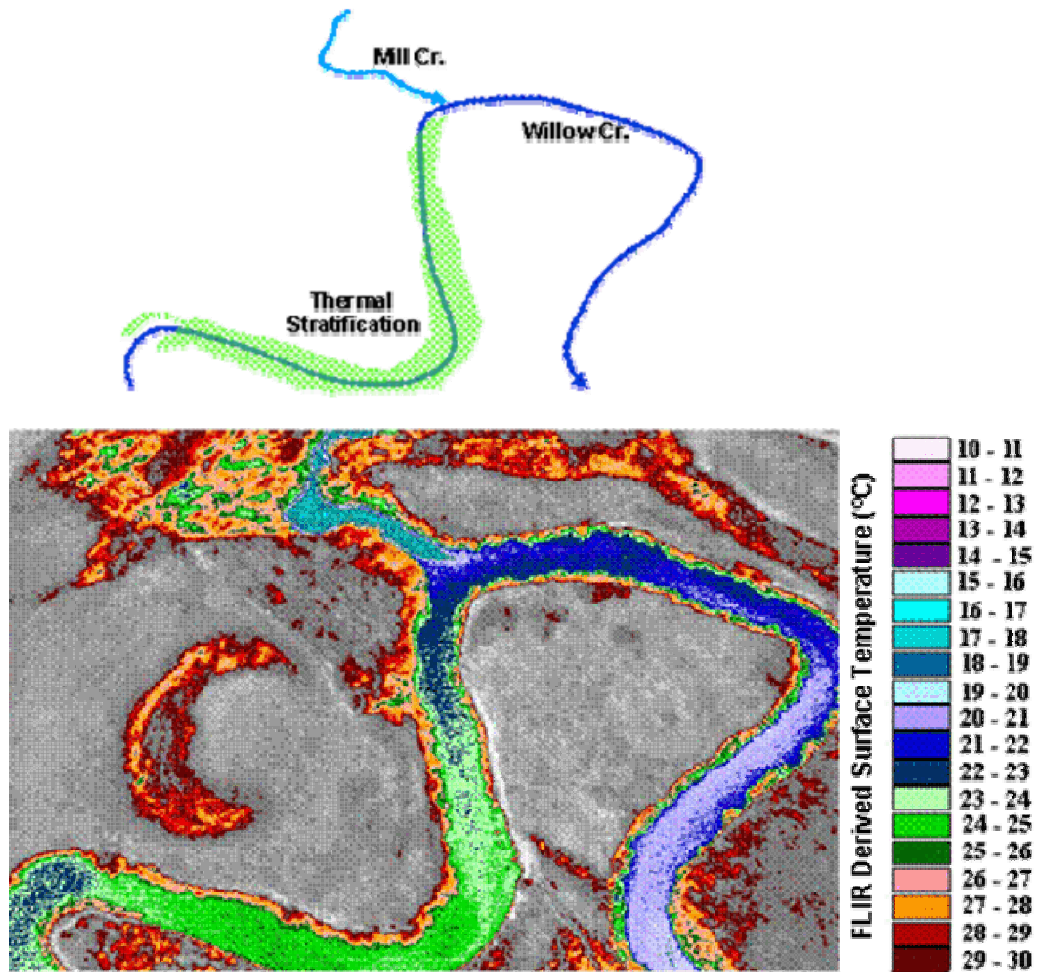


FIGURE 5.14
An Example of Thermal Stratification Identified from FLIR Image - Willow Creek and Mill Creek Confluence, Grande Ronde River Basin, Oregon (~16:40, August 25, 1999) (Watershed Sciences, LLC 1999)

5.5.3 TTOOLS SAMPLING OF TIR DATA

TIR grid data contain surface water temperatures that can be sampled and statistically summarized. These data are then converted to a GIS point data layer, where the positional data represents the position of the sample (helicopter position) and the temperature data is the ten sample median of the water surface temperature. The TIR point data layer offers very high resolution and needs to be associated with the stream data nodes created by TTools. A procedure is available to associate TIR temperature data to stream segment data nodes, where the closest TIR temperature value is associated (recorded) to the most proximate stream data node.

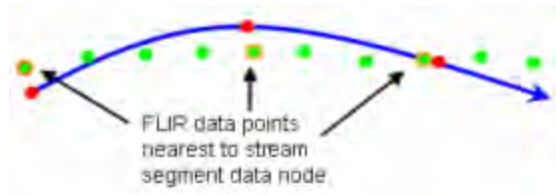


FIGURE 5.14
Method Used to Associate FLIR
Temperatures

5.6 OTHER TTOOLS APPLICATIONS:

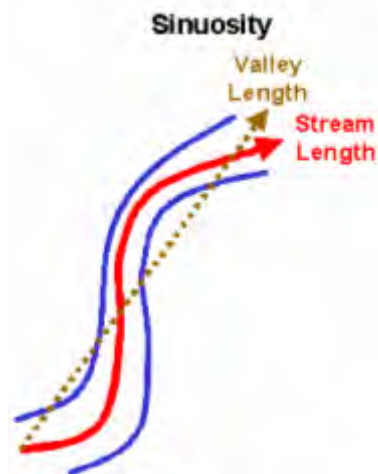
In addition to the standard suite of sampling operations, TTools can be used to sample other geographic parameters. One can digitize the valley edges, flood prone widths, bankfull widths, or meander widths according to Rosgen (1996) stream channel classification protocols. These widths can then be sampled with TTools, and the results can be manipulated within a spreadsheet (i.e., Excel) to calculate sinuosity, meander width ratio, and entrenchment ratios.

5.6.1 STREAM SINUOSITY

Several morphology assessment methods consider stream sinuosity, especially in unconfined stream reaches, as an important parameter of stream health. With data compiled with Tools, sinuosity becomes a fairly easy parameter to quantify. Stream sinuosity is the stream length to valley length ratio.

Sinuosity is calculated as,

$$\text{Stream Sinuosity} = \frac{\text{Stream Length}}{\text{Valley Length}} \quad (5-3)$$

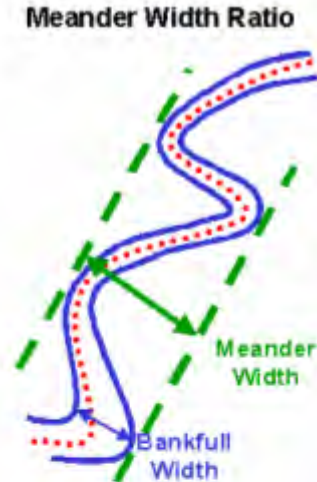


5.6.2 MEANDER WIDTH RATIO

Meander width ratio is the meander width to bankfull width ratio. Meander width is the belt width or amplitude of the meander geometry.

Meander Width Ratio,

$$\text{Meander Width Ratio} = \frac{\text{Meander Width}}{\text{Bankfull Width}} \quad (5-4)$$

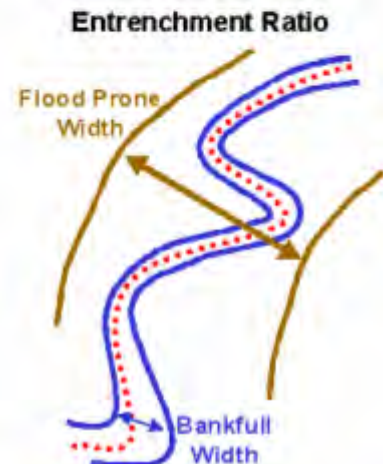


5.6.3 ENTRENCHMENT RATIO

Entrenchment ratio refers to the vertical containment of the channel. It is quantified as the flood prone width to bankfull width ratio.

Entrenchment Ratio,

$$\text{Entrenchment Ratio} = \frac{\text{Flood Prone Width}}{\text{Bankfull Width}} \quad (5-5)$$



5.7 DIGITIZING A STREAM LAYER

Conceptually, what you need to do to create a stream layer from the aerial imagery by tracing the stream. Following are the steps that need to be completed:

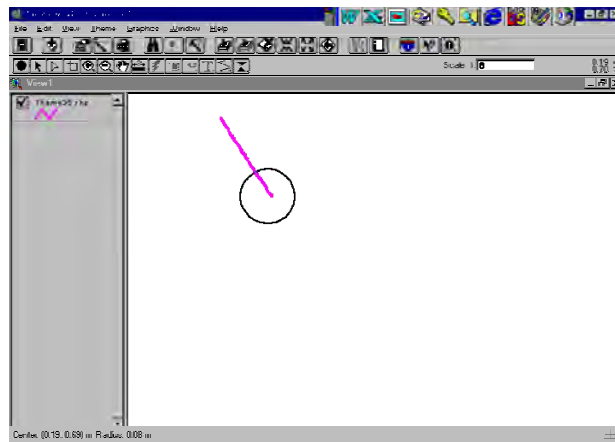
1. Add an existing 1:100,000 or 1:24,000 stream coverage to your view.
2. Add the appropriate aerial imagery to your view.

Now you have a view containing the aerial imagery and coarse stream coverage. The coarse stream coverage will help guide you during digitization in case you lose track of the stream and/or its tributaries. (You may be required to re-project the coarse stream coverage in order to match the aerial imagery projection.) Now, you are ready to begin creating your 1:5,000 digitized stream layer.

1. Zoom in to 1:5,000 or closer if the aerial imagery resolution is sufficient.
2. Go to View/New Theme...
3. In the Feature Type dialog box, select Line.
4. Give your theme a name and save it.
5. Go into the Legend Editor for this new line theme and make it easier to see. That is, change the line width from 0.1 to 2 and make the color something that will show up against the aerial imagery.
6. Go to Theme/Properties...
7. Select the Editing button on the left side of the dialog box.
8. Under "Snapping", check the boxes next to both "General" and "Interactive" and in each of the "Tolerance" dialog boxes. Then click OK to get out of this dialog box.
9. Now click on the Interactive Snap tool, which appears in your Toolbar as follows:



10. Now right-mouse-click in the view, holding the button down, and this will create a circle (snapping radius) around your cursor. This will help you connect the ends of two lines, by making sure that the end of a previously drawn line is within the circle when you start the new line.



11. Select the Draw Line tool, which looks like:



12. Beginning at the mouth of the stream, start tracing the center of the wetted channel.
13. Click whenever the stream channel makes a bend (since you can't draw curves with your mouse).
14. When you get close to the edge of the screen frame, right-mouse-click and select "Pan". This will move the frame over so you can continue digitizing.
15. To stop drawing the stream line, double-click.

HERE ARE SOME TIPS REGARDING THIS STREAM DIGITIZING PROCESS:

- Save your work often. To do this, go to Theme/Save Edits.
- Save each stream that you digitize as a **separate theme**.
- If the channel splits, trace only one channel, whichever appears to be the main one.
- Remember to use that Snap tool, in order to minimize "cleaning up" that you have to do later.
- If you are trying to digitize a stream in a heavily forested area, which is likely to be the case in an upper watershed area, you may also need DRGs for the area. DRG stands for Digital Raster Graphic. The DRG for a particular quad is simply the scanned version of the USGS topo map for that area. The scale for DRGs is therefore the same as that for USGS topo maps, or 1:24,000. **Because we are interested in developing stream and vegetation layers that will be accurate to 1:5000, DRGs may be used as a point of reference when the aerial imagery for a particular area is difficult to read, but they are not a substitute for developing stream or vegetation layers from aerial imagery.**

You will not know if you need to obtain DRGs to create a stream layer until you have worked with the aerial imagery for awhile. If you do decide you need them, they can be obtained through the following website: www.reo.gov. This is the website for the Regional Ecosystem Office, which is part of the Northwest Forest Plan. To get the quad maps you want, you must know either the lat/long or the map names.

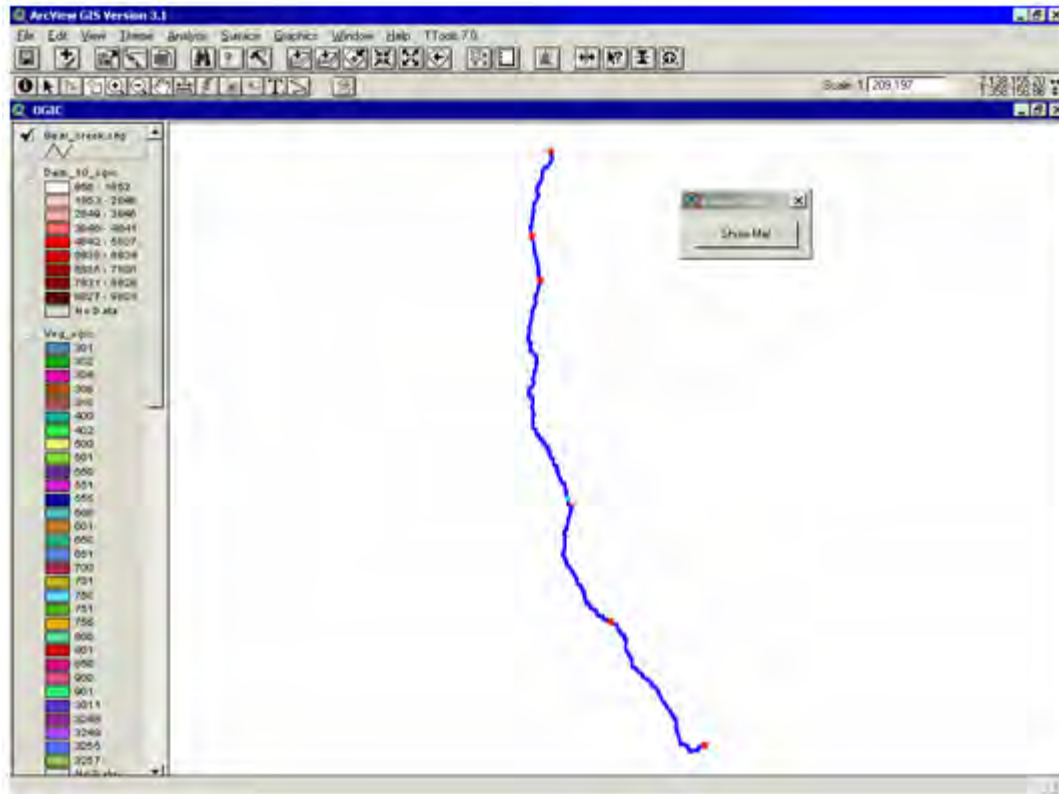
5.7.1 CLEANING AND UNIONIZING A STREAM LAYER

TTools requires that your stream layer be cleaned of all undershoots/overshoots, and then unionized into a single line (i.e., merge the separate segments). This section describes how to check your stream layer for overshoots/undershoots, and how to fix those errors.

1. Make sure that you have your stream layer selected in your view.
2. Select the TTools menu.

3. Select the “Show Loose Ends” option in the TTools menu.
4. Click the “Show Me” button to identify overshoots/undershoots within your stream polyline.

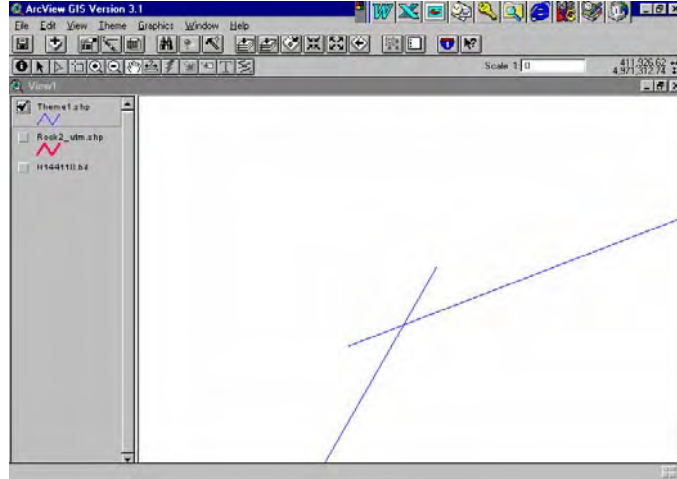
Now your stream polyline will have all of its nodes highlighted in red or blue. Blue is good and red is bad. Red indicates that you have an overshoot/undershoot that needs to be fixed. You are only allowed to have a red dot at each terminal end of the stream polyline in your finished product.



5.7.2 CLEANING THE OVERSHOTS

Now that you have highlighted the overshoots/undershoots with the Show Loose Ends tool, you can get to work fixing the stream polyline. Remember, you will have to click the “Show Me” button each time you pan or zoom in/out of your view.

Use your magnifying glass tool to zoom in to an overshoot/undershoot. The image below illustrates an overshoot, which was highlighted in red by the “Show Loose Ends” tool.

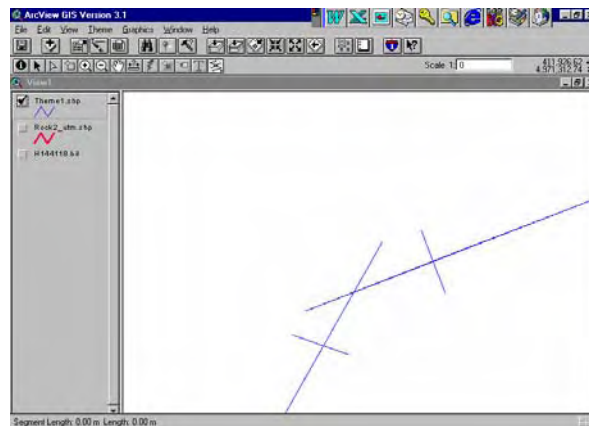


SO NOW YOU NEED TO MAKE SOME REPAIRS.

1. Select your stream polyline theme in your view.
2. Go to Theme/Start Editing.
3. Go to Theme/Properties. In the pop-up window, select the Editing icon on the left. Check both the interactive and general snapping boxes. Click OK.
4. Now you need to select the Line Splicing tool from your tool bar. It is in the drop-down of the line-drawing button, and looks like this:



5. Use your cursor to draw splicing lines on each side of the overshoot, as seen below:



- Now you can use the Select Feature tool to select each of the line segments that you don't want to appear in the end product. After you have selected each one, hit the delete key to get rid of it.

Your goal is to delete the overlapping lines and the splice lines that you just created. DO NOT delete the stream polylines outside of the splice lines that you created!

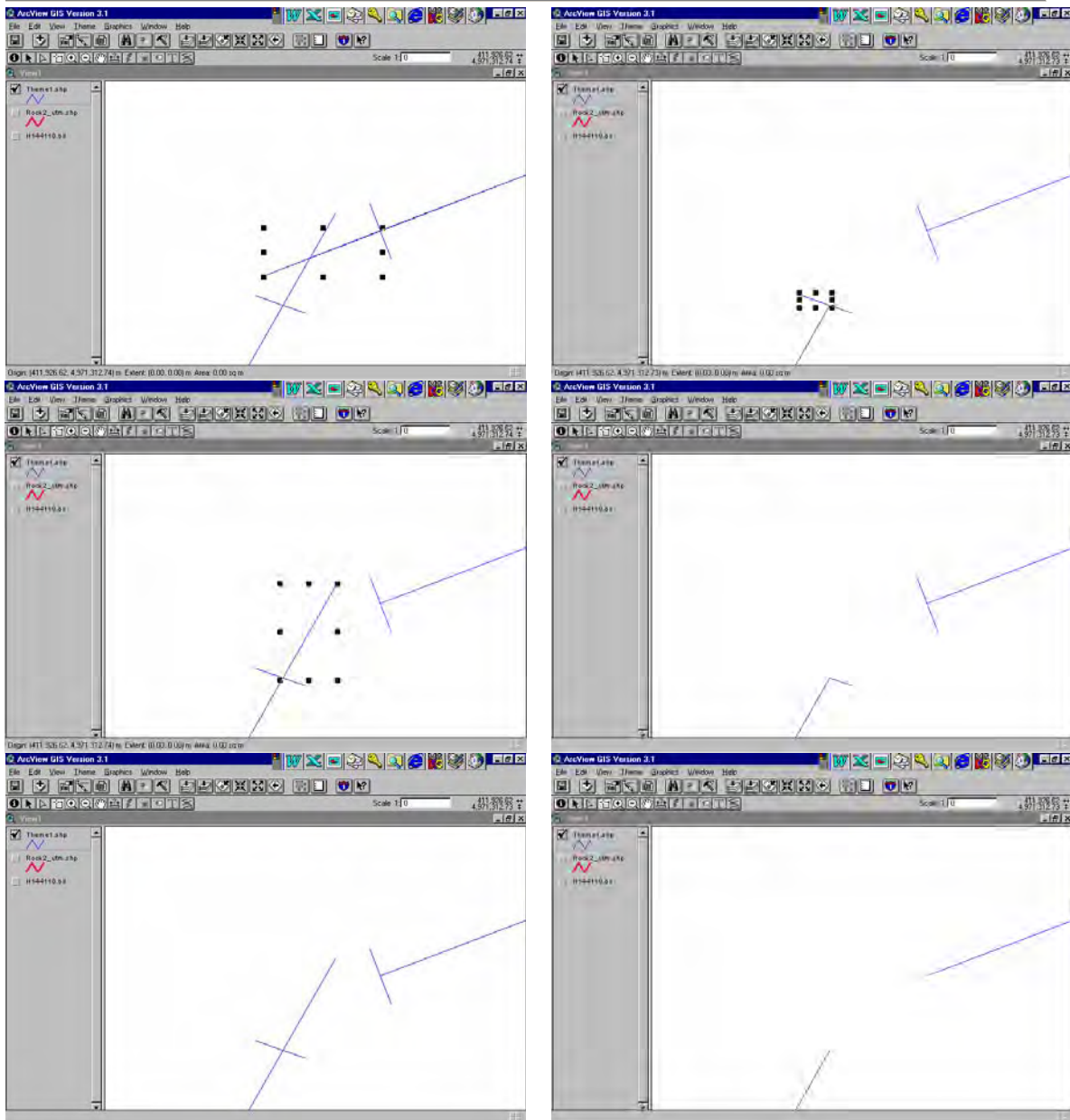


FIGURE 5.15
Example of Delete the Overlapping Lines and the Splice Lines

5.7.3 CLEANING THE UNDERSHOOTS

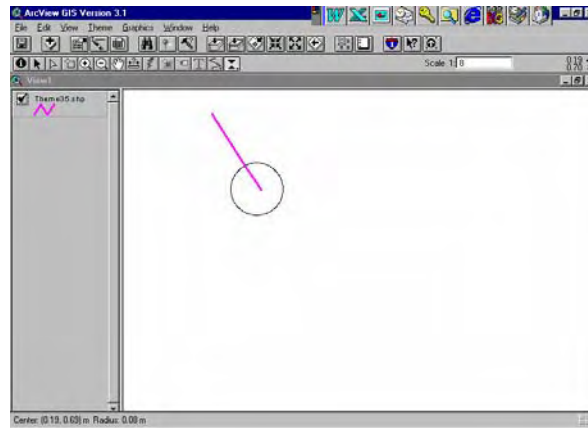
Undershoots may occur during the digitizing process if you had forgotten to turn on the snapping feature, or if you did not start a new line close enough to an old line. Undershoots also are an intermediate product of cleaning an overshoot (i.e., once you splice out the overshoot segments, you are left with an undershoot that still needs to be fixed).

1. Make sure that your stream theme is the edit mode. (Theme/Start Editing).
2. Click on the Interactive Snapping Tool on the tool bar. It looks like this:



(If the Snapping Tool button is not visible, then go to Theme/Properties. In the pop-up window, select the Editing icon on the left. Check both the interactive and general snapping boxes. Click OK.)

3. Now, use the cursor to draw a snapping radius around one of the loose ends.



4. Click on the Draw Line button in the tool bar. It looks like this:



5. Draw a line that connects the two loose ends. (You should see your snapping radius circles appear as you are drawing the connection line.)

You know you are done cleaning when...

- A. You zoom out to the full extent of your digitized stream theme, and
- B. You use the Show Loose Ends tool to identify overshoots/undershoots, and
- C. There are no red dots within your stream polyline – only one on each terminal end.

5.7.4 UNIONIZING THE CLEANED STREAM POLYLINE

Once you have cleaned your digitized stream polyline of all undershoots/overshoots, you must unionize the records within the table. This process essentially takes multiple segments that comprise your stream layer, and “melts” them into one single, continuous line (i.e., it converts a multi-record database table into a single-record database table). TTools only works on a unionized line theme.

1. Open the TTools menu, and select the Unionize Polyline option.
2. Name the new file – this will be your cleaned and unionized stream polyline that TTools sampling will be based from.

Helpful Hint: It is a good idea to use a naming convention like:
ColdCreek_clean_utm.

This file name includes the stream name, identifies it as cleaned, and indicates the projection.

3. Now, open the Table of your new theme, and make sure that it consists of only one single record. If there are multiple records, there is an error in your stream polyline and you must repeat the cleaning process to check for missed overshoots or undershoots.

5.8 DIGITIZING CHANNEL WIDTH (NEAR STREAM DISTURBANCE ZONE WIDTH²⁰)

The near stream disturbance zone width serves as an estimate of the bankfull width. This parameter is used to determine the distance of the near stream vegetation to the wetted channel. In essence, the near stream disturbance zone allows for positioning of the near stream land cover relative to the stream channel. A statistical validation of GIS sampled channel width polylines digitized from aerial imagery and ground level bankfull width measurements is available in **Figure 5.6**.

Similarly, wetted widths can be estimated using aerial imagery. Because wetted widths are highly dependent on instream flow conditions, field verification data must be used.

TTools has the capability to sample the NSDZ. The image below illustrates the digitized right and left channel edges for a section of stream (red lines). The blue dots in the image below indicate the 100-foot stream reaches.

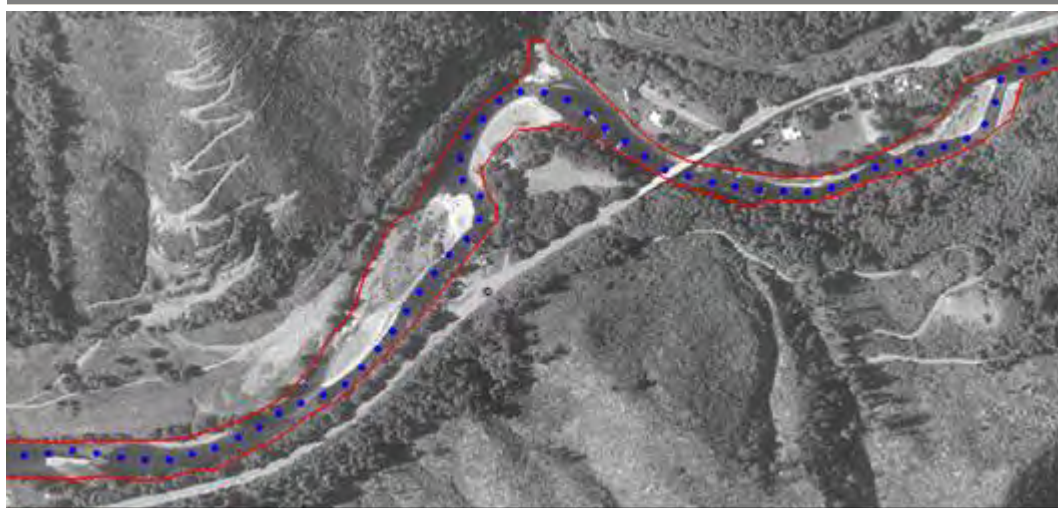


FIGURE 5.16
Channel Width Polylines Digitized from Aerial Imagery (Wilson River, Oregon)

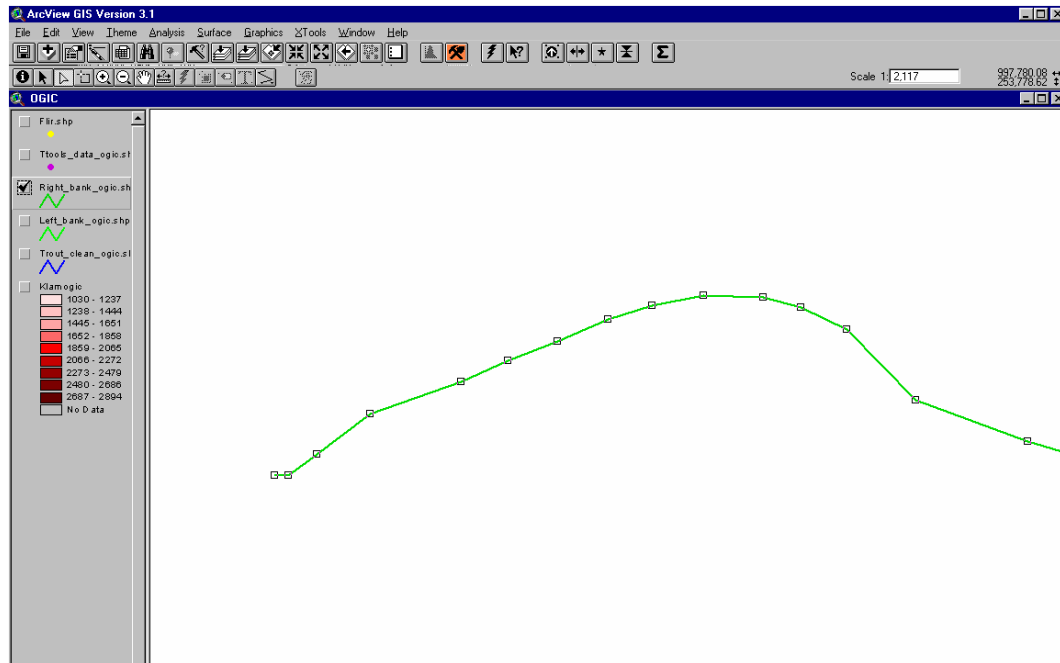
²⁰ Near stream disturbance zone width is the measurement of channel width performed by TTools. It is named (by the authors) because there is not an exact reference to GIS sampled channel width that correlates with a commonly used ground level measurement. It is intended to serve as an estimate of the bankfull width, but the authors acknowledge that measurement limitations may affect the accuracy of this estimate. Statistical validation of derived channel widths with ground level measurements is highly recommended.

The following steps will guide you digitizing channel width:

1. Select your cleaned 1:5,000 stream theme in your view.
2. Go to Theme/Convert to Shapefile...
3. Name the new theme (this will be either your right bank or left bank theme).
4. Select your new bank theme in your view.
5. Zoom to the beginning of your stream (at least 1:5,000). (You should have your aerial photograph or DOQ turned on as well.)
6. Go to Theme/Start Editing.
7. Click on the Vertex Editing tool in your button bar:



8. Now click on your bank polyline with the cursor. All the nodes will now be highlighted with a small box (see image below).



9. Center your Vertex Editing cursor on a node, and you will see cross-hairs appear. Click and hold while you move the vertex to the desired location on the channel edge.
10. In order to add a node to a section of the line that needs a bend, place your Vertex Editing cursor over the desired location on the line and right-mouse-click once.
11. Repeat this process for both the right bank and the left bank, until you have moved the polyline theme to the appropriate location.

Helpful Hint:

In some areas, the channel edges may be obscured by vegetation canopy closure, or the stream may be too narrow to interpret the channel edges from the aerial imagery. You should leave the nodes in such locations undisturbed. The result will be a bank line that is exactly on top of your digitized stream line (i.e., you will have moved the line ONLY where the channel edges are visible in the aerial imagery). When you run TTools to sample the channel widths, the values recorded will be ZERO where you could not digitize the channel edge. You may then modify the TTools database manually, and insert ground level measurements into the segments where the channel widths could not be interpreted from the aerial imagery.

5.9 DIGITIZING NEAR STREAM LAND COVER

You must have digitized your stream polyline and the channel edge (NSDZ) polylines before attempting to digitize vegetation. TTools uses your digitized stream polyline as a reference point for sampling vegetation.

CREATING THE BUFFER - IF YOU COULD NOT DIGITIZE THE CHANNEL EDGES...

Follow these steps if you could not digitize the NSDZ anywhere along your stream. You need to create a buffer that extends 300 feet from the stream center line.

1. Add your digitized stream theme and the aerial imagery to your view.
2. In the View menu, select the Properties option, and make sure that your “map units” correspond to those of the projection you are in.
3. In the Theme menu, select the Create Buffers option. (If this option is grayed out, you probably have not set your view and map units.)
4. Choose your stream polyline theme.
5. Choose “At a specified distance”, and type in 300.
6. Set the “Distance Units” to *feet*.
7. Select “In a new theme”, and name the new file.

Now you have a buffer that extends 300 feet from your digitized stream. The next step will be to cut that buffer into multiple polygons that represent the riparian vegetation.

CREATING THE BUFFER - IF YOU COULD DIGITIZE THE CHANNEL EDGES...

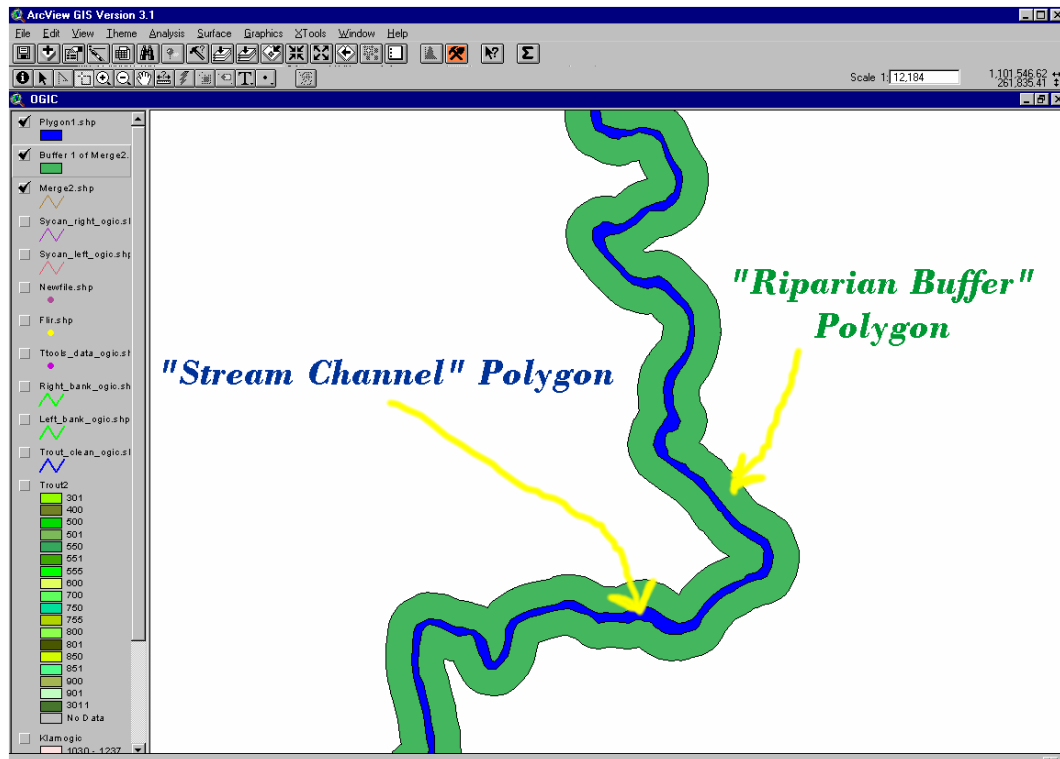
Follow these steps if you could digitize the NSDZ, even if there are some stream reaches that you could not. You need to create the buffer to extend 300 feet from the bank edges, not from the stream center line.

1. Add your Right Bank polyline and your Left Bank Polyline to your view.
2. In the View menu, select the Properties option, and make sure that your “map units” correspond to those of the projection you are in.
3. Make sure that you have the **Xtools** (not *TTools*) extension installed and turned on. (You can download this free extension from the Oregon Department of Forestry website at <http://www.odf.state.or.us>)
4. In the Xtools menu, select the Merge Themes option.
5. When asked which theme to preserve output from, choose *either* your Right Bank polyline theme, or your Left Bank polyline theme.
6. When asked which theme to merge with, choose the *other* bank polyline theme.
7. Name the output file (this is a temporary file that you can eventually delete after this).
8. Go to the “Theme/Create Buffers...” . (If this option is grayed out, you probably have not set your view and map units.)
9. Choose your *merged* banks theme that you just created.
10. Choose “At a specified distance”, and type in 300.
11. Set the “Distance Units” to *feet*.
12. Select “In a new theme”, and name the new file.

Now you have a buffer that will be the basis for your riparian vegetation map. Since you have digitized the banks, you know that the area between the banks is stream channel. This needs to become a single polygon within the riparian vegetation map, and here is how to do it:

13. Under the “**XTools**” drop-down menu, select “Make one polygon from polylines”.
14. Select the MERGED stream banks theme that you created in step 7.
15. Name the new file (this is also a temporary file that can eventually be deleted).

Now you have your 300-foot “riparian buffer” polygon and a “stream channel” polygon. Your next task is to combine these polygons. (See image below.)



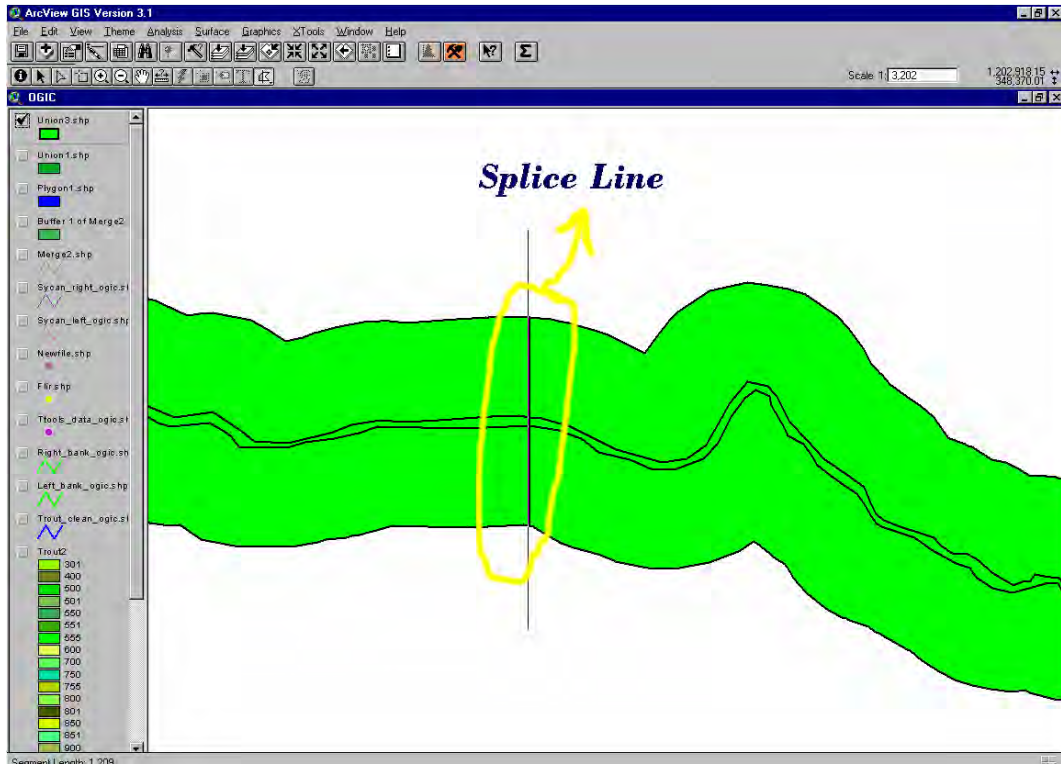
16. Turn on the extension called “Geoprocessing”.
17. In the View menu, select the Geoprocessing Wizard option.
18. Select “Union two themes”.
19. The “input theme to union” must be your *stream channel polygon*. The “polygon overlay theme to union” must be your *riparian buffer polygon*. Name the output file. (This output file will become your working riparian vegetation map.)

The new buffer is like a “donut”, and there is one last step before it is ready for vegetation mapping.

20. Zoom somewhere near the middle of the buffer.
21. Go to “Theme/Start Editing”.
22. On the tool button bar, select your polygon splicing tool (it is a drop-down button beneath the rectangle graphic button). It looks like this:



23. Now draw a line all the way across the middle of your buffer polygon theme (see image below). This will separate the continuous “donut” polygon, preparing it for the mapping process. Be patient, splitting may take a few minutes to appear in your view.



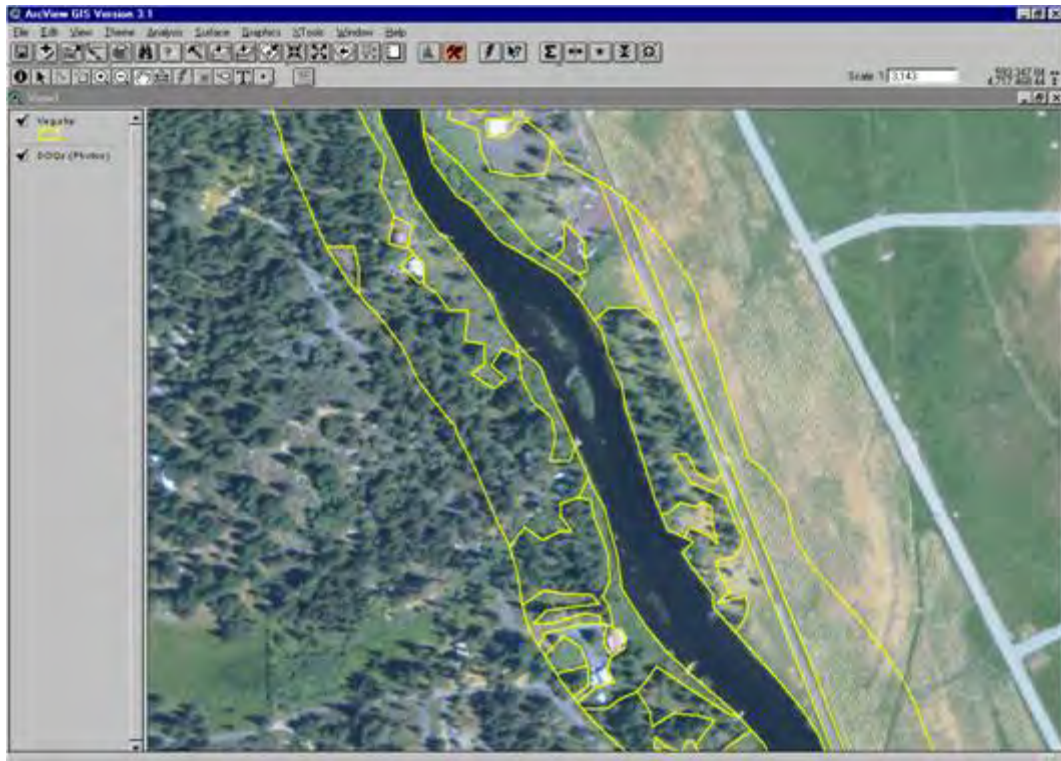
You now have a base polygon layer that will be used to map the riparian vegetation. The following steps will get you started on the aerial imagery interpretation and mapping process.

DELINEATING RIPARIAN LAND COVER POLYGONS

Vegetation mapping should be done using the highest resolution and most recent aerial imagery available. Streams change over time, and so does the riparian vegetation. Higher resolutions allow you to see more detail, such as smaller willow galleries along a stream bank. Multispectral, or color imagery enhances the vegetation mapping process by making the various riparian communities more decipherable. A typical view extent for mapping riparian vegetation is between 1:2,500 and 1:5,000 maximum.

The image below shows an example of mapped riparian features along the Williamson River in southern Oregon. Mapped features in this image include a road, house, farm field, willows along the bank, grassy areas, dense conifer stands, less dense conifer stands, and the river itself. The basic rule of thumb when delineating riparian vegetation polygons is to identify areas with the following three distinctions:

1. Species Composition
2. Canopy Density
3. Height



It may be difficult to identify species and heights from the aerial imagery, but that is where GROUND LEVEL DATA comes into play. It is critical that you have collected a sufficient amount of ground level riparian information so that you can comfortably assign species compositions and heights to the vegetation map that you are creating. While collecting the data (species, height, density), be sure to record the precise location so that you can match that data to the aerial imagery.

The steps for creating the vegetation polygons from your buffer are described below.

1. Make sure that your aerial imagery and buffer polygon theme are in the view.
2. Zoom to one end of the buffer theme.
3. Open the table to your vegetation buffer theme.
4. Go to "Table/Start Editing".
5. Go to "Edit/Add Field...".
6. Name the field something like "Vegcode", as a number field with zero decimal places.
7. Go to "Table/Stop Editing", and save the changes.
8. Return to your view.
9. Go to "Theme/Start Editing".
10. Select the polygon splicing tool:



11. Working from the outside of your buffer, inward, begin outlining the various riparian features.

IMPORTANT NOTE: Only create one polygon at a time (i.e., do not splice more than one polygon) or the records within the theme's table will be linked and adding the polygon attributes will not be easy.

12. Now you have a choice. You can draw all of the polygons in your riparian vegetation map, then add the codes. Or you can add the codes to the polygons as you do the digitizing.

CODING YOUR RIPARIAN FEATURE POLYGONS

There should be one field within your riparian vegetation theme that will contain a numeric code, which describes the species, canopy density, and height of the riparian feature.

Species: Species identification relies on the ground level data and knowledge of the area in which you are mapping vegetation. In forested areas, you are often only able to distinguish between conifer and deciduous species compositions. Therefore, an example of species classes to map would be conifer, deciduous, and mixed conifer/deciduous.

Canopy Density: This is an ocular estimate of the canopy closure, as observed from the aerial imagery. Precise measurements are not possible, so it is sufficient to derive classes such as: 0-25%, 25-50%, 50-75%, 75-100%.

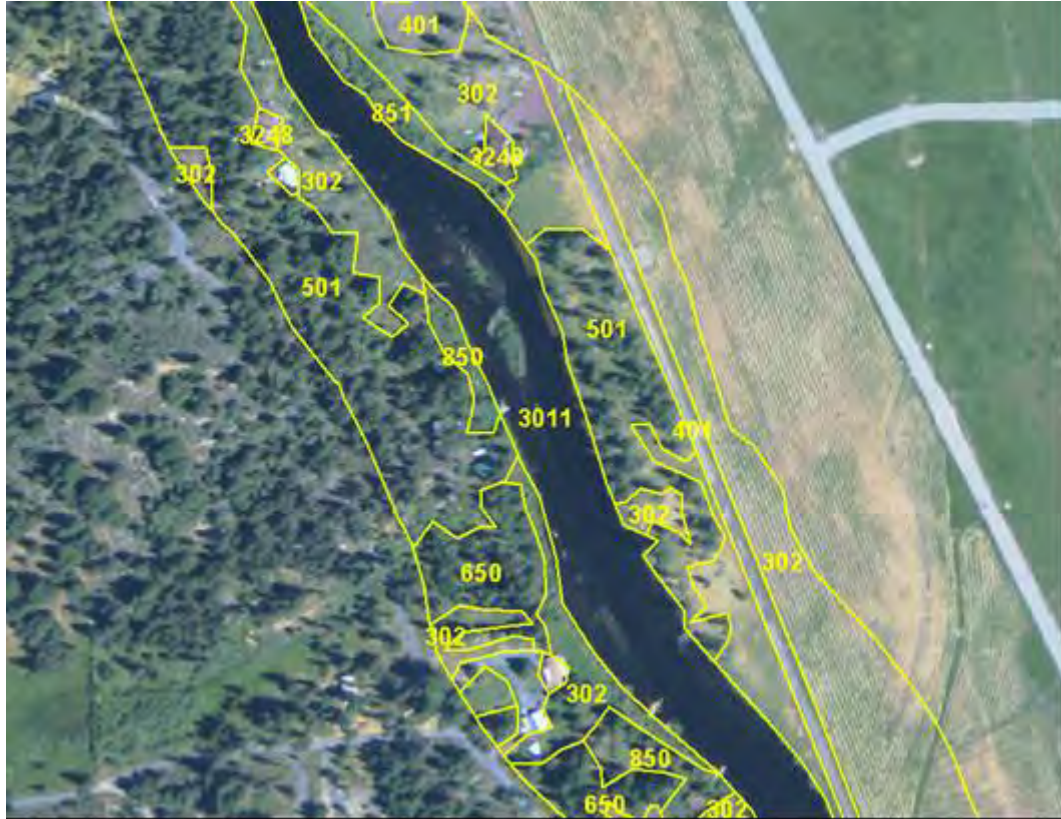
Height: Since you cannot measure precise stand height from the aerial imagery, it is sufficient to derive a few different height classes for your vegetation, such as tall, medium, and short. You can eventually apply your ground level data to estimate height ranges or values for these classes.

The table on the following page lists some example riparian vegetation codes and their corresponding species, canopy density, and height values. The codes may cover narrower ranges of the attributes, depending upon the aerial imagery quality, experience of the person doing the mapping, and amount of ground level data collected.

Remember: These are some simple examples of riparian feature codes and descriptions. They may vary in type and complexity, depending upon the sub-basin or stream that is being analyzed.

Code	Riparian Feature Description	Height (m)	Density (%)
301	Water	0.0	0%
3011	River Bottom - Floodplain	0.0	0%
302	Pastures/Cultivated Field/Lawn	0.0	0%
3025	Young Orchard	3.0	75%
303	Mature Orchard	12.2	75%
304	Barren - Rock	0.0	0%
305	Barren - Embankment	0.0	0%
306	Barren - Campground/Park	0.0	0%
307	Barren - Gravel Pit	0.0	0%
308	Barren - Clearcut	0.0	0%
309	Clearcut, below 50% dense regeneration	4.6	25%
321	Lumber Yard	0.0	0%
400	Barren - Road	0.0	0%
401	Barren - Forest Road	0.0	0%
402	Barren - Railroad	0.0	0%
403	Barren - Ag. Road	0.0	0%
500	Large Mixed Conifer/Hardwood (>75% Canopy)	24.4	75%
501	Small Mixed Conifer/Hardwood (>75% Canopy)	12.2	75%
550	Large Mixed Conifer/Hardwood (>25% Canopy)	24.4	25%
551	Small Mixed Conifer/Hardwood (>25% Canopy)	12.2	25%
600	Large Hardwood	22.9	75%
601	Small Hardwood	12.2	75%
650	Large Hardwood	22.9	25%
651	Small Hardwood	12.2	25%
700	Large Conifer	27.4	75%
701	Small Conifer	12.2	75%
750	Large Conifer	27.4	25%
751	Small Conifer	12.2	25%
800	Shrubs	4.6	75%
850	Shrubs	4.6	25%
900	Grasses	1.0	75%
3248	Developed – Residential buildings	6.1	100%
3249	Developed – Industrial buildings	9.1	100%
3252	Dam	0.0	0%
3253	Pipeline	0.0	0%
3254	WWTP	0.0	0%

The image below demonstrates the codes assigned to riparian feature polygons. It is essential that each and every polygon within your riparian vegetation polygon layer has a value associated with it. The value **MUST** also be a number, and not a string.



CONVERTING THE RIPARIAN POLYGON THEME INTO A GRID:

Now that you have completed the riparian vegetation mapping, you must convert the polygon theme into a GRID so that TTools can sample it. Here is the way to do it:

1. Make sure that your riparian vegetation polygon theme is in the projection that you want to use TTools in. Since re-projecting grids requires ArcInfo, you may not have the ability to do so. Thus whatever projection your mosaic DEM is in, will determine the projection that you will be using TTools in.
2. Turn on the Spatial Analyst extension if you have not already done so.
3. Select your riparian vegetation polygon theme in your view (make sure that none of the features are highlighted).
4. In the Theme menu, select the Convert to Grid option.
5. Name your output file. **IMPORTANT:** Do not have a space anywhere in the path to your file. Do not have a space in the name of the file. Underscore is OK. Do not have a path to your file that is extremely long. All of these issues will result in a corrupt conversion process.

6. In “Output grid extent”, choose “same as ‘your_veg_shapefile’.shp” (i.e., the extent should be same as your vegetation polygon layer).
7. In “Output Grid Cell Size” enter 1 meter (3.28 feet). **THEN HIT THE ENTER KEY.** Failure to hit the enter key after typing in the number will not update the “number of rows” and “number of columns” fields, and your conversion will crash.
8. Now click OK.
9. Under “Pick field for cell values” select the name of the field in your riparian vegetation polygon layer that contains your vegetation code numbers.
10. Then wait a minute or two.

5.10 TTOOLS OPERATION

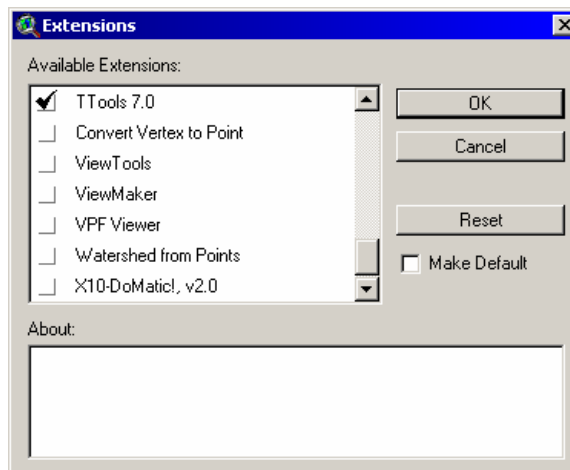
TURNING ON THE TTOOLS EXTENSION

PREREQUISITES:

- You must have the Spatial Analyst extension. TTools will not work without it.
- You must have a copy of “TTools7.avx” within the following folder:
Esri/Av_gis30/Arcview/Ext32/ (probably located on your C drive).

STEPS:

1. In the “File” drop-down, select “Extensions...”
2. Check the box next to TTools 7.0 and click “OK” (see picture below).



3. Click the TTools 7.0 menu for a drop-down of the TTools sampling options.

STEP 1: SEGMENTING THE STREAM AND CALCULATING THE ASPECT

PREREQUISITES:

- 1:5000 digitized *and* cleaned stream polyline theme.

STEPS:

1. Check the Map Units under View/Properties. You **MUST** be in a projection that uses the Map Units of FEET or METERS (for example, OGIC has feet for Map Units, while UTM has meters for Map Units). *Plan to stay in this projection/Map Units for the remainder of using TTools.*
2. Highlight your 1:5000 stream theme in your view's table of contents.
3. Select the Segment/Calculate Aspect option in the TTools
4. You will be asked to select the projection properties that you are in. (If you are using Ogic, and Oregon Lambert is not an option, you must cancel. Then load the "Projector! OL" extension and click on its button (the hourglass) in the view. This will load Oregon Lambert projection properties into your project.)
5. Name the point coverage that you are creating. This will be the database file that TTools uses from here on out. (Do not use spaces in your file name or in the path to your file.)
6. You will be asked if you want to "Reverse Line Segments". If you digitized your stream from the mouth up, choose "Yes". Otherwise, choose "No". (If you are unsure, just guess, and you can check the results shortly.)
7. You will be asked to input the spacing distance. This determines the longitudinal distance between the nodes that will be placed on your stream polyline. The units must be meters.

The *Length* column of your TTools point coverage now contains the cumulative longitudinal distance, in meters. The *Aspect* column contains the downstream segment direction (units are degrees from north).

Important: You **MUST** now double-check the TTools point coverage that you created to be sure you did not select the wrong option when you were asked to Reverse Line Segments. The following steps will guide you:

1. Select your TTools point theme in your View.
2. Select the uppermost point visible in your view (the point nearest the headwaters).
3. Open the Table to your TTools point theme.

4. If the first record (Id = 0) is not highlighted, then you made the wrong choice when asked if you want to reverse line segments. You will need to delete this TTools point coverage from the ArcView project, and start the “Segment/Calculate Aspect” step over.

The first record in the TTools point theme table (Id = 0) MUST correspond to your uppermost node (nearest the headwaters). The remainder of TTools uses this information to determine which direction is downstream.

STEP 2: MEASURING CHANNEL WIDTHS

PREREQUISITES:

- You must have performed Step 1 of TTools – “Segment/Calculate Aspect”.
- You need a Right Bank polyline theme and a Left Bank polyline theme. Both must have been cleaned and unionized like your stream polyline was.
- The bank polylines must extend the full length on both sides of your TTools point coverage (i.e., extend the entire length of the stream).

STEPS:

1. Select the “Measure Channel Widths” option on the TTools menu.
2. Select your TTools point theme.
3. Select your Right Bank polyline theme.
4. Select your Left Bank polyline theme.
5. When asked whether to overwrite existing data. If you choose “Yes”, all channel width data will be erased and re-sampled. If you choose “No”, sampling will be performed only where there are zero values in the Channel column of the TTools data table.

Helpful Hint:

- The output units in the field titled “Channel” will be meters.
- Remember that areas where you could not interpret the NSDZ from the aerial imagery, you did not move the bank line away from the stream line. Thus, TTools will report values of ZERO in the channel width column for such locations. It is your responsibility to manually insert field-measured NSDZ values into the TTools database file.

STEP 3: MEASURING STREAM ELEVATION AND GRADIENT

This procedure uses Spatial Analyst to sample a grid theme. Spatial Analyst can perform a limited number of commands (about 32,000) in a given ArcView session before causing a “Segmentation Violation”, and crashing ArcView. Therefore, it is **strongly recommended** that you save the project, completely close out of ArcView, and re-open the project before beginning this step of TTools. Doing so will clear ArcView and Spatial Analyst memory, and TTools will then be able to accurately predict and prevent a potentially disastrous crash.

PREREQUISITES:

- You must have your TTools point theme in the view.
- You must have a 10-meter or 30-meter DEM in the view. The DEM must have been mosaiced and must extend at least nine miles around the stream that is being sampled.

Helpful Hint:

Before proceeding with TTools sampling, make sure that your DEM and TTools point coverage are located on your local hard drive. If your DEM resides on a network drive, TTools sampling will take about three times longer.

STEPS:

1. Select the "Measure Elevation/Gradient" option in the TTools menu.
2. Select your TTools point theme.
3. Select your DEM grid theme.
4. When asked to "select your DEM elevation units", choose the units of the values that are in the actual DEM that you are using. Be careful – depending on the source, your DEM may have elevations in feet or meters.
5. When asked whether to overwrite existing data – if you choose "Yes", all elevation and gradient data will be erased and re-sampled – if you choose No, sampling will begin at the first zero value.
6. Spatial Analyst (developed by ESRI) has a bug, which limits the number of grid samples that it may perform. Beyond which, ArcView fatally crashes and reports a "Segmentation Violation" error. TTools will prevent this disaster from happening. Depending on the size of your TTools point theme, you may get a message that says, "Spatial Analyst has reached its sampling capacity....". Click OK, and TTools will automatically save your project and close your ArcView session. At this point, re-open your ArcView project and start the measuring elevation/gradient process again. This time, DO NOT overwrite existing values, and TTools will begin sampling where it left off last time.
7. Repeat this process as many times as necessary, until you see a window pop up that says, "Elevations and gradients have been sampled..."

STEP 4: MEASURING TOPOGRAPHIC SHADE

This procedure uses Spatial Analyst to sample a grid theme. Spatial Analyst can perform a limited number of commands in a given ArcView session before causing a "Segmentation Violation", and crashing ArcView. Therefore, it is **strongly recommended** that you save the project, completely close out of ArcView, and re-open the project before beginning this step of TTools. Doing so will clear ArcView and Spatial Analyst memory, and TTools will then be able to accurately predict and prevent a potentially disastrous crash.

PREREQUISITES:

- You must have your TTools point theme in the view.
- You must have a mosaiced 10-meter or 30-meter DEM in the view. The DEM must cover the entire 4th field subbasin that you are sampling within.
- You must have performed the “Measure Elevation/Gradient” step of TTools.

Helpful Hint:

Before proceeding with TTools sampling, make sure that your DEM and TTools point coverage are located on your local hard drive. If your DEM resides on a network drive, TTools sampling will take about three times longer.

STEPS:

1. Select the “Measure Topographic Shade” option in the TTools menu.
2. Select your TTools point theme.
3. Select your DEM grid theme.
4. When asked to “select your DEM elevation units”, choose the units of the values that are in the actual DEM that you are using. Be careful – depending on the source, your DEM may have elevations in feet or meters.
5. When asked whether to overwrite existing data – if you choose "Yes", all elevation and gradient data will be erased and re-sampled – if you choose No, sampling will begin at the first zero value.
6. Spatial Analyst (developed by ESRI) has a bug, which limits the number of grid samples that it may perform. Beyond which, ArcView fatally crashes and reports a “Segmentation Violation” error. TTools will prevent this disaster from happening. Depending on the size of your TTools point theme, you may get a message that says, “Spatial Analyst has reached its sampling capacity....”. Click OK, and TTools will automatically save your project and close your ArcView session. At this point, re-open your ArcView project and start the “Measure Topographic Shade” process again. This time, DO NOT overwrite existing values, and TTools will begin sampling where it left off last time.
7. Repeat this process as many times as necessary, until you see a window pop up that says, “Topographic Shade Angles have been calculated...”.

STEP 5: SAMPLING THE RIPARIAN LAND COVER

This procedure uses Spatial Analyst to sample a grid theme. Spatial Analyst can perform a limited number of commands in a given ArcView session before causing a “Segmentation Violation”, and crashing ArcView. Therefore, it is **strongly recommended** that you save the project, completely close out of ArcView, and re-open the project before beginning this step of TTools. Doing so will clear ArcView and Spatial Analyst memory, and TTools will then be able to accurately predict and prevent a potentially disastrous crash.

PREREQUISITES:

- You must have your TTools point theme in the view.
- You must have a riparian vegetation grid theme in the view.
- You must have your DEM in the view.

Helpful Hint:

Before proceeding with TTools sampling, make sure that your DEM, vegetation grid, and TTools point coverage are located on your local hard drive. If your DEM or vegetation grid resides on a network drive, TTools sampling will take about three times longer.

STEPS:

1. Select the “Sample Riparian Land Cover” option in the TTools menu.
2. Select your TTools point theme.
3. Select your 1:5000 digitized riparian vegetation grid theme.
4. Select your DEM.
5. Select your DEM elevation units.
6. Type in your sampling distance interval (in meters). This is the distance between sampling steps.
7. Spatial Analyst (developed by Esri) has a bug, which limits the number of grid samples that it may perform. Beyond which, ArcView fatally crashes and reports a “Segmentation Violation” error. TTools will prevent this disaster from happening. Depending on the size of your TTools point theme, you may get a message that says, “Spatial Analyst has reached its sampling capacity....” Click OK, and TTools will automatically save your project and close your ArcView session. At this point, re-open your ArcView project and start the “Sample Vegetation Grid” process again. This time, DO NOT overwrite existing values, and TTools will begin sampling where it left off last time.
8. Repeat this process as many times as necessary, until you see a window pop up that says, “Riparian land cover has been sampled...”

STEP 6: SAMPLE FLIR DATA

PREREQUISITES:

- You must have your TTools point theme in the view.
- You must have your FLIR point theme in the view.

STEPS:

1. Select the “Sample FLIR Data” option in the TTools menu.
2. Select your TTools point theme.
3. Select the FLIR point coverage that you will be sampling.
4. Select the field from your FLIR point theme that contains the temperature values you wish to sample. (Typically, the “Median” field is sampled from Watershed Sciences, LLC data sources.)
5. Select the temperature units that exist in the FLIR point coverage.

SYMBOLS

- a: Wind Function Coefficient (m/mb's)
- α : Atmospheric Elevation (degrees)
- α_{CL} : Volumetric Weighted Thermal Diffusivity ($\frac{m^2}{s}$)
- α_{H_2O} : Water Thermal Diffusivity (0.0000001433m²/s)
- α_{sed} : Substrate Thermal Diffusivity (0.0000045m²/s)
- A_{CL} : Surface Area of Conduction Layer (m²)
- A_s : Cross-Sectional Across Seepage Face (m²)
- A_W : Stream Segment Surface Area (m²)
- A_x : Cross-Sectional Wetted Area (m²)
- b: Wind Function Coefficient (mb⁻¹)
- B_R : Bowens Ratio (unitless)
- C_E : Embeddedness
- C_I : Clearness Index
- C_L : Cloudiness (0 to 1)
- $C_1...C_4$: Muskingum Coefficients
- C_R : Refraction Coefficient (degrees)
- c_{CL} Volumetric Weighted Specific Heat Capacity ($\frac{J}{kg^{\circ}C}$)
- c_{H_2O} Water Specific Heat Capacity (4187 J/kg^{°C})
- c_K : Wave Celerity ($\frac{m}{s}$)
- c_{sed} : Substrate Specific Heat Capacity (2219 J/kg^{°C})
- D: Day of Month (1 to 31)
- D_F : Diffuse Fraction of Solar Radiation
- D_L : Dispersion Coefficient Used in MacCormick Method ($\frac{m^2}{s}$)
- D_x : Diffusion Coefficient Used in Muskingum-Cunge Method ($\frac{m^2}{s}$)
- dt: Model Time Step (s)
- dx: Model Distance Step (m)
- d_{BF} : Bankfull Depth (m)
- \bar{d}_{BF} : Average Bankfull Depth (m)
- d_{CL} : Depth of Conduction Layer (m)
- d_W : Water Column Depth (m)
- \bar{d}_W : Average Water Column Depth (m)
- δ : Solar Declination (degrees)
- Δ : Slope of the Saturation Vapor v. Air Temperature Curve ($\frac{mb}{^{\circ}C}$)
- ϵ_{atm} : Emissivity of the Atmosphere (unitless)
- \bar{E} : Evaporation Rate ($\frac{m}{s}$)
- E_C : Eccentricity of Earth's Orbit (unitless)
- E_t : Equation of Time (minutes)
- E_a : Aerodynamic Evaporation ($\frac{m}{s}$)

SYMBOLS

- e_a : Vapor Pressure (mbar)
 e_s : Saturation Vapor Pressure (mbar)
 e_a' : Vapor Pressure Based on e_s' (mb)
 e_s' : Saturation Vapor Pressure Based on T_W (mb)
 e : Density Gradient ($10^{-6} \frac{1}{m}$)
 $\Phi_{\text{convection}}$: Convection Flux ($\frac{W}{m^2}$)
 $\Phi_{\text{conduction}}$: Substrate Conduction Flux ($\frac{W}{m^2}$)
 $\Phi_{\text{evaporation}}$: Evaporation Flux ($\frac{W}{m^2}$)
 Φ_{longwave} : Longwave Radiation Flux ($\frac{W}{m^2}$)
 $\Phi_{\Delta Q}$: Change in Stored Heat ($\frac{W}{m^2}$)
 $\Phi_{\Delta M}$: Water Advected Heat ($\frac{W}{m^2}$)
 Φ_{LW}^A : Atmospheric Emitted Longwave Radiation Flux ($\frac{W}{m^2}$)
 $\Phi_{\text{LW}}^{\text{LC}}$: Land Cover Emitted Longwave Radiation Flux ($\frac{W}{m^2}$)
 Φ_{LW}^S : Water Column Emitted Longwave Radiation Flux ($\frac{W}{m^2}$)
 g : Acceleration of gravity (9.8 (m/s²))
 Φ_{SRG} : Global Solar Flux ($\frac{W}{m^2}$)
 Φ_{SRB} : Direct Beam Solar Radiation Estimate above Topography ($\frac{W}{m^2}$)
 Φ_{SRB1} : Direct Beam Solar Radiation above Topography ($\frac{W}{m^2}$)
 Φ_{SRD1} : Diffuse Solar Radiation above Topography ($\frac{W}{m^2}$)
 Φ_{SRB2} : Direct Beam Solar Radiation below Topography ($\frac{W}{m^2}$)
 Φ_{SRD2} : Diffuse Solar Radiation below Topography ($\frac{W}{m^2}$)
 Φ_{SRB3} : Direct Beam Solar Radiation below Land Cover ($\frac{W}{m^2}$)
 Φ_{SRD3} : Diffuse Solar Radiation below Land Cover ($\frac{W}{m^2}$)
 Φ_{SRB4} : Direct Beam Solar Radiation above Stream Surface ($\frac{W}{m^2}$)
 Φ_{SRD4} : Diffuse Solar Radiation above Stream Surface ($\frac{W}{m^2}$)
 Φ_{SRB5} : Direct Beam Solar Radiation Penetrating Stream Surface ($\frac{W}{m^2}$)
 Φ_{SRD5} : Diffuse Solar Radiation Penetrating Stream Surface ($\frac{W}{m^2}$)
 Φ_{SRB6} : Direct Beam Solar Radiation Attenuated in Water Column ($\frac{W}{m^2}$)
 Φ_{SRD6} : Diffuse Solar Radiation Attenuated in Water Column ($\frac{W}{m^2}$)
 Φ_{SR6} : Solar Radiation Attenuated in Water Column ($\frac{W}{m^2}$)
 Φ_{SRB7} : Direct Beam Solar Radiation Attenuated in Stream Bed ($\frac{W}{m^2}$)

SYMBOLS

- Φ_{SRD7} : Diffuse Solar Radiation Attenuated in Stream Bed ($\frac{W}{m^2}$)
- Φ_{SR7} : Solar Radiation Attenuated in Stream Bed ($\frac{W}{m^2}$)
- Φ_{solar} : Solar Radiation Attenuated in Water Column ($\frac{W}{m^2}$)
- Φ_{total} : Total Heat Flux ($\frac{W}{m^2}$)
- F_d : Densimetric Froude Number (unitless)
- γ : Psychrometric Constant ($\frac{mb}{^\circ C}$)
- k : Wind Velocity Coefficient ($k = 0.4$)
- K : Travel time Parameter (s)
- K_{CL} : Volumetric Weighted Thermal Conductivity ($\frac{J}{m \cdot s \cdot ^\circ C}$)
- $K_{\text{H}_2\text{O}}$: Water Thermal Conductivity ($0.600 \frac{J}{m \cdot s \cdot ^\circ C}$)
- K_{sed} : Sediment Thermal Conductivity ($15.977 \frac{J}{m \cdot s \cdot ^\circ C}$)
- K_{S} : Dominant Substrate Hydraulic Conductivity (m/s)
- K_{S} : Composite Substrate Hydraulic Conductivity ($\frac{m}{s}$)
- h : Hour based on daylight savings time (hr)
- h_D : Hydraulic Head for Darcy Calculation (m)
- h_S : Hydraulic Head Across Seepage Face (m)
- H_{LC} : Land Cover Height for each Zone (m)
- η : Porosity of the Stream Bed (unitless)
- JD : Julian Day (1 to 365)
- L_e : Latent Heat of Vaporization ($\frac{J}{kg}$)
- M_A : Air Mass Thickness
- m : Minute based on daylight savings time (min)
- n : Manning's Roughness Coefficient
- θ_{AL} : Apparent Longitude of the Sun (degrees)
- θ_{AS} : Geometric Mean of Anomaly of the Sun (degrees)
- θ_{AZ} : Solar Azimuth (degrees)
- θ_{CS} : Equation of the Center of the Sun (degrees)
- θ_{HA} : Hour Angle (degrees)
- θ_{LS} : True Longitude of the Sun (degrees)
- θ_{LS} : Geometric Mean of the Longitude of the Sun (degrees)
- θ_{OB} : Mean Obliquity of the Elliptic (degrees)
- θ_{OB} : Obliquity of the Elliptic (degrees)
- θ_{SA} : Solar Altitude (degrees)
- θ_{SZ} : Solar Zenith – Uncorrected (degrees)
- θ_{SZ} : Solar Zenith – Corrected (degrees)
- θ_{TA} : Solar True Anomaly (degrees)
- θ_{TW} : Topographic Shade Angle – West (degrees)
- θ_{TS} : Topographic Shade Angle – South (degrees)

SYMBOLS

- θ_{TE} : Topographic Shade Angle – East (degrees)
 θ_{VTS} : View to Sky (unitless)
 P_A : Adiabatic Atmospheric Pressure (mb)
 P : Solar Radius Vector (AU)
 P_W : Wetted Perimeter (m)
 PL_{LC} : Direct Beam Path Length through each land cover zone (m)
 PL_W : Direct Beam Path Length through Water Column (m)
 Q : Flow Rate (m^3)
 Q_{evap} : Evaporation Loss Rate ($\frac{m^3}{s}$)
 Q_{TRIB} : Surface Inflow Flow Rate ($\frac{m^3}{s}$)
 Q_{GW} : Subsurface Inflow Rate (m^3)
 Q_{hyp} : Hyporheic Exchange Rate Across Seepage Face ($\frac{m^3}{s}$)
 Q_{IN} : Surface Inflow Rate (m^3)
 Q_{OUT} : Withdrawal Flow Rate (m^3)
 Q_{TRIB} : Instantaneous Flow Summation of Surface Inflows ($\frac{m^3}{s}$)
 Q_{WITH} : Withdrawal Flow Rate ($\frac{m^3}{s}$)
 R_{SS} : Stream Surface Reflectivity (unitless)
 R_{SB}^B : Reflectivity of Stream Bed if Direct Beam Radiation (unitless)
 R_{SB}^D : Reflectivity of Stream Bed if Diffuse Radiation (unitless)
 r : Radius Vector (radians)
 ρ_{CL} : Volumetric Weighted Density ($\frac{kg}{m^3}$)
 S : Storage (m^3)
 S_f : Friction slope (unitless)
 SL_{LC} : Shadow Length Cast from each Zone (m)
 $s_{1,t}, s_{2,t}$: Approximation of the Slope ($\frac{^{\circ}C}{s}$)
 T_A : Air Mass Transmissivity
 T_W^B : Direct Beam Transmissivity of Water Column (unitless)
 T_W^D : Diffuse Transmissivity of Water Column (unitless)
 τ : Shear Stress ($\frac{kg}{m \cdot s^2}$)
 t_{JD} : Julian days since epoch 1900 January 0.5 ET
 t_{JDC} : Julian centuries since epoch 1900 January 0.5 ET
 t_{DST} : Daylight Savings Time (day fraction)
 t_{GMT} : Greenwich Mean Time (day fraction)
 t_s : Solar Time (minutes)
 t_{zone} : Time Zone (see Table 2.1)
 T_a : Air Temperature ($^{\circ}C$)
 T_{GW} : Subsurface Inflow Temperature ($^{\circ}C$)
 T_{TRIB} : Surface Inflow Temperature ($^{\circ}C$)
 T_W : Water Temperature ($^{\circ}C$)

SYMBOLS

- ΔT_{CL}^{solar} : Change in Conduction Layer Temperature from Solar Radiation ($^{\circ}C$)
 ΔT_{CL}^{cond} : Change in Conduction Layer Temperature from Conduction ($^{\circ}C$)
 T_{CL} : Conduction Layer Temperature ($^{\circ}C$)
 T_{CL}^{solar} : Conduction Layer Temperature Accounting for Solar Irradiance ($^{\circ}C$)
 T_{CL}^{cond} : Conduction Layer Temperature Accounting for Conduction ($^{\circ}C$)
 T_{GW} : Subsurface Inflow Temperature ($^{\circ}C$)
 T_{IN} : Surface Inflow Temperature ($^{\circ}C$)
 T_{OUT} : Withdrawal Flow Temperature $\approx T_W$ ($^{\circ}C$)
 T_{TRIB} : Instantaneous Flow Weighted Temperature of Surface Inflows ($^{\circ}C$)
 U : Average Flow Velocity ($\frac{m}{s}$)
 U_s : Shear Velocity ($\frac{m}{s}$)
 V : Water Column Volume (m^3)
 VD : Land Cover Density (unitless)
 V_{sed} : Substrate Volume in Conduction Layer (m^3)
 V_{H_2O} : Water Volume in Conduction Layer (m^3)
 V_{CL} : Conduction Layer Volume (m^3)
 V_W : Water Reach Volume (m^3)
 W_B : Bottom Width (m)
 W_W : Stream Surface Width (m)
 $W:D$: Bankfull width to depth ratio (dimensionless)
 $f(\overline{W})$: Wind Function ($\frac{m}{mb \cdot s}$)
 \overline{W} : Wind Velocity Measured at ≈ 2 meters Above Surface ($\frac{m}{s}$)
 \overline{W}_s : Wind Velocity Measured at Water Surface ($\frac{m}{s}$)
 X : Wedge Weighting Coefficient
 Ψ_{LC} : Land Cover Shade Density (unitless)
 Y : Year (If month is less than 2, then $Y = \text{Year}-1$)
 Z : Channel Side Slope Ratio (dimensionless)
 z : Elevation (m)
 z_d : Zero-Plane Displacement (m) $z_d = 0.7 \cdot H_{LC}$
 z_0 : Roughness Height (m) $z_d = 0.1 \cdot H_{LC}$
 z_M : Measurement Height (2 m) $z_M > z_d + z_0$
 z_s : Stream Elevation (m)

References

- Adams, T.A. and K. Sullivan. 1990.** The physics of forest stream heating: a simple model. Timber-Fish-Wildlife Report No. TFW-WQ3-90-007. Washington Department of Natural Resources, Olympia, Washington.
- Anderson, D.A., J.C. Tannehill and R.H. Pletcher. 1984.** Computational Fluid Mechanics and Heat Transfer. McGraw-Hill, New York.
- Anderson, E.R. 1954.** Energy-budget studies. In: Water Loss Investigations, Lake Hefner Studies Technical Report. Prof. Pap. 269, US Geological Survey, Department of the Interior, Washington D.C.
- Atwell, B. H., McDonald, R. B., & Bartolucci, L. A. 1971.** Thermal remote sensing of streams from airborne radiometric scanning. Water Resources Bulletin, 7 228-243.
- Austin, R. W. and G. Halikas. 1976.** The index of refraction of seawater. Scripps Instit. Oceanogr., San Diego, CA., Tech. Report SIO 76-1. 121 pp.
- Avery, T. E. and Berlin, G. L. 1992.** Fundamentals of remote sensing and airphoto interpretation. New York: Mcmillan.
- Bedient, P.B. and W.C. Huber. 1992.** Hydrology and Floodplain Analysis. Reading, Massachusetts: Addison-Wesley Publishing Company.
- Bell, M.C. 1986.** Fisheries handbook of engineering requirements and biological criteria. Fish Passage Development and Evaluation Program, U. S. Army Corps of Engineers, North Pacific Division. Portland, Oregon, 290 pp.
- Berk, A., Bernstien, L. S., and Roberson, D. C. 1989.** MODTRAN: A Moderate Resolution Model for LOWTRAN 7, Tech. Rep. GL-TR-89-0122, Geophys. Lab., HAFB, Bedford, MA.
- Beschta, R. L., R. E. Bilby, G. W. Brown, L. B. Holtby, and T. D. Hofstra. 1987.** Stream temperature and aquatic habitat: Fisheries and forestry interactions. Pages 191-232 in E. O. Salo and T. W. Cundy, eds. *Streamside management: Forestry and fishery interactions*. University of Washington, Institute of Forest Resources, Seattle, USA.
- Beschta, R.L. and J. Weatherred. 1984.** A computer model for predicting stream temperatures resulting from the management of streamside vegetation. USDA Forest Service. WSDG-AD-00009.
- Bowie, G.L., Mills, W.B., Porcella, D.B., Campbell, C.L., Pagenkopf, J.R., Rupp, G.L., Johnson, K.M., Chan, P.W., and Gherini, S.A. 1985.** Rates, Constants and Kinetics Formulations in Surface Quality Modeling, 2nd Edition, EPA/600/3-85/040, U.S. Environmental Protection Agency, Athens, GA.
- Bowen, I.S. 1926.** The ratio of heat loss by convection and evaporation from any water surface. Physical Review. Series 2, Vol. 27:779-787.
- Boyd M. and B. Kasper. 2002.** Upper Klamath Lake Drainage: Vegetation, Hydrology and Morphology. Oregon Department of Environmental Quality.
- Boyd, M. 1996.** Heat Source: stream temperature prediction. Master's Thesis. Departments of Civil and Bioresource Engineering, Oregon State University, Corvallis, Oregon.

- Brady, D.K., W.L. Graves and J.C. Geyer. 1969.** Surface heat exchange at power plant cooling lakes, cooling water studies for Edison Electric Institute. Report No. 5, John Hopkins University.
- Brett, J.R. 1952.** Temperature Tolerance in Young Pacific Salmon, Genus *Oncorhynchus*. *J. Fish. Res. Bd. Can.*, 9(6):265-323.
- Brown, G.W. 1983.** Chapter III, Water Temperature. Forestry and Water Quality. Oregon State University Bookstore. Pp. 47-57.
- Brown, G.W. 1970.** Predicting the effects of clearcutting on stream temperature. *Journal of Soil and Water Conservation*. 25:11-13.
- Brown, G.W. 1969.** Predicting temperatures of small streams. *Water Resour. Res.* 5(1):68-75.
- Brown, L. and Barnwell, T.O., Jr. 1987.** The Enhanced Stream Water Quality Models QUAL2E and QUAL2E-UNCAS: Documentation and USER Manual, Report EPA/600/3-87/007, U.S. Environmental Protection Agency, Athens, GA.
- Chapra, S.C. 1997.** Surface Water-Quality Modeling. Boston: WCB/McGraw-Hill.
- Chen, Y. 1994.** Hydrologic and water quality modeling for aquatic ecosystem protection and restoration in forest watersheds: a case study of stream temperature in the Upper Grande Ronde River, Oregon. PhD Dissertation. University of Georgia. Athens, Georgia.
- Cuenca, R.H. 1989.** Irrigation System Design: An Engineering Approach. Englewood Cliffs, New Jersey, Prentice-Hall, Inc.
- Cunge, K.A. 1969.** On the subject of a flood propagation method (Muskingum Method). *J. Hyd. Res.*, vol. 7, no. 2, pp. 205-230.
- Dingman, S.L. 2002.** Physical Hydrology. 2nd Ed. New Jersey: Prentice Hall.
- Domenico P.A. and F.W. Schwartz. 1990.** Physical and Chemical Hydrogeology. New York, John Wiley and Sons, Inc.
- Dunne, T. and L.B. Leopold. 1978.** Water in Environmental Planning. San Francisco, California, W.H. Freeman and Company.
- Faux, R. N., P. Maus, C. Torgersen, and M. Boyd. 2001.** Airborne Thermal Infrared (TIR) Remote Sensing Application to USDA USFS Stream Temperature Monitoring Programs: New Approaches for monitoring thermal variability. USFS Remote Sensing Applications Center, Salt Lake City, Utah.
- Fisher, H. B., E. J. List, R. C. Koh, J. Imberger, and N. H. Brooks. 1979.** Mixing in Inland and Coastal Waters. Academic Press, New York, 1979.
- Hall, F.C. 1998.** Pacific Northwest Ecoclass Codes for Seral and Potential Natural Communities. USDA Forest Service. Pacific Northwest Research Station. PNW-GTR-418.
- Harbeck, G.E. and J.S. Meyers. 1970.** Present day evaporation measurement techniques. J. Hydraulic Division. A.S.C.E., Proceed. Paper 7388.
- Harbeck, G.E., Kohler, M.A. Koberg, G.E., and others, 1958.** Water-Loss Investigations: Lake Mead Studies: USGS Prof. Pap. 298, 100 p.

- Heath A.G. and G.M. Hughes. 1973.** Cardiovascular and respiratory changes during heat stress in rainbow trout (*Salmo gairneri*). *J. Exp. Biol.*, 59:323-338.
- Hogan, J.W. 1970.** Water temperature as a source of variation in specific activity of brain acetylcholinesterase of bluegills. *Bull. Environment. Contam. Toxicol.*, 5:347-353.
- Hokanson, K., C.F. Kleiner and T.W. Thorslund. 1977.** Effects of Constant Temperatures and Diel Temperature Fluctuations on Specific Growth and Mortality Rates and Yield of Juvenile Rainbow Trout, *Salmo gairneri*. *J. Fish. Res. Bd. Can.*, 34:639-648.
- Ibqal, M. 1983.** An Introduction to Solar Radiation. Academic Press. New York. 213 pp.
- Issacson, E., J.J. Stoker and B.A. Troesch. 1956.** Numerical solution of flood prediction and river regulation problems. *Inst. Math. Sci., Report No. IMM-235*, New York University, New York.
- Jerlov, W.G. 1976.** Marine optics. Elsevier Scient. Publ. Comp., Elsevier Oceanography Series, 14. 231 p.
- Jobson, H.E. and T.N. Keefer. 1979.** Modeling highly transient flow, mass and heat transfer in the Chattahoochee River near Atlanta, Georgia. Geological Survey Professional Paper 1136. U.S. Gov. Printing Office, Washington D.C.
- Kay, J, Allen, T., Fraser, R., Luvall, J., Ulanowicz, R., 2001.** "Can we use energy based indicators to characterize and measure the status of ecosystems, human, disturbed and natural?" in Ulgiati, S., Brown, M.T., Giampietro, M., Herendeen, R., Mayumi, K., (eds) Proceedings of the international workshop: Advances in Energy Studies: exploring supplies, constraints and strategies, Porto Venere, Italy, 23-27 May, 2000 pp. 121-133.
- Kovalchik, B.L. 1987.** Riparian zone associations. R6 ECOL TP-279-87. USDA Forest Service. Pacific Northwest Region.
- Kustas, W.P., A Rango and R. Uijlenhoet. 1994.** A simple energy balance algorithm for snowmelt runoff model. *Water Resources Research* 30:1515-1527.
- Leopold, L. B., M. G. Wolman and J. P. Miller. 1964.** Fluvial Processes in Geomorphology. Freeman, San Francisco, California. 522 pp.
- MacCormick, R.W. 1969.** The effect of viscosity in hypervelocity impact cratering. *Am. Inst. Aeronaut. Astronaut. Paper* 69-364.
- Marciano, J.J. and G.E. Harbeck. 1952.** Mass transfer studies in water loss investigations: Lake Hefner studies. USGS Prof. Paper 269.
- Martin, J. L. and McCutcheon, S. C. 1999.** Hydrodynamics and Transport for Water Quality Modeling, Lewis Publishers, New York, NY, 1999.
- McCutcheon, S.C. 1989.** Water Quality Modeling: Vol. 1, Transport and Surface Exchange in Rivers. CRC Press, Boca Raton. pp. 183-209.
- Meeus, J. 1988.** Astronomical Formulae for Calculators. 4th Ed. Richmond, Virginia: Willmann-Bell Inc.
- Meeus, J. 1991.** Astronomical Algorithms. 2nd Ed. Richmond, Virginia: Willmann-Bell Inc.

- Meyer, A. F. 1928.** Elements of hydrology: 2d ed. revised, New York, John Wiley & Sons, 522 p.
- Meyer, A.F. 1942.** Evaporation from lakes and reservoirs. Minnesota Resources Commission, St. Paul, MN.
- Moore, J., Miner, J. and R. Bower. 1999.** The effect of shade on water: a tub study. Department of Rangeland Resources. Oregon State University.
- Morton, F.I. 1965.** Potential evaporation and river basin evaporation. J. Hydraul. Dive Prac. Am. Soc. Civ. Eng. 91(HY96)67-97.
- National Oceanic and Atmospheric Administration.** Surface Radiation Branch, Solar position calculator website. (<http://www.srrb.noaa.gov/highlights/sunrise/azel.html>)
- Norton, W.R., L.A. Roesner and G.T. Orlob. 1968.** Mathematical models for predicting thermal changes in impoundments, EPA Water Pollution Control Research Series, U.S. Environmental Protection Agency, Washington D.C.
- Oke, T. R. 1978.** Boundary Layer Climates. Maethuen and Company, Ltd. London, England. 372 pp.
- Oregon Department of Environmental Quality. 2000.** Upper Grande Ronde River Subbasin Total Maximum Daily Load.
- Park, C. 1993.** SHADOW: stream temperature management program. User's Manual v. 2.3. USDA Forest Service. Pacific Northwest Region.
- Parker, F.L. and P.A. Krenkel. 1969.** Thermal pollution: status of the art. Rep. 3. Department of Environmental and Resource Engineering, Vanderbilt University, Nashville, TN.
- Penman, H.L. 1948.** Natural evaporation from open water, bare soil, and grass. Royal Society of London Proceedings, Series A, 193:120-145.
- Petersen, B., T. Stringham and W. Krueger. 1999.** The impact of shade on the temperature of running water. Department of Rangeland Resources. Oregon State University.
- Poole, G.C., J.A. Stanford, S.W. Running and C.A. Frissell. 2000.** A linked GIS/modeling approach to assessing the influences of flood-plain structure on surface- and ground-water routing in rivers. Proceedings 4th International Conference on Integrating GIS and Environmental Modeling (GIS/EM4).
- Poole, G.C. and C.H. Berman. 2000.** Pathways of human influence on water temperature dynamics in stream channels. Submitted to Environmental Management (pending publication).
- Potter M.C. and D.C. Wiggert. 1991.** Mechanics of Fluids. Englewood Cliffs, New Jersey, Prentice Hall, Inc.
- Raudkivi, A.J. 1979.** Hydrology. Pergamon, Oxford, England.
- Rishel, G.B., Lynch, J.A. and E.S. Corbett.. 1982.** Seasonal stream temperature changes following forest harvesting. J. Environ. Qual. 11:112-116.
- Rosgen, D. 1996.** Applied River Morphology. Wildland Hydrology. Pagosa Springs, Colorado.

- Ryan, P.J. and D.F. Harleman.** 1976. Transient cooling pond behavior. *Hydraul. Eng. and the Environ.*, Proc 21st Ann. Hydraul. Div. Specialty Conf., A.S.C.E., Boseman, Montana.
- Scatterlund, D. R. and P. W. Adams.** 1992. Wildland watershed management. 2nd edition. John Wiley and Sons, Inc.
- Sellers, W.D.** 1965. Physical Climatology. University of Chicago Press. Chicago, IL. 272 pp.
- Shanahan, P.** 1984. Water temperature modeling: a practical guide. Proceedings of statormwater and water quality model users group meeting. April 12-13. U.S. EPA-600/6-85-003.
- Sinokrot, B.A. and H.G. Stefan.** 1993. Stream temperature dynamics: measurement and modeling. *Water Resour. Res.* 29(7):2299-2312.
- Stoker, J.J.** 1957. Water Waves. Intersciences Press, New York.
- Torgersen, C.E., D.M. Price, H.W. Li, and B.A. McIntosh.** 1995. Thermal refugia and chinook salmon habitat in Oregon: Applications of airborne thermal videography. Proceedings of the 15th Biennial Workshop on Color Photography and Videography in Resource Assessment, Terre Haute, Indiana. May, 1995. American Society for Photogrammetry and Remote Sensing.
- Torgersen, C. E., D. M. Price, H. W. Li, and B. A. McIntosh.** 1999. Multiscale thermal refugia and stream habitat associations of chinook salmon in northeastern Oregon. *Ecological Applications* 9: 301-319.
- Torgersen, C.E., R. Faux, B.A. McIntosh, N. Poage, and D.J. Norton.** 2001. Airborne thermal remote sensing for water temperature assessment in rivers and streams. *Remote Sensing of Environment* 76(3): 386-398.
- United States Government Printing Office.** 1998. [*The Astronomical Almanac for the Year 1998*](#). Washington, DC: Navy Dept., Naval Observatory, Nautical Almanac Office.
- Watershed Sciences, LLC.** 1999. Remote sensing survey of the Grande Ronde River Basin: thermal infrared and color videography. Prepared for ODEQ. Corvallis, Oregon. 24 pp.
- Wen-Yao, L., R. T. Field, R.G. Gantt R. G., and V. Klemas.** 1987. Measurement of the Surface Emissivity of Turbid Waters. *Remote Sensing of the Enviornment* 21:97-109.
- Wunderlich, T.E.** 1972. Heat and mass transfer between a water surface and the atmosphere. Water Resources Research Laboratory, Tennessee Valley Authority. Report No. 14, Norris Tennessee. Pp 4.20.

The methods presented in this document formulate the programmed modules utilized by Heat Source and TTools (versions 7.0). These computer models are used to create spatial data sets for stream networks, simulate dynamic hydraulics and thermodynamics. Appropriate use and application are the sole responsibility of the user.

This document may be downloaded from the web site at the following URL:
<http://www.deq.state.or.us/wq/TMDLs/tools.htm>

Updated February 12, 2003 & February 20, 2007

Cite this document as:

Boyd, M., and Kasper, B. 2003. Analytical methods for dynamic open channel heat and mass transfer: Methodology for heat source model Version 7.0.